ISBN 978-82-326-4046-1 (printed version)
ISBN 978-82-326-4047-8 (electronic version)
ISSN 1503-8181

Doctoral theses at NTNU, 2019:225

John Clauß

Energy flexibility of Norwegian residential buildings using demand response of electricity-based heating systems

A study on residential demand side flexibility, heating system control, and time-varying $CO_{2eq.}$ intensities of the electricity mix

NTNU
Norwegian University of
Science and Technology
Faculty of Engineering
Department of Energy and Process Engineering

NTNU
Norwegian University of
Science and Technology

Doctoral theses at NTNU, 2019:225

NTNU

NTNU
Norwegian University of
Science and Technology

John Clauß

Energy flexibility of Norwegian residential buildings using demand response of electricity-based heating systems

A study on residential demand side flexibility, heating system control, and time-varying $CO_{2eq.}$ intensities of the electricity mix

Trondheim, August 2019

Norwegian University of Science and Technology
Faculty of Engineering
Department of Energy and Process Engineering

NTNU
Norwegian University of
Science and Technology

NTNU
Norwegian University of Science and Technology

Thesis for the degree of Philosophiae Doctor

Faculty of Engineering
Department of Energy and Process Engineering

ISBN 978-82-326-4046-1 (printed version)
ISBN 978-82-326-4047-8 (electronic version)
ISSN 1503-8181

Doctoral theses at NTNU, 2019:225

Printed by Skipnes Kommunikasjon as

PREFACE

In summer 2006, we spent our family holidays in northern Norway. On our way back to Germany we passed Trondheim and stopped to have a look around the University Campus of NTNU. Even though I was in my final year of high school at the time, I told my parents that "One day, I would like to study here!" – Little did we know…! I went to Trondheim for two semesters during my Bachelor studies in 2010/2011 and simply got hooked on the place, which is why I came back to Trondheim to write my Master Thesis at NTNU and SINTEF. This was the first time that I have worked with heat pump technologies and their integration into a local heating grid.

I liked the working environment and the interaction with my supervisors at NTNU and SINTEF during the time of my master thesis, and of course, I liked the everyday-life in Trondheim. Therefore, I was delighted when an opening for a PhD position at NTNU came up. I took up contact with the supervisor-to-be, Laurent Georges, and after a short meeting, I decided to apply for the position.

In the end, I got the job as a PhD fellow, and after years of studies, I was ready to have a regular job. Again, little did I know…! It was soon apparent that being a PhD fellow is not a normal job, but it is much more than that. It is a journey filled with lots of excitement, frustration, small personal breakthroughs, patience and in the end satisfaction. It took quite some time and efforts, but after many steps, rather small steps in the beginning and bigger steps towards the end, I finished my PhD studies, thanks to the guidance and encouragements of my supervisor, and the support of my family, friends, fellow PhD students, and other colleagues.

The topic of this thesis is interdisciplinary and requires knowledge from several different topics. I learned more about heat pump systems, heat pump system control, and heat pump system modeling in building performance simulation. Furthermore, I learned about input-output models and the European power grid. All of this was applied and investigated with regards to building energy flexibility.

This PhD thesis is a great accomplishment for me personally, and I hope that it also inspires and encourages others to contribute to a more sustainable future.

Trondheim, August 2019

John Clauß

ABSTRACT

The transition to a sustainable energy system requires a shift to intermittent renewable energy sources, which call for increased flexibility on the demand side. Heat pumps offer the possibility to couple the electricity sector and the heating sector, and when connected to thermal energy storages, they can provide demand side flexibility.

This thesis investigates the flexibility potential of residential buildings in Scandinavia, and more specifically in Norway. In this regard, three different boundary levels are considered: *power grid level*, *building level,* and *heat pump system level*.

At the *power grid level*, a methodology to evaluate the hourly average $CO_{2eq.}$ intensity of the electricity mix, while also considering electricity trading is developed. In general, the $CO_{2eq.}$ intensity of the electricity mix may indicate the share of renewable energies in the mix. The proposed method is based on the logic of input-output models and avails the balance between electricity generation and demand. This thesis shows that it is essential to consider electricity imports and their varying $CO_{2eq.}$ intensities for the evaluation of the $CO_{2eq.}$ intensity in Scandinavian bidding zones. Generally, the average $CO_{2eq.}$ intensity of the Norwegian electricity mix increases during times of electricity imports since the average $CO_{2eq.}$ intensity usually is low because electricity is mainly generated from hydropower. This hourly $CO_{2eq.}$ intensity can be used as a penalty signal for demand response strategies applied to residential heating.

At the *building level*, the flexibility potential of predictive rule-based controls (PRBC) in the context of Scandinavia and Norway is studied. For this purpose, demand response measures are applied to electricity-based heating systems, such as heat pumps and direct electric heating. In one case study, the demand response potential for heating a single-family residential building based on the hourly average $CO_{2eq.}$ intensity of six Scandinavian bidding zones is investigated. The results show that control strategies based on the $CO_{2eq.}$ intensity can achieve emission reductions if daily fluctuations of the $CO_{2eq.}$ intensity are large enough to compensate for the increased electricity use due to load shifting. Furthermore, the results reveal that price-based control strategies usually lead to increased overall emissions for the Scandinavian bidding zones as the operation is shifted to nighttime when cheap carbon-intensive electricity is imported from the continental European power grid.

In another case study, the building energy flexibility potential of a Norwegian single-family detached house is investigated using PRBC. Four insulation levels are studied for this building: (1) passive house, based on the Norwegian standard for residential passive houses, (2) zero emission building, based on the LivingLab located at the Gløshaugen Campus at NTNU, (3) TEK10, based on the Norwegian building standard from 2010, and (4) TEK87, based on the Norwegian building standard from 1987. The three PRBC investigated aim at reducing energy costs for heating, reducing

annual $CO_{2eq.}$ emissions and reducing the energy use for heating during peak hours. This last objective is probably the most strategic in the Norwegian context where cheap electricity is mainly produced by hydropower. It is shown that the price-based control does not generate cost savings because lower electricity prices are outweighed by the increase in electricity use for heating. The implemented price-based control would create cost savings in electricity markets with higher daily fluctuations in electricity prices, such as Denmark. For the same reasons, the carbon-based control cannot reduce the yearly $CO_{2eq.}$ emissions due to limited daily fluctuations in the average $CO_{2eq.}$ intensity of the Norwegian electricity mix. The PRBC that reduces the energy use for heating during peak hours turns out to be very efficient, especially for direct electric heating. As an example, for the ZEB insulation level and direct electric heating, the price-based control reduces the energy use during peak hours by 18%, and the carbon-based control by about 37%. The control strategy dedicated to reduce the energy use during peak hours leads to a 93% reduction. For air-source heat pumps, the control of the heat pump system is complex and reduces the performance of the three PRBC. Therefore, it is suggested to model a heat pump system with enough detail for a proper assessment of the building energy flexibility.

The model complexity required to adequately describe the heat pump system behavior with regards to demand response of residential heating is investigated on the *heat pump system level*. In the course of this thesis, the influence of the modeling complexity of the heat pump system control on distinct energy-related and heat pump system-related performance indicators is studied. The results prove that the modeling complexity of the system control has a significant impact on the key performance indicators, meaning that this aspect should not be overlooked. If the heat pump operation is investigated in detail and a high time resolution is required, it is shown that a PI-controller leads to a smoother operation than a P-controller, but tuning of the controller is highly recommended. It is shown that the choice of the controller (P or PI) is not crucial as long as the control signal to the heat pump is not of importance and power is not investigated at very short time scales. Regarding demand response measures, a strong interaction between the prioritization of domestic hot water and the control of auxiliary heaters significantly increases electricity use of a bivalent mono-energetic heat pump system, if demand response is performed for both, domestic hot water and space heating. The electricity use for heating is only slightly increased if demand control using predictive rule-based control is performed for space heating only.

To summarize, energy flexible buildings can play a major role in the transition towards a more sustainable energy system. The use of the hourly $CO_{2eq.}$ intensity as a penalty signal for demand response strategies applied to residential heating, can facilitate achieving the emission targets of the European Union. At the building level, different objectives of demand response, such as reducing operational costs, reducing CO_2 emissions or increasing system efficiency are often incompatible and thus

difficult to achieve at the same time when using PRBC. When aiming at a realistic control of the heating system of a single building, it is found that heat pump controller tuning and DHW prioritization of the heat pump are two significant aspects that should be considered regardless of the control strategy applied. The combination of heating system, heat distribution system, system control and building envelope is always case-specific and it is suggested that future work focuses on the design of a heat pump system that considers energy flexibility. In this PhD thesis, standard sizing of a heat pump system that is operated in an energy flexible way is applied.

Keywords

Energy flexibility; hourly $CO_{2eq.}$ intensity; demand response; demand side flexibility; predictive control; rule-based control; heat pump system; heat pump modeling; model complexity; direct electric heating; time-varying $CO_{2eq.}$ intensities; time varying electricity prices; Scandinavian power market

ACKNOWLEDGMENTS

Many persons have accompanied me on the way of this PhD. Big Thanks especially to Laurent Georges, my main supervisor, for all the scientific and personal advice throughout my PhD studies. I highly appreciate your open-door policy. My deepest gratitude for your trust in me, your guidance, all our discussions, your patience and your motivation that helped shape this PhD research into what it is.

To my co-supervisor Igor Sartori at SINTEF Community for introducing me to the IEA EBC Annex 67 Energy Flexible Buildings, which undoubtedly boosted my PhD.

To the researchers involved in Annex 67 for motivational and fruitful meetings and discussions. Special thanks to Rui Lopes from Nova University of Lisbon and James Parker from Leeds Beckett University, especially for the joyful conversations during Annex meetings. Furthermore, I would like to thank Christian Finck from Eindhoven University, Pierre Vogler-Finck from Neogrid Technologies ApS and Sebastian Stinner from RWTH Aachen for the excellent collaboration. I want to thank Sebastian for introducing me to code-writing and his support in MATLAB. Your expertise made coding much easier for me. I found new friends in each of you.

To my office mates Martin Thalfeldt, Amar Aganovic and Xingji Yu for the good atmosphere and discussions about football and motorsports. Special thanks to Martin for your help and support in IDA ICE during the start of my PhD.

Furthermore, I would like to thank Maria Justo Alonso from SINTEF Community / NTNU for discussions and support throughout my whole PhD. I highly appreciate your proposal to get me involved in one of your projects at SINTEF towards the end of my PhD period. It paved the way for my employment after my PhD studies.

To Daniel Rohde for all the informal breaks with joyful conversations and Wiener Melange, I enjoyed our breaks during the last year of my PhD as we were in the same position regarding our PhD studies, which never seemed to end.

To Adriana Reyes Lua from NTNU for all the explanations on control theory and controller tuning.

I am grateful to Amalie and Seán for reading and commenting on this thesis.

To the Master students that I have co-supervised, Thea, Katrine and Christoph, I would like to thank each of you for your interest and dedication to study energy flexibility.

To the co-authors of my papers: among previously mentioned colleagues, my thanks to Paul Beagon from UCD, to Christian Solli from NTNU, to Karen Byskov Lindberg from SINTEF Community and to Henrik Madsen from DTU Copenhagen. Thank you, Christian, for introducing me to input-output models. Thank you, Karen, for our discussions and your very valuable suggestions and feedback on some of my articles.

To EQUA for their never-ending support in IDA ICE. It is good to have you on speed dial. The EQUA Simulation Summit was a highlight and a boost for my PhD studies for sure! Special thanks to Daniel, Sven, Tobias, and Christoph from EQUA Solutions AG in Switzerland and to Mika and Erkki from EQUA Simulation Finland Oy.

To my friends. To my friends back home in Germany, especially to Aule, Sön, Mieze, Benni, Michi and Maik for all good times and nonsense during our annual trips and for just being there. To my friends and former roommates in Trondheim, especially to Eirik, Antonios and Giannis. Antonios and Giannis for welcoming me into your group of friends with open arms shortly after I have moved to Trondheim. Eirik for simply being a great friend, for all our discussions about everything and nothing, for all the ski-touring trips during the last three years and for always having a sympathetic ear.

To my family. To my parents for bringing me up in a carefree home, for always having my back and for being my role models in so many ways. To my fantastic brother for being the brother and friend you are and for reminding me to ease up more often. To my parents-in-law for your support during our hectic everyday life, for always having an open door and for many Friday evening pizzas.

Last but not least, to Andrea and Alfred. To Alfred especially for brightening our everyday life and for all the smiles every single day. To Andrea for simply being you, for all your support, cakes, dinners, patience and understanding throughout the whole period of my PhD.

LIST OF PAPERS

Paper 1:

Clauß J, Stinner S, Solli C, Lindberg KB, Madsen H, Georges L. A generic methodology to evaluate hourly average $CO_{2eq.}$ intensities of the electricity mix to deploy the energy flexibility potential of Norwegian buildings. *Proceedings of the 10th International Conference on System Simulation in Buildings*, Liege, Belgium, pp. 1-19, 2018. [1]

Paper 2:

Clauß J, Stinner S, Solli C, Lindberg KB, Madsen H, Georges L. Evaluation Method for the Hourly Average $CO_{2eq.}$ Intensity of the Electricity Mix and Its Application to the Demand Response of Residential Heating. *Energies*. 2019; 12(7):1345. [2]

Paper 3:

Clauß J, Stinner S, Sartori I, Georges L. Predictive rule-based control to activate the energy flexibility of Norwegian residential buildings: Case of an air-source heat pump and direct electric heating. *Applied Energy*. 2019; 237:500–18. [3]

Paper 4:

Johnsen T, Taksdal K, Clauß J, Yu X, Georges L. Influence of thermal zoning and electric radiator control on the energy flexibility potential of Norwegian detached houses. *Accepted at CLIMA 2019 Conference*, 2019. [4]

Paper 5:

Clauß J, Georges L. Model complexity of heat pump systems to investigate the building energy flexibility and guidelines for model implementation. *Revised version submitted to Applied Energy,* 2019. [5]

Paper 6:

Clauß J, Finck C, Vogler-Finck P, Beagon P. Control strategies for building energy systems to unlock demand side flexibility – A review. *Proceedings of the 15th IBPSA Conference*, San Francisco, USA, pp. 1750-1759, 2017. [6]

Paper 7:

Clauß J, Vogler-Finck P, Georges L. Calibration of a High-Resolution Dynamic Model for Detailed Investigation of the Energy Flexibility of a Zero Emission Residential Building. *Springer Proceedings in Energy "Cold Climate HVAC Conference 2018"*, Kiruna, Sweden, pp. 725-736, 2018. [7]

Paper 8:

Clauß J, Sartori I, Alonso M J, Thalfeldt M, Georges L. Investigations of different control strategies for heat pump systems in a residential nZEB in the Nordic climate. *Proceedings of the 12th IEA Heat Pump Conference*, Rotterdam, Netherlands, 2017. [8]

ABBREVIATIONS

ASHP	Air-source heat pump
BAU	Business as usual
BPS	Building performance simulation
BZ	Bidding zone
CSC	Control strategy carbon
CSP	Control strategy price
CSS	Control strategy schedule
DE	Direct electric
DHW	Domestic hot water
DSM	Demand side management
DR	Demand response
FH	Floor heating
HCT	High carbon threshold
HP	Heat pump
HPT	High price threshold
HTSP	High temperature set-point
HVAC	Heating, ventilation and air-conditioning
KPI	Key performance indicator
LCA	Life-cycle assessment
LCT	Low carbon threshold
LPT	Low price threshold
LTSP	Low temperature set-point
MHP	Modulating heat pump
MPC	Model-predictive control
MRIO	Multi-regional input-output
OHP	On-off heat pump
P	Proportional
PH	Passive house
PI	Proportional integral
PMV	Predicted mean vote
PRBC	Predictive rule-based control
Q_{Aux}	Auxiliary heater

ABBREVIATIONS

RTSP	Reference temperature set-point
SH	Space heating
TEK10	Norwegian building standard from 2010
TEK87	Norwegian building standard from 1987
TM	Temperature measurement
TSP	Temperature set-point
ZEB	Zero emission building

LIST OF CONTENTS

LIST OF TABLES

LIST OF FIGURES

1 INTRODUCTION

The transition to a sustainable energy system relies on the application of intermittent renewable energy sources. Historically, the operation of electricity generation plants was scheduled to meet the electricity demand, but with the introduction of more intermittent renewable energy sources on the generation side, demand side flexibility is essential to make full use of the electricity generated from intermittent renewable sources. The introduction of renewable energy sources, however, implies several challenges for system operation that need to be addressed by means of changes in the way energy systems are operated.

1.1 Motivation

On a global perspective, the building sector is responsible for 30% of the total energy use [9] and contributes to 40% of the total greenhouse gas emissions. In Norway, the building sector accounted for 36% of the energy consumption in 2015. Approximately 75% of the building sector`s energy consumption was covered by electricity, which is due to the widespread use of direct electric heating. 96% of the total domestic electricity generation was covered by hydropower [10].

However, the Scandinavian power system is highly interconnected leading to electricity trading between Scandinavian bidding zones as well as with the continental European power grid. Electricity generation in continental Europe is often dependent on thermal power plants and is thus more carbon-intensive. Norway is usually a net exporter of electricity on an annual perspective, but also imports electricity at times. During these times, the Norwegian electricity mix becomes more carbon-intensive and avoiding electricity consumption during those periods is a way to reduce the total greenhouse gas emissions. Therefore, this thesis investigates the carbon intensity of the electricity mix and considers electricity trading between Norway and its neighboring countries on an hourly resolution. The applicability of the hourly average $CO_{2eq.}$ intensity for heating demand response is discussed.

According to the EPBD recast, all new buildings built after 2020 have to be nearly zero energy buildings. The Norwegian Research Centre on Zero Emission Buildings (ZEB) focused on the balance of CO_2 emissions rather than on primary energy. Regarding residential buildings in cold climate countries like Norway, space heating needs are dominant over space cooling demands. The transition to a more sustainable building sector is typically promoted by (1) highly-insulated building envelopes in order to decrease space heating needs, (2) energy efficient thermal systems, as well as (3) covering the final energy use by renewable energy sources.

Heat pump systems are recognized as a promising technology to contribute to a further de-carbonization of the building sector, especially in Norway where the electricity generation is almost entirely from hydropower. Furthermore, heat pumps

provide the possibility of bridging the electricity sector and the heating sector and furthermore, the possibility to decouple the electricity demand for charging thermal storages and the heat demand of a building. Typically, a residential heat pump is connected to a water storage tank which can provide the opportunity of a more flexible operation. With regards to buildings, demand side flexibility is also called building energy flexibility.

According to the Building Performance Institute Europe, future buildings, e.g., termed nZEBs 2.0, should play a significant role in transforming the European energy market, as they become interactive players in balancing the grid by demand side management (DSM) or demand response (DR) measures [11]. DSM in power systems is a way to overcome potential challenges of the electricity grid, such as balancing the generation and consumption, voltage regulation or high peak loads. The progress in computation and communication technology in recent years has paved the way to a more widespread application of DR measures. DR can enable to fully exploit the electricity generated from intermittent renewable energy sources by deploying demand side flexibility [12]. DR measures can be applied to control the electricity use in a building depending on signals from the power grid [13].

Several studies point out the importance of DSM to improve the interaction between buildings and the electricity grid [12,14–18]. A number of studies have investigated the building energy flexibility with special focus on the building heating system [13,19–22]. In those studies, DR measures have been applied to electric heating systems, such as heat pump systems or direct electric heating systems. These measures are implemented into control strategies, such as predictive rule-based controls (PRBC) or more advanced controls, e.g., optimal control or model-predictive controls (MPC). PRBCs rely on a set of pre-defined rules to control the energy system, where temperature set-points (TSP) for space heating (SH) or domestic hot water (DHW) heating are usually varied to start or delay the operation of the heating system depending on the control signal. PRBCs can be a good compromise to advanced controls because PRBC is more straightforward, but can still be effective to reduce operational costs or to save carbon emissions [22].

This thesis investigates the DR of electricity-based heating systems in energy-flexible residential buildings. For this purpose, a methodology to evaluate the hourly average $CO_{2eq.}$ intensity of the electricity mix also considering electricity trading is developed. This hourly $CO_{2eq.}$ intensity will be used as a penalty signal for DR strategies applied to residential heating, more specifically to direct electric heating and air-to-water heat pumps. The flexibility potential of PRBC in the specific context of Norway will be studied. Furthermore, this thesis seeks to understand which level of modeling complexity is required to properly describe the heat pump system operation with regards to DR of residential heating.

1.2 Research questions and research tasks

The main objective of this thesis is to contribute to the transition to a more sustainable energy system. For this purpose, the thesis focuses on the implementation of demand response strategies for residential heating in energy flexible buildings. The following original research questions are investigated:

Q 1: What are the characteristics of the hourly average $CO_{2eq.}$ intensity of the electricity mix in Scandinavia?

Task 1: Develop a methodology to evaluate the hourly average $CO_{2eq.}$ intensity also considering electricity trading within an interconnected power grid.

Q 1.1: What are the characteristics of the hourly average $CO_{2eq.}$ intensity for the specific case of Norway?

Task 1.1: Analyze the relationship between the $CO_{2eq.}$ intensity in a Norwegian bidding zone and the (a) hourly electricity spot price, (b) hourly electricity use, (c) hourly electricity imports from Denmark and the Netherlands and (d) the hydropower reservoir level.

Q 1.2: How do the characteristics of the $CO_{2eq.}$ intensity used as a control signal for residential heating influence the overall emission savings in Scandinavian bidding zones?

Task 1.2: Develop a case study of residential heating where demand response is performed using the $CO_{2eq.}$ intensity of several Scandinavian bidding zones as penalty signal.

Q 2: What is the energy flexibility potential of PRBC in the specific context of Norway?

Task 2: Three demand response strategies are studied for four different building insulation levels and three different heating systems.

Q 2.1: Which key performance indicators are typically used to express building energy flexibility?

Task 2.1: Perform a literature review to study this question.

Q 2.2: How does the thermal zoning impact the energy flexibility potential?

Task 2.2: Consider the preferences of Norwegians to have cold bedrooms. A calibrated multi-zone building is used to determine how the thermal mass activation using PRBC influences bedroom temperatures.

Q 2.3: How does the modeling complexity of the heat pump system influence the operation of the heating system and thus the energy flexibility potential?

Task 2.3: For this purpose, an air-source heat pump (ASHP) is able to modulate continuously between 30% and 100%. It has an imposed minimum cycle and pause time and a realistic control to prioritize DHW over SH. The heat pump is connected to a detailed model of a storage tank with a realistic control of the auxiliary heaters.

Q 2.4: How does PRBC influence the operating conditions of the heat pump in terms of duration and frequency of cycles?

Task 2.4: Analyze in detail the operation of a modulating and an on-off heat pump system.

Q 3: Which level of modeling complexity of the heat pump system control is required to describe the heat pump behavior with regards to demand response of residential heating?

Task 3: Set up a control model of a comprehensive heat pump system in a dynamic building performance simulation tool to investigate the influence of the modeling complexity on the chosen key performance indicators by a stepwise simplification of the control model.

Q 3.1: How is the system operation influenced by different levels of modeling complexity for the heat pump system control?

Task 3.1: Analyze key performance indicators with focus on system operation, such as the frequency and duration of heat pump cycles.

This work focuses on residential buildings. Three heating systems that are commonly applied in Norwegian residential buildings are investigated: air-source heat pumps (modulating, on-off) and direct electric heating. Residential heat pumps are often connected to water storage tanks and used in combination with a low-temperature heat distribution system. In that way, pre-heating of domestic hot water and the building thermal mass can be performed. Electric resistance heaters installed in water storage tanks and electric radiators can be applied for the same purpose.

Demand response measures can be applied to control the operation of a building heating system depending on signals from outside the building to deploy the demand side flexibility [13]. For this reason, different system boundaries are considered in this thesis. Figure 1-1 puts the research questions in context to the different boundary levels.

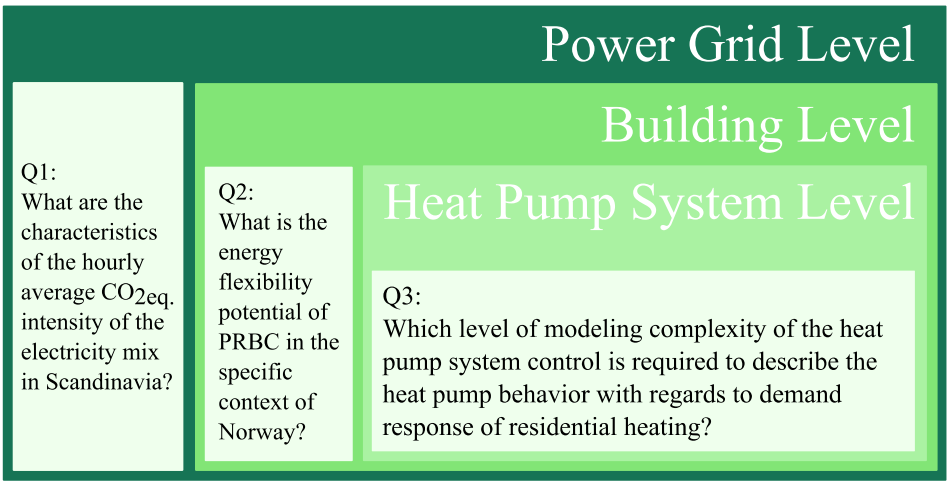

Figure 1-1. *Research questions in context to the different boundary levels.*

1.3 Structure of the thesis

The remainder of the thesis is structured as follows:

Chapter 2 presents the research context and background of the thesis. Chapter 3 describes the building model and briefly introduces the demand response scenarios of the case studies. The main results of the papers are presented, and the research questions are discussed in Chapter 4. Section 4.1 illustrates the results for the $CO_{2eq.}$ intensity in Scandinavian bidding zones. Section 4.2 covers the flexibility potential of predictive rule-based control in the specific context of Norway. The required modeling complexity for the heat pump system in building performance simulation is presented in Section 4.3. Chapter 5 outlines the main conclusions and gives recommendations for future research.

1.4 List of publications

Three journal papers and five conference papers build the foundation of this PhD thesis. An overview of the papers is presented in Figure 1-2. It is here distinguished between *primary papers* and *supporting papers*, where the primary papers address the main research questions, and the *supporting papers* present preparative work for the primary papers. The papers that are included in this thesis are presented in the following together with my contribution to each of the papers:

Primary papers:

Paper 1:

Clauß J, Stinner S, Solli C, Lindberg K B, Madsen H, Georges L. A generic methodology to evaluate hourly average $CO_{2eq.}$ intensities of the electricity mix to deploy the energy flexibility potential of Norwegian buildings. *Proceedings of the 10th International Conference on System Simulation in Buildings*, Liege, Belgium, pp. 1-19, 2018.

Contribution: The conceptualization was done together with Laurent Georges. I collected the data. Structuring the data and the development of the methodology was done in collaboration with Christian Solli. The results were analyzed and visualized together with Sebastian Stinner. I wrote the majority of the paper draft. Revision and editing were done in collaboration with all co-authors.

Paper 2:

Clauß J, Stinner S, Solli C, Lindberg KB, Madsen H, Georges L. Evaluation Method for the Hourly Average $CO_{2eq.}$ Intensity of the Electricity Mix and Its Application to the Demand Response of Residential Heating. *Energies*. 2019; 12(7):1345.

Contribution: This paper is based on Paper 1, which is extended by a case study. Regarding the extended part, I developed the building simulation model, implemented the control, run the simulations, analyzed the data, visualized the results and wrote the original draft of the article. Conceptualization and methodology were done in collaboration with Laurent Georges.

Paper 3:

Clauß J, Stinner S, Sartori I, Georges L. Predictive rule-based control to activate the energy flexibility of Norwegian residential buildings: Case of an air-source heat pump and direct electric heating. *Applied Energy*. 2019; 237:500–18.

Contribution: Conceptualization was done in collaboration with Laurent Georges. I implemented the different building models and control strategies into IDA ICE. The detailed modeling and control of the heat pump system in IDA ICE was done in collaboration with Laurent Georges. The data analysis was done together with Sebastian Stinner. Evaluation of the results was done together with Sebastian

Stinner and Laurent Georges. I wrote the initial draft of the paper. Revision and editing were done in collaboration with all co-authors.

Paper 4:

Johnsen T, Taksdal K, Clauß J, Yu X, Georges L. Influence of thermal zoning and electric radiator control on the energy flexibility potential of Norwegian detached houses. *Accepted at CLIMA 2019 Conference*, 2019.

Contribution: This paper originates from a Master thesis. Most of the research methodology originates from my PhD work, I supervised the students and contributed to the paper revision and editing.

Paper 5:

Clauß J, Georges L. Model complexity of heat pump systems to investigate the building energy flexibility and guidelines for model implementation. *Revised version submitted to Applied Energy,* 2019.

Contribution: I did the conception and design of the paper together with Laurent Georges. I wrote the initial draft of the paper. Editing and revision was done in collaboration with Laurent Georges.

Paper 6:

Clauß J, Finck C, Vogler-Finck P, Beagon P. Control strategies for building energy systems to unlock demand side flexibility – A review. *Proceedings of the 15th IBPSA Conference*, San Francisco, USA, pp. 1750-1759, 2017.

Contribution: The idea for this paper came from a collaboration on an IEA EBC Annex 67 report. The conceptualization and structure of the paper was done in collaboration with the three co-authors. I wrote the initial draft of the paper. Editing and revision was done in collaboration with the three co-authors.

Supporting papers:

Paper 7:

Clauß J, Vogler-Finck P, Georges L. Calibration of a High-Resolution Dynamic Model for Detailed Investigation of the Energy Flexibility of a Zero Emission Residential Building. *Springer Proceedings in Energy "Cold Climate HVAC Conference 2018"*, Kiruna, Sweden, pp. 725-736, 2018.

Contribution: The conceptualization was done in collaboration with Laurent Georges. I calibrated and validated the IDA ICE model of the case study building. The dedicated experiments were done in collaboration with Pierre Vogler-Finck. I wrote the initial draft. Editing and revision of the article was done in collaboration with both co-authors.

Paper 8:

Clauß J, Sartori I, Alonso M J, Thalfeldt M, Georges L. Investigations of different control strategies for heat pump systems in a residential nZEB in the Nordic climate. *Proceedings of the 12th IEA Heat Pump Conference*, Rotterdam, Netherlands, 2017.

Contribution: I did the conceptualization together with Laurent Georges. I developed the building model in IDA ICE, implemented the control strategies together with Martin Thalfeldt, analyzed the data and wrote the initial draft of the paper. Editing and revising were done in collaboration with the co-authors.

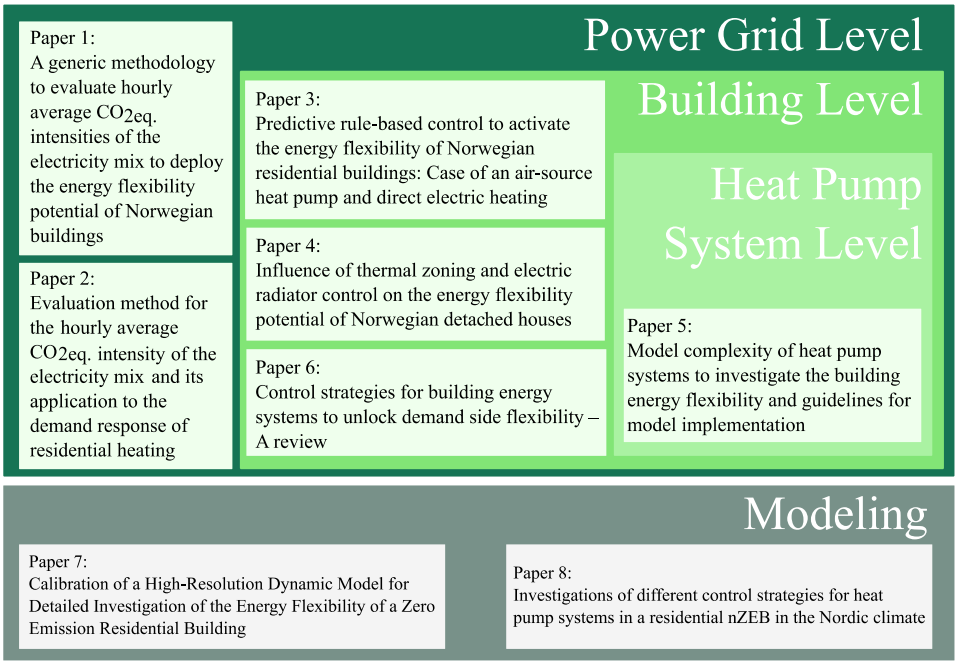

Figure 1-2. *Overview of the publications considered in this thesis.*

The causal connections of all the papers included in this PhD thesis are illustrated in Figure 1-3. The Journal papers are marked with bold lines.

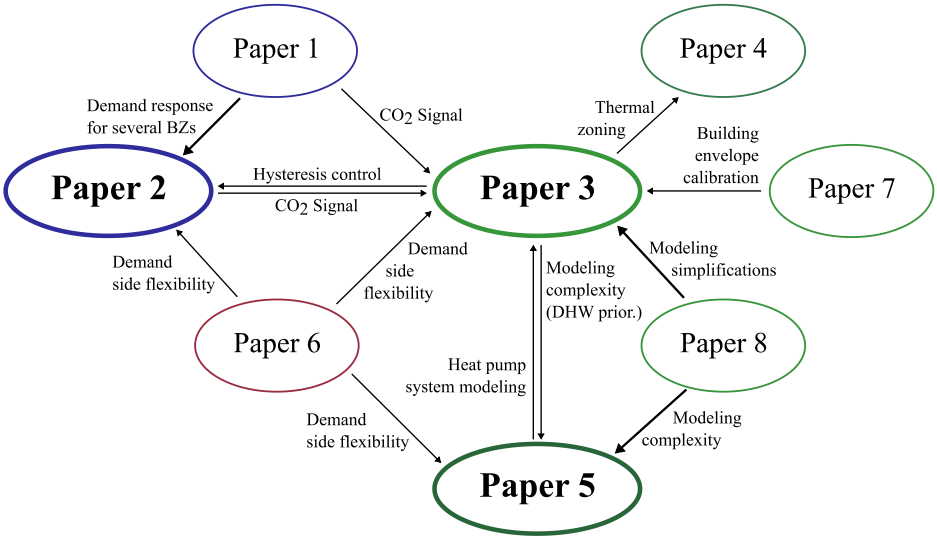

Figure 1-3. *Causal connection of the papers included in this thesis.*

Additional publications

Student supervision, national and international collaborations and my activity in international IEA Annexes lead to further publications:

Conference contributions:

Vogler-Finck P, Clauß J, Georges L, Sartori I. Wisniewski R. Inverse Model Identification of the Thermal Dynamics of a Norwegian Zero Emission House. *Springer Proceedings in Energy "Cold Climate HVAC Conference 2018"*, Kiruna, Sweden, pp. 533-543, 2018. [23]

Solli C, Clauß J., Korpås M. Combining energy use profiles and time dependent import-export corrected GWP-factors for deeper understanding of an organizations' energy use' contribution to the carbon footprint. *ISCN 2018*, Stockholm, Sweden, 2018.

Backe S, Sørensen Å L, Pinel D, Clauß J, Lausselet C. Opportunities for Local Energy Supply in Norway: A Case Study of a University Campus Site. *Submitted to the 1st Nordic Conference on Zero Emission and Plus Energy Buildings,* Trondheim, Norway, 2019.

Contributions to IEA Annex reports:

Finck C, Beagon P, Clauß J, Péan T, Vogler-Finck P, Zhang K, Kazmi H. Review of applied and tested control possibilities for energy flexibility in buildings. *Technical Report* from IEA EBC Annex 67 Energy Flexible Buildings, 2018. [24]

Santos A Q, Jørgensen B N. *IEA EBC Annex 67 report Control strategies and algorithms for obtaining energy flexibility in buildings*. 2019. My contribution: Clauß J. Predictive rule-based control to perform heating demand response in Norwegian residential buildings.

Jensen S Ø, Parker J, Engelmann P, Marszal-Pomianowska A J. *IEA EBC Annex 67 report Examples of Energy Flexibility in buildings*. 2019. My contribution: Clauß J. Predictive rule-based control to perform heating demand response in Norwegian residential buildings.

Master thesis supervision:

Johnsen T and Taksdal K. *Energy flexibility characterization of Norwegian residential buildings heated by direct electricity*. Master thesis, Norwegian University of Science and Technology, 2018.

Nickl C H. *Influence of the space heating distribution system on the energy flexibility of Norwegian residential buildings*. Master thesis, Norwegian University of Science and Technology, 2018.

Other contributions:

Backe S, Sørensen Å L, Pinel D, Clauß J, Lausselet C, Woods R. *Consequences of local energy supply in Norway – A case study on ZEN pilot Campus Evenstad.* ZEN Report, 2019.

Vogler-Finck P, Clauß J, Georges L. A dataset to support dynamical modelling of the thermal dynamics of a super-insulated building. *Zenodo*. 2017. [25]

2 RESEARCH CONTEXT AND BACKGROUND

This chapter provides information on energy-flexible buildings in Section 2.1. Typical approaches for heating demand response and an introduction to thermal zoning in residential buildings are given in Section 2.2. Furthermore, Section 2.3 gives a brief introduction of methodologies used to evaluate time-varying $CO_{2eq.}$ intensities. Also, the evaluation method developed during this PhD work is briefly introduced. Section 2.4 briefly introduces the modeling complexity of heat pump systems to study the heating demand response of residential buildings.

2.1 Energy flexible buildings

A comprehensive definition of energy flexibility is hard to obtain, since researchers with different academic backgrounds may have different objectives when investigating energy flexibility. In a literature review by Lopes et al. [26] several definitions of "flexibility" and methodologies used to quantify the energy flexibility in buildings have been proposed. In general, an energy-flexible building is a building that can react to an external signal that it receives from outside the building. Three rather general definitions are presented in the following:

- Energy flexibility can be seen as the ***ability*** to manage a building's demand and generation according to local climate conditions, user needs and grid requirements [27].
- It can also be understood as a building ***property***, if it is seen as the margin in which the building can be operated while respecting its functional requirements.
- Furthermore, energy flexibility can be regarded as a ***service*** which can be provided. In that sense, energy flexibility will allow for demand side management/load control and demand response based on the requirements of the surrounding grids.

It is difficult to dissociate the three definitions from each other, when it comes to the use of energy flexibility. In this thesis, energy flexibility is seen as a building *property* which is used to provide a *service*.

In general, a smart meter or a building management system that can receive signals from outside the building are required to make use of the building energy flexibility. Communication, sensing, and computing devices have become more affordable in recent years and open up new possibilities for improved controls for demand response. Furthermore, thermal energy storages are required to exploit the flexibility potential. In residential buildings, thermal storages are typically water storage tanks or the building thermal mass. These thermal storages can be activated, meaning that they temporarily get loaded to higher temperatures (in case of heating), which often leads to increased total energy use for heating, but at the same time total operational costs or total CO_2 emissions can be decreased, or a service to the grid can be provided depending on the control objective.

2.2 Current approaches for heating demand response

Demand response strategies can be applied to deploy the building energy flexibility and to target different control objectives. DR measures are implemented into control strategies, such as PRBC or more advanced controls, e.g., optimal control or MPC. PRBCs rely on a set of pre-defined rules to control the energy system, where temperature set-points for space heating or domestic hot water heating are usually varied to start or delay the operation of the heating system depending on the control signal. These pre-defined rules are rather straightforward to implement into dynamic building simulation tools, but careful design of the control rules is necessary. MPC solves an optimization problem but is more expensive to develop, for instance, the identification of a model used for control is acknowledged as the most critical part in the design of an MPC [22,28]. PRBCs can be a decent compromise to advanced controls because PRBC is simpler, but can still be effective to reduce operational costs or to save carbon emissions [22]. Furthermore, as PRBCs can deal with time-varying operating conditions and can interact with the energy system and the grid [29], they have a potential to contribute to peak shaving and load shifting of the electricity consumption [30].

Even though it is a promising measure, MPC is out of the scope of this thesis, and the sole focus is on PRBC to perform heating demand response.

Commonly used penalty signals for DR are:

- the electricity spot price [31–34],
- the $CO_{2eq.}$ intensity of the electricity mix [35–39],
- the share of renewables in the electricity mix [19,40],
- or voltage fluctuations [41].

Depending on the decision criteria of the RBC (e.g., weather, price, occupancy, $CO_{2eq.}$ intensity), RBC typically aims at activating the energy flexibility of the building to improve (one of) the following objectives:

- *Load shifting:* Regular daily peak periods can usually be identified in a national energy grid. The controller aims to avoid or force the operation of the systems during fixed hours. Fixed scheduling strategies are simple and easy to implement, but they cannot adapt to changing conditions in the daily profile of the grid.
- *Peak shaving:* It is aimed at a reduction of the demand peak to support the grid. For this purpose, the power exchange of a building with the grid is monitored, and thresholds are defined for the import and export of power [34,42].
- *Reducing the energy costs for the end-users:* This objective relies on time-varying energy prices. The energy system aims to operate at low-price periods. Here, it is important to identify proper low-price and high-price thresholds [33].
- *Improving the energy use from renewable energy sources:* At single-building scale, an increased self-consumption leads to increased use of on-site generated

electricity [43] whereas, at the scale of the power grid, the residual load at a national level or bidding zone level is of interest.

Numerous studies have been already conducted on building energy flexibility with focus on the heating system [21,33,35,36,44–46]. In these studies, heat pump systems play a major role, and the electrification of heating using heat pumps in combination with thermal energy storage has been recognized as a promising measure for increasing the flexibility potential [13,47]. This potential for a heat pump system is dependent on the type of buildings, the type of heat pump and thermal storage, as well as, the applied control strategy [22].

An overview of control strategies that aim at deploying the building energy flexibility is provided in Paper 6 of this thesis.

Several relevant studies confirmed that PRBC can decrease the energy costs for the building operation [31,32,34]. In order to define the PRBC rules, Georges et al. [48] introduced a lower and upper price threshold so that energy is stored during low-price periods and energy use is lowered during high-price periods. Alimohammadisagvand et al. [31] successfully implemented a price-based PRBC to control the thermal energy storage of a residential building heated by a ground source heat pump. Fischer et al. [49] used PRBC for scheduling the heat pump operation depending on predictions of the electricity price, PV generation and thermal loads of the building. Here, the heat pump was run either at times of high PV generation to maximize the PV self-consumption or at times of minimum electricity prices to charge the storage tank of the heat pump system. Dar et al. [34] investigated the energy flexibility of a Net-ZEB heated by an air-source heat pump. They concluded that the peak power could be reduced significantly with a well-tuned RBC.

In this thesis, the demand response scenarios are based on different penalty signals. Predictive rule-based controls are implemented into the building performance simulation tool IDA ICE to investigate demand response scenarios based on the predicted electricity spot price, the predicted $CO_{2eq.}$ intensity of the electricity mix or a simple schedule. TSPs for DHW heating and SH are varied depending on the signal. The reference scenario maintains constant TSPs for SH (21°C) and DHW heating (50°C). These TSPs are varied for the DR strategies. The DHW TSP can be increased by 10K or decreased by 5K depending on the current value of the penalty signal. Regarding SH, the TSPs are increased by 3K or decreased by 1K. A detailed description of the specific PRBC mechanisms is provided in Section 3.2.

Regarding the influence of thermal zoning on the energy flexibility potential of residential buildings, this problem has been addressed in a very limited number of studies only [21,50,51], whereas most studies assume the same indoor temperature in all the rooms of the building, including bedrooms. Nevertheless, it has been proven that many Norwegians like cold bedrooms (< 16 °C) and may open windows for several hours a day to reach the desired bedroom temperature [52]. The risk of

flushing the heat stored in bedrooms is more important with increasing insulation levels. It is thus important to determine how the thermal mass activation using PRBC influences bedroom temperatures.

2.3 Evaluating the hourly average $CO_{2eq.}$ intensity

The operation of a heating system can be shifted to times of low $CO_{2eq.}$ intensity in the grid mix using thermal storage if the carbon intensity is applied as a penalty signal for control. In general, the $CO_{2eq.}$ intensity can be used as an indicator of the share of renewable energies in the electricity mix. In Norway, electricity is mostly generated from hydropower. However, increased interaction between the continental European and the Norwegian power grids is expected in the future [47].

As Norway has a very limited number of fossil fuel power plants for electricity generation, the hourly average $CO_{2eq.}$ intensity of the electricity mix already strongly depends on the electricity exchanges with neighboring bidding zones (BZ). Generally, the CO_2 price is seen as an essential driver for the transition to a low-carbon society [47]. This CO_2 price is expected to increase in the future so that the application of a $CO_{2eq.}$ intensity signal for control purposes is likely to gain importance. Compared to the electricity spot price, the use of the $CO_{2eq.}$ intensity of the electricity mix as a penalty signal is not as common because this penalty signal is not readily available.

The European power grid is highly interconnected. In order to avoid bottlenecks in the transmission system, BZs are created with different electricity prices. One country can have several BZs [53]. Norway consists of five BZs, each of them having physical connections to neighboring BZs that enables electricity imports and exports (Figure 2-1).

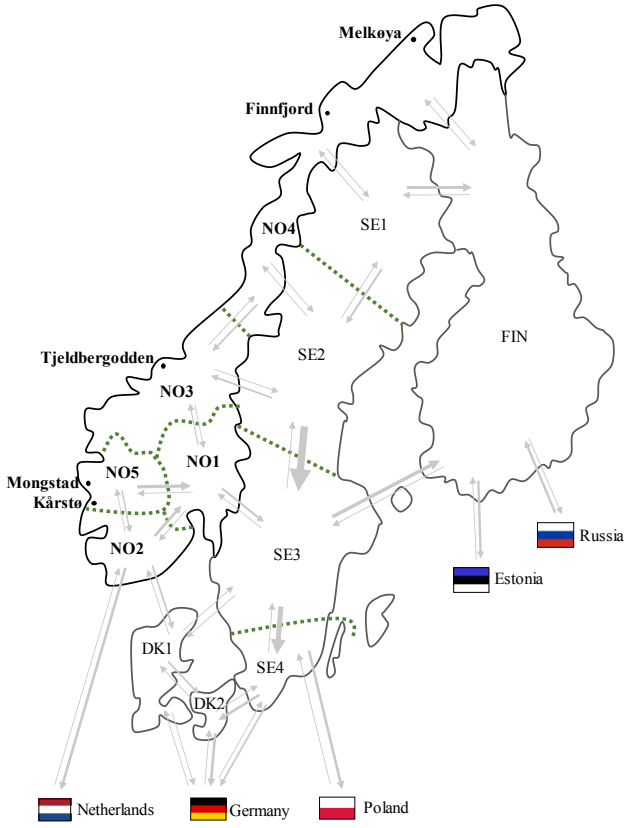

Figure 2-1. *Overview of the Scandinavian power market bidding zones, also including gas-fired power plants in Norway (adjusted from [47]).*

2.3.1 Review of existing evaluation methods for the $CO_{2eq.}$ intensity

Generally, evaluation methods for the hourly $CO_{2eq.}$ intensities of the electricity mix can be categorized as presented in Table 2-1. In a de-coupled approach, the electricity demand and supply sides do not influence each other. On the contrary, in a coupled approach, the interaction between the demand and supply sides is taken into account. For example, if a large number of buildings would apply the average $CO_{2eq.}$ intensity as a penalty signal, the resulting electric load could be affected, and thus the predicted generation would not be optimized for this load anymore. Ideally, a coupled approach should be used to take into account DR in the prediction of the electricity generation and the respective $CO_{2eq.}$ emissions [40,51]. Furthermore, average and marginal $CO_{2eq.}$ intensities are two distinct concepts. Marginal emissions are the emissions from one additional kWh generated/consumed and, consequently, it results from a single power plant. On the contrary, the average $CO_{2eq.}$ intensity is the $CO_{2eq.}$/kWh emitted on average from the entire electricity generation of the BZ. It thus results from a mix of power plants. On the one hand, it could be argued that the marginal $CO_{2eq.}$ intensity is most coherent for the control of a limited number of buildings

because they will rather affect a single plant than the overall production. On the other hand, average $CO_{2eq.}$ intensities (or factors) have been used extensively in the past for buildings exporting electricity to the grid, e.g., Zero Emission Buildings or Nearly Zero Energy Buildings. Studies mostly focusing on the life-cycle assessment (LCA) of buildings often use average $CO_{2eq.}$ intensities rather than marginal intensities.

Table 2-1. *Categorization of methodologies to (a) evaluate $CO_{2eq.}$ intensities of the electricity mix (marked as "CO_2") or (b) determine the optimal dispatch and unit commitment in electricity grids (marked as "EL").*

De-coupled approach		**Coupled approach**	
Average	Marginal	Average	Marginal
Energinet [54] *(CO_2)*	Bettle et al. [58] *(CO_2)*	Graabak [61] *(CO_2)*	Patteeuw et al. [40] *(EL)*
Vandermeulen et al. [19] *(CO_2)*	Hawkes [59] *(CO_2)*		Arteconi et al. (based on Patteeuw) [51] *(EL)*
Milovanoff et al. [55] *(CO_2)*	Peán et al. (based on Hawkes) [38] *(CO_2)*		Graabak et al. [61] *(CO_2, EL)*
Roux et al. [56] *(CO_2)*	Corradi [60] *(CO_2)*		Askeland et al. [62] *(EL)*
Tomorrow [57] *(CO_2)*			Quoilin et al. [63] *(EL)*

A comprehensive description of the studies presented in Table 2-1 is provided in Paper 2 of this thesis.

2.3.2 Evaluation of the hourly average $CO_{2eq.}$ intensity

The literature review (references in Table 2-1) has shown that electricity trading between bidding zones is often simplified or fully neglected. Therefore, a methodology has been developed to calculate the hourly average $CO_{2eq.}$ intensity of the electricity mix in an interconnected power grid. The methodology is generic and takes into account the hourly average $CO_{2eq.}$ intensities of the electricity traded between neighboring BZs (imports and exports). The proposed method resorts to the logic of multi-regional input-output models (MRIO) [64]. In MRIO models, interdependencies within the whole system can be captured, while preserving regional differences [65]. Input-output models are usually used to perform energy system modeling in combination with an economic analysis considering different industry sectors [66–68]. The logic is based on the assumption that there always is a balance between consumption and generation for the whole system. In the present work, this logic can be applied for electricity where BZs are used instead of industry sectors.

Both Paper 2 and Paper 1 describe in detail the methodology to evaluate the hourly average $CO_{2eq.}$ intensity of the electricity mix. On top of that, Paper 1 studies the average $CO_{2eq.}$ intensity in Norway as a function of (a) the electricity use in a BZ, (b) the electricity spot price, (c) the electricity import from foreign countries and (d) the filling level of the water reservoirs. Paper 2 investigates how the characteristics of the $CO_{2eq.}$ intensity used as a control signal influence the overall emission savings. This

is done using the case study of residential heating where DR is performed using the $CO_{2eq.}$ intensity of six Scandinavian BZs.

Regarding the proposed methodology, input data about the hourly electricity generation per generation technology is retrieved from ENTSO-E. Information on the CO_2 factors of an electricity generation technology is based on Ecoinvent. Comparing the CO_2 factors from Ecoinvent and the IPCC report, it is noticed that they are significantly different depending on the assumptions taken to evaluate these factors.

2.4 Modeling complexity

In general, the required modeling complexity of the heat pump system control depends on the objective of a respective study. For example, simplified models may be sufficient to analyze the annual energy use, whereas a more detailed model of a heat pump system is required if the physical behavior of the heat pump operation is of interest. In this thesis, *modeling complexity* of the heat pump system refers to the models for the water storage tank, the heat pump control, the auxiliary heater control and the heat pump system control. Madani et al. [69] address the question of the required model complexity for comprehensive heat pump systems with the aim to find the minimum required level of detail to capture the behavior of a real heat pump system with satisfying accuracy. They suggest a roadmap (see Figure 2-2) to find the necessary level of model complexity for the heat pump unit on the one hand, and the heat source on the other hand, based on the type of analysis to be carried out.

Existing studies on DR using mostly building performance simulation (BPS) typically combine one or several of the following simplifications for the modeling of the heat pump system:

(1) The heat pump modulates perfectly between 0 and 100%, or is on/off.
(2) Minimum duration and pause times in the heat pump cycle are not considered.
(3) The water storage tank is simplified by either neglecting thermal stratification or the tank has a perfect stratification at all times. This is especially important for studies that consider SH and a DHW tank.
(4) DHW prioritization over SH is not considered.
(5) The heat pump delivers any required temperature.
(6) The control strategy of the auxiliary heater(s) is idealized.

An extended review is provided in Paper 5 of this PhD thesis. Ideally, knowledge about the short-time dynamics of heat pump systems is considered when DR measures for heating are performed to study the energy flexibility potential of these systems. These short-time dynamics depend to a great extent on the tuning of the heat pump controller, which usually is a proportional-integral (PI) controller. The controller tuning is often overlooked in studies regarding DR and energy flexibility using BPS and cannot be captured in detail by strongly simplified models for heat pump systems. Regarding these DR applications, the specific level of modeling

complexity of the heat pump (system) control has not yet been addressed in the literature.

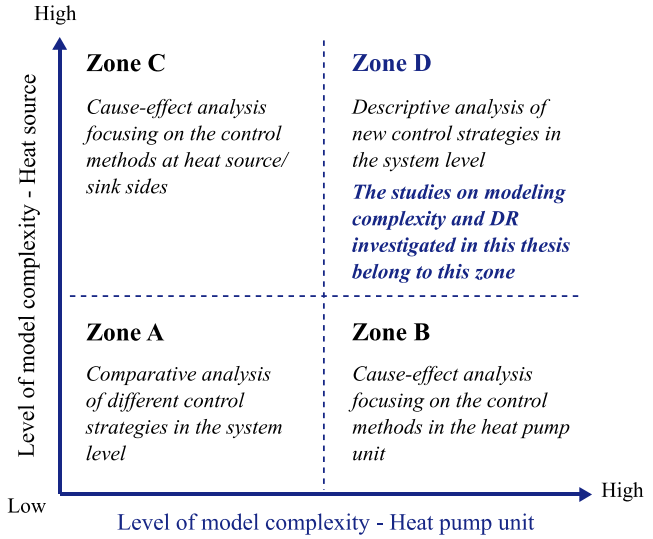

Figure 2-2. *Roadmap for required model complexity depending on the type of study (adapted from [69]: the work carried out in this thesis ranks among Zone D).*

The responsiveness of the heat pump to an external penalty signal for DR influences the short-time behavior of the heat pump system. Therefore, it is essential to carefully consider the heat pump characteristics when developing the respective component models of the heat pump system and its control.

The importance of heat pump sizing is addressed in several studies, e.g. [69–71]. For a monovalent heat pump system, the heat pump is sized to fully cover the heating demands of the building, even during very low outdoor temperatures. As these conditions occur only for very limited parts of the year, the heat pump behavior in part load should be considered carefully. The use of inverter-driven heat pumps offers the possibility to modulate the heat pump capacity also to meet the heating loads required by the building [72] during periods with higher outdoor temperatures and thus lower building heating demands. On the contrary, for a bivalent heat pump system, the heat pump covers the heating load above the so-called bivalent temperature, whereas below this temperature the auxiliary heater covers heating demands. Therefore, it can be chosen to size the heat pump so that it covers only a fraction of the peak heat demand of the building.

Other system characteristics that are of interest are cycling losses, an improved performance during part load operation for modulating heat pumps, and controller tuning. Cycling losses occur during the start-up of each cycle because the compressor has to re-establish the pressure difference between the evaporator and the condenser and thus the heating capacity of the heat pump unit is lower until steady-state

conditions are reached [73]. Several studies found that performance is improved for modulating heat pumps compared to on-off heat pumps [70,73,74]. Dongellini et al. [73] found that the maximum efficiency of the heat pump is obtained for frequencies between 40 Hz and 60 Hz, where the COP increases up to 20% by scaling from the nominal frequency (120 Hz) to 50 Hz, depending on the outdoor air temperature. Bagarella et al. [71]. point out that the tuning of the controller parameters (gain parameter k and integral time T_i) is important for the reactivity of the controller, which determines how fast the controller reacts to a variation in the controlled variable. A very reactive controller usually oscillates until it reaches the required compressor frequency that satisfies the heat load. If the controller is less reactive, it has less or even no oscillations and is thus more stable, but it takes more time for the heat pump to match the required heating load.

Paper 5 of this thesis addresses two questions. Firstly, it investigates the model complexity of the heat pump system control required to study the behavior of heat pump systems in detail, with a special focus on DR. More specifically, the controller for the heat pump unit and the influence of the DHW prioritization on the auxiliary heater operation during DR is analyzed. Secondly, the paper documents in a generic way how to implement temperature-based control of heat pump systems into a BPS tool to investigate DR. A case study of a residential building is chosen to present the implementation approach and to investigate the effect of modeling complexity based on a residential air-source heat pump system. A complex model for the heat pump control has been simplified step-by-step to see the influence on the chosen key performance indicators (KPIs), such as energy use, average tank temperatures, number of heat pump cycles per year and average heat pump run time. Paper 5 aims at answering how the complexity of the model for the heat pump system control affects the previously mentioned KPIs and how it affects the short-time behavior of a heat pump system when performing DR.

3 BUILDING MODEL AND HEATING DEMAND RESPONSE

This chapter explains briefly the building model implemented in IDA ICE, together with the configuration of the energy system and its control. Furthermore, the studied demand response scenarios are summarized.

3.1 Building model

The same building model has been used in all Papers of this thesis, except for Paper 4. The case study building is a Living Lab, which is a Norwegian residential zero emission building with a heated floor area of 105 m² located on the Gløshaugen campus in Trondheim (Norway) [75]. The building floor plan is shown in Figure 3-1. The on-site electricity generation from the photovoltaic panels is designed to compensate for the building CO_{2eq} emissions from the operational phase as well as for embodied emissions over the lifetime of the building. The building has a highly-insulated envelope and lightweight timber construction as well as energy efficient windows with low emissivity. Furthermore, it contains 90 m^2 of phase change material in the roof construction in order to limit the peak indoor temperatures. The Living Laboratory consists of five heated zones: two bedrooms, a bathroom, a living room north and one large room combining a kitchen and a living room south.

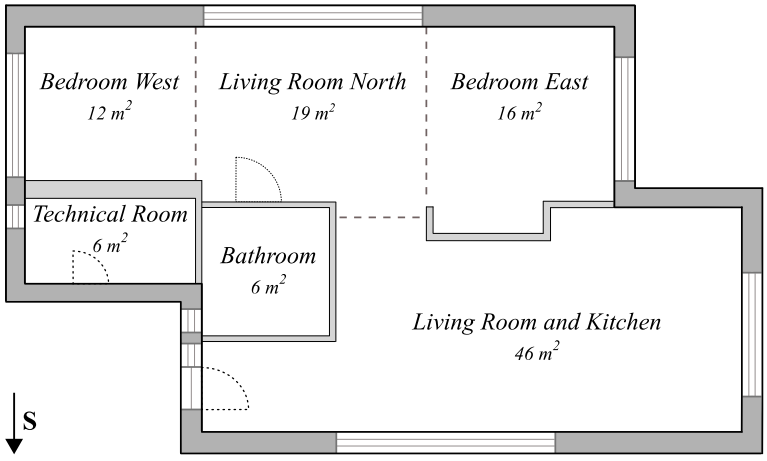

Figure 3-1. *Floor plan of the studied building.*

A detailed multi-zone model of the Living Lab has been created using the software IDA ICE version 4.8. IDA ICE is a dynamic building simulation software which applies equation-based modeling [76]. It allows investigation of the detailed dynamics of the components of the energy supply system and enables the user to evaluate the indoor climate as well as the energy use of a building.

3.1.1 Building envelope model

The model of the building envelope has been calibrated and validated using dedicated experiments (February 2017 to May 2017), where the building was heated by an electric radiator. Knowing the short-term thermal dynamics of the building envelope as a response to time-varying space heating temperature set-points is of importance for active demand response measures as well as for the development of resulting control strategies for heat pumps. It has been found that the model is reliable for predicting the temperature trend for cases with intermittent heating and closed internal doors. The model is also reliable for predicting the thermal dynamics of the building if bedroom doors are opened. A comprehensive description of the calibration is presented in Paper 7.

3.1.2 Configuration of the energy system

Three different heating systems have been considered across the case studies: a modulating air-source heat pump, an on-off air-source heat pump, and direct electric heating. The ASHPs are connected to a water storage tank used for both SH and DHW. For the ZEB insulation level, the heat pump is assisted by 4 m² of solar thermal collectors which is in line with the most common concepts of Norwegian ZEB [77]. With the ASHP, the SH distribution is performed using floor heating (FH). The peak and back-up heating are done by electric resistances. The layout of the heat pump system is presented in Figure 3-2. For the case of direct electric heating, electric radiators supply SH, and a resistance heater inside the storage tank is used for DHW heating. A comprehensive description of the system is presented in Paper 3.

Water storage tank

IDA ICE has a one-dimensional model of a stratified tank that accounts for the heat conduction and convection effects in the tank. The storage tank is divided into ten horizontal layers: the DHW part consists of the four upper layers and the SH part of the six lower layers. The DHW and SH buffer tanks are dimensioned based on [78].

Heat pump

The heat pump is sized according to “bivalence point” principle and is working in bivalent mono-energetic mode at low outdoor temperatures [79]. On/off auxiliary heaters are installed at the upper layers of the SH and DHW parts of the tank to ensure that the required water distribution temperatures are always met. The auxiliary heater in the DHW tank has a capacity of 3 kW, whereas the auxiliary heater for the SH tank has a capacity of 9 kW [80]. The heat pump model is calibrated with manufacturer data for full load operation based on the procedure recommended by Niemelä [81].

For this work, the default heat pump model in IDA ICE (called ESBO plant) has been extended to account for additional physical phenomena. First, the heat pump modulates continuously between 30% and 100% of the nominal compressor capacity while it cycles on-off below 30%. Second, a minimum run and pause time has been

implemented (here taken at 10 minutes) in order to prevent on-off cycling from occurring too frequently. Third, a realistic prioritization of the DHW over the SH production is implemented so that the heat pump cannot support SH when producing DHW. All these three actions require supplementing an anti-windup to the PI control in order to prevent the saturation of the integral action. The implementation of these phenomena is presented in Paper 5.

Furthermore, it is worth mentioning that the DHW prioritization and the minimum run and stop times may lead to the violation of the temperature set-points for SH. Then, auxiliary heaters have to operate.

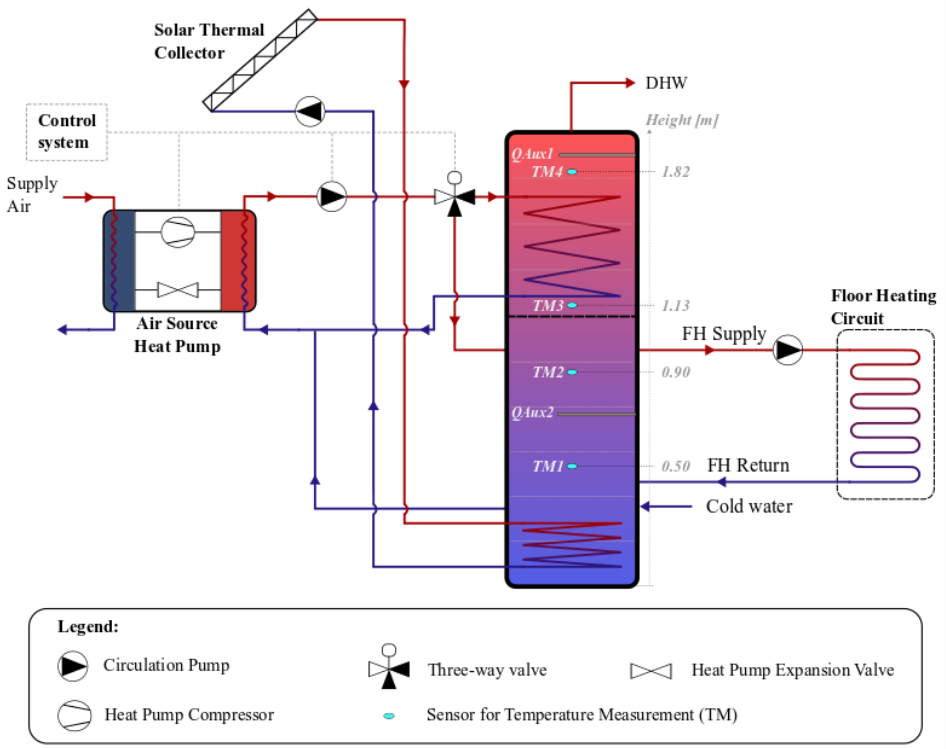

Figure 3-2. *Configuration of the heating system in the ZEB.*

Regarding DHW, the heat pump is first operated at full load, and the mass flow through the circulation pump is adjusted by a P-controller in order to meet a given temperature set-point at the outlet of the condenser. As soon as the circulation pump runs at full speed, the heat pump compressor speed is adjusted. The heat pump is connected to the DHW tank through a heat exchanger. Then, the maximum supply temperature of the heat pump is slightly higher than the temperature set-point in the DHW storage tank.

Direct electric heating

Direct electric heating is the most common SH system in Norwegian residential buildings [82]. For the case of direct electric heating for both, DHW and SH, an electric resistance heater with a power of 3 kW is used for DHW heating whereas electric radiators are used for SH. One electric radiator is placed in each room with a power equal to the nominal SH power of the room.

Temperature-based heat pump control

A hysteresis control based on measured water temperatures in the tank is used for DHW heating as well as for heating the SH tank. There are four temperature sensors in the water tank. Each part of the tank (i.e., the DHW and SH parts) has two sensors to control their charging according to a hysteresis. With a bivalent heat pump system, the control of the auxiliary heaters should be clearly defined as the auxiliary heater operation can have a strong impact on the total electricity use for heating [43,83,84]. The temperature set-points of both electric auxiliary heaters are set 3K below the start temperature of the heat pump. In that way, the heat pump is started when the temperature drops below a certain threshold. If the heat pump cannot cover the heat demand and the tank temperature continues to decrease, the auxiliary heater eventually starts. The auxiliary heaters are controlled by a thermostat with a differential of 4K.

3.1.3 Boundary conditions

Internal heat gains from electrical appliances, occupants, and lighting are according to Norwegian technical standard, SN/TS 3031:2016 [85]. Schedules for electrical appliances are based on SN/TS 3031:2016, whereas the schedules for occupancy and lighting are taken from prEN16798-1 and ISO/FDIS 17772-1 standards [86,87]. The daily profile for DHW consumption is taken from SN/TS 3031:2016 [85]. All profiles have an hourly resolution and are applied for every day of the year.

Using the Predicted Mean Vote (PMV) method, indoor operative temperature set-points can be defined depending on the activity and clothing level of the occupants [88]. With thermal activation by SH, indoor operative temperatures can be varied between 20°C and 24°C. When thermal zoning is investigated, a temperature set-point of 16°C is used in bedrooms to account for the temperature preferences of Norwegians.

Hourly weather data is taken from [89]. Hourly electricity spot prices are provided by NordPool [90], whereas the hourly average $CO_{2eq.}$ intensity is determined according to the methodology proposed in Paper 1 and Paper 2. Weather data, spot prices, and $CO_{2eq.}$ intensity of the electricity mix in NO3 are correlated so that historical data from 2015 for the city of Trondheim is applied.

3.2 Demand response scenarios

Predictive rule-based controls are implemented into IDA ICE to investigate demand response scenarios based on the predicted electricity spot price, the predicted $CO_{2eq.}$ intensity of the electricity mix or a simple schedule. Temperature set-points for DHW heating and SH are varied depending on the signal. Temperature set-points that are related to DHW heating are the start and stop temperatures of the hysteresis, as well as the supply temperature of the heat pump. Temperature set-points that are related to SH are the room temperature, the start and stop temperatures of the hysteresis as well as the FH supply temperature. The DR strategies are briefly described in the following:

- **Price-based DR:** Electricity prices vary throughout a day so that energy costs could be reduced if the heating system is operated outside high-price periods. The control aims at reducing overall heating costs.
- **CO_2-based DR:** The $CO_{2eq.}$ intensity of the electricity mix can be used to increase the consumption of electricity generated from non-fossil fuels. The control aims at decreasing overall $CO_{2eq.}$ emissions.
- Two different principles are introduced to determine the penalty signals for the price-based and CO_2-based DR strategies: Principle (a) is established to make use of the lowest spot prices or $CO_{2eq.}$ intensities, whereas Principle (b) aims at pre-heating the thermal energy storages in the hours before a maximum spot price or $CO_{2eq.}$ intensity occurs. Both principles are illustrated in Figure 3-3. Furthermore, a comprehensive description of both principles is provided in Paper 2 and Paper 3.
- **Schedule-based DR:** In the Norwegian electricity grid, a major concern regarding residential buildings is the maximum power and electricity use during peak hours. The temperature set-points are changed based on a schedule. Temperature set-points are increased three hours before a defined peak period and decreased during peak periods. Regarding load shifting, peak periods are defined to be between 7 a.m. and 10 a.m. as well as between 5 p.m. and 8 p.m. based on a typical hourly profile for the electricity use in Norwegian households [91]. Pre-peak and after-peak hours are defined as the three hours before and two hours after a respective peak period.

The reference scenario, termed BAU (for business as usual), maintains the constant TSPs for SH and DHW heating at 21°C and 50°C respectively. Using constant TSPs is the most common way to control the heating system in Norwegian residential buildings. These TSPs are varied for the DR strategies. The DHW TSP can be increased by 10K or decreased by 5K depending on the current value of the penalty signal. Regarding SH, the TSPs are increased by 3K or decreased by 1K.

The performance of the control with regards to emission savings is sensitive to the selection of thresholds, low-carbon threshold (LCT), and high-carbon threshold

(HCT). The influence of LCTs and HCTs on the number of hours per TSP has been evaluated for bidding zone NO3 in a sensitivity analysis in Paper 3. An LCT of 30% and an HCT of 70% have been chosen for calculating the penalty signal.

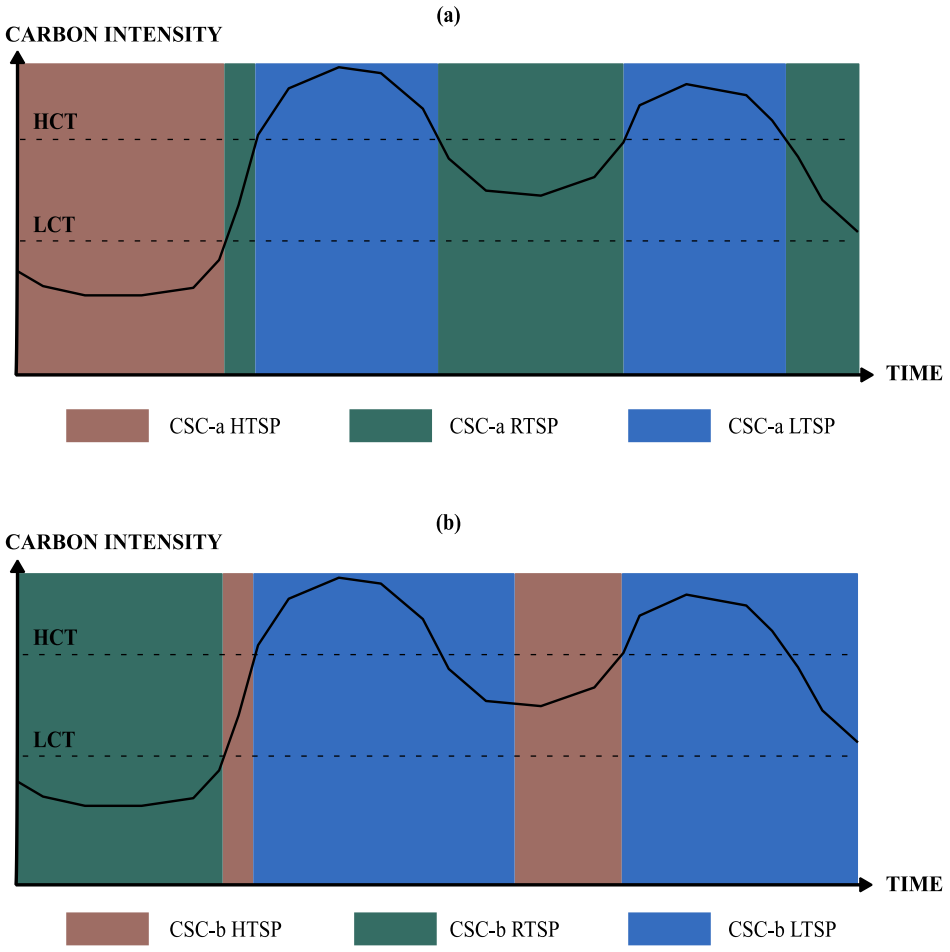

Figure 3-3. *Principle of the determination of the carbon-based control signal according to (a) CSC-a and (b) CSC-b (CSC-a is control strategy carbon based on principle a, CSC-b is control strategy carbon based on principle b, HTSP is high temperature set-points, RTSP is reference temperature set-points, LTSP is low temperature set-points).*

As an example, Figure 3-4 illustrates the working principle (b) for a modulating heat pump system controlled by a PRBC that aims at decreasing energy costs according to an hourly spot price signal. This indirect control increases the TSPs for DHW and SH just before high-price periods to charge the thermal storages and to avoid electricity use during high-price periods. Figure 3-4 shows that DHW heating is prioritized over SH because the TSP for DHW heating is increased as soon as the spot price signal allows it (Figure 3-4 (b)), whereas the SH-related TSPs are increased

after the DHW tank has been charged (Figure 3-4 (c)). Exemplary, this can be seen in the early afternoon on 19 February. A detailed description is provided in Paper 3.

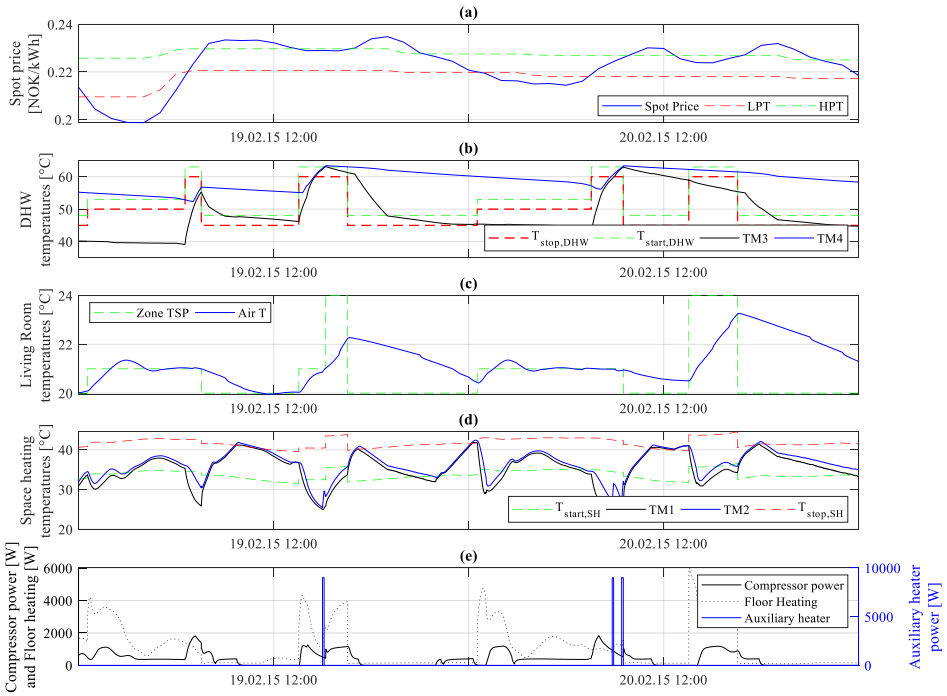

Figure 3-4. *Control principle of a price-based control for the modulating heat pump during an exemplary 48h period [18], where (a) shows the spot price, (b) shows the DHW temperatures and hysteresis set-points, (c) shows the measured air temperature and the temperature set-point for space heating in the Living Room, (d) shows the SH temperatures and hysteresis set-points in the SH tank and (e) shows the power of the compressor, the floor heating and the electric auxiliary heater (LPT and HPT are the low-price and high-price thresholds for the PRBC;* $T_{start,DHW}$ *and* $T_{stop,DHW}$ *are the start and stop temperatures for DHW heating; TM is temperature measurements in the water tank;* $T_{start,SH}$ *and* $T_{stop,SH}$ *are the start and stop temperatures for SH).*

4 RESULTS AND DISCUSSION

This chapter presents the key results of Papers 1 to 6 and answers the defined research questions.

Section 4.1 covers the results regarding the hourly average $CO_{2eq.}$ intensity of the electricity mix. Paper 1 and Paper 2 both introduce the methodology that has been developed to evaluate the hourly average $CO_{2eq.}$ intensity of the electricity mix in a bidding zone. Both papers address research question Q1, and on top of that Paper 1 focuses on research question Q1.1, while Paper 2 answers research question Q1.2.

Section 4.2 presents the results of Paper 3, 4 and 6 looking into the flexibility potential of PRBC in Norway. Furthermore, the influence of thermal zoning on the flexibility potential is investigated. Research questions Q2 to Q2.4 are answered.

Section 4.3 presents the results of Paper 5 focusing on the modeling complexity of the heat pump control model required to properly represent the operation of the heat pump system when performing heating demand response. Research questions Q3 and Q3.1 are answered.

4.1 $CO_{2eq.}$ intensities in Scandinavia (Paper 1 and 2)

The generic methodology for evaluating the average $CO_{2eq.}$ intensity of the electricity mix in a bidding zone also considers dynamic $CO_{2eq.}$ intensities of electricity imports from neighboring bidding zones. The method is based on the balance between *electricity production plus imports* and *electricity consumption plus exports*. The balance is satisfied for all BZs at each hour of the year. The methodology complies with the logic of a multi-regional input-output framework. Among possible applications, this $CO_{2eq.}$ intensity signal can be used to control the operation of a building HVAC system to reduce overall $CO_{2eq.}$ emissions.

Q 1: What are the characteristics of the hourly average $CO_{2eq.}$ intensity of the electricity mix in Scandinavian bidding zones?

The hourly average $CO_{2eq.}$ intensities for all Norwegian BZs are evaluated for the year 2015. Times series of the average $CO_{2eq.}$ intensities in the Norwegian bidding zones are plotted in Figure 4-1 (a). NO5 has the highest annual average $CO_{2eq.}$ intensity which is due to the electricity generation from the thermal power plant in Mongstad (see Figure 2-1 and Table 4-1).

Furthermore, it is obvious that the highest $CO_{2eq.}$ intensity peaks occur in NO2. Figure 4-1 (b) presents the average $CO_{2eq.}$ intensities for NO2, NO3, SE1, SE4, DK1, and FIN. It is clear that the Norwegian electricity mix has low average $CO_{2eq.}$ intensities compared to non-Norwegian BZs. Resulting from the large differences in $CO_{2eq.}$ intensity, the average $CO_{2eq.}$ intensity in NO2 usually increases when electricity is imported from DK1, which also explains the $CO_{2eq.}$ peaks in the BZ. A more detailed

analysis of the correlation of the average $CO_{2eq.}$ intensity and electricity imports to Norway is provided in Paper 1.

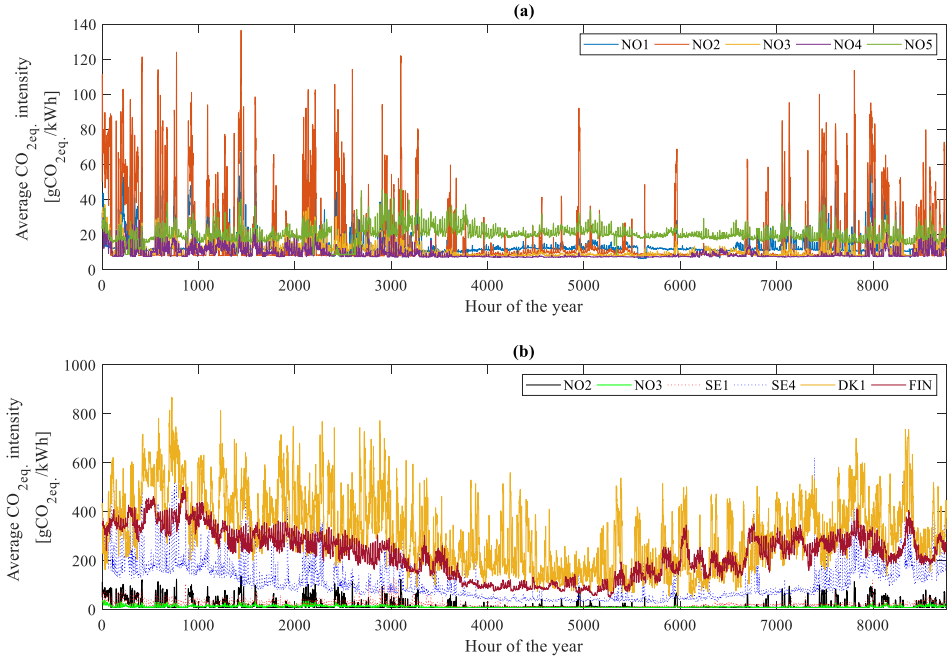

Figure 4-1. *Hourly average $CO_{2eq.}$ intensity of the electricity mix for (a) the Norwegian bidding zones and (b) for several Scandinavian bidding zones.*

An overview of the annual average $CO_{2eq.}$ intensities for several Scandinavian bidding zones is provided in Table 4-1. DK1 has the highest annual average $CO_{2eq.}$ intensities, followed by FIN and SE4. It can also be seen that electricity trading should be considered for the determination of the annual average $CO_{2eq.}$ intensity.

Table 4-1. *Comparison of the annual average $CO_{2eq.}$ intensities of the electricity mix for several Scandinavian bidding zones.*

BZ	NO1	NO2	NO3	NO4	NO5	SE1	SE4	DK1	FIN
Average $CO_{2eq.}$ intensity [$gCO_{2eq.}$/kWh]	15	17	11	9	20	21	114	316	227
Average $CO_{2eq.}$ intensity without imports [$gCO_{2eq.}$/kWh]	7	8	8	7	20	21	259	461	241

Paper 1 and 2 prove the importance of considering electricity imports and dynamic $CO_{2eq.}$ intensities of these imports when evaluating the average $CO_{2eq.}$ intensity of the

electricity mix of a BZ for the case of Norway. It is shown that high electricity demands, high spot prices, and low average $CO_{2eq.}$ intensities typically occur simultaneously. These correlations are specific to Norway, while in other countries with a higher share of thermal power plants, the correlations between electricity spot prices, electricity demands and average $CO_{2eq.}$ intensities of the electricity mix can be different.

Since the electricity generation in Norway is almost entirely from hydropower, the impact of imports of fossil fuel-based electricity on the average $CO_{2eq.}$ intensity is very strong. In other countries, for example, Finland or the Netherlands, the impact of fossil fuels on the average $CO_{2eq.}$ intensity is lower. Figure 4-2 illustrates the dependency of the average $CO_{2eq.}$ intensity on the electricity imports for four Scandinavian BZs: NO2, SE4, DK1, and FIN.

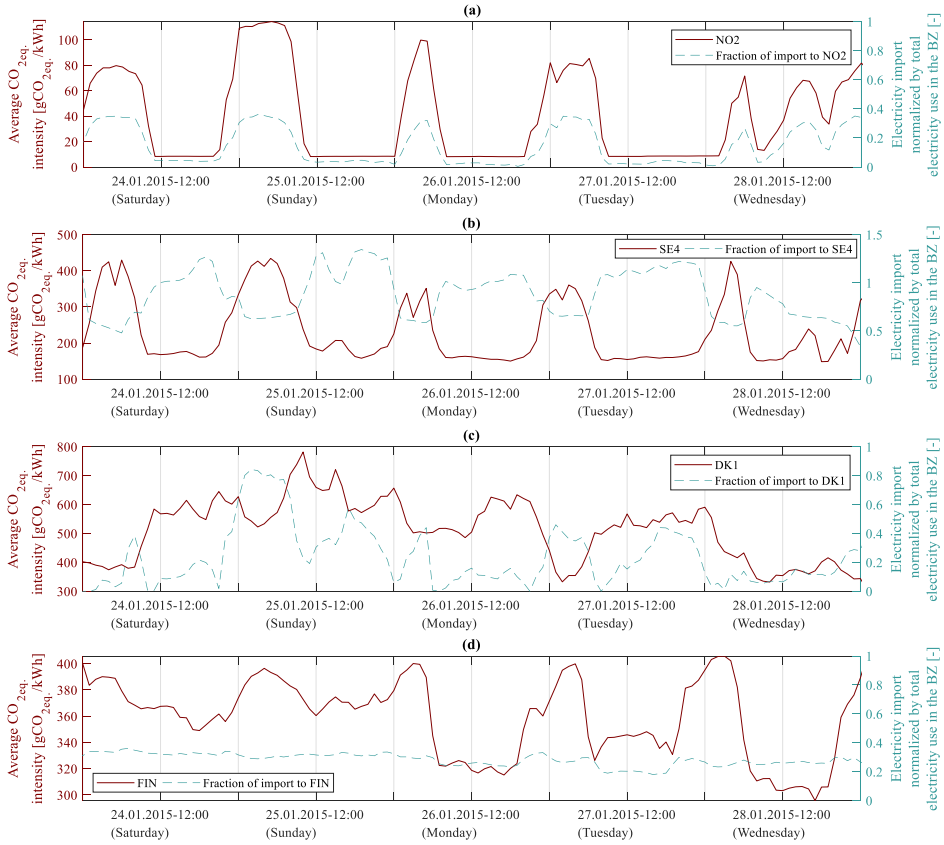

Figure 4-2. *Average $CO_{2eq.}$ intensity and fraction of imports on the total electricity use of a BZ for five exemplary days for four Scandinavian BZs: (a) NO2, (b) SE4, (c) DK1 and (d) FIN.*

It can be seen that the average $CO_{2eq.}$ intensity of NO2 systematically increases with an increasing share of imports in the electricity mix. On the contrary, the dependency

is the opposite in SE4. Every time there is a higher fraction of imports, the $CO_{2eq.}$ intensity decreases because electricity is mostly imported from SE3 which has a higher share of renewables in the grid.

Q 1.1: What are the characteristics of the hourly average $CO_{2eq.}$ intensity for the specific case of Norway?

Regarding the relation between the average $CO_{2eq.}$ intensity and the total electricity use for the Norwegian BZs, Figure 4-3 shows that the average $CO_{2eq.}$ intensity is low when the electricity use is high. In Norway, electricity is produced from hydropower in times of high demands. Therefore, the average $CO_{2eq.}$ intensities are typically low during peak load hours because flexible hydropower plants prefer to operate at high electricity prices (when also the electricity demand is high). Cheap electricity is usually bought from abroad during periods of low electricity use, while electricity generation using hydropower only starts during periods of higher electricity prices corresponding to periods with higher loads.

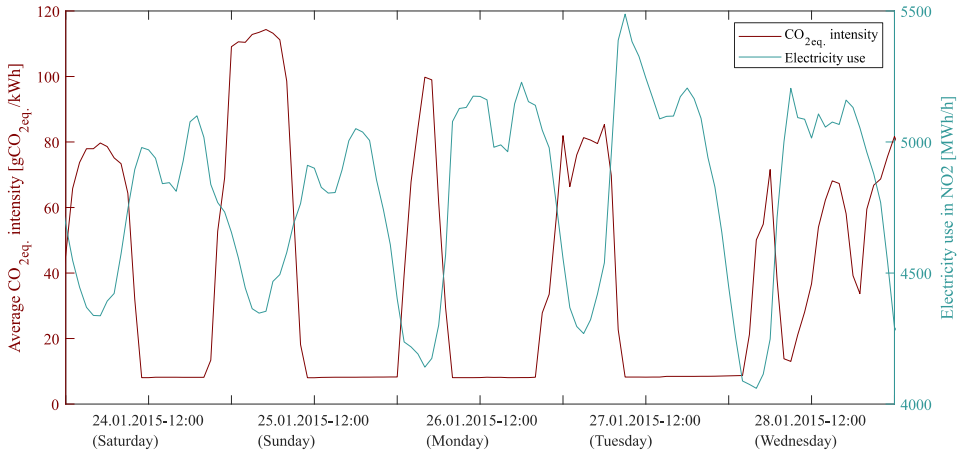

***Figure 4-3**. Average $CO_{2eq.}$ intensity and electricity use in NO2 for five exemplary days in January 2015.*

Average $CO_{2eq.}$ intensities in Norway are low during high-price hours. The $CO_{2eq.}$ intensity can increase significantly as soon as cheap electricity is imported from neighboring BZs because of a more carbon-intensive electricity generation outside Norway. Figure 4-4 presents the spot price in NO2 and the average $CO_{2eq.}$ intensities of all Norwegian BZs for five exemplary days in January 2015. As electricity is usually generated from hydropower during periods of high prices, the average $CO_{2eq.}$ intensity is low during these high-price periods typically leading to low $CO_{2eq.}$ intensities in the mornings and early evenings. The average $CO_{2eq.}$ intensity is usually high during night times due to electricity imports from the Netherlands and Denmark. This does not only affect the $CO_{2eq.}$ intensity of NO2, but subsequently impact the intensities of the other Norwegian BZs as a BZ can both import and export at the

same time. This shows that it can be important to consider imports from 2nd tier BZs in some cases.

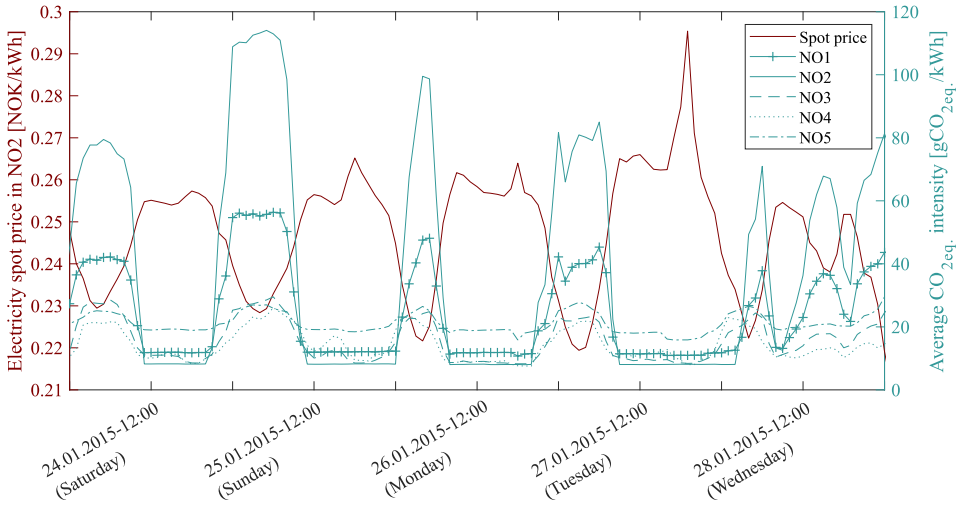

Figure 4-4. *Electricity spot price in NO2 and average $CO_{2eq.}$ intensity in all Norwegian BZs for five exemplary days in January 2015.*

It has to be mentioned that, in general, the management of the hydropower reservoirs is based on cost-optimal planning depending on (a) the expected future electricity price, (b) the expected precipitations and the resulting expected water level in reservoirs as well as (c) the expected future electricity demands. Within this optimization, the minimum water reservoir level is determined by national restrictions for waterways, while the maximum level that is possible without losing water and thus money is limited by the capacity of the reservoirs. Electricity imports to Norway are necessary for winter and early spring even though the water reservoirs are still rather full because precipitation and thus the water level of reservoirs are not predictable many months ahead. Some water is kept in the reservoirs to ensure electricity supply at all times.

Q 1.2: How do the characteristics of the $CO_{2eq.}$ intensity used as a control signal for residential heating influence the overall emission savings in several Scandinavian bidding zones?

This question is answered in Paper 2. A case study has been developed to study the demand response of residential heating using the $CO_{2eq.}$ intensity of several Scandinavian bidding zones as a penalty signal. A single-family detached house built according to the Norwegian building standard from the 1980s is chosen as a case [92] to represent a large share of the residential building stock. Electric radiators are used for SH whereas an electric resistance heater is used for DHW heating. The DR study is performed for the following six Scandinavian bidding zones: NO2, NO3, SE1, SE4,

DK1, and FIN. The carbon-based penalty signals for DR are obtained according to the two principles proposed in Section 3.2.

It is found, that the energy use increases for all DR cases. It is shown that annual $CO_{2eq.}$ emissions decrease for NO2 while they remain almost unchanged for the other BZs. For NO3, the daily fluctuations in average $CO_{2eq.}$ intensity is too low to benefit from DR measures. Comparing results for NO2 and NO3 regarding overall emission savings, it demonstrates that electricity imports should be properly considered as they influence the variations of $CO_{2eq.}$ intensities significantly. These variations have shown to be important to make the CO_{2eq}-based DR effective. The study has shown that it is possible to achieve emission reductions, but this is very dependent on the characteristics of the $CO_{2eq.}$ intensity signal.

Furthermore, DHW heating and SH were separated to study the $CO_{2eq.}$ emission saving potentials. It is shown that SH is the main contributor to total emission savings because, for such a building with limited thermal insulation, the share of electricity use is much more significant for SH than for DHW heating. This will be different for buildings with better insulation levels. For example, regarding CSC-a (see Figure 3-3) in DK1, it was found that, even though DR measures for DHW heating lead to 12% emission savings, the overall emissions increase by 1% because the emissions resulting from SH increase by 3%. Finally, $CO_{2eq.}$ emissions for DHW heating are decreased significantly in most of the zones using CSC-a. On the contrary, in the Norwegian and Swedish BZs, these emissions increase significantly using CSC-b. A comprehensive description of the results is given in Paper 2.

4.2 Energy flexibility potential of residential single-family houses (Paper 3, 4 and 6)

Paper 3 investigates three types of predictive rule-based control (PRBC) to perform the demand response for heating a Norwegian residential building. The three PRBC strategies are designed to reduce (a) energy costs for heating using the hourly spot prices as input (called control strategy price CSP), (b) the annual $CO_{2eq.}$ emissions for heating based on the hourly $CO_{2eq.}$ intensity of the electricity mix in Norway (called control strategy carbon CSC) and (c) the energy use during peak-load hours using a pre-defined schedule (called control strategy schedule CSS). In the Norwegian context, reducing the energy use during peak-load hours is probably the most important objective for control, as bottlenecks in the distribution grids are expected in the near future. Paper 3 addresses research questions Q2, Q2.2, Q2.3, and Q2.4.

Paper 4 investigates the influence of thermal zoning on the energy flexibility potential in Norwegian detached houses. Most studies about energy flexibility consider a single indoor temperature, but this is questionable in residential buildings where people may want different temperature zones. This is critical in Norway where many occupants

prefer cold bedrooms (~16°C) and open bedroom windows for this purpose. Therefore, both Paper 3 and Paper 4 address research question Q2.2.

Paper 6 is a review of control strategies for building energy systems to unlock demand side flexibility. Besides control strategies for heating systems, key performance indicators to express energy flexibility are found. Therefore, Paper 6 addresses research question Q2.1.

Q 2: What is the energy flexibility potential of PRBC in the specific context of Norway?

The hourly averaged compressor power is shown in Figure 4-5 for the modulating heat pump in a ZEB. In the BAU scenario (Figure 4-5 (a)), the heat pump is often run during peak hours because these hours also coincide with the peak DHW demand. The CSP-b strategy (Figure 4-5 (c)), enforces heat pump operation in the early morning and early afternoon because spot prices are usually increasing at these times. The CSC-b strategy (Figure 4-5 (b)) amplifies the heat pump operation during late evening and peak hours in the morning in close accordance with the typical daily fluctuations of the $CO_{2eq.}$ intensity. The CSS strategy (Figure 4-5 (d)) enforces the heat pump operation during pre-defined periods.

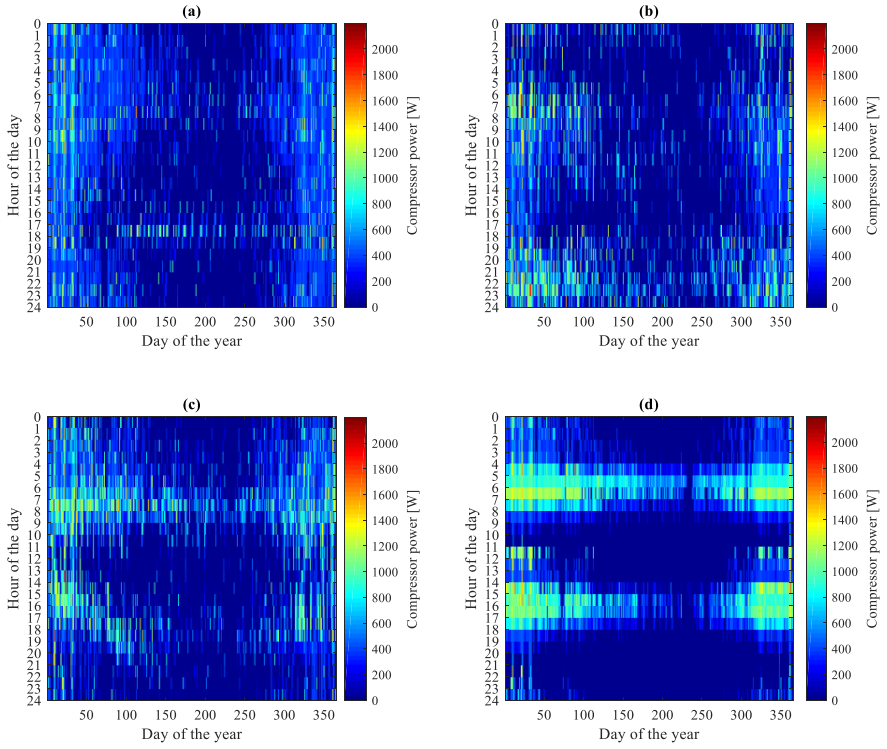

Figure 4-5. *Carpet plot of the hourly averaged compressor power of the modulating heat pump in the ZEB: (a) BAU, (b) CSC-b, (c) CSP-b and (d) CSS.*

Figure 4-6 illustrates the influence of the control scenarios on the annual electricity use for heating during pre-peak, peak and after-peak hours for the different PRBC scenarios applied in the ZEB. Figure 4-6 (a) and (b) correspond to the modulating heat pump system whereas Figure 4-6 (c) and (d) correspond to the direct electric heating.

The case of direct electric heating is discussed first. The CSS control leads to a higher increase in electricity use during pre-peak hours compared to the CSP-b and CSC-b control scenarios. The CSS is hugely effective to reduce energy use during peak hours but may generate new peaks during pre-peak periods. In conclusion, all controls (except for CSC-a) reduce the energy use during peak hours, especially CSS. CSC-a on the contrary would lead to increased electricity use during peak hours as well as after-peak hours. The annual electricity use for heating is increased slightly for CSP-b and CSS compared to the references (BAU), whereas it is decreased for the CSC-b strategy (Figure 4-6 (d)).

For the case of a modulating ASHP, the CSS control is much less effective to reduce electricity use during peak hours. CSC-b has almost unchanged energy use during that time period while CSP-b has increased energy use during peak hours. Regarding CSP-b, an increased use of the auxiliary heater during peak hours, which is due to the strict prioritization of DHW heating for the heat pump, is indicated previously in Figure 3-4 (c).

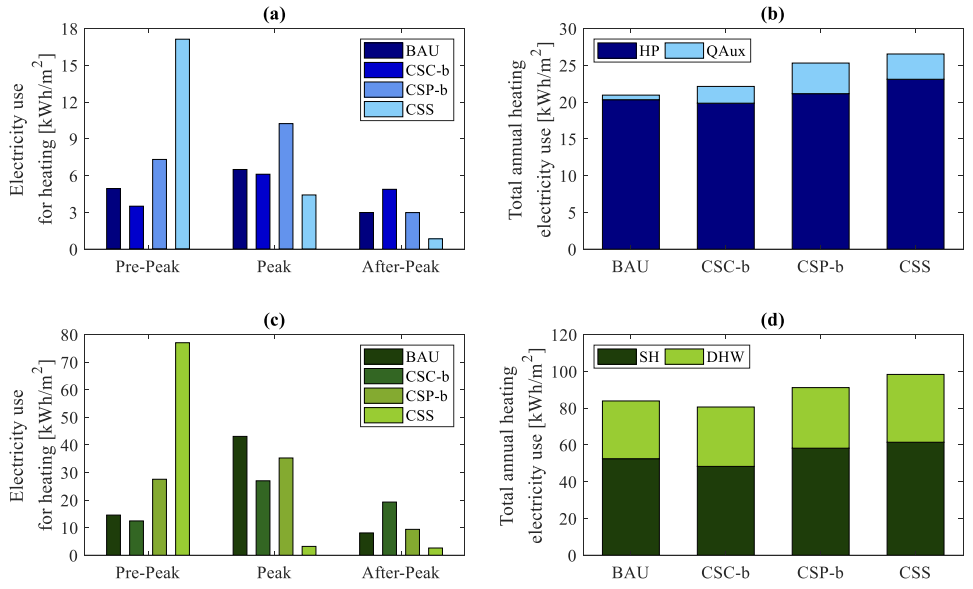

Figure 4-6. *Electricity use for heating of the ZEB using a modulating heat pump (a, b) or direct electric heating (c, d).*

There is an increase in the annual electricity use for heating for all three control scenarios. The reasons for increased electricity use for heating are the TSP variations for DHW heating and SH, hence increased thermal losses from the water storage tank and through the walls as well as the DHW prioritization for the heat pump. Because of the prioritization of DHW heating, the SH tank is less frequently charged to higher temperatures by the heat pump. Thus, the auxiliary heater is used more often for CSC-b, CSP-b, and CSS cases as the water temperature in the SH tank drops below the respective set-point for the auxiliary heater more frequently.

The price-based PRBC leads to increased heating costs even though it aims to avoid heating during high-price periods. The potential cost savings for the tested PRBC are outweighed by the increase in electricity use for heating. For the ASHP system, costs are increased by up to 21%. For direct electric heating, heating costs are increased by 5%, even though the electricity use is increased by 13%. This suggests that applying a PRBC to reduce energy costs for heating does not work in Norway. In fact, price-based control is more favorable in countries with greater price fluctuations, but in Norway spot prices do not fluctuate as much during the day as in other countries.

The carbon-based PRBC is associated with higher electricity use during early mornings and late evenings. As for the price-based control, increased energy use and limited daily fluctuations of the $CO_{2eq.}$ intensities (compared to other European bidding zones) limit the reduction of the annual $CO_{2eq.}$ emissions. Reductions can only be achieved for direct electric heating, but not for the studied ASHP.

The schedule-based control proved to be very efficient to reduce the energy use for heating during peak hours, especially for the direct electric heating. In the case of the heat pump, the reduction is significantly lowered due to the complexity of the heat pump control (see Q2.3 below). In the Norwegian context, the schedule-based control manages to significantly reduce energy use during peak hours, which is a main goal.

Q 2.1: Which key performance indicators (KPIs) are typically used to express building energy flexibility?

Multiple specific energy flexibility KPIs exist, which allow quantifying different aspects of demand side flexibility. Services covered by energy flexibility KPIs (mainly focusing on the building) do not cover all possible services for demand side management such as grid integration or grid ancillary services.

Besides conventional KPIs, such as final energy use, energy costs or CO_2 emissions, common KPIs related to building energy flexibility are self-generation, self-consumption, peak power generation, flexibility factors in terms of load shifted or costs reduced. Furthermore, there are KPIs related to building properties that can express flexibility, such as the available structure storage capacity or storage efficiency.

Most KPIs that are specific to energy flexibility are found in RBC studies. A detailed overview and description of KPIs related to energy flexibility is provided in Paper 6.

Q 2.2: How does the thermal zoning impact the energy flexibility potential?

Regarding Paper 3, energy flexibility has been evaluated for warm and cold bedrooms with open and closed doors, respectively. A lower temperature in bedrooms reduces the annual electricity use for heating (typically by 10%) compared to a uniform temperature in the building. It leads to a similar reduction in the energy costs for heating and annual $CO_{2eq.}$ emissions.

For DR controls, it was found that thermal zoning has a limited effect on the reduction of energy use during peak periods. For colder bedrooms with closed doors, it is shown that the bedroom temperatures are not strongly dependent on the heating control strategies applied in the other rooms. Similar results are found in Paper 4, which also shows that in buildings with low insulation levels, cold bedrooms can be easily created by applying a low temperature set-point in these rooms (e.g., ~16°C). With high insulation levels including a centralized heat recovery of the ventilation air and in combination with internal heat gains, it is intrinsically difficult to create cold bedrooms. Periods with moderate to high bedroom temperatures will be found systematically during the space-heating season (as long as bedroom windows are not open). If DR strategies are not applied to bedrooms (but only to the rest of the building), they do not amplify this phenomenon.

Consequently, the findings from Paper 4 suggest that activation of the building thermal mass, if not applied in bedrooms, will not further increase the risk of window opening or user dissatisfaction in bedrooms. The window opening should be avoided as it would lead to a noticeable increase in the space-heating needs. In addition, the thermal mass activation without considering bedrooms leads to a moderate reduction of the load-shifting potential compared to the activation of the entire building. This again coincides with the findings from Paper 3.

Q 2.3: How does the modeling complexity of the heat pump system influence the operation of the heating system and thus the energy flexibility potential?

The impact of the modeling complexity of the heat pump system on the energy flexibility potential is studied. With DR controls using time-varying set-points, results show that the DHW prioritization, the minimum cycle length as well as the hysteresis between the start and stop temperatures (when the heat pump operates below its minimum power modulation capabilities) prevent the heat pump stopping immediately after it is required by the PRBC. This may also trigger the operation of the auxiliary heater too frequently and significantly increase the energy use for heating. These phenomena have a major impact on the performance of the DR controls.

Compared to a simpler heating system, direct electric heating, the performance of DR controls with the ASHP is systematically lower. Modeling these details in a heat pump system are most often neglected in the literature but are important to predict a realistic energy flexibility potential. Therefore, a detailed and comprehensive heat pump model can be used to optimize PRBC. For instance, improving the prioritization control strategy between DHW and SH should be considered to make maximum use of the heat pump and minimize the use of auxiliary heaters while respecting the temperature set-points. The modeling complexity of a heat pump system required to study the operation of a heat pump in a detailed manner is investigated in Paper 5 and results are outlined comprehensively in Section 4.3 of this thesis, which answers research questions Q3 and Q3.1.

Q 2.4: How does PRBC influence the operating conditions of the heat pump in terms of duration and frequency of cycles?

This research question addresses the influence of the PRBC on the operating conditions of the heat pump in terms of duration and frequency of heat pump cycles. Paper 3 confirms the advantages of a modulating heat pump over an on-off heat pump. For the reference case (BAU) with constant heating set-points, the modulating heat pump leads to roughly half the number of heat pump cycles throughout the year. Compared to BAU, the DR controls lead to a comparable number of cycles for the modulating heat pump whereas an on-off heat pump will have fewer cycles with longer durations. As the number of cycles is related to the mechanical wear and the lifetime of the heat pump, an increased (or decreased) number of cycles corresponds to a cost (or a saving) that needs to be investigated in future work.

Figure 4-7 shows the influence of the DR strategies on the number of heat pump cycles throughout the year for both, the modulating heat pump and the on-off heat pump. The year can be typically divided into two periods. From October to April, both SH and DHW are important while, between May and September, the DHW needs are dominant. In this last period, the number of heat pump cycles is similar between the DR control strategies as well as between the on-off and modulating heat pumps (i.e. in the range of 40 to 100 cycles per month). On the contrary during the period when SH needs are significant, the number of heat pump cycles differs between cases.

Regarding the BAU control, the number of heat pump cycles for the modulating heat pump increases with the rising outdoor temperature from January to April, whereas an opposite trend can be seen for the on/off heat pump. The modulating heat pump cycles less often with colder outdoor temperatures due to the power sizing procedure. The heat pump is sized to operate continuously for outdoor temperatures that are typical for winter. Above a certain outdoor temperature, the modulating heat pump behaves more like an on/off heat pump and has shorter cycles for heating the storage tanks.

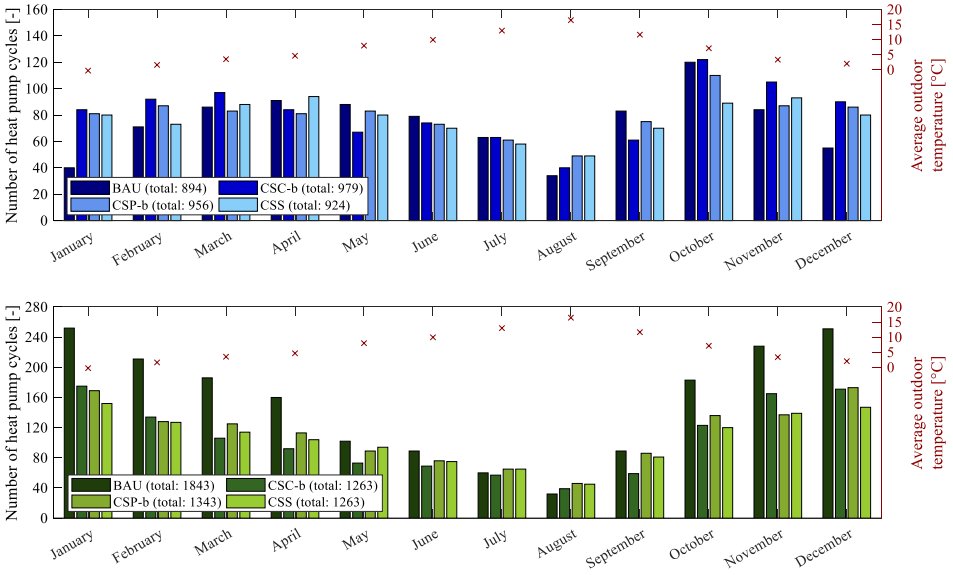

Figure 4-7. *Influence of the control strategies on the number of heat pump cycles for a modulating and an on/off ASHP and the ZEB case.*

Figure 4-8 compares the total number of heat pump cycles and the average heat pump cycle length for one year for different building insulation levels, namely passive house (PH), the ZEB and a building constructed according to TEK10 (Norwegian building standard from 2010).

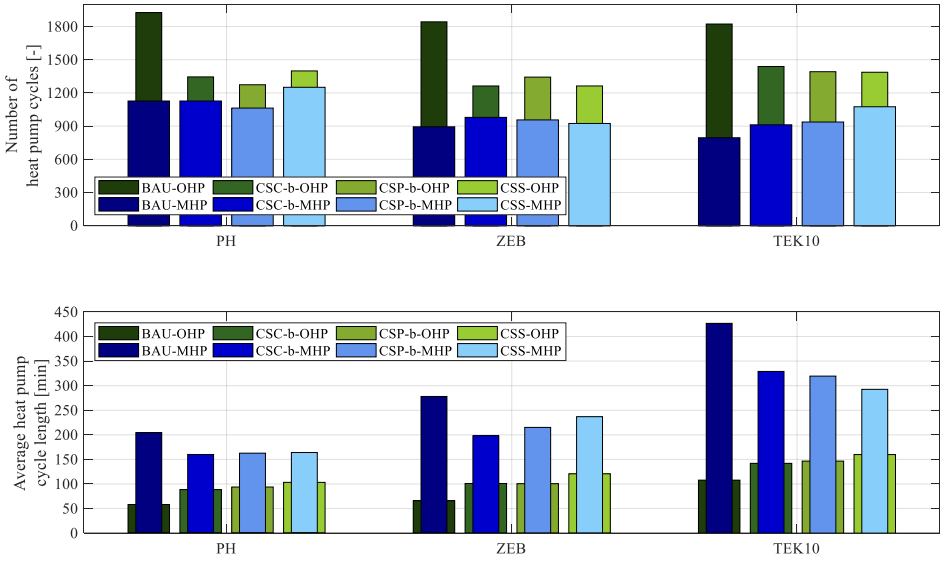

Figure 4-8. *Influence of the building insulation level on the total number of heat pump cycles per year for a modulating (MHP) and an on/off ASHP (OHP).*

Comparing these building insulation levels, the total number of heat pump cycles is similar, but the average duration of a cycle is different. The SH tank volume is smaller for higher insulation levels because of lower nominal SH power. As the heat pump capacity is the same for all three cases, the average cycle length is shorter for higher levels of insulation. It is obvious that proper sizing of the heat pump system (i.e. both the heat pump and storage tank) is essential.

4.3 Model complexity (Paper 5)

The results on the influence of the modeling complexity for the heat pump system control on chosen performance indicators are presented in this section. The influence of the DHW prioritization and the impact of the auxiliary heater operation on the annual electricity use for heating is discussed for the scenario with constant TSPs and a price-based DR scenario.

Q 3: Which level of modeling complexity of the heat pump system control is required to describe the heat pump behavior with regards to demand response of residential heating?

The influence of the modeling complexity of the heat pump system control on distinct energy-related and heat pump system-related performance indicators was investigated in Paper 5. For that purpose, six different cases with varying model complexity were studied. Results prove that the modeling complexity of the heat pump system control has a significant impact on the final results, proving that this aspect should not be overlooked.

For the chosen performance indicators, it is shown that a tuned P-controller and a tuned PI-controller can lead to similar results. In this regard, as long as the control signal to the heat pump is not of importance and power is not investigated at very short time scales, the choice of controller (P or PI) is not crucial. If the heat pump operation is investigated in detail and a high time resolution is required, it is shown that a PI-controller leads to a smoother operation than a P-controller, but a tuning of the controller is highly recommended.

Regarding DR measures, a strong interaction between the prioritization of domestic hot water and the control of auxiliary heaters significantly increases electricity use of a bivalent mono-energetic heat pump system when DR is performed for both, domestic hot water and space heating. The electricity use for heating is only slightly increased if demand control using predictive rule-based control is performed only for space heating. Figure 4-9 (b) illustrates the annual electricity use for heating for the modulating and on-off heat pump system distinguishing between the electricity use for the heat pump and the electric auxiliary heater. For each of the DR scenarios, the electricity use for heating is compared to a reference case (BAU) where constant temperature set-points for the room air temperature (21°C) and for DHW heating (53°C) are applied. The share of electricity use from the auxiliary heater is most

significant for CSP when DR measures are applied to both, DHW and SH. During the SH season, SH needs are usually present when DHW is produced by the heat pump. This leads to a temperature decrease in the SH tank that ultimately triggers the operation of the auxiliary heater. As the duration of DHW mode is prolonged by DR compared to BAU, the resulting increase in electricity use is larger when DR is applied to DHW. This confirms that the primary cause of increased electricity use for heating is the prioritization of DHW. Even though DHW is prioritized in the CSP-SH case, the auxiliary heater does not contribute significantly to the electricity use for heating. Comparing the MHP and the OHP, it can be seen that the electric auxiliary heater of the OHP system contributes less to the annual electricity demand for heating. Unlike MHP, the OHP control is exclusively based on a hysteresis and thus, somehow, on a charging of the SH tank. Therefore, with OHP, the SH tank has a larger autonomy when the HP is in DHW mode before the SH auxiliary heater has to be triggered. The auxiliary heater is then used less frequently by the OHP compared to the MHP.

Regarding the electricity use during pre-peak, peak and after-peak hours, the MHP and OHP show similar results for the same DR scenario (e.g. MHP-CSP vs. OHP-CSP) (Figure 4-9 (a)). Compared to the respective BAU scenario, increased electricity use during peak periods occurs for both heat pump systems. Direct electric heating has been investigated to ensure that the predictive rule-based control works properly for a simple heat distribution system. For direct electric heating, the price-based control (CSP) leads to reduced electricity use during peak periods, whereas the electricity use increases during pre-peak and after-peak periods. This conclusion does not hold for the two heat pump systems.

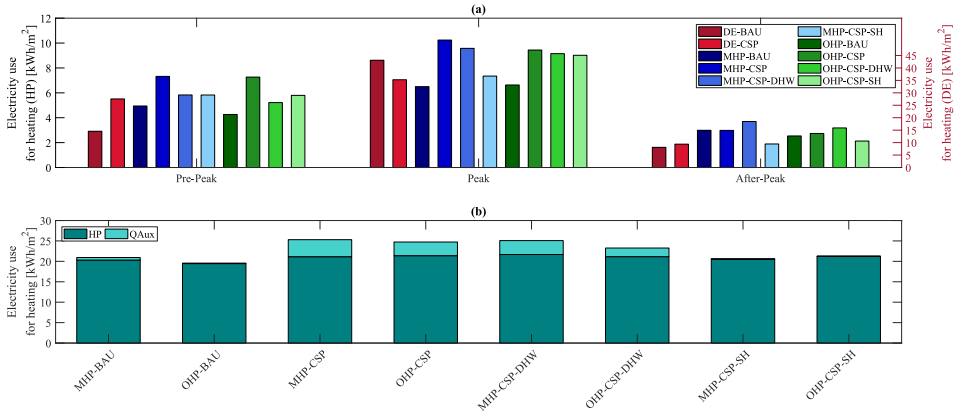

Figure 4-9. *(a) Electricity use for heating using direct electric heating (DE) (right axis), a modulating heat pump (MHP) and an on-off heat pump (OHP) (both left axis) and (b) annual electricity use for heating for the MHP and OHP for the different DR scenarios.*

Q3.1: How is the system operation influenced by different levels of modeling complexity for the heat pump system control?

The influence of modeling complexity on (1) energy-related KPIs, such as energy use for heating and average tank temperatures and (2) KPIs related to the heat pump system, such as the number of heat pump cycles per year and the average heat pump run time was investigated.

Six different cases were investigated: (1) an MHP with a tuned PI-controller (called MHP-PI-tuned), (2) an MHP with a PI-controller with a high integral time compared to the tuned integral time (called MHP-PI-highTi), (3) an MHP with a P-controller (called MHP-P), (4) an OHP, (5) a MHP as defined in case (1) but without a minimum run time (called MHP-noCT, with noCT meaning "no cycling time") and (6) an MHP modulating between 0% and 100% (called MHP-PM, with PM meaning "perfect modulation"). If not mentioned differently, the cases include a minimum heat pump run time and a heat pump that is able to modulate between 30% and 100%. Table 4-2 shows the influence of different heat pump model characteristics on the chosen KPIs.

The electricity use is rather similar for all studied cases. The heat pump with a perfect modulation (MHP-PM) performs best, whereas the on-off heat pump has the highest electricity use for heating. The modulating heat pumps with different P- or PI-controls show very similar heating electricity use.

The tank temperatures for the SH and the DHW tanks are the average temperature of the uppermost two layers of each tank. These temperatures are averaged over the SH season which is assumed to be from 1 September to 15 May. During summer time, only DHW heating is required so that all the investigated heat pumps behave in a same way, namely like an OHP. Regarding the DHW tank, the temperature differences among all cases are within 1.1K. The differences are small because DHW heating is always controlled by a hysteresis.

Table 4-2. *Influence of the modeling complexity and the controller parameters on the chosen KPIs.*

Case	Controller parameters		E_{Use} [kWh]		Average tank temperature [°C]		No. of HP cycles [-]	Average HP run time [min]	SCOP
	k [-]	T_i [s]	HP	Q_{Aux}	SH	DHW			
MHP-PI-tuned	0.1	300	2025	8	36.7	52.5	983	260	3.72
MHP-P	1	-	2028	9	36.8	52.6	808	322	3.73
MHP-PI-highTi	0.1	3300	2035	9	36.8	52.5	1059	239	3.69
OHP	-	-	2197	2	38.2	53.0	1988	59	3.41
MHP-noCT	0.1	300	2033	8	36.8	52.6	870	297	3.71
MHP-PM	0.1	300	1891	17	33.7	51.9	438	767	4.43

Regarding the SH tank, the maximum temperature difference between the studied cases is 4.5K. The OHP has the highest average temperature in the SH tank because

it charges the tank to higher temperatures for each cycle based on the hysteresis. For the MHP cases, the compressor speed is controlled to keep the temperature in the tank close to the floor heating supply temperature. In average, this leads to a lower tank temperature during the heating season and thus to lower heat losses from the tank. Due to higher condenser temperatures and tank thermal losses, the OHP has the lowest SCOP. On the contrary, the MHP-PM the highest SCOP.

Even though the electricity use and average tank temperatures are relatively similar for all cases, there are significant differences in the number of heat pump cycles and the average heat pump run time. The OHP has approximately twice the number of heat pump cycles compared to the MHP with a tuned PI-controller. The average run time is lowest for the OHP, while this average run time increases with a decreasing number of heat pump cycles. This confirms the advantage of modulating heat pumps over on-off heat pumps. The number of heat pump cycles is influenced by the choice of the control (P- or PI-control) and the tuning of the control parameters.

Figure 4-10 compares the output control signal to the heat pump for the P-control (MHP-P) and two PI-controls (MHP-PI-tuned and MHP-PI-highTi) for different time resolutions. Generally, the output of the PI-controls is smoother than the P-control which can have sudden variations in the signal. If the aim is to achieve a smooth operation of the heat pump, a PI-controller should be preferred over a P-controller. As it can be seen in Figure 4-10 (a) between minutes 420 and 545, the tuned PI-control leads to larger oscillations. The PI-controller with a higher integral time has weaker oscillations. These differences are directly related to the PI tuning rules applied in Paper 5. Regarding the tuning parameter τ_c, it could be chosen so that a P-controller and a PI-controller would give a very similar behavior. The large difference of output signals between the three controllers will lead to different electricity use in the short-term. These differences between the controllers almost disappear for a resolution time of 60 minutes. Actually, Figure 4-10 shows that the control signals for the P- and PI-controls are under-resolved above an averaging time of 15 minutes. Therefore, a time resolution lower than 15 minutes should be chosen if the aim is to investigate the dynamics of the heat pump in detail. The choice of controller is also important when power is investigated. The maximum power required during a year is very similar between a P- and a PI-controller as a controller output signal of 1 leads to the heat pump operating at full load. However, for time intervals lower than 15 minutes, the controllers will lead to different electrical powers.

In summary, the most appropriate modeling complexity depends on the type of investigation. Is the focus solely on energy and operational costs or is the detailed behavior of the heat pump or power of interest? The KPIs in Table 4-2 show that a P-controller and a PI-controller can lead to similar results as long as the heat pump operation and power are not investigated at short time scales. A P-controller has the advantage to simplify significantly the modeling setup. Its tuning is easier and the problem of integral windup avoided. On the contrary, if the heat pump operation is

investigated for short time scales, the heat pump control and tuning cannot be simplified.

All in all, with regards to a detailed investigation of the heat pump operation, it is shown that commonly-used energy-related performance indicators are not sufficient. Therefore, energy-related performance indicators should be complemented by additional indicators, such as the number of heat pump cycles and the average heat pump cycle time. A time-series analysis with a high resolution time is inevitable and thus highly recommended to spot potential problems like integral windup of a PI-controller.

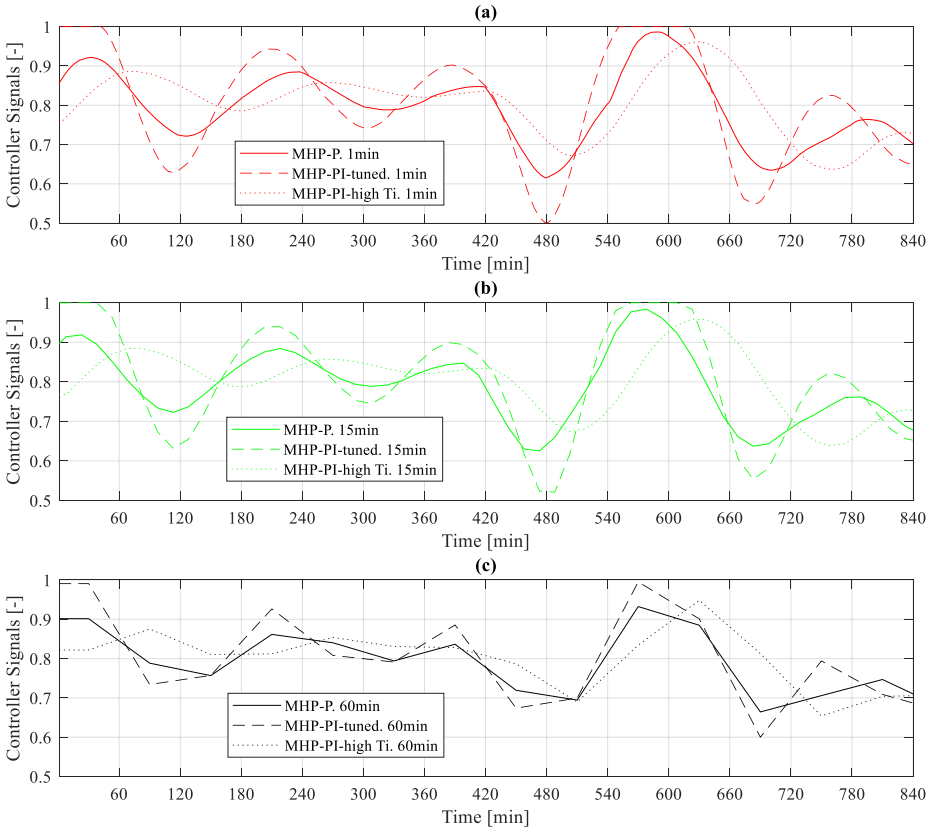

Figure 4-10. *Comparison of P-Controller and two PI-Controller output signal to the heat pump for a time resolution of (a) 1min, (b) 15 min and (c) 60 min during an exemplary period of 14 h.*

5 CONCLUSIONS AND FUTURE RESEARCH

This chapter summarizes the main findings of the work conducted during the PhD. Key conclusions are presented for each of the three main parts in Section 5.1. Limitations of the studies are discussed in Section 5.2. Possibilities for future research are identified and presented in Section 5.3.

5.1 Concluding remarks

Regarding average $CO_{2eq.}$ intensities of the electricity mix

Norway is a special case in Europe because the electricity generation is almost fully renewable. The impact of fossil fuel-based electricity imports on the average $CO_{2eq.}$ intensity is particularly strong for the case of Norway because the electricity in Norway is almost entirely generated from hydropower.

When controlling a building's electricity use according to the average $CO_{2eq.}$ intensity of the electricity mix in Norway, it has been shown that electricity use would be increased during peak hours, thus causing more stress on the grid. Thus, increased power loads at times of low $CO_{2eq.}$ intensities may amplify already existing peak loads, which could lead to grid congestions and possibly higher electricity prices. This would admittedly lead to decreased carbon emissions, but the transmission and distribution grid could get stressed even more.

Regarding building HVAC control, it is interesting to see that in Norway a control based on the average $CO_{2eq.}$ intensity of the electricity mix and a price-based control would lead to contradictory operation periods of the energy system meaning that minimizing operating costs is not compatible with minimizing CO_2 emissions (see Figure 4-4). This will be different in countries where the electricity generation relies more on fossil fuels, and thus average $CO_{2eq.}$ intensities are typically high at times of high electricity demand and thus high prices. A reasonable design of the penalty signal for heating control purposes is therefore essential. The use of a well-designed penalty signal based on the $CO_{2eq.}$ intensity can facilitate achieving the emission targets of the European Union, when applied in demand response strategies for residential heating.

The proposed methodology to calculate the hourly $CO_{2eq.}$ intensity of the electricity mix is not limited to studies on heating demand response, but can also be used in other fields of research, such as LCA. In LCA, the use of a fixed/constant $CO_{2eq.}$ intensity of the electricity mix is a major flaw, especially with regards to the calculation of the emissions from the operational phase of a building.

Regarding flexibility potential

As usual, the control objectives have to be chosen carefully and stated clearly. It has been shown that the price-based predictive rule-based control strategy that makes use

of the lowest spot prices leads to an increased heating electricity use and annual heating costs because it also involves longer periods with increased temperature set-points. A price-based PRBC that aims at charging the thermal energy storage right before high-price periods also fails to realize cost savings for the case of Norway. Generally, price-based PRBC is more profitable in electricity markets with greater daily fluctuations in the electricity price, such as Denmark. It has been shown that the investigated price-based controls, which do not lead to cost savings in the Norwegian context, result in cost savings if they were applied to the same building in Denmark.

It has been found that demand response strategies applied to DHW heating are very promising to decrease operational costs for direct electric heating systems. In conclusion, efficient demand response measures using PRBC can be implemented for DHW heating. However, the performance of the same controls is moderate for SH in buildings with a poor insulation level. This confirms that buildings with higher insulation level show a stronger potential for a flexible heating operation as they have a higher storage efficiency.

The results prove that carbon-based controls can achieve emission reductions if daily fluctuations of the $CO_{2eq.}$ intensity are large enough to counterbalance for the increased electricity use generated by load shifting. In some cases, the additional energy use to charge the storage and additional storage losses outweigh the potential emissions savings.

Regarding the Norwegian case, $CO_{2eq.}$ intensity fluctuations in NO2 are mainly generated by electricity imports, which further confirms the need to account for these electricity imports in the demand response analysis. If the heating system is controlled according to spot prices, it was found that price-based controls lead to increased emissions in the Scandinavian countries as operation is usually shifted towards night-time (for the case of Norway) when cheap but carbon-intensive electricity is indirectly imported from Germany, Poland or the Netherlands (via Denmark and Sweden).

The effect of thermal zoning on the flexibility potential has been investigated as well. For colder bedrooms with closed doors, it is shown that the bedroom temperatures are only sparsely dependent on the heating control strategies applied in the other rooms. These are important conclusions because it suggests that energy flexibility potential is moderately impacted by thermal zoning which is an important aspect of user behavior. In addition, the risk of open bedroom windows to keep the bedroom cold will not be increased by the different DR controls. In Norway, buildings are often constructed in wood which leads to thermal insulation in partition walls to limit the sound propagation. The conclusion may be different for construction modes with non-insulated partition walls, such as concrete.

Regarding modeling complexity

Based on a summary of typical modeling simplifications for heat pump systems, Paper 5 of this thesis analyses two key components: the heat pump controller and the

domestic hot water prioritization of the heat pump. The results prove that the modeling complexity of the system control has a significant impact on the key performance indicators, proving that this aspect should not be overlooked:

- (1) The model complexity affects the short-time behavior of a heat pump system when performing demand response. It is recommended to consider controller tuning for studies on heat pump systems with focus on DR regardless of the applied control strategies, e.g. PRBC or model-predictive control (MPC).
- (2) It has been shown that the perfectly modulating heat pump idealizes the performance of the system and thus overestimates the potential for cost or emissions savings.
- (3) P- and PI-controls for modulating heat pump systems lead to a similar number of heat pump cycles per year while these numbers are significantly different for on-off and perfectly modulating heat pumps.
- (4) The controller type (i.e. P- or PI-control) and tuning are important when heat pump operation is investigated at short time scales. In practice, a PI-controller would be preferred to achieve a smoother operation of the heat pump. The controller tuning is often overlooked in studies on DR and energy flexibility using building performance simulation (BPS) and cannot be captured in detail by strongly simplified models for heat pump systems.

The difference between P- and PI-controllers and their parameter tuning should be considered in a realistic way if the heat pump operation is investigated at short time scales. Besides PRBC, these conclusions are also valid for other controls, such as MPC, where typically temperature set-points are controlled and not the compressor power directly. The choice of controller for a modulating heat pump (i.e. P- or PI-control) and its tuning is not crucial if the heat pump operation and electric power are not investigated at short time scales. A P-controller can be advantageous as it significantly simplifies the modeling setup. Its tuning is easier and the problem of integral windup is avoided.

Regarding the DHW prioritization, the results demonstrate a strong influence of this prioritization on the control of the electric auxiliary heaters. Electricity use increases significantly when the DR is applied to DHW as this increases the use of the auxiliary heater for space-heating.

5.2 Limitations

Demand response for residential heating is an interdisciplinary study, where it is necessary to make assumptions at different levels. Specific assumptions taken in this thesis are discussed in the following so that results can be interpreted, discussed and understood in a better way.

Regarding average $CO_{2eq.}$ intensities of the electricity mix

The proposed methodology to evaluate the hourly average $CO_{2eq.}$ intensity of the electricity mix is an adaptation of multi-regional input-output models (MRIO). Regarding the CO_2 factor for a specific electricity generation technology, it is shown that these factors can vary significantly among references depending on their respective assumptions for emission allocations. To improve the proposed methodology, the used dataset could be more detailed, so that a CO_2 factor is not only technology-dependent but also bidding zone-dependent.

The major advantage of the proposed methodology is its simplicity compared to the other existing methodologies presented in Table 2-1. Nevertheless, it also has limitations. The proposed methodology to evaluate the hourly average $CO_{2eq.}$ intensity is a decoupled approach meaning that the interaction between the supply and demand side is not considered. This limitation counts for all decoupled approaches, not only for the proposed method. A coupled approach should be used to take into account these interactions into the forecast of the electricity generation if a significant number of buildings takes part in the demand response control. If a large number of buildings applies this $CO_{2eq.}$ intensity as a control signal, the overall electric load could be sufficiently affected so that the forecasted generation would not be optimized anymore for this load. For instance, if the $CO_{2eq.}$ signal is low, a large number of buildings may decide to favor consumption during this period of time. If the number of buildings is significant, a strong imbalance will appear between the real and predicted energy consumption. Balancing power would be needed, potentially with a power plant generating electricity with relatively high $CO_{2eq.}$ intensity (such as a gas-fired power plant). The resulting overall $CO_{2eq.}$ emissions can, therefore, be suboptimal. Ideally, a coupled model is required so that the impact of the demand response control is taken into account in the forecast of the electricity generation and corresponding $CO_{2eq.}$ emissions [40,51].

As discussed in section 2.3.1, average and marginal $CO_{2eq.}$ intensities are two distinct concepts. Marginal emissions are the emissions from one additional kWh generated/consumed and, consequently, result from a single power plant. Therefore, it could be argued that the marginal $CO_{2eq.}$ intensity is most coherent for the control of a limited number of buildings because they will rather affect a single plant than the overall production. Generally, the fluctuations of marginal emissions are typically larger than the fluctuations of average emissions and are thus expected to have a stronger emission savings potential. For the case of Norway, where the electricity generation is almost fully from hydropower, the fluctuations in marginal emission might still be limited since the hydropower plants can already be operated in a flexible way. Therefore, the marginal emissions depend very much on the operation strategy of the hydropower and the hydropower reservoirs, as discussed in section 4.1 under Q1.1. For power systems that rely on fossil fuels to a larger extent, a study on CO_2 emissions of the electricity generation in Europe by [93] has shown that marginal

emissions could actually increase if load shifting from peak to off-peak hours is performed and if the peak loads are covered by gas power plants. According to the merit order curve, fossil gas has higher marginal costs than hard coal, but reducing peak loads may lead to a lower share of gas power plants in the electricity mix, which will lead to an increase in marginal emissions as coal has a higher $CO_{2eq.}$ intensity than gas.

Regarding flexibility potential

By definition, predictive rule-based control is based on predefined control rules that may not be optimal. The load shifting potential depends on the tuning of these rules, in the case of this PhD, the low-price and high-price thresholds.

Different principles to determine the penalty signal (based on spot price or $CO_{2eq.}$ intensity) could lead to a different load shifting potential. In this thesis, the thresholds were determined using a 24 h sliding horizon, but other principles could be used for the determination. The use of percentiles is another possibility. In that sense, it can be made sure that the thresholds will lead to the same amount of hours in the high-price or low-price segments for each prediction horizon, e.g. one day. Furthermore, the thresholds could be determined for every single day, rather than for a sliding horizon.

For the chosen principle that considers a 24h sliding horizon, it has been found that ideally the thresholds are chosen for each area of interest (bidding zone) because spot price or $CO_{2eq.}$ intensity signals are different. With the Norwegian spot price and $CO_{2eq.}$ intensity signal it is not sufficient to simply design the control based on the lowest $CO_{2eq.}$ intensities or prices, as it may be the case for other bidding zones because they have more rapid price or $CO_{2eq.}$ intensity fluctuations. Nevertheless, for energy costs and $CO_{2eq.}$ emissions it should be investigated whether model-predictive control could generate significant benefit even though the price and $CO_{2eq.}$ signals have limited fluctuations in Norway.

Regarding system design, the choice and sizing of components of a heat pump system and the control of the system go hand in hand and need to be considered carefully. Throughout this thesis, a four-pipe tank connection has been used in the case studies. Other hydraulic connections exist but have not been considered here.

Furthermore, frosting and defrosting of air-source heat pumps have been neglected in this thesis. This may lead to an overestimation of the heat pump performance and the flexibility potential.

Regarding modeling complexity

The required modeling complexity of a heat pump system has been investigated in IDA ICE. The heat pump model in IDA ICE has some shortcomings. Firstly, it is a steady-state model. Secondly, transient effects of the heat pump are not considered in the IDA ICE model. This means that efficiency losses during start-up and shut-down

periods are not accounted for. Thirdly, so far it is not possible to take into account the increase of COP in part load operation in IDA during continuous operation. As already mentioned, the (de)frosting of air-source heat pumps should be better modeled.

5.3 Future research

This thesis investigates the flexibility potential of predictive rule-based control to perform heating demand response in residential buildings. Based on the findings of this thesis and the limitations of the studies, possibilities for future research can be outlined.

Regarding average $CO_{2eq.}$ intensities of the electricity mix

Regarding the methodology proposed in this thesis, CO_2 factors specific for each technology and each bidding zone could be implemented instead of using the same CO_2 factor of an electricity generation technology for all bidding zones.

The proposed methodology for the determination of the $CO_{2eq.}$ intensity is a de-coupled approach. A next step can be the development of a coupled model. Then the energy system and a large number of buildings that take part in a demand response scheme can be combined and the effect on the average and marginal $CO_{2eq.}$ intensities can be investigated. Furthermore, $CO_{2eq.}$ intensity of the electricity mix and electricity prices can be coupled so that the effect of increasing CO_2 prices on the electricity mix can be studied for future scenarios.

Another possibility for future work is the development of a model to forecast $CO_{2eq.}$ intensities. The model could be based on historical data and could be used for forecasting if ENTSO-E does not provide data on the electricity generation.

Regarding flexibility potential

The price-based predictive rule-based controls applied in this PhD thesis apply hourly electricity spot prices. Different electricity prices could be investigated in future studies, such as time-of-use price, real-time prices or intra-day prices.

Besides different prices, other principles can be used to determine price thresholds, in case a similar PRBC is used, e.g. percentiles of the price signals. In this regard, indirect control for peak shaving can be performed.

With price-based control applied to DHW, the annual heating costs increase because the advantage of consuming during lower electricity prices is outweighed by the large increase in electricity use. The use of additional set-points for DHW heating along lower electricity spot prices to operate the heat pump more frequently should be considered in future studies to avoid a too frequent operation of the electric auxiliary heater.

Furthermore, more advanced controls, such as model-predictive control, can be developed to see whether they actually lead to significantly higher cost or emission savings compared to PRBCs for the same spot prices or $CO_{2eq.}$ intensities. In other studies, MPC has shown a strong potential for cost and emission savings for residential heating, but the major drawback for an extensive implementation in real buildings is still the identification of a simplified building model which can be used in the optimization within the MPC. (P)RBC is easier to implement into real buildings as no building model has to be identified. RBC strategies are the state-of-the-art for residential heating, and will continue to play a significant role for the heating of single buildings in the years to come. Nevertheless, despite the challenges that have to be overcome regarding MPC, with (a) the necessary Information and Communications Technologies in place, and (b) stronger incentives to make use of the energy flexibility of buildings, the importance of MPC (and other advanced controls) will be increased not only at the single-building level, but also at the aggregated level where several buildings are interconnected. Advanced controls will be of value especially when the operation of the heating systems of several buildings has to be scheduled in an optimal way. Then, it will be difficult to meet the requirements with (P)RBC.

In this thesis, the occupant behavior or occupants comfort preferences are solely based on national or international standards (except for Paper 4). The same occupancy profiles for the rooms are used throughout this research. In reality, the occupant behavior may differ strongly from person to person, and these variations could be accounted for in future research.

This PhD thesis, like most of the existing studies in the literature, is based on simulations. Even though the models are relatively detailed, many physical phenomena are simplified. Therefore, field measurements should be performed, for instance to validate simulation results, to verify whether some important details of the HVAC system operation have not been omitted in simulations, to measure the detailed temperature distribution in the buildings (such as the air temperature stratification), and to investigate the user acceptance and thermal comfort during thermal mass activation.

Investigations have been performed using a specific case study so that the work should be extended to other configurations:

- Different hydraulic layouts of the heat distribution system should be tested, such as a two-pipe connection of the tank instead of a four-pipe connection.
- Furthermore, the flexibility potential for different heat emission systems should be compared, for example, a water-based radiator instead of floor heating should be studied.
- The flexibility potential of ground-source heat pumps can be investigated and compared to air-source heat pumps.

- The case of detached single-family house has been taken as it represents a large share of the building stock in Norway. Other residential building types can be investigated, such as row houses and apartment blocks. Office buildings also represent a large segment of the building stock. For office buildings, the mechanical ventilation is expected to play a more important role than in residential buildings so that both ventilation and local space heating should be properly coordinated by the control.

Future work could also focus on the design of the heat pump system that considers energy flexibility. In this PhD thesis, standard sizing of a heat pump system that is operated in an energy flexible way is applied.

In line with the focus on zero emission neighborhoods in Norway, the flexibility potential of heat pumps in neighborhoods should be investigated.

Regarding modeling complexity

For future work, the transient behavior of the heat pump and the increased part load efficiency of modulating heat pumps should be considered to investigate the impact on the flexibility potential. The (de)frosting of air-source heat pumps should be better modeled.

BIBLIOGRAPHY

[1] Clauß J, Stinner S, Solli C, Lindberg KB, Madsen H, Georges L. A generic methodology to evaluate hourly average CO2eq . intensities of the electricity mix to deploy the energy flexibility potential of Norwegian buildings. to be Publ. Proc. 10th Int. Conf. Syst. Simul. Build., Liege, Belgium: 2018.

[2] Clauß J, Stinner S, Solli C, Lindberg KB, Madsen H, Georges L. Evaluation Method for the Hourly Average CO2eq. Intensity of the Electricity Mix and Its Application to the Demand Response of Residential Heating. Energies 2019;12:1345. doi:10.3390/en12071345.

[3] Clauß J, Stinner S, Sartori I, Georges L. Predictive rule-based control to activate the energy flexibility of Norwegian residential buildings: Case of an air-source heat pump and direct electric heating. Appl Energy 2019;237:500–18. doi:10.1016/J.APENERGY.2018.12.074.

[4] Johnsen T, Taksdal K, Clauß J, Yu X, Georges L. Influence of thermal zoning and electric radiator control on the energy flexibility potential of Norwegian detached houses. Accept. CLIMA 2019 Conf., 2019.

[5] Clauß J, Georges L. Model complexity of heat pump systems to investigate the building energy flexibility and guidelines for model implementation. Revis Version Submitt to Appl Energy 2019:1–25.

[6] Clauß J, Finck C, Vogler-Finck P, Beagon P. Control strategies for building energy systems to unlock demand side flexibility – A review. 15th Int. Conf. Int. Build. Perform. Simul. Assoc. San Fr. USA, San Francisco: 2017.

[7] Clauß J, Vogler-Finck P, Georges L. Calibration of a high-resolution dynamic model for detailed investigation of the energy flexibility of a zero emission residential building. In: Johansson D, editor. Springer Proc. Energy, Cold Clim. HVAC 2018 Conf., Kiruna, Sweden: Springer Nature Switzerland AG 2019; 2018. doi:https://doi.org/10.1007/978-3-030-00662-4_61.

[8] Clauß J, Sartori I, Alonso MJ, Thalfeldt M, Georges L. Investigations of different control strategies for heat pump systems in a residential nZEB in the nordic climate. Proc. 12th IEA Heat Pump Conf. 2017, Rotterdam, Netherlands: 2017.

[9] IEA. International Energy Agency - Buildings. Key World Energy - Stat 2015:82. doi:10.1787/9789264039537-en.

[10] OECD/IEA. ENERGY POLICIES OF IEA COUNTRIES Norway 2017 Review. 2017.

[11] D´Angiolella R, De Groote M, Fabbri M. Buildings as micro energy hubs. REHVA J 2016:52–5.

[12] Aduda KO, Labeodan T, Zeiler W, Boxem G, Zhao Y. Demand side flexibility: Potentials and building performance implications. Sustain Cities

Soc 2016;22:146–63. doi:10.1016/j.scs.2016.02.011.

[13] Finck C, Li R, Kramer R, Zeiler W. Quantifying demand flexibility of power-to-heat and thermal energy storage in the control of building heating systems. Appl Energy 2017;209:409–25. doi:10.1016/j.apenergy.2017.11.036.

[14] Arteconi A, Hewitt NJ, Polonara F. State of the art of thermal storage for demand-side management. Appl Energy 2012;93:371–89. doi:10.1016/j.apenergy.2011.12.045.

[15] Chen Y, Xu P, Gu J, Schmidt F, Li W. Measures to improve energy demand flexibility in buildings for demand response (DR): A review. Energy Build 2018;177:125–39. doi:10.1016/J.ENBUILD.2018.08.003.

[16] Yin R, Kara EC, Li Y, Deforest N, Wang K, Yong T, et al. Quantifying flexibility of commercial and residential loads for demand response using setpoint changes. Appl Energy 2016;177:149–64. doi:10.1016/j.apenergy.2016.05.090.

[17] Haider HT, See OH, Elmenreich W. A review of residential demand response of smart grid. Renew Sustain Energy Rev 2016;59:166–78. doi:10.1016/j.rser.2016.01.016.

[18] Vandermeulen A, van der Heijde B, Helsen L. Controlling district heating and cooling networks to unlock flexibility: A review. Energy 2018. doi:10.1016/j.energy.2018.03.034.

[19] Vandermeulen A, Vandeplas L, Patteeuw D, Sourbron M, Helsen L. Flexibility offered by residential floor heating in a smart grid context : the role of heat pumps and renewable energy sources in optimization towards different objectives . Proc. 12th IEA Heat Pump Conf. 2017, Rotterdam, Netherlands: 2017.

[20] Junker RG, Azar AG, Lopes RA, Lindberg KB, Reynders G, Relan R, et al. Characterizing the energy flexibility of buildings and districts. Appl Energy 2018;225:175–82. doi:10.1016/j.apenergy.2018.05.037.

[21] Péan T, Ortiz J, Salom J. Impact of Demand-Side Management on Thermal Comfort and Energy Costs in a Residential nZEB. Buildings 2017;7:37. doi:10.3390/buildings7020037.

[22] Fischer D, Madani H. On heat pumps in smart grids: A review. Renew Sustain Energy Rev 2017;70:342–57. doi:10.1016/j.rser.2016.11.182.

[23] Vogler-Finck P, Clauß J, Georges L, Sartori I, Wisniewski R. Inverse model identification of the thermal dynamics of a Norwegian zero emission house. In: Johansson D, editor. Springer Proc. Energy, Cold Clim. HVAC 2018 Conf., Springer Nature Switzerland AG 2019; 2018.

[24] Finck C, Clauß J, Vogler-Finck P, Beagon P, Zhang K, Kazmi H. Review of applied and tested control possibilities for energy flexibility in buildings 2018. doi:10.13140/RG.2.2.28740.73609.

[25] Vogler-Finck P, Clauß J, Georges L. A dataset to support dynamical modelling of the thermal dynamics of a super-insulated building. Zenodo: 2017. doi:https://doi.org/10.5281/zenodo.1034819.

[26] Lopes RA, Chambel A, Neves J, Aelenei D, Martins J. A literature review of methodologies used to assess the energy flexibility of buildings. Energy Procedia 2016;91:1053–8. doi:10.1016/j.egypro.2016.06.274.

[27] Jensen SØ, Marszal-Pomianowska A, Lollini R, Pasut W, Knotzer A, Engelmann P, et al. IEA EBC Annex 67 Energy Flexible Buildings. Energy Build 2017;155:25–34. doi:10.1016/j.enbuild.2017.08.044.

[28] Killian M, Kozek M. Ten questions concerning model predictive control for energy efficient buildings. Build Environ 2016;105:403–12. doi:10.1016/j.buildenv.2016.05.034.

[29] De Coninck R, Helsen L. Quantification of flexibility in buildings by cost curves - Methodology and application. Appl Energy 2016;162:653–65. doi:10.1016/j.apenergy.2015.10.114.

[30] Haghighi MM. Controlling Energy-Efficient Buildings in the Context of Smart Grid : A Cyber Physical System Approach. University of California at Berkeley, 2013.

[31] Alimohammadisagvand B, Jokisalo J, Kilpeläinen S, Ali M, Sirén K. Cost-optimal thermal energy storage system for a residential building with heat pump heating and demand response control. Appl Energy 2016;174:275–87. doi:10.1016/j.apenergy.2016.04.013.

[32] Alimohammadisagvand B, Jokisalo J, Sirén K. Comparison of four rule-based demand response control algorithms in an electrically and heat pump-heated residential building. Appl Energy 2018;209:167–79. doi:10.1016/j.apenergy.2017.10.088.

[33] Le Dréau J, Heiselberg P. Energy flexibility of residential buildings using short term heat storage in the thermal mass. Energy 2016;111:991–1002. doi:10.1016/j.energy.2016.05.076.

[34] Dar UI, Sartori I, Georges L, Novakovic V. Advanced control of heat pumps for improved flexibility of Net-ZEB towards the grid. Energy Build 2014;69:74–84. doi:10.1016/j.enbuild.2013.10.019.

[35] Heidmann Pedersen T, Hedegaard RE, Petersen S. Space heating demand response potential of retrofitted residential apartment blocks. Energy Build 2017;141:158–66. doi:10.1016/j.enbuild.2017.02.035.

[36] Hedegaard RE, Pedersen TH, Petersen S. Multi-market demand response using economic model predictive control of space heating in residential buildings. Energy Build 2017;150:253–61. doi:10.1016/j.enbuild.2017.05.059.

[37] Dahl Knudsen M, Petersen S. Demand response potential of model predictive

control of space heating based on price and carbon dioxide intensity signals. Energy Build 2016;125:196–204. doi:10.1016/j.enbuild.2016.04.053.

[38] Péan TQ, Salom J, Ortiz J. Environmental and Economic Impact of Demand Response Strategies for Energy Flexible Buildings. Proc BSO 2018 2018:277–83.

[39] Vogler-Finck PJC, Wisniewski R, Popovski P. Reducing the carbon footprint of house heating through model predictive control - A simulation study in Danish conditions. Sustain Cities Soc 2018;42:558–73. doi:10.1016/j.scs.2018.07.027.

[40] Patteeuw D, Bruninx K, Arteconi A, Delarue E, D'haeseleer W, Helsen L. Integrated modeling of active demand response with electric heating systems coupled to thermal energy storage systems 2015;151:306–19. doi:10.1016/j.apenergy.2015.04.014.

[41] De Coninck R, Baetens R, Saelens D, Woyte A, Helsen L. Rule-based demand-side management of domestic hot water production with heat pumps in zero energy neighbourhoods. J Build Perform Simul 2014;7:271–88. doi:10.1080/19401493.2013.801518.

[42] Baetens R, De Coninck R, Helsen L, Saelens D. The Impact of Load Profile on the Grid-Interaction of Building Integrated Photovoltaic (BIPV) Systems in Low-Energy Dwellings. J Green Build 2010;5:137–47. doi:10.3992/jgb.5.4.137.

[43] Salpakari J, Lund P. Optimal and rule-based control strategies for energy flexibility in buildings with PV. Appl Energy 2016;161:425–36. doi:10.1016/j.apenergy.2015.10.036.

[44] Vanhoudt D, Geysen D, Claessens B, Leemans F, Jespers L, Van Bael J. An actively controlled residential heat pump: Potential on peak shaving and maximization of self-consumption of renewable energy. Renew Energy 2014;63:531–43. doi:10.1016/j.renene.2013.10.021.

[45] Georges E, Cornélusse B, Ernst D, Lemort V, Mathieu S. Residential heat pump as flexible load for direct control service with parametrized duration and rebound effect. Appl Energy 2017;187:140–53. doi:10.1016/j.apenergy.2016.11.012.

[46] D'hulst R, Labeeuw W, Beusen B, Claessens S, Deconinck G, Vanthournout K. Demand response flexibility and flexibility potential of residential smart appliances: Experiences from large pilot test in Belgium. Appl Energy 2015;155:79–90. doi:10.1016/J.APENERGY.2015.05.101.

[47] IEA, Nordic Energy Research. Nordic Energy Technology Perspectives 2016 Cities, flexibility and pathways to carbon-neutrality. Oslo: 2016.

[48] Georges E, Garsoux P, Masy G, DeMaere D`Aetrycke G, Lemort V. Analysis of the flexibility of Belgian residential buildings equipped with Heat Pumps

and Thermal Energy Storages. CLIMA 2016 - Proc. 12th REHVA World Congr., Aalborg: 2016.

[49] Fischer D, Bernhardt J, Madani H, Wittwer C. Comparison of control approaches for variable speed air source heat pumps considering time variable electricity prices and PV. Appl Energy 2017;204:93–105. doi:10.1016/j.apenergy.2017.06.110.

[50] Reynders G, Nuytten T, Saelens D. Potential of structural thermal mass for demand-side management in dwellings. Build Environ 2013;64:187–99. doi:10.1016/j.buildenv.2013.03.010.

[51] Arteconi A, Patteeuw D, Bruninx K, Delarue E, D'haeseleer W, Helsen L. Active demand response with electric heating systems: Impact of market penetration. Appl Energy 2016;177:636–48. doi:10.1016/j.apenergy.2016.05.146.

[52] Berge M, Georges L, Mathisen HM. On the oversupply of heat to bedrooms during winter in highly insulated dwellings with heat recovery ventilation. Elsevier Ltd, 2016. doi:10.1016/j.buildenv.2016.07.011.

[53] NordPoolGroup. NordPool Bidding Areas 2018. https://www.nordpoolgroup.com/the-power-market/Bidding-areas/. (accessed April 28, 2018).

[54] Energinet. Retningslinjer for miljødeklarationen for el 2017:1–16.

[55] Milovanoff A, Dandres T, Gaudreault C, Cheriet M, Samson R. Real-time environmental assessment of electricity use: a tool for sustainable demand-side management programs. Int J Life Cycle Assess 2018;23:1981–94. doi:10.1007/s11367-017-1428-2.

[56] Roux C, Schalbart P, Peuportier B. Accounting for temporal variation of electricity production and consumption in the LCA of an energy-efficient house. J Clean Prod 2016:532–40. doi:10.1016/j.jclepro.2015.11.052.

[57] Tomorrow. CO2-equivalent Model Explanation 2018. https://github.com/tmrowco/electricitymap-contrib/blob/master/CO2eq Model Explanation.ipynb (accessed May 4, 2018).

[58] Bettle R, Pout CH, Hitchin ER. Interactions between electricity-saving measures and carbon emissions from power generation in England and Wales. Energy Policy 2006;34:3434–46. doi:10.1016/j.enpol.2005.07.014.

[59] Hawkes AD. Estimating marginal CO2 emissions rates for national electricity systems. Energy Policy 2010;38:5977–87. doi:10.1016/j.enpol.2010.05.053.

[60] Corradi O. Estimating the marginal carbon intensity of electricity with machine learning 2018. https://medium.com/electricitymap/using-machine-learning-to-estimate-the-hourly-marginal-carbon-intensity-of-electricity-49eade43b421 (accessed February 28, 2019).

[61] Graabak I, Bakken BH, Feilberg N. Zero emission building and conversion factors between electricity consumption and emissions of greenhouse gases in a long term perspective. Environ Clim Technol 2014;13:12–9. doi:10.2478/rtuect-2014-0002.

[62] Askeland M, Jaehnert S, Mo B, Korpas M. Demand response with shiftable volume in an equilibrium model of the power system. 2017 IEEE Manchester PowerTech, IEEE; 2017. doi:10.1109/PTC.2017.7980990.

[63] Quoilin S, Hidalgo Ganzalez I, Zucker A. Modelling Future EU Power Systems Under High Shares of Renewables The Dispa-SET 2.1 open-source model. Petten, Netherlands: 2017. doi:10.2760/25400.

[64] Wiebe KS. The impact of renewable energy diffusion on European consumption-based emissions. Econ Syst Res 2016;28:133–50. doi:10.1080/09535314.2015.1113936.

[65] Bachmann C, Roorda MJ, Kennedy C. DEVELOPING A MULTI-SCALE MULTI-REGION INPUT-OUTPUT MODEL. Econ Syst Res 2015;27:172–93. doi:10.1080/09535314.2014.987730.

[66] Pan L, Liu P, Li Z, Wang Y. A dynamic input–output method for energy system modeling and analysis. Chem Eng Res Des 2018;131:183–92. doi:10.1016/j.cherd.2017.11.032.

[67] Guevara Z, Domingos T. The multi-factor energy input–output model. Energy Econ 2017;61:261–9. doi:10.1016/j.eneco.2016.11.020.

[68] Palmer G. An input-output based net-energy assessment of an electricity supply industry. Energy 2017;141:1504–16. doi:10.1016/J.ENERGY.2017.11.072.

[69] Madani H, Claesson J, Lundqvist P. Capacity control in ground source heat pump systems: Part I: modeling and simulation. Int J Refrig 2011;34:1338–47. doi:10.1016/J.IJREFRIG.2011.05.007.

[70] Bagarella G, Lazzarin R, Noro M. Annual simulation, energy and economic analysis of hybrid heat pump systems for residential buildings. Appl Therm Eng 2016;99:485–94. doi:10.1016/J.APPLTHERMALENG.2016.01.089.

[71] Bagarella G, Lazzarin R, Noro M. Sizing strategy of on–off and modulating heat pump systems based on annual energy analysis. Int J Refrig 2016;65:183–93. doi:10.1016/J.IJREFRIG.2016.02.015.

[72] Lee CK. Dynamic performance of ground-source heat pumps fitted with frequency inverters for part-load control. Appl Energy 2010;87:3507–13. doi:10.1016/J.APENERGY.2010.04.029.

[73] Dongellini M, Abbenante M, Morini GL. A strategy for the optimal control logic of heat pump systems: impact on the energy consumptions of a residential building. Proc. 12th IEA Heat Pump Conf. 2017, 2017.

[74] Cheung H, Braun JE. Performance comparisons for variable-speed ductless and single-speed ducted residential heat pumps. Int J Refrig 2014;47:15–25. doi:10.1016/J.IJREFRIG.2014.07.019.

[75] Goia F, Finocchiaro L, Gustavsen A. The ZEB Living Laboratory at the Norwegian University of Science and Technology : a zero emission house for engineering and social science experiments. 7 . Passiv. Nord. - Sustain. Cities Build., Copenhagen: 2015.

[76] EQUA. EQUA Simulation AB 2015. http://www.equa.se/en/ida-ice.

[77] Kristjansdottir TF, Houlihan-Wiberg A, Andresen I, Georges L, Heeren N, Good CS, et al. Is a net life cycle balance for energy and materials achievable for a zero emission single-family building in Norway? Energy Build 2018;168:457–69. doi:10.1016/j.enbuild.2018.02.046.

[78] Fischer D, Lindberg KB, Madani H, Wittwer C. Impact of PV and variable prices on optimal system sizing for heat pumps and thermal storage. Energy Build 2017;128:723–33.

[79] Stiebel Eltron. Planung und Installation: Wärmepumpen. 2013.

[80] OSOHotwater. OSO Hotwater, “OSO Optima EPC series”. Patent 328503, 02 2014, 2014.

[81] Niemelä T, Vuolle M, Kosonen R, Jokisalo J, Salmi W, Nisula M. Dynamic simulation methods of heat pump systems as a part of dynamic energy simulation of buildings. Proc. 3rd Ibpsa-engl. Conf. BSO 2016, Newcastle: 2016.

[82] Brattebø H, O’Born R, Sandberg NH, Vestrum MI, Sartori I. Fremtidig utvikling i energiforbruk og CO2-utslipp for Norges boligmasse. 2016.

[83] Renaldi R, Kiprakis A, Friedrich D. An optimisation framework for thermal energy storage integration in a residential heat pump heating system. Appl Energy 2017;186:520–9. doi:10.1016/j.apenergy.2016.02.067.

[84] Psimopoulos E, Bee E, Widén J, Bales C. Techno-economic analysis of control algorithms for an exhaust air heat pump system for detached houses coupled to a photovoltaic system. Appl Energy 2019;249:355–67. doi:10.1016/j.apenergy.2019.04.080.

[85] SN/TS3031:2016. Bygningers energiytelse, Beregning av energibehov og energiforsyning 2016.

[86] Ahmed K, Akhondzada A, Kurnitski J, Olesen B. Occupancy schedules for energy simulation in new prEN16798-1 and ISO/FDIS 17772-1 standards. Sustain Cities Soc 2017;35:134–44. doi:10.1016/j.scs.2017.07.010.

[87] ISO17772-1. Energy performance of buildings - Indoor environmental quality - Part1: Indoor environmental input parameters for the design and assessment of energy performance of buildings. 2017.

[88] ISO7730:2005. Ergonomics of the thermal environment - Analytical determination and interpretation of thermal comfort using calculation of the PMV and PPD indices and local thermal comfort criteria 2005.

[89] OpenStreetMap. Shiny weather data 2017. https://rokka.shinyapps.io/shinyweatherdata/ (accessed May 20, 2017).

[90] Nord Pool Spot. www.nordpoolspot.com/historical-market-data 2016. www.nordpoolspot.com/historical-market-data.

[91] Rendum J, Vik AL, Knutsen AS. Innføring av AMS i norske husstander, og mulighetene dette gir for nettfleksibilitet. Norwegian University of Science and Technology, 2016.

[92] Brattebø H, O'Born R, Sartori I, Klinski M, Nørstebø B. Typologier for norske boligbygg - Eksempler på tiltak for energieffektivisering. 2014.

[93] Graabak I, Feilberg N. CO2 emissions in a different scenarios of electricity generation in Europe. 2011.

RESEARCH PUBLICATIONS

This part contains the complete results of the research which are communicated through the following international publications.

PAPER 1

A generic methodology to evaluate hourly average $CO_{2eq.}$ intensities of the electricity mix to deploy the energy flexibility potential of Norwegian buildings

Clauß J[1], Stinner S[1], Solli C[2], Lindberg KB[3,4], Madsen H[5,6], Georges L[1,6]

[1] Norwegian University of Science and Technology NTNU, Department of Energy and Process Engineering, Trondheim, Norway

[2] NTNU, Property Division, Trondheim, Norway

[3] NTNU, Department of Electric Power Engineering, Trondheim, Norway

[4] SINTEF Building and Infrastructure, Oslo, Norway

[5] DTU Technical University of Denmark, DTU Compute, Copenhagen, Denmark

[6] NTNU, (ZEN-project), Trondheim, Norway

This paper is published in *Proceedings of the 10th International Conference on System Simulation in Buildings* held in Liege, Belgium on 10 - 12 December 2018.

A generic methodology to evaluate hourly average $CO_{2eq.}$ intensities of the electricity mix to deploy the energy flexibility potential of Norwegian buildings

J. Clauß[1]*, S. Stinner[1], C. Solli[2], K. B. Lindberg[3,4], H. Madsen[5,6], L. Georges[1,6]

(1) Norwegian University of Science and Technology NTNU, Department of Energy and Process Engineering, Trondheim, Norway

(2) NTNU, Property Division, Trondheim, Norway

(3) NTNU, Department of Electric Power Engineering, Trondheim, Norway

(4) SINTEF Building and Infrastructure, Oslo, Norway

(5) DTU Technical University of Denmark, DTU Compute, Copenhagen, Denmark

(6) NTNU, (ZEN-project), Trondheim, Norway

*john.clauss@ntnu.no

1. ABSTRACT

This work presents a generic methodology to calculate the average $CO_{2eq.}$ intensity of the electricity mix in a bidding zone for every hour. The evaluation is based on the logic of a *multi-regional input-output approach*. The methodology includes the $CO_{2eq.}$ intensities of the electricity imports from neighboring bidding zones. To apply this methodology, input data about electricity generation is here taken from ENTSO-E and $CO_{2eq.}$ emissions per fuel type from the database Ecoinvent. This article demonstrates that it is important to take electricity imports into account when evaluating the $CO_{2eq.}$ intensity in many Scandinavian bidding zones. Correlations between the average $CO_{2eq.}$ intensity in Norway and the electricity spot price, the electricity import from foreign countries and the filling level of the Norwegian water reservoirs are investigated. The average $CO_{2eq.}$ intensity of the Norwegian electricity mix is relatively high during times with electricity imports and low when electricity is generated from hydropower. Making use of the building energy flexibility, a large potential for load shifting and emission reductions can be offered. As ENTSO-E provides 72h forecasts for the electricity generation, the $CO_{2eq.}$ intensity evaluated using this methodology can be applied as a penalty signal in predictive controls of buildings (such as model-predictive control or predictive rule-based control). The paper discusses the applicability of such a $CO_{2eq.}$ intensity as a control signal for the operation of an energy system.

Keywords: building energy flexibility, dynamic $CO_{2eq.}$ intensity, predictive control, Scandinavian power market

2. INTRODUCTION

A low-carbon energy system is required to reduce its environmental impact in the future. The energy use in buildings constitutes a large part of the total energy use. Two ways to achieve a more sustainable system could be to (1) increase the energy efficiency of buildings and (2) de-carbonize the energy supplied to buildings (IEA & Nordic Energy Research, 2016). According to the IEA, the CO_2 price is expected to sharply increase in the future and will thus be a fundamental driver for the transformation of energy systems towards carbon neutrality. Furthermore, an increased interaction between the Norwegian power grid and the "continental" European power grids is expected. Introducing demand side flexibility into the power system may lead to more stable electricity prices in the Norwegian energy grid (IEA & Nordic Energy

Research, 2016). In Norway, electricity is mostly generated by hydropower and since there is a very limited number of fossil fuel power plants for electricity generation, hourly average $CO_{2eq.}$ intensities of the electricity mix are strongly influenced by electricity exchanges with neighboring bidding zones and countries. If the $CO_{2eq.}$ intensity is used as an indicator for the fraction of renewables in the electricity mix, it can be used as a control signal for buildings. By making use of the energy flexibility of a building, energy use can be shifted to times with high fraction of renewables in the electricity mix.

The objective of this work is the development of a methodology for calculating the hourly average $CO_{2eq.}$ intensity of the electricity mix in an interconnected power grid from existing electricity production data sets. This methodology aims to evaluate the average $CO_{2eq.}$ intensities for each bidding zone (BZ) in Scandinavia taking $CO_{2eq.}$ intensities of electricity imports into account. The average $CO_{2eq.}$ intensity includes the emissions of a technology from a life cycle perspective. Electricity losses in the transmission and distribution grid are neglected in this study. The methodology is generic and not restricted to the Norwegian power system. Input data for calculating the $CO_{2eq.}$ intensity of the electricity mix is not readily available. Therefore, this work will provide the calculation methodology as well as will hint on where to retrieve and how to structure the input data in order to apply this methodology

2.1 State-of-the-art for determining average $CO_{2eq.}$ intensities for building energy system control

Usually, the $CO_{2eq.}$ intensity of imports from neighboring countries is assumed to be fixed (i.e. constant in time) when calculating the $CO_{2eq.}$ intensity of the domestic grid mix. For example, the Danish transmission system operator (TSO) Energinet provides hourly data of the average $CO_{2eq.}$ intensity of the electricity consumption in Denmark where imports from Norway are assumed as 0 g/kWh, from Sweden as 40 g/kWh and from Germany as 500 g/kWh (ENERGINET.DK, 2011). Knudsen and Petersen (Dahl Knudsen & Petersen, 2016), Hedegaard et al. (Hedegaard, Pedersen, & Petersen, 2017) and Pedersen et al. (Heidmann Pedersen, Hedegaard, & Petersen, 2017) study the demand response potential for space heating in Danish residential buildings applying hourly average $CO_{2eq.}$ intensities using the data from Energinet. Vandermeulen et al. (Vandermeulen, Vandeplas, Patteeuw, Sourbron, & Helsen, 2017) aim at maximizing the electricity use of residential heat pumps at times of high renewable energy penetration in the Belgian power grid. They use data from the Belgian TSO, Elia, but it is not stated how electricity imports are considered (i.e. if dynamic $CO_{2eq.}$ intensities of the imported electricity are considered). The company "Tomorrow" has launched a website, which shows the average $CO_{2eq.}$ intensity in most European countries in real time (Tomorrow, 2016). They consider trading between bidding zones as well as dynamic $CO_{2eq.}$ intensities in their models (Tomorrow, 2018), but a license is required to get access to the data.

2.2 The Scandinavian power market

NordPool is the leading power market in Europe (NordPoolGroup, 2018b) and operates mainly in Scandinavia, the Baltics, Germany and the UK. It has a day-ahead as well as an intra-day market. NordPool is owned by the Nordic TSOs (Norway, Sweden, Finland and Denmark) and the Baltic TSOs (Estonia, Latvia and Lithuania) (NordPoolGroup, 2018a). Each country can be divided into several bidding zones. As shown in Figure 1, Norway consists of five BZs, each of these zones have physical connections with neighboring bidding zones that enable import and export of electricity. Generally, BZs are created to avoid bottlenecks in the transmission system. By allocating different electricity prices for each BZ, they can help indicating constraints in the transmission system (NordPoolGroup, 2018c).

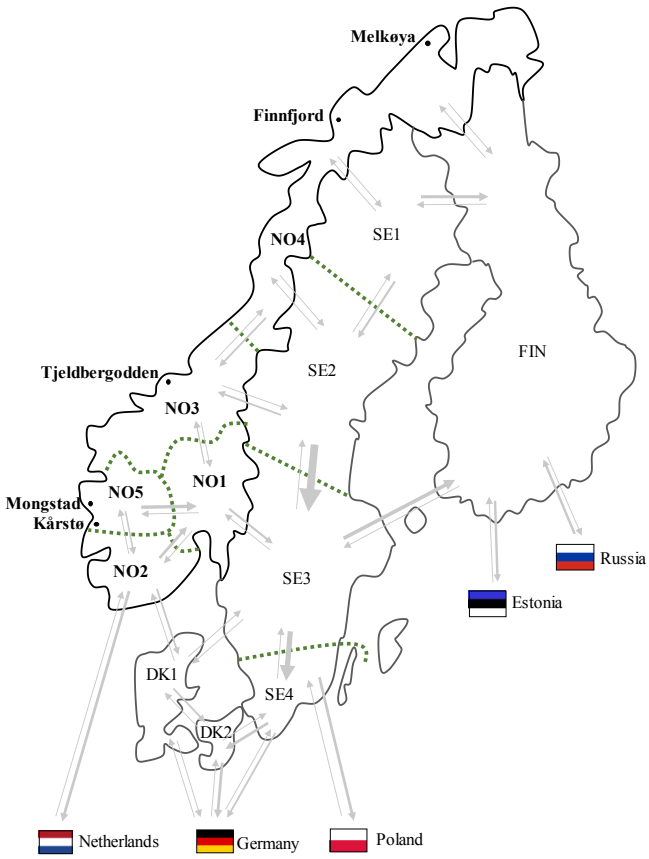

Figure 1: Overview of the Scandinavian power market bidding zones also including gas-fired power plants in Norway (adjusted from (IEA & Nordic Energy Research, 2016)*).*

3. EVALUATION METHOD FOR HOURLY AVERAGE $CO_{2EQ.}$ INTENSITY

This paper compares two scenarios for the calculation of the average $CO_{2eq.}$ intensity of the electricity mix. The calculation methodology is exactly the same, but the input data is treated differently:

(1) Scenario 1: The average $CO_{2eq.}$ intensity of the electricity mix is evaluated using the electricity generation per fuel type (retrieved from ENTSO-E).
(2) Scenario 2: For some gas power plants, the sales of their electricity generation to the grid is limited. Consequently, the second scenario evaluates the average $CO_{2eq.}$ intensity of the electricity mix using the same data as scenario (1) but with additional information on sales licenses of gas power plants. These licenses are granted by NVE (Norwegian water resources and energy directorate).

In the case of Norway, both scenarios lead to significant differences in the average $CO_{2eq.}$ intensity. Both scenarios are compared in section 4.1. As already mentioned, the impact of fossil fuels on the average $CO_{2eq.}$ intensity is very strong since the electricity generation in Norway originates almost entirely from hydropower. The dataset from ENTSO-E contains hourly values for the *total electricity generation per production type within a BZ*. It also includes data for thermal power plants which consume most of the generated electricity onsite. It is necessary to have knowledge about sales licenses of such power plants. As the electricity is not sold to the

electricity grid, it should not be considered in the calculation of the *average $CO_{2eq.}$ intensity of the electricity grid mix* (Scenario 2).

This section presents the sources for the input data, the assumptions made for processing the data and the calculation methodology to evaluate hourly average $CO_{2eq.}$ intensities. Although generic, the calculation methodology is explained using Norway as a particular case.

3.1 Data retrieval

3.1.1 Electricity generation per bidding zone

Electricity generation per production type within a bidding zone can be retrieved from ENTSO-E, which is the European Network of TSOs for Electricity. Each European TSO is asked to provide data to ENTSO-E to promote closer cooperation across the TSOs as well as to promote market transparency. The data can be downloaded after setting up a free user account.

In this work, missing data is handled in the following way: missing data for individual hours are populated with interpolated values based on the hour before and after; missing data for a whole day is populated with data of the previous day. Depending on the case, it can be sufficient to interpolate between hours or to duplicate individual previous hours. It may also be better to include data of the same hours from the day before or day ahead. If the dataset from ENTSO-E is incomplete for specific bidding zones, data may be retrieved from the respective national TSOs. For instance, in the Norwegian case study, the hourly electricity generation per production type for Sweden was obtained from the Swedish TSO because data for Swedish BZs was not available from ENTSO-E.

Pre-processing of the electricity generation data

For Scenario 1, ENTSO-E data for the hourly values of the electricity generation is considered and no further information about sales licenses for individual power plants is considered. The dataset from ENTSO-E remains unchanged regarding the electricity generation, except for treating missing data. Data regarding the hourly electricity imports and exports between BZs is usually provided by the market operator. For the particular case of Norway, data related to electricity imports was taken from both, ENTSO-E and NordPool (Nord Pool Spot, 2016).

Scenario 2 calculates the average $CO_{2eq.}$ intensity of the electricity mix taking information of the power plant fleet into account as well as the sales license of the thermal power plants. In other words, this is representative for the $CO_{2eq.}$ intensity of the electricity mix consumed by households. Norway has a very limited number of thermal power plants which normally are not allowed to sell electricity to the grid by agreement. The thermal power plants with the highest capacities are shown in Figure 1. In Scenario 2, the electricity generation of these power plants is not considered in the evaluation of the $CO_{2eq.}$ intensity, except for the power plant in Mongstad, which sells electricity to the grid. Regarding the other thermal power plants, their electricity generation has been removed from the ENTSO-E data. Nevertheless, data on the electricity generation from these power plants is either logged under the production technology "*fossil gas*" or "*other*" in the ENTSO-E dataset. It is not explained in the ENTSO-E documentation what exactly is considered as "other". The utilization of waste heat from industrial processes is not explicitly considered in any production type of the ENTSO-E dataset. Therefore, it is here assumed that the utilization of waste heat is meant by "other" in the dataset. Furthermore, it is difficult to allocate a CO_2 factor for this production type "other", since the meaning of this category is not specified by ENTSO-E and could be different in every country. Here, the factor is simply assumed to be the average of the different fossil fuel technologies. Information regarding sales licenses of power plants can usually be obtained from either the

TSO, the company owning the power plants or state directorates. It has to be mentioned that this information is here restricted to Norway, the dataset for Scenario 2 remains unchanged for other BZs. Regarding Scenario 2, when electricity is generated from waste heat in Norway, electricity is mostly for self-consumption and therefore the hourly electricity generation from "other" is set to 0.

Structure of the dataset

This paper also describes in detail how the methodology can be implemented into a specific environment, here using Excel and MATLAB. In general, the input data can be arranged in the following matrix:

$$BZ_j = \begin{bmatrix} P_{BZ_j,EGT_1}(t_1) & \cdots & P_{BZ_j,EGT_m}(t_1) \\ \vdots & P_{BZ_j,EGT_i}(t_g) & \vdots \\ P_{BZ_j,EGT_1}(t_{8760}) & \cdots & P_{BZ_j,EGT_m}(t_{8760}) \end{bmatrix} \quad (1)$$

where
- *i* is the *"index of EGTs"* ranging from 1 to m
- *j* is the *"index of a specific BZ"*
- *g* is the *"hour of the year"* ranging from 1 to 8760 (or 8784)

Matrix BZ (where "BZ" stands for Bidding Zone) includes the electricity generation from each electricity generation technology (EGT_i) at every hour of the year (t_g). EGT_i contains data about the electricity generation from each technology in the BZ, but, by extension, also includes the imports from 1st tier BZs. In other words, imports from other BZs are considered as an EGT in the matrix. For instance, in Excel, one sheet per BZ can be used with each sheet having exactly the same layout. The input data can be arranged in the same way as the data sheets from the ENTSO-E website.

3.1.2 Emission factors per electricity generation technology

The average $CO_{2eq.}$ intensity of a bidding zone depends directly on the CO_2 factor that is associated to each EGT. Two ways of acquiring CO_2 factors of a given EGT are the IPCC report (Krey et al., 2014; Schlömer et al., 2014) or the Ecoinvent database (Ecoinvent, 2016). Ecoinvent provides a vast variety of CO_2 factors for electricity generation from a given fuel type depending on the type of power plant or the specific country. A license is necessary to use Ecoinvent, whereas the IPCC report is available free of charge. An identical CO_2 factor has been applied for each EGT in every country and thus the CO_2 factor is assumed to be independent of the country. Therefore, it is assumed that each power plant using a same EGT has the same CO_2 factor, disregarding the thermal efficiency or the age of the power plant. The choice of the CO_2 factor of an EGT strongly affects the final result of the evaluation. Differences of the CO_2 factors between references mainly result from different allocations of emissions, especially for combined heat-and-power plants. More detailed information regarding emission allocations are given in references (Ecoinvent, 2016; Krey et al., 2014; Schlömer et al., 2014). Regarding annual average $CO_{2eq.}$ intensities of a country, they can be calculated from Ecoinvent or taken from the website of the European Environment Agency (EEA, 2018), for instance. Table 1 gives an overview of typical CO_2 factors for different fuel types. For this work, data from the Ecoinvent database has been used. Here, the phases that are considered in the CO_2 factor of an EGT consider the extraction of fuels, the construction of the power plant including infrastructure and transport as well as its operation and maintenance and the end of use of the power plant. For the sake of simplicity, the CO_2 factor for *hydro pumped storage* is here assumed constant in time, 62 $gCO_{2eq.}$/kWh. In fact, it is dependent on the $CO_{2eq.}$ intensity of the electricity mix used when pumping water into the storage reservoir. Unlike Norway, this assumption can be critical for bidding zones that usually have a relatively high $CO_{2eq.}$ intensity.

Table 1. Comparison of CO_2 factors per electricity generation technology (EGT) from different references

Electricity generation technology (EGT)	**Emission factor [$gCO_{2eq.}/kWh_e$]**		**Name of EGT in Ecoinvent** (for reproduction purposes)	**Emission factor [$gCO_{2eq.}/kWh_e$]**
	IPCC	**EEA**		**Ecoinvent** (applied here)
Biomass	740	-	Electricity, high voltage {SE}| heat and power co-generation, **wood chips**, 6667 kW, state-of-the-art 2014 | Alloc Rec, U	60[1]
Fossil brown coal/Lignite	820	-	Electricity, high voltage {DE}| electricity production, **lignite** | Alloc Rec, U	1240
Fossil coal-derived gas		-	Electricity, high voltage {DE}| treatment of **coal gas**, in power plant | Alloc Rec, U	1667
Fossil gas	490	-	Electricity, high voltage {DK}| heat and power co-generation, **natural gas**, conventional power plant, 100MW electrical | Alloc Rec, U	529
Fossil hard coal	1001	-	Electricity, high voltage {DK}| heat and power co-generation, **hard coal** | Alloc Rec, U	1266
Fossil oil		-	Electricity, high voltage {DK}| heat and power co-generation, **oil** | Alloc Rec, U	1000
Fossil oil shale		-	No data in Ecoinvent (assumed value)	1000
Fossil peat		-	Electricity, high voltage {FI}| electricity production, **peat** | Alloc Rec, U	1071
Geothermal	38	-	Electricity, high voltage {DE}| electricity production, **deep geothermal** | Alloc Rec, U	95
Hydro pumped storage	24	-	Electricity, high voltage {NO}| electricity production, **hydro, pumped storage** | Alloc Rec, U	62
Hydro run-of-river and poundage	24	-	Electricity, high voltage {SE}| electricity production, **hydro, run-of-river** | Alloc Rec, U	5
Hydro water reservoir	24	-	Electricity, high voltage {NO}| electricity production, **hydro, reservoir**, alpine region | Alloc Rec, U	8
Marine	24	-	No data in Ecoinvent (assumed value - as wind offshore)	18
Nuclear	12	-	Electricity, high voltage {SE}| electricity production, **nuclear**, pressure water reactor | Alloc Rec, U	13
Other		-	No data in Ecoinvent (assumed value - avg. fossil fuels)	979
Other RES		-	No data in Ecoinvent (assumed value - avg. RES)	46
Solar	45	-	Electricity, low voltage {DK}| electricity production, **photovoltaic**, 3kWp slanted-roof installation, single-Si, panel, mounted | Alloc Rec, U	144
Waste		-	Electricity, for reuse in municipal waste incineration only {DK}| **treatment of municipal solid waste**, incineration | Alloc Rec, U	500
Wind offshore	12	-	Electricity, high voltage {DK}| electricity production, **wind**, 1-3MW turbine, **offshore** | Alloc Rec, U	18
Wind onshore	11	-	Electricity, high voltage {DK}| electricity production, **wind**, 1-3MW turbine, **onshore** | Alloc Rec, U	14
Imports from all bidding zones with calculated hourly data	-	0		0
Imports from Russia	-	-	Electricity, high voltage {**RU**}| market for | Alloc Rec, U	862
Imports from Estonia	-	762	Electricity, high voltage {**EE**}| market for | Alloc Rec, U	1179
Imports from Poland	-	671	Electricity, high voltage {**PL**}| market for | Alloc Rec, U	1225
Imports from Belgium	-	212	Electricity, high voltage {**BE**}| market for | Alloc Rec, U	365
Imports from Great Britain	-	389	Electricity, high voltage {**GB**}| market for | Alloc Rec, U	762

[1] Assuming that biogenic CO_2 is climate neutral; 100 year spruce rotation assumption and dynamic GWP for climate impact of burning wood; does not consider climate impact from CO_2 from wood combustion

Strictly speaking, if the constant CO_2 factor considered for pumped hydro storage is much lower than the $CO_{2eq.}$ intensity of the electricity mix when water is pumped into the storage, it would correspond to a "greenwashing" of the electricity mix.

3.2 Calculation methodology

This work evaluates the hourly average $CO_{2eq.}$ intensity of the electricity mix in an interconnected power grid, where hourly average $CO_{2eq.}$ intensities of the electricity mix of the electricity imports are considered for most of the BZs. Constant annual average values for the $CO_{2eq.}$ intensity are allocated to the electricity imports from a few specific countries (Russia, Estonia, Poland, Belgium and Great Britain), here also called boundary BZs. This section provides a step-by-step guidance on how to determine the hourly average $CO_{2eq.}$ intensity of the electricity mix of a bidding zone. Tables are presented in matrix-form for illustration purposes and easier reproduction.

In the present case study, hourly average $CO_{2eq.}$ intensities are calculated for all Norwegian, Swedish and Danish bidding zones as well as for Finland, Germany and the Netherlands. In each BZ, the electricity mix is assumed homogeneous, leading to a same $CO_{2eq.}$ intensity for the entire BZ at each hour of the year. For neighboring countries where the $CO_{2eq.}$ intensities are not evaluated (meaning Great Britain, Belgium, Poland, Estonia and Russia), a yearly-averaged $CO_{2eq.}$ intensity are considered. It is nonetheless reasonable to assume that these countries have a limited impact on the $CO_{2eq.}$ intensity of the Norwegian electricity mix. They either are 2nd tier countries (i.e. which do not have a direct grid connection to Norwegian bidding zones) or have limited electricity export to Norway (which is typically the case for Russia).

Matrix T(t) (where "T" stands for Technology) includes the electricity generation from each generation type (EGT_i) in all BZs and is calculated for each hour of the year (t):

$$T(t) = \begin{bmatrix} P_{BZ_1,EGT_1}(t) & \cdots & P_{BZ_n,EGT_1}(t) \\ \ddots & \iddots & \\ \vdots & P_{BZ_j,EGT_i}(t) & \vdots \\ \iddots & \ddots & \\ P_{BZ_1,EGT_m}(t) & \cdots & P_{BZ_n,EGT_m}(t) \end{bmatrix} \quad (2)$$

where
- i is the *"index of EGTs"* ranging from 1 to m
- j is the *"index of BZs"* ranging from 1 to n

The size of matrix T(t) depends on the number of EGTs and number of BZs that are considered in a respective study.

The next step is a normalization to 1 MWh by dividing by the total hourly electricity generation (Σ EGT_i) in a bidding zone (BZ_j) (also considering imports) during each hour (t) of the year. This step will be necessary to determine the $CO_{2eq.}$ intensity for 1 MWh of generated electricity in a respective BZ has. Matrix N(t) (where "N" stands for Normalization) is set up as follows:

$$N(t) = \begin{bmatrix} \frac{1}{\sum_i P_{BZ_1,EGT_i}}(t) & 0 & 0 & 0 & 0 \\ 0 & \ddots & 0 & 0 & 0 \\ 0 & 0 & \frac{1}{\sum_i P_{BZj,EGT_i}}(t) & 0 & 0 \\ 0 & 0 & 0 & \ddots & 0 \\ 0 & 0 & 0 & 0 & \frac{1}{\sum_i P_{BZ_n,EGT_i}}(t) \end{bmatrix} \quad (3)$$

where
- i is the *"index of EGTs"* ranging from 1 to m
- j is the *"index of a specific BZ"* ranging from 1 to n

The matrix P(t) (where "P" stands for Production) is the share of electricity generation from each EGT ($P_{EGT,t}$) and the imports on the total hourly electricity generation in a respective BZ, still considering electricity imports as an EGT. Regarding the electricity imports to a BZ, it is distinguished between imports from BZs with a fixed $CO_{2eq.}$ intensity of the electricity mix ($P_{Import,fix,t}$)[2] and imports from BZs with a variable electricity mix ($P_{Import,var,t}$). P(t) considers the share of each EGT in the electricity mix of a specific BZ, but does not consider the share of each EGT in the imports. P(t) is calculated by multiplying T(t) and N(t):

$$P(t) = T(t) \cdot N(t) = \begin{bmatrix} P_{EGT,t} \\ P_{Import,fix,t} \\ P_{Import,var,t} \end{bmatrix} \quad (4)$$

$P_{EGT,t}$ and $P_{Import,fix,t}$ can be combined to $P_{EGT,fix}$:

$$P_{EGT,fix} = \begin{bmatrix} P_{EGT,t} \\ P_{Import,fix,t} \end{bmatrix} \quad (5)$$

The next steps show how to include the share of each EGT in the electricity mix of neighboring BZs into the electricity mix of the BZ in question. In general, the balance between electricity consumption and electricity generation has to be satisfied at all times for each BZ. For each BZ, the sum of import and generation of electricity generated by a specific EGT should be consumed in the BZ or exported. This complies with the logic of a multi-regional input-output (MRIO) framework, which can be used for calculating consumption-based emissions for an entire country or region (Wiebe, 2016). Based on the MRIO approach, the electricity balance can be expressed as

$$M = P_{EGT,fix} + M \cdot P_{Import,var,t}, \quad (6)$$

with *M* (where "M" stands for Mix) as the share of each EGT (and boundary BZ) on the electricity use of BZ *j* and the exports from BZ *j*. Solving equation (6) for *M* is done by

$$M_{(i,j)} = P_{EGT,fix} \cdot \left(I - P_{Import,var,t}\right)^{-1} \cdot \quad (7)$$

where *I* is an identity matrix. *Matrix $M_{(i,j)}$ contains the share of each EGT (i) (and boundary BZ) on the electricity use and exports from BZ (j).* A new matrix is computed for each hour of the year.

The ***average $CO_{2eq.}$ intensity of a BZ for every hour of the year*** is calculated by

$$e_j(t) = \sum_{i=1}^{m} ef_{EGT_i} \cdot M_{(i,j),} \quad (8)$$

where *t* is the hour of the year, *i* is the *"index of EGTs"* ranging from 1 to m, *j* is the *"index of a specific BZ"* ranging from 1 to n and ef_{EGT_i} is a vector containing the emission factors of the EGTs.

If a different $CO_{2eq.}$ factor should be considered for a same electricity generation technology, but for a different plant efficiency, plant age or country, a new EGT should be defined for each different $CO_{2eq.}$ factor considered.

[2] These are the boundary BZs where the $CO_{2eq.}$ intensity is given as a boundary condition to the calculation and therefore not calculated (such as Russia, Estonia, Poland, Belgium and Great Britain).

4. RESULTS

The import from 2nd tier BZs have a lower impact on the average $CO_{2eq.}$ intensity of the target BZs (here Norway) than 1st tier BZs. Therefore, the influence of the direct imports from 1st tier BZs on the average $CO_{2eq.}$ intensities of Norwegian BZs are rather investigated. Average $CO_{2eq.}$ intensities for *Scenario 1* and *Scenario 2* are presented in Figure 2(a) and (b). The case study is done for the year 2015.

4.1 Hourly average $CO_{2eq.}$ intensities for all Norwegian bidding zones

Figure 2(a) shows the calculated $CO_{2eq.}$ intensity for each Norwegian BZ using *Scenario 1*. It can be seen that NO2 has the lowest intensity most of the year, which can be explained by the absence of gas power plants in this BZ. NO2 also shows the highest variations in the hourly average $CO_{2eq.}$ intensities because it is the only Norwegian BZ with direct transmission lines to the Netherlands and Denmark. It can thus reach high peaks during hours of import from these two countries. NO4 has the highest average $CO_{2eq.}$ intensity because a relatively large share of the generation comes from the LNG production plant in Melkøya. Nevertheless, according to its sales license, this power plant generates electricity mostly for self-consumption. The power plant is connected to the grid either to buy electricity from the grid during the start-up of the power plant (e.g. after maintenance) or for frequency control of the grid (i.e. participation to the intra-day market), if required. The average $CO_{2eq.}$ intensities calculated using *Scenario 2* is presented in Figure 2(b). It is evident that the average $CO_{2eq.}$ intensity decreases significantly in all BZs compared to Scenario 1 except for NO2 and NO5.

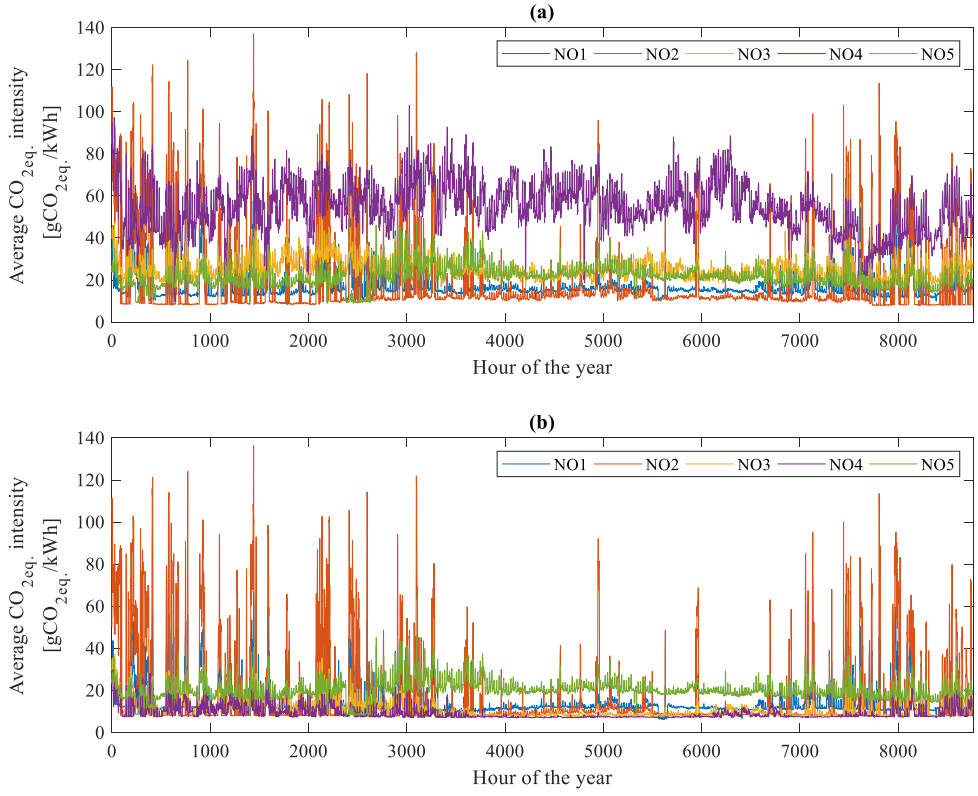

Figure 2: Hourly average $CO_{2eq.}$ intensity of the electricity mix in Norwegian bidding zones for (a) Scenario 1 and (b) Scenario 2.

In fact, the annual-averaged $CO_{2eq.}$ intensity of NO2 decreases as well but only slightly compared to other BZs. As NO2 does not have fossil fuel power plants, the peaks in NO2 remain similar to Scenario 1 since electricity imports from the Netherlands and Denmark remain unchanged between Scenario 1 and Scenario 2. The average $CO_{2eq.}$ intensities in NO5 remain similar because the thermal power plant in Mongstad is selling its electricity to the grid and is therefore also considered in Scenario 2. The average $CO_{2eq.}$ intensities for SE1, SE4, DK1, Finland and the Netherlands are plotted for comparison in Figure 3. As expected, the Norwegian electricity mix has low average $CO_{2eq.}$ intensities compared to other countries. For instance, it can be seen that the $CO_{2eq.}$ intensity in NO2 is only a fraction of the intensities of other non-Norwegian BZs. Therefore, the average $CO_{2eq.}$ intensity in NO2 is expected to increase during times of electricity imports from the BZs DK1 and NL.

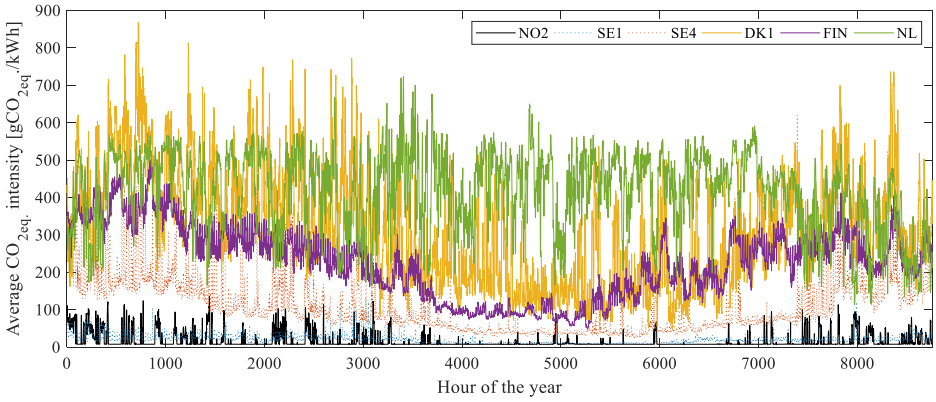

Figure 3: Hourly $CO_{2eq.}$ intensity of the electricity mix for several bidding zones (data of Scenario 2).

Due to the fact that the electricity generation in Norway is almost entirely from hydropower, the impact of imports of fossil fuel-based electricity on the average $CO_{2eq.}$ intensity is very strong. In other countries, for example Finland or the Netherlands, the impact of fossil fuels on the average $CO_{2eq.}$ intensity is lower.

Figure 4 illustrates the dependency of the average $CO_{2eq.}$ intensity on the electricity imports for four Scandinavian BZs: NO2, SE4, DK1 and FIN. It can be seen that the average $CO_{2eq.}$ intensity of NO2 systematically increases with an increasing share of imports in the electricity mix. On the contrary, the dependency is the opposite in SE4. Every time there is a higher fraction of imports, the $CO_{2eq.}$ intensity decreases because electricity is mostly imported from SE3 which has a higher share of renewables in the grid. A fraction of imports normalized by the total electricity use above 1 can occur when a BZ is importing from another BZ while at the same time the total electricity use in this BZ is lower than the total electricity imports (then this BZ imports and exports electricity at the same time). This happens frequently in SE4. Regarding DK1, it can be seen that the average $CO_{2eq.}$ intensity is only slightly dependent on the electricity imports while the average $CO_{2eq.}$ intensity of the Finnish electricity mix is barely influenced by the electricity imports. This clearly shows that the need to account for imports in the evaluation of the average $CO_{2eq.}$ intensity strongly depends on the country.

In the following, a closer look is taken at the average $CO_{2eq.}$ intensities in NO2 because this is the Norwegian BZ with the highest fluctuations in the $CO_{2eq.}$ intensity. Several correlations are investigated: $CO_{2eq.}$ intensity as a function of (a) the hourly electricity use in NO2, (b) the hourly electricity spot price in NO2, (c) the hourly electricity imports from the Netherlands and Denmark to NO2 and (d) the hydropower reservoir level. The investigation considers the average $CO_{2eq.}$ intensity of Scenario 2.

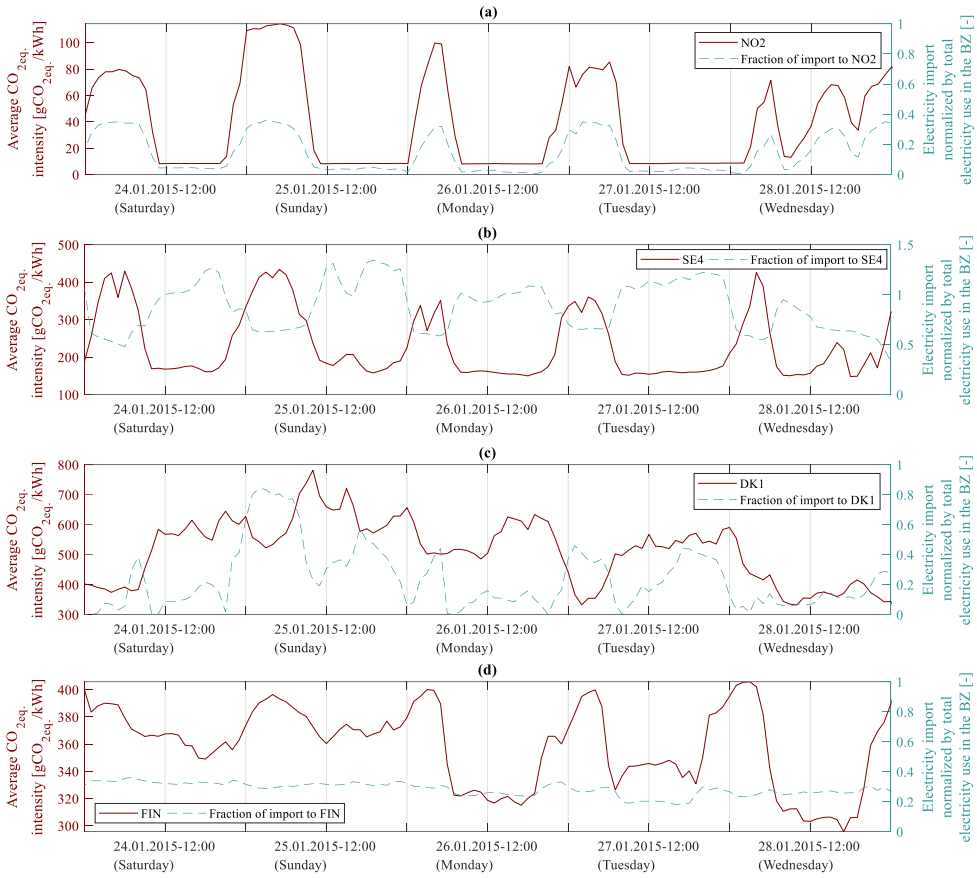

Figure 4. Average $CO_{2eq.}$ intensity and fraction of imports on the total electricity use of a BZ for five exemplary days for 4 Scandinavian BZs: (a) NO2, (b) SE4, (c) DK1 and (d) FIN.

4.2 Correlation of average $CO_{2eq.}$ intensity and electricity use

Figure 5 shows that the average $CO_{2eq.}$ intensity is usually low during times of high electricity use and vice versa. Cheap electricity is usually bought from abroad during periods of low electricity use, while electricity generation using hydropower only starts during periods of higher electricity prices corresponding to periods with higher loads.

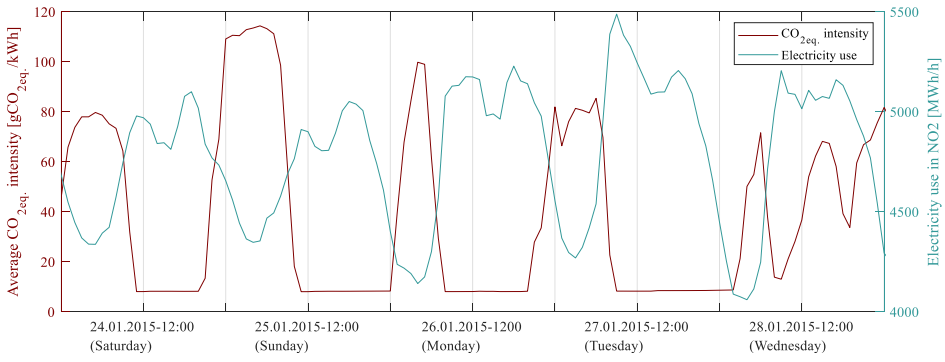

Figure 5: Average $CO_{2eq.}$ intensity and electricity use in NO2 for five exemplary days in January 2015.

This dependency is of importance when discussing the average $CO_{2eq.}$ intensity as a control signal for building energy systems (see section 5).

4.3 Correlation of average $CO_{2eq.}$ intensity and electricity spot price

Figure 6 presents the correlation between the average $CO_{2eq.}$ intensity and the electricity spot price in NO2. It is obvious that low average $CO_{2eq.}$ intensities occur during hours of high prices. High average $CO_{2eq.}$ intensities occur mostly during low-price hours with prices being typically low during night time when the electricity use is low. It should be mentioned that prices are fluctuating daily as well as seasonally. Spot prices during summer time are typically lower than during winter time.

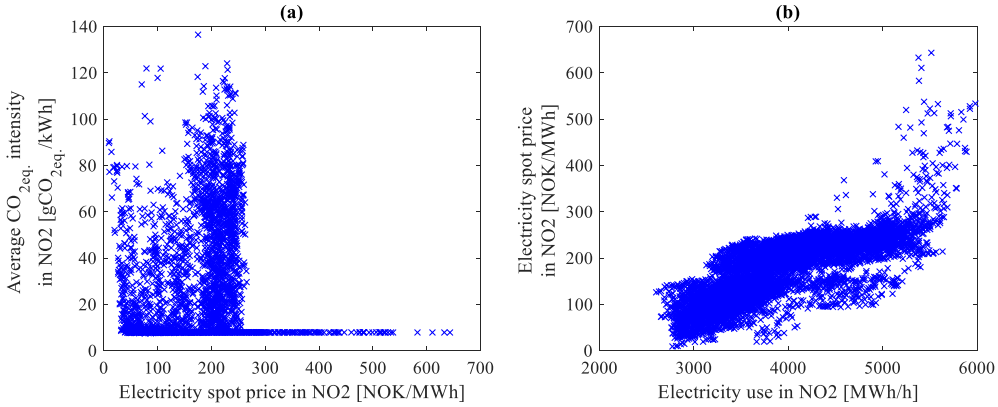

Figure 6: Correlation between (a) the $CO_{2eq.}$ intensity and electricity spot price in NO2 and (b) the electricity spot price and the electricity use in NO2, both in 2015.

Therefore, a same electricity price can be a relatively low price in winter time, but a relatively high price in summer time. It can be seen from Figure 6(a) that there is a clear break at a spot price of about 270 NOK/MWh. Most of the electricity is used when spot prices are between 180 and 280 NOK/MWh (for 2015). As already mentioned, electricity is usually generated from hydropower as soon as the daily electricity demand is relatively high and thus the price as well. Figure 7 presents the spot price in NO2 and the average $CO_{2eq.}$ intensities of all Norwegian BZs for five exemplary days in January 2015.

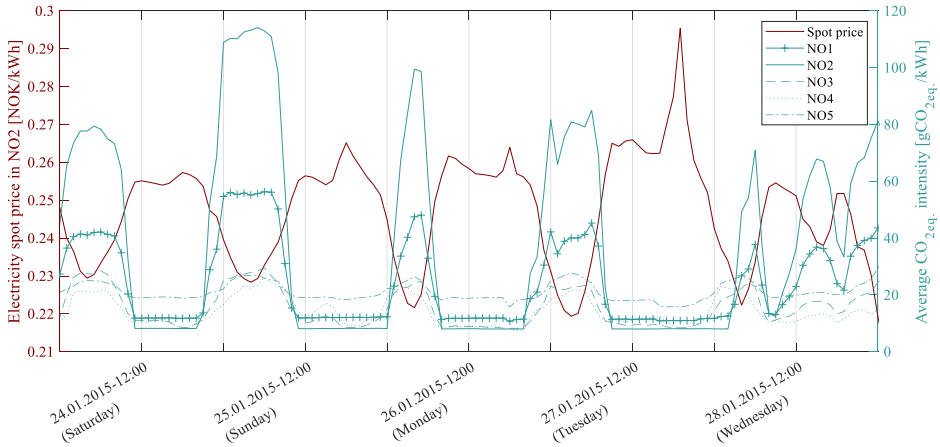

Figure 7: Electricity spot price in NO2 and average $CO_{2eq.}$ intensity in all Norwegian BZs for five exemplary days in January 2015.

As electricity is usually generated from hydropower during periods of high prices, the average $CO_{2eq.}$ intensity is low during these high-price periods typically leading to low $CO_{2eq.}$ intensities in the mornings and early evenings. The average $CO_{2eq.}$ intensity is usually high during night times due to electricity imports from the Netherlands and Denmark. This does not only affect the $CO_{2eq.}$ intensity of NO2 but subsequently impact the intensities of the other Norwegian BZs as a BZ can both import and export at the same time. This shows that it can be important to consider imports from 2nd tier BZs in some cases.

4.4 Correlation of average $CO_{2eq.}$ intensity and imports from DK and NL

The correlation between the average $CO_{2eq.}$ intensity in NO2 and its electricity imports from Denmark and the Netherlands is illustrated in Figure 8. It is evident that the average $CO_{2eq.}$ intensity in NO2 increases with more imported electricity. The different colors show three different ranges of the average $CO_{2eq.}$ intensity of DK1 to show the impact that the imported electricity with certain $CO_{2eq.}$ intensity has on the average $CO_{2eq.}$ intensity in NO2. Generally, the average $CO_{2eq.}$ intensity in NO2 is increased more rapidly if the average $CO_{2eq.}$ intensity of the imported electricity is high.

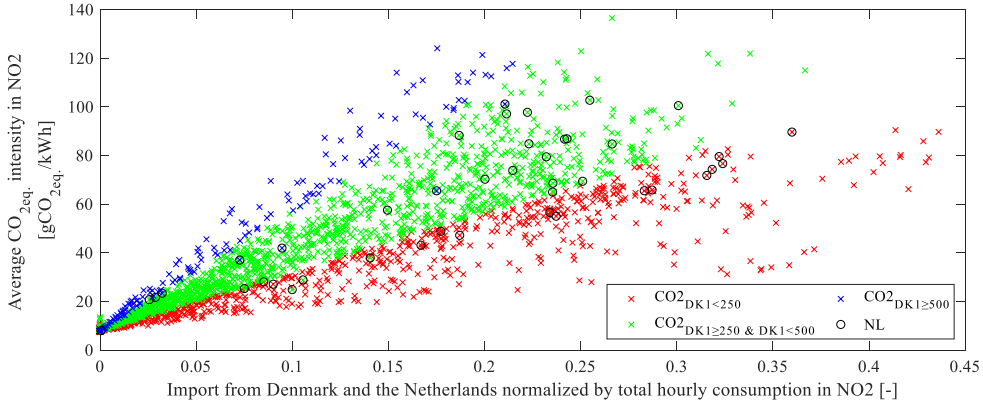

Figure 8: Correlation between the average $CO_{2eq.}$ intensity in NO2 and the electricity imports from NL and DK1 to NO2 in 2015 (colors show different magnitude of $CO_{2eq.}$ intensity of the imported electricity).

Electricity of low average $CO_{2eq.}$ intensity can be imported without increasing the intensity in NO2 significantly. If the share of imports from Denmark is high, but the average $CO_{2eq.}$ intensity in NO2 is still rather low, it indicates that the imported electricity has been generated from less

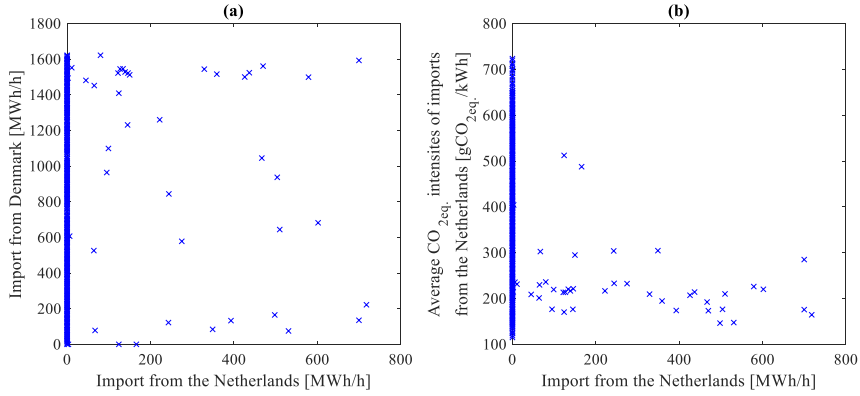

Figure 9: Correlation between (a) the imports from DK1 and imports from NL and (b) the average $CO_{2eq.}$ intensity of the imports from NL and the imports from NL.

carbon-intense technologies, such as wind power. Figure 8 does not directly show whether electricity is generated from wind or fossil fuels in DK1. It is reasonable to believe that the production is most probably from wind if the intensities in NO2 are below 20 $gCO_{2eq.}$/kWh. Figure 9 displays that electricity is imported from the Netherlands almost only in hours when there is also import from Denmark. There are only two hours throughout the whole year when NO2 imported from the Netherlands, but not from Denmark. The average $CO_{2eq.}$ intensity of the electricity imported from the Netherlands is between 150 and 300 $gCO_{2eq.}$/kWh for most of the hours.

4.5 Correlation of average $CO_{2eq.}$ intensity, hydropower reservoir level and total imports

Data for the hydropower reservoir levels in Norway is available with a weekly time resolution. In Figure 10(a), the weekly level of hydropower reservoirs in Norway is shown throughout the year. The level is at its highest at the end of autumn (week 40) when all the snow in the mountains has melted. A high electricity use during winter and shoulder season (Figure 10(b)) leads to depletion of the reservoirs. The filling level of the reservoirs is lowest just before the snow starts to melt in the mountains in spring (week 17) (Figure 10(a)). To find a correlation between weekly reservoir levels and hourly average $CO_{2eq.}$ intensities, these intensities are averaged over one week. Figure 11 shows that there is a positive correlation between the $CO_{2eq.}$ intensity in NO2 and the reservoir level, if the reservoir level is decreasing (winter and spring), but almost no correlation for increasing reservoir levels (summer and autumn). This is also supported by Figure 10(a) showing that there is less electricity import to NO2 when the water reservoir levels are increasing (week 18 to week 40 in 2015).

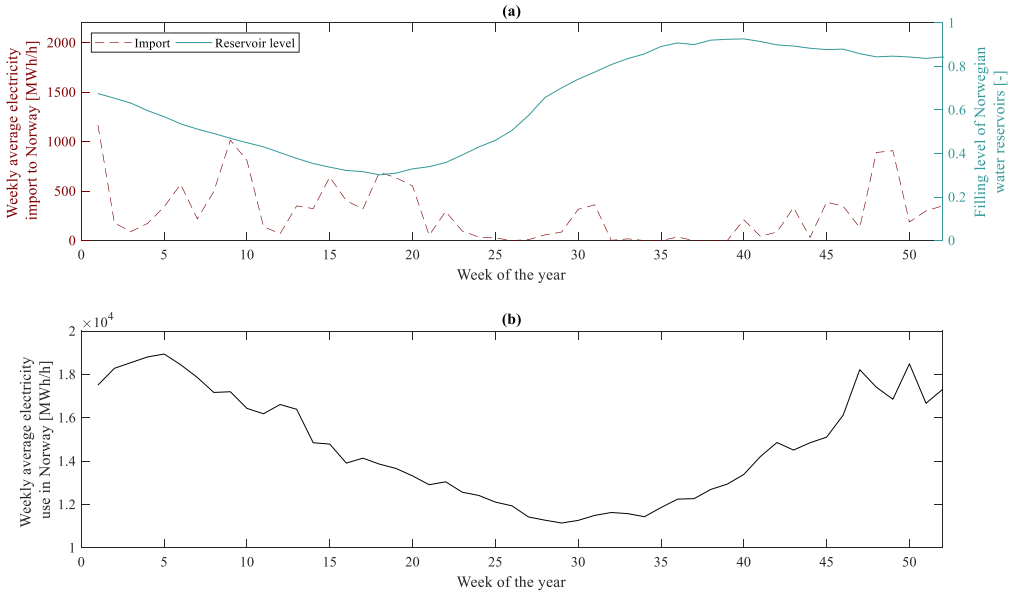

Figure 10: (a) Electricity imports to Norway (MWh/h) and weekly level of the Norwegian water reservoirs (-) and (b) electricity use in Norway (MWh/h) in 2015 (weekly average values).

It has to be pointed out that the management of the hydropower reservoirs is based on a cost-optimal planning depending on (a) the expected future electricity price, (b) the expected precipitations and the resulting expected water level in reservoirs as well as (c) the expected future electricity demands. Within this optimization, the minimum water reservoir level is

determined by national restrictions for waterways, while the maximum level that is possible without losing water and thus money is limited by the capacity of the reservoirs. Electricity imports to Norway are necessary in winter and early spring even though the water reservoirs are still rather full because precipitation and thus the water level of reservoirs are not predictable many months ahead. Some water is kept in the reservoirs to ensure electricity supply at all times. As discussed in section 4.3, Norway imports electricity on a daily basis when prices are low and exports when prices are high, independent of the season of the year.

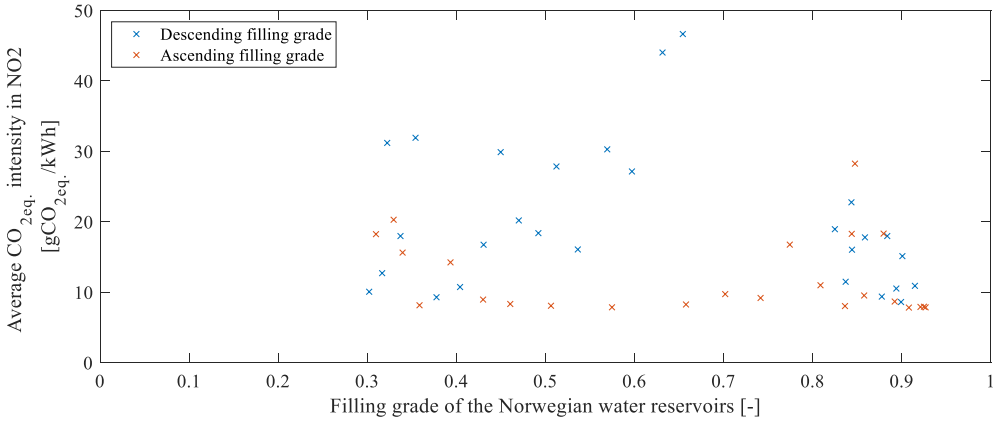

Figure 11: Correlation of $CO_{2eq.}$ intensity in NO2 and the hydropower reservoir level in Norway in 2015 (weekly average values)

5. DISCUSSION: APPLICABILITY IN BUILDING ENERGY SYSTEM CONTROL

In general, a low $CO_{2eq.}$ intensity is an indication for a high share of renewables and/or nuclear electricity generation. The application of the $CO_{2eq.}$ intensity as a control signal for the operation of building energy systems may help to reach the emission targets of the European Union. Even though it is a rather new approach, it has been used in several studies across Europe, for instance in Denmark (Dahl Knudsen & Petersen, 2016; Hedegaard et al., 2017; Heidmann Pedersen et al., 2017; Junker et al., 2018), Belgium (Patteeuw et al., 2015; Vandermeulen et al., 2017) and in Spain (Péan, Salom, & Ortiz, 2018). The control principle is rather straightforward as the basic idea is to avoid the use of electricity at times of high $CO_{2eq.}$ intensities of the electricity mix. This paper focuses on the evaluation of an hourly *average $CO_{2eq.}$ intensity* signal. Although the evaluation of a marginal $CO_{2eq.}$ intensity is not part of the scope, it is briefly mentioned here for the sake of completeness. Compared to an average $CO_{2eq.}$ intensity signal, a marginal $CO_{2eq.}$ intensity signal has the distinction of having stronger emission fluctuations and thus a higher emission savings potential, but a much more advanced methodology is required to calculate these marginal emissions.

Average and marginal $CO_{2eq.}$ intensities are two different concepts. The average $CO_{2eq.}$ intensity is the $CO_{2eq.}$/kWh emitted on average for the entire electricity consumption of the bidding zone, thus resulting from a mix of power plants. The marginal $CO_{2eq.}$ intensity is the $CO_{2eq.}$/kWh emitted for an additional kWh consumed, thus resulting from a single power plant. It may be argued that controlling a building will not affect the overall production but rather a single plant (or limited number of plants) and that marginal $CO_{2eq.}$ intensities are more coherent. Nevertheless, average factors have been extensively used in the past for buildings exporting electricity to the grid, such as Nearly Zero Energy Buildings or Zero Emission Buildings. These buildings often have large photovoltaic systems onsite.

The method proposed computes the average $CO_{2eq.}$ intensity based on the forecast of the electricity generation for the next days. It is a decoupled approach since the interaction between the supply side and the demand side is not considered. If a large number of buildings applies this $CO_{2eq.}$ intensity as a control signal, the overall electric load could be sufficiently affected so that the forecasted generation would not be optimized anymore for this load. For instance, if the $CO_{2eq.}$ signal is low, a large number of buildings may decide to favour consumption during this period of time. If the number of buildings is significant, a strong imbalance will appear between the real and predicted energy consumption. Balancing power would be needed, potentially with a power plant generating electricity with relatively high $CO_{2eq.}$ intensity (such as a coal-fired power plant). The resulting overall $CO_{2eq.}$ emissions can therefore be suboptimal. Ideally, a coupled model is required so that the impact of the demand response control is taken into account in the forecast of the electricity generation and corresponding $CO_{2eq.}$ emissions (Arteconi et al., 2016; Patteeuw et al., 2015).

Consequently, the proposed method suffers some limitations. Nevertheless, the market penetration of demand response in buildings is still limited and the method can be used as long as the number of buildings participating is rather low. Even though limited this approach is representative for most studies in building energy flexibility and, more generally, in building energy performance simulation. For example, regarding the evaluation of zero emission buildings, fixed average $CO_{2eq.}$ intensities of the electricity mix are usually assumed to calculate the emission balance. The use of an hourly average $CO_{2eq.}$ intensity for demand response would then remain coherent with that approach. In the EPBD method, the performance of buildings is evaluated using an average primary energy factor and not a marginal. Finally, the major advantage of the proposed methodology is its simplicity.

In general, a reduction of the energy use as well as the peak load during peak hours are desired to avoid exceeding the capacity of the transmission and/or the distribution grid. Advanced controls, such as predictive rule-based control or model-predictive control, can schedule the operation of energy systems to reduce the peak load. A study on CO_2 emissions of the electricity generation in Europe by (Graabak & Feilberg, 2011) has shown that marginal emissions could actually increase, if load shifting from peak to off-peak hours is performed and if the peak loads are covered by gas power plants. According to the merit order curve, fossil gas has higher marginal costs than hard coal, but reducing peak loads may lead to a lower share of gas power plants in the electricity mix, which will lead to an increase in marginal emissions as coal has a higher $CO_{2eq.}$ intensity than gas.

Norway is a special case in Europe because the electricity generation is almost fully renewable. When controlling a building's electricity use according to the average $CO_{2eq.}$ intensity in Norway, this paper has shown that the electricity consumption will be increased during peak hours, thus causing more stress on the grid. Thus, increased power loads at times of low $CO_{2eq.}$ intensities may amplify already existing peak loads, which could lead to grid congestions and possibly higher electricity prices, according to Figure 6. This would admittedly lead to decreased carbon emissions, but the transmission and distribution grid could get stressed even more. Regarding building HVAC control it is interesting to see that a control based on the average $CO_{2eq.}$ intensity of the electricity mix and a price-based control would lead to contradictory operation periods of the energy system meaning that minimizing operation costs is not compatible with minimizing CO_2 emissions (see Figure 7). This will be different in other countries with more thermal power plants.

6. CONCLUSION

This work presents a generic methodology for evaluating the average $CO_{2eq.}$ intensity of the electricity mix in a bidding zone also considering dynamic $CO_{2eq.}$ intensities of electricity imports from neighboring bidding zones. The method is based on the balance between *electricity production plus imports* and *electricity consumption plus exports*. The balance is satisfied for all BZs at each hour of the year. The methodology complies with the logic of a multi-regional input-output framework. Among possible applications, this $CO_{2eq.}$ intensity signal can be used to control the operation of a building HVAC system in order to minimize the overall $CO_{2eq.}$ emissions.

Input data about the hourly electricity generation per generation technology was retrieved from ENTSO-E. Information on the CO_2 factors of an electricity generation technology was based on Ecoinvent. Comparing the CO_2 factors from Ecoinvent and the IPCC report, it can be seen that these factors are significantly different depending on the assumptions taken for the specific CO_2 factors.

As a particular case of this method, the average $CO_{2eq.}$ intensity in Norway is evaluated as a function of (a) the electricity use in a BZ, (b) the electricity spot price, (c) the electricity import from foreign countries and (d) the filling level of the water reservoirs. In Norway, the average $CO_{2eq.}$ intensities are typically low during peak load hours because flexible hydropower plants prefer to operate at high electricity prices, when the electricity demand is usually high. Therefore, average $CO_{2eq.}$ intensities in Norway are low during high-price hours. The $CO_{2eq.}$ intensity can increase significantly as soon as electricity is imported from neighboring BZs because of a more carbon-intensive electricity generation outside Norway. For the particular case of Norway with high renewable share in the electricity generation, it is shown that it is important to consider electricity imports when evaluating the average $CO_{2eq.}$ intensity. The $CO_{2eq.}$ intensities are correlated to the filling grade of the Norwegian water reservoirs to a smaller extent. The amount of weekly electricity imports, and thus the average $CO_{2eq.}$ intensity, is to a certain extent correlated to an ascending and descending trend for the Norwegian reservoir level.

This work proves the importance of considering electricity imports and dynamic $CO_{2eq.}$ intensities of these imports when evaluating the average $CO_{2eq.}$ intensity of the electricity mix of a BZ for the case of Norway. It is shown that high electricity demands, high spot prices and low average $CO_{2eq.}$ intensities typically occur simultaneously. These correlations are specific to Norway, while in other countries with a higher share of thermal power plants, the correlations between electricity spot prices, electricity demands and average $CO_{2eq.}$ intensities of the electricity mix can be different.

Lastly, the paper discusses the applicability of a $CO_{2eq.}$ intensity control signal for the operation of building energy systems. The average $CO_{2eq.}$ intensity signal that is determined in this methodology can be applied in predictive controls for building energy systems, such as model-predictive control or predictive rule-based controls, by using the forecast of the hourly electricity generation provided by ENTSO-E. The proposed methodology to evaluate the hourly average $CO_{2eq.}$ intensity is a decoupled approach meaning that the interaction between the supply and demand side is not considered. A coupled approach should be used to take into account these interactions into the forecast of the electricity generation, if a significant number of buildings takes part in the demand response control.

ACKNOWLEDGEMENTS

The authors would like to acknowledge IEA EBC Annex 67 “Energy Flexible Buildings”, IEA HPT Annex 49 “Design and Integration of Heat Pumps for nZEBs” as well as the Research Centre on Zero Emission Neighbourhoods in Smart Cities (FME ZEN). Sebastian Stinner gratefully acknowledges that his contribution was supported by a research grant from E.ON Stipendienfonds im Stifterverband für die Deutsche Wissenschaft (project number T0087/29896/17).

REFERENCES

Arteconi, A., Patteeuw, D., Bruninx, K., Delarue, E., D’haeseleer, W., & Helsen, L. (2016). Active demand response with electric heating systems: Impact of market penetration. *Applied Energy*, *177*, 636–648. https://doi.org/10.1016/j.apenergy.2016.05.146

Dahl Knudsen, M., & Petersen, S. (2016). Demand response potential of model predictive control of space heating based on price and carbon dioxide intensity signals. *Energy and Buildings*, *125*, 196–204. https://doi.org/10.1016/j.enbuild.2016.04.053

Ecoinvent. (2016). www.ecoinvent.org. Retrieved from www.ecoinvent.org

EEA. (2018). Overview of electricity production and use in Europe. Retrieved April 12, 2018, from https://www.eea.europa.eu/data-and-maps/indicators/overview-of-the-electricity-production-2/assessment

ENERGINET.DK. (2011). CO 2 -prognoser. Retrieved from https://www.energinet.dk/-/media/Energinet/El-RGD/El-CSI/Dokumenter/Data/CO2-prognoser.pdf.

Graabak, I., & Feilberg, N. (2011). *CO2 emissions in a different scenarios of electricity generation in Europe. SINTEF Energy Research*.

Hedegaard, R. E., Pedersen, T. H., & Petersen, S. (2017). Multi-market demand response using economic model predictive control of space heating in residential buildings. *Energy and Buildings*, *150*, 253–261. https://doi.org/10.1016/j.enbuild.2017.05.059

Heidmann Pedersen, T., Hedegaard, R. E., & Petersen, S. (2017). Space heating demand response potential of retrofitted residential apartment blocks. *Energy & Buildings*, *141*, 158–166. https://doi.org/10.1016/j.enbuild.2017.02.035

IEA, & Nordic Energy Research. (2016). *Nordic Energy Technology Perspectives 2016 Cities, flexibility and pathways to carbon-neutrality*. Oslo. Retrieved from http://www.nordicenergy.org/wp-content/uploads/2016/04/Nordic-Energy-Technology-Perspectives-2016.pdf

Junker, R. G., Azar, A. G., Lopes, R. A., Lindberg, K. B., Reynders, G., Relan, R., & Madsen, H. (2018). Characterizing the energy flexibility of buildings and districts. *Applied Energy*, *225*(February), 175–182. https://doi.org/10.1016/j.apenergy.2018.05.037

Krey, V., Masera, O., Blanforde, G., Bruckner, T., Cooke, R., Fish-Vanden, K., Haberl, H., Hertwich, E., Kriegler, E., Müller, D., Paltsev, S., Price, L., Schlömer, S., Uerge-Vorsatz, D., Van Vuuren, D., Zwickel, T. (2014). Annex II: Metrics & Methodology. *Climate Change 2014: Mitigation of Climate Change. Contribution of Working Group III to the Fifth Assessment Report of the Intergovernmental Panel on Climate Change*, 1281–1328. Retrieved from http://www.ipcc.ch/pdf/assessment-report/ar5/wg3/ipcc_wg3_ar5_annex-ii.pdf

Nord Pool Spot. (2016). www.nordpoolspot.com/historical-market-data. Retrieved from www.nordpoolspot.com/historical-market-data

NordPoolGroup. (2018a). NordPool-About us. Retrieved from https://www.nordpoolgroup.com/About-us/

NordPoolGroup. (2018b). NordPool. Retrieved June 13, 2018, from https://www.nordpoolgroup.com/message-center-container/newsroom/exchange-message-list/2018/q2/nord-pool-key-statistics--may-2018/

NordPoolGroup. (2018c). NordPool Bidding Areas. Retrieved April 28, 2018, from https://www.nordpoolgroup.com/the-power-market/Bidding-areas/.

Patteeuw, D., Bruninx, K., Arteconi, A., Delarue, E., D'haeseleer, W., & Helsen, L. (2015). Integrated modeling of active demand response with electric heating systems coupled to thermal energy storage systems, *151*, 306–319. https://doi.org/10.1016/j.apenergy.2015.04.014

Péan, T. Q., Salom, J., & Ortiz, J. (2018). Environmental and Economic Impact of Demand Response Strategies for Energy Flexible Buildings. *Proceedings of BSO 2018*, (September), 277–283.

Schlömer, S., Bruckner, T., Fulton, L., Hertwich, E., McKinnon, A., Perczyk, D., Roy, J., Schaeffer, R., Sims, R., Smith, P., Wiser, R. (2014). Annex III: Technology-Specific Cost and Performance Parameters. *Climate Change 2014: Mitigation of Climate Change. Contribution of Working Group III to the Fifth Assessment Report of the Intergovernmental Panel on Climate Change*, 1329–1356. https://doi.org/https://www.ipcc.ch/pdf/assessment-report/ar5/wg3/ipcc_wg3_ar5_annex-iii.pdf

Tomorrow. (2016). Electricity map Europe. Retrieved April 13, 2018, from https://www.electricitymap.org/?wind=false&solar=false&page=country&countryCode=NO

Tomorrow. (2018). CO2-equivalent Model Explanation. Retrieved May 4, 2018, from https://github.com/tmrowco/electricitymap-contrib/blob/master/CO2eq Model Explanation.ipynb

Vandermeulen, A., Vandeplas, L., Patteeuw, D., Sourbron, M., & Helsen, L. (2017). Flexibility offered by residential floor heating in a smart grid context : the role of heat pumps and renewable energy sources in optimization towards different objectives . In *12th IEA Heat Pump Conference 2017*. Rotterdam, Netherlands.

Wiebe, K. S. (2016). The impact of renewable energy diffusion on European consumption-based emissions†. *Economic Systems Research*, *28*(2), 133–150. https://doi.org/10.1080/09535314.2015.1113936

PAPER 2

Evaluation Method for the Hourly Average $CO_{2eq.}$ Intensity of the Electricity Mix and Its Application to the Demand Response of Residential Heating

Clauß J[1], Stinner S[1], Solli C[2], Lindberg KB[3,4], Madsen H[5,6], Georges L[1,6]

[1] Norwegian University of Science and Technology NTNU, Department of Energy and Process Engineering, Trondheim, Norway

[2] NTNU, Property Division, Trondheim, Norway

[3] NTNU, Department of Electric Power Engineering, Trondheim, Norway

[4] SINTEF Building and Infrastructure, Oslo, Norway

[5] DTU Technical University of Denmark, DTU Compute, Copenhagen, Denmark

[6] NTNU, (ZEN-project), Trondheim, Norway

This paper is published in *Energies*, March 2019; 12(7):1345.

energies

MDPI

Article

Evaluation Method for the Hourly Average $CO_{2eq.}$ Intensity of the Electricity Mix and Its Application to the Demand Response of Residential Heating

John Clauß [1,*], Sebastian Stinner [1], Christian Solli [2], Karen Byskov Lindberg [3,4], Henrik Madsen [5,6] and Laurent Georges [1,6]

1 Norwegian University of Science and Technology NTNU, Department of Energy and Process Engineering, Kolbjørn Hejes vei 1a, 7491 Trondheim, Norway; sebastian.stinner@rwth-aachen.de (S.S.); laurent.georges@ntnu.no (L.G.)
2 NTNU, Property Division, Høgskoleringen 8, 7034 Trondheim, Norway; christian.solli@ntnu.no
3 NTNU, Department of Electric Power Engineering, 7491 Trondheim, Norway; karen.lindberg@sintef.no
4 SINTEF Building and Infrastructure, Pb 124 Blindern, 0314 Oslo, Norway
5 DTU Technical University of Denmark, DTU Compute, Asmussens Allé, Building 303B, 2800 Kgs. Lyngby, Denmark; hmad.dtu@gmail.com
6 Research Center on Zero Emission Neighbourhoods in Smart Cities, Trondheim 7491, Norway
* Correspondence: john.clauss@ntnu.no

Received: 1 March 2019; Accepted: 2 April 2019; Published: 8 April 2019

Abstract: This work introduces a generic methodology to determine the hourly average $CO_{2eq.}$ intensity of the electricity mix of a bidding zone. The proposed method is based on the logic of input–output models and avails the balance between electricity generation and demand. The methodology also takes into account electricity trading between bidding zones and time-varying $CO_{2eq.}$ intensities of the electricity traded. The paper shows that it is essential to take into account electricity imports and their varying $CO_{2eq.}$ intensities for the evaluation of the $CO_{2eq.}$ intensity in Scandinavian bidding zones. Generally, the average $CO_{2eq.}$ intensity of the Norwegian electricity mix increases during times of electricity imports since the average $CO_{2eq.}$ intensity is normally low because electricity is mainly generated from hydropower. Among other applications, the $CO_{2eq.}$ intensity can be used as a penalty signal in predictive controls of building energy systems since ENTSO-E provides 72 h forecasts of electricity generation. Therefore, as a second contribution, the demand response potential for heating a single-family residential building based on the hourly average $CO_{2eq.}$ intensity of six Scandinavian bidding zones is investigated. Predictive rule-based controls are implemented into a building performance simulation tool (here IDA ICE) to study the influence that the daily fluctuations of the $CO_{2eq.}$ intensity signal have on the potential overall emission savings. The results show that control strategies based on the $CO_{2eq.}$ intensity can achieve emission reductions, if daily fluctuations of the $CO_{2eq.}$ intensity are large enough to compensate for the increased electricity use due to load shifting. Furthermore, the results reveal that price-based control strategies usually lead to increased overall emissions for the Scandinavian bidding zones as the operation is shifted to nighttime, when cheap carbon-intensive electricity is imported from the continental European power grid.

Keywords: predictive rule-based control; hourly $CO_{2eq.}$ intensity; demand response; energy flexibility

1. Introduction

A transition to a low-carbon energy system is necessary to reduce its environmental impact in the future. This implies a reduction of $CO_{2eq.}$ emissions on the electricity supply side by making use of intermittent renewable energy sources. To fully exploit the electricity generated from these

intermittent energy sources, deploying demand side flexibility is crucial [1]. Regarding building heating systems, demand side flexibility is the margin by which a building can be operated while still fulfilling its functional requirements [2]. From a global perspective, potential emission savings from the building sector are large since the building sector is responsible for 30% of the total energy use [3]. Several studies point out the importance of demand side management to improve the interaction between buildings and the electricity grid [1,4–8]. Progressively decreasing prices for sensing, communication, and computing devices will open up possibilities for improved controls for demand response (DR) as future management systems will be more affordable. A number of studies have investigated the building energy flexibility with a special focus on building heating systems [9–16]. In those studies, DR measures have been applied to electric heating systems, such as heat pump systems or direct electric heating systems.

DR measures can be applied to control the electricity use for the heating of buildings depending on power grid signals [12]. The most common signal for DR is the electricity spot price [15–20], but the $CO_{2eq.}$ intensity of the electricity mix [15,21–25], the share of renewables in the electricity mix [9,26] or voltage fluctuations [27] are applied as well.

DR measures are implemented into control strategies, such as predictive rule-based controls (PRBC) or more advanced controls, e.g., optimal control or model-predictive controls (MPC). PRBCs rely on pre-defined rules to control the energy system, where temperature set-points (TSP) for space heating (SH) or domestic hot water (DHW) heating are usually varied to start or delay the operation of the heating system depending on the control signal. These rules are rather straightforward to implement, but a careful design of the control rules is necessary. MPC solves an optimization problem but is more expensive to develop, for instance the identification of a model used for control is acknowledged as the most critical part in the design of an MPC [28,29]. PRBCs can be a good compromise to advanced controls because PRBC is simpler, but can still be effective in reducing operational costs or saving carbon emissions [29].

By applying the carbon intensity as a penalty signal for indirect control, the operation of a heating system can be shifted to times of low $CO_{2eq.}$ intensity in the grid mix using thermal storage. In general, the $CO_{2eq.}$ intensity can be used as an indicator of the share of renewable energies in the electricity mix. Applying the $CO_{2eq.}$ intensity as a penalty signal to operate building energy systems can help to reach the emission targets of the European Union. In Norway, electricity is mostly generated from hydropower. However, an increased interaction between the continental European and the Norwegian power grids is expected in the future [30]. As Norway has a very limited number of fossil fuel power plants for electricity generation, the hourly average $CO_{2eq.}$ intensity of the electricity mix already strongly depends on the electricity exchanges with neighboring bidding zones (BZ). Generally, the CO_2 price is seen as an essential driver for the transition to a low-carbon society [30]. This CO_2 price is expected to increase in the future so that the application of a $CO_{2eq.}$ intensity signal for control purposes is likely to gain importance. Compared to the electricity spot price, the use of the $CO_{2eq.}$ intensity of the electricity mix as a control signal is not as common because this control signal is not readily available. To the author's knowledge, in Europe, only the transmission system operator (TSO) for Denmark, Energinet, provides information on the average $CO_{2eq.}$ intensity of the electricity mix with an hourly resolution and at no charge. This may also be the reason why most studies that use $CO_{2eq.}$ intensity as a penalty signal for heating were performed for Denmark and conducted only rather recently: Vogler-Finck et al. [21], Pedersen et al. [22], Hedegaard et al. [23], and Knudsen et al. [24] use the data from Energinet in their DR studies for the heating of residential buildings.

They European power grid is highly interconnected. The leading power market in Europe is NordPool, which provides a day-ahead as well as an intra-day market. NordPool mainly operates in Scandinavia, UK, Germany, and the Baltics [31]. It is owned by the Scandinavian TSOs (Norway, Sweden, Denmark, and Finland) and the Baltic TSOs (Estonia, Lithuania, and Latvia) [32]. In order to avoid bottlenecks in the transmission system, BZs are created with different electricity prices.

One country can have several BZs [33]. Norway consists of five BZs, each of them having physical connections to neighboring BZs that enables electricity imports and exports (Figure 1).

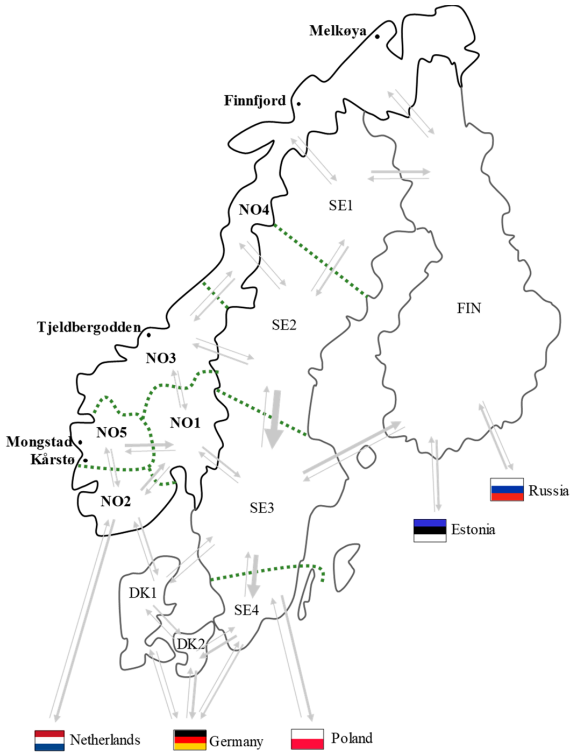

Figure 1. Overview of the Scandinavian power market bidding zones, also including gas-fired power plants in Norway (adjusted from [30]).

The main contributions of this paper are twofold. Firstly, a methodology for calculating the hourly average $CO_{2eq.}$ intensity of the electricity mix in an interconnected power grid is developed. The methodology is generic and takes into account the hourly average $CO_{2eq.}$ intensities of the electricity traded between neighboring BZs (imports and exports). The proposed method resorts to the logic of multi-regional input–output models (MRIO) [34]. Input–output models are usually used to perform energy system modeling in combination with an economic analysis considering different industry sectors [35–37]. They are based on the assumption that there always is a balance between consumption and generation for the whole system. In the present work, this logic can be applied for electricity where BZs are used instead of industry sectors. As an example, this paper evaluates the hourly average $CO_{2eq.}$ intensity for several Scandinavian BZs using the electricity production data for the year 2015. Emissions related to an electricity generation technology are considered on a life-cycle perspective. Electricity losses in the transmission and distribution grid are neglected. The input data required to calculate the average $CO_{2eq.}$ intensity is not readily available. Therefore, this work does not only provide the methodology to determine the $CO_{2eq.}$ intensities but also guidelines on where to retrieve and how to structure the input data to apply the proposed methodology.

Secondly, studies that focus on the evaluation of hourly $CO_{2eq.}$ intensities usually do not consider the detailed control of the HVAC system, whereas most studies that specifically focus on the heating system control do not comment on the methodology for determining the $CO_{2eq.}$ intensity. Therefore, the paper investigates how the characteristics of the $CO_{2eq.}$ intensity used as control signal influence

the overall emission savings. This is done using the case study of residential heating where DR is performed using the $CO_{2eq.}$ intensity of several Scandinavian BZs. A detailed description of the HVAC system and its control is provided which has been spotted as a major short-coming of the other existing approaches that primarily focus on the $CO_{2eq.}$ intensity evaluation.

2. Review of Existing Evaluation Methods for $CO_{2eq.}$ Intensity

Generally, evaluation methods for the hourly $CO_{2eq.}$ intensities of the electricity mix can be categorized as presented in Table 1. In a de-coupled approach, the electricity demand and supply sides do not influence each other. On the contrary, in a coupled approach, the interaction between the demand and supply sides is taken into account. For example, if a large number of buildings would apply the average $CO_{2eq.}$ intensity as a penalty signal, the resulting electric load could be affected and thus the predicted generation would not be optimized for this load anymore. Ideally, a coupled approach should be used to take into account DR in the prediction of the electricity generation and the respective $CO_{2eq.}$ emissions [26,38,39]. Furthermore, average and marginal $CO_{2eq.}$ intensities are two distinct concepts. Marginal emissions are the emissions from one additional kWh generated/consumed and, consequently, it results from a single power plant. On the contrary, the average $CO_{2eq.}$ intensity is the $CO_{2eq.}$/kWh emitted on average from the entire electricity generation of the BZ. It thus results from a mix of power plants. On the one hand, it could be argued that the marginal $CO_{2eq.}$ intensity is most coherent for the control of a limited number of buildings because they will rather affect a single plant than the overall production. On the other hand, average $CO_{2eq.}$ intensities (or factors) have been used extensively in the past for buildings exporting electricity to the grid, e.g., Zero Emission Buildings or Nearly Zero Energy Buildings. Studies mostly focusing on the life-cycle assessment (LCA) of buildings often use average $CO_{2eq.}$ intensities rather than marginal intensities.

Table 1. Categorization of methodologies to evaluate $CO_{2eq.}$ intensities of the electricity mix (marked as 'CO_2') or determine the optimal dispatch and unit commitment in electricity grids (marked as 'EL').

De-Coupled Approach		Coupled Approach	
Average	**Marginal**	**Average**	**Marginal**
Energinet [40] (CO_2) Vandermeulen et al. [9] (CO_2) Milovanoff et al. [41] (CO_2) Roux et al. [42] (CO_2) Tomorrow [43] (CO_2)	Bettle et al. [44] (CO_2) Hawkes [45] (CO_2) Peán et al. (based on Hawkes) [25] (CO_2) Corradi [46] (CO_2)	Graabak [47] (CO_2)	Patteeuw et al. [26] (EL) Arteconi et al. (based on Patteeuw) [38] (EL) Graabak et al. [47] (CO_2, EL) Askeland et al. [48] (EL) Quoilin et al. [49] (EL)

2.1. De-Coupled Approach

The evaluation methodology of the TSO Energinet for determining the $CO_{2eq.}$ intensity of the Danish electricity mix has two distinct simplifications: (1) the methodology considers only the operational phase (meaning without the life-cycle perspective) and (2) the $CO_{2eq.}$ intensity of the imports from neighboring countries are assumed to be constant. For example, electricity imports from Norway are assumed to be 9 g/kWh, from Germany 415 g/kWh and from Sweden 28 g/kWh [40].

Vandermeulen et al. [9] aim at maximizing the electricity use of residential heat pumps at times of high shares of renewable energy generation in the Belgian power grid. Data from the Belgian TSO, Elia, is used. It is not stated whether electricity imports are considered.

Milovanoff et al. [41] determine the environmental impacts of the electricity consumption in France for the years 2012 to 2014. They calculate 'impact factors' for electricity generation and consumption, where the impact factor for consumption agrees with the environmental impacts per kWh consumed including country-specific electricity production and trades. Regarding the electricity trades with neighboring BZs, it is assumed that the impact of the electricity imports to France equals the impact of the electricity generated in the BZ France is importing from, without taking exports and imports between France' neighboring BZs into account. Even though the methodology does not take

into account the electricity trades between neighboring BZs, it is pointed out that dynamic data of electricity imports and exports should be considered for calculating $CO_{2eq.}$ intensities of the electricity consumption. Milovanoff et al. as well as Roux et al. [42] make use of the Ecoinvent data base version 3.1 which provides CO_2 factors for electricity generation technologies considering the whole life-cycle of a technology. Roux et al. calculate hourly average $CO_{2eq.}$ intensities of the electricity generation and consumption in France for the year 2013. Their study focuses on the magnitude of errors when a yearly-average factor for the electricity mix is used instead of an hourly-average factor varying throughout the year. However, it is not stated how the $CO_{2eq.}$ intensities of the imports are considered in the study.

The company Tomorrow launched a website which shows the hourly average $CO_{2eq.}$ intensity for most European countries in real time [50]. Data on the electricity generation per production technology in a BZ is taken from ENTSO-E. Furthermore, trading between BZs as well as time-varying $CO_{2eq.}$ intensities are considered in their models (Tomorrow, 2018), but a license has to be purchased to get access to the data. Their method is based on the electricity balance between the supply and demand side. The hourly $CO_{2eq.}$ intensities of each BZ are considered as vectors in a linear equation system, which is solved for the $CO_{2eq.}$ intensity for each hour of year.

Bettle et al. [44] calculate marginal emission factors for Wales and England for the year 2000, based on 30 min data of a full year for all generating power plants considering all plants individually. Imports are not considered in their study. They found that the marginal emission factor is usually higher than the average emission factor (up to 50% higher). Thus, the average factor is likely to underestimate the carbon-savings potential.

Hawkes [45] estimates marginal CO_2 emission rates for Great Britain, based on data from 2002 to 2009. The emission rate is termed marginal emission factor and corresponds to the CO_2 intensity of the electricity not used as a result of a DR measure. The approach follows a merit-order approach and thus applies only to countries where the electricity generation is primarily based on fossil-fuel technologies. The methodology does not consider electricity imports from neighboring BZs. They point out a clear correlation between the total system load and the marginal emission factor, showing high emission factors during times of high system loads.

Peán et al. [25] determine marginal emission factors for Spain for the year 2016 based on the methodology proposed by Hawkes [45]. Similar to Hawkes, electricity imports are not considered.

Corradi [46] aims at calculating the marginal $CO_{2eq.}$ intensity of the electricity using machine learning. Flow tracing [51] is used to trace the flow of the electricity back to the area where the marginal electricity is generated. Following Corradi's approach, in the end, the total marginal emissions of a BZ are the weighted average of the emissions from the marginal electricity generation plant of that BZ and the marginal electricity generation plant of the imports (in case of imports), using the percentage of origin as a weight.

2.2. Coupled Approach

Graabak et al. [47] determine yearly average marginal emission factors for the European power grid and marginal emission factors for the Norwegian power grid based on a European Multi-area Power-market Simulator (EMPS). EMPS is a stochastic optimization model for hydro-thermal electricity markets where the electricity market is arranged so that electricity prices balance supply and demand in each area and time step. It is used by all main actors in the Nordic power market, such as the TSOs, and for energy system planning, production scheduling, and price forecasting. Average emission factors are estimated for several scenarios of production portfolio for the European power grid. They point out that an average emission factor should be used for the control of a large number of buildings while a marginal emission factor should be applied for the control of a limited number of buildings.

Patteeuw et al. [26], Arteconi et al. [38], Askeland et al. [48] and Quoilin et al. [49] determine optimal dispatch and unit commitment in electricity grids. None of the models calculates $CO_{2eq.}$ intensities. Nevertheless, their models could determine the carbon intensity by considering CO_2 factors for each

electricity generation technology. Patteeuw et al. [26] developed an approach to model active demand response with electric systems while considering both the supply and demand sides. The model takes thermal comfort and techno-economic constraints of both sides of the power system into account. Formulated as an optimization problem, it minimizes the overall operational cost of the electricity generation. The case study is based on the Belgian power system using the year 2010. This model enables to investigate the influence of different levels of market penetration of DR on the decision of the marginal generation technology. The approach does not consider imports. Arteconi et al. [38] apply the same model for the choice of the generation technology and use a low-order resistance–capacitance building model as a case study to investigate the DR potential of a building.

Askeland et al. [48] developed an equilibrium model for the power market that couples the demand and supply sides. The model provides time series for the electricity demand as well as for the renewable energy generation. A case study for the Northern European power system is performed where the effect of DR on the potential shift in the generation mix is studied. Quoilin et al. [49] developed a model called Dispa-SET, which is an open-source model that solves the optimal dispatch and unit commitment problem at the EU level, applying one node per country, instead of per BZs.

3. Evaluating the Hourly Average $CO_{2eq.}$ Intensity

In the following, the sources for required input data are first presented. The assumptions for processing the data are then stated. Finally, a step-by-step guidance is given to determine the hourly average $CO_{2eq.}$ intensity of the electricity mix per BZ. In the case study, hourly average $CO_{2eq.}$ intensities are calculated for Scandinavia, meaning Norwegian, Swedish, and Danish bidding zones, but also for Finland, Germany, and the Netherlands.

3.1. Data Retrieval and Pre-Processing

3.1.1. Electricity Use per Bidding Zone

Data regarding the electricity generation per production type within a BZ can be retrieved from ENTSO-E, which is the European Network of TSOs for Electricity. The European TSOs are supposed to provide data to ENTSO-E to promote market transparency and closer cooperation across the TSOs. A free user account at ENTSO-E has to be set up to download the data. Furthermore, data may also be retrieved directly from national TSOs, if the dataset from ENTSO-E is incomplete for specific BZs. For instance, hourly electricity generation data for the Swedish BZs was here obtained from the Swedish TSO (as this data was not available from ENTSO-E).

The ENTSO-E dataset contains hourly values for the total electricity generated per production type within a BZ. Thermal power plants are included as a production type. In practice, these power plants can consume most of the generated electricity onsite. Therefore, it is necessary to have knowledge about the sales licenses to the grid of these power plants. When onsite-generated electricity is not sold to the grid, it should ideally not be considered for the average $CO_{2eq.}$ intensity of the electricity mix. Information regarding sales licenses can usually be obtained from either the TSO, state directorates or directly from the company owning the power plant. For our case study of Scandinavia, these sales licenses were only determined for Norway. The Norwegian thermal power plants with the highest installed capacities are shown in Figure 1. Only the power plant of Mongstad sells electricity to the grid. Comprehensive information on data treatment and assumptions is provided in [39].

The input data can be arranged in the following way:

$$\mathrm{BZ} = \begin{bmatrix} P_{BZ_j,EGT_1}(t_1) & \cdots & P_{BZ_j,EGT_m}(t_1) \\ & \ddots \quad \vdots & \\ \vdots & P_{BZ_j,EGT_i}(t_g) & \vdots \\ & \vdots \quad \ddots & \\ P_{BZ_j,EGT_1}(t_{8760}) & \cdots & P_{BZ_j,EGT_m}(t_{8760}) \end{bmatrix} \quad (1)$$

where

- i is the "index of EGTs" ranging from 1 to m
- j is the "index of a specific BZ"
- g is the "hour of the year" ranging from 1 to 8760 (or 8784)

The matrix BZ (where 'BZ' stands for bidding zone) includes the electricity generation from each electricity generation technology (EGT_i) at every hour of the year (t_g). EGT_i represents electricity generation from each technology in the BZ, but, by extension, it also includes the imports from first tier BZs. In other words, imports from other BZs are considered as an EGT in the matrix.

3.1.2. Emission Factors per Electricity Generation Technology

The average $CO_{2eq.}$ intensity of a BZ depends directly on the CO_2 factor that is associated to each EGT. This choice of the CO_2 factor strongly affects the final result of the evaluation. Two possible ways of acquiring CO_2 factors of a given EGT are the IPCC report [52,53] or the Ecoinvent database [54]. Ecoinvent provides a vast variety of CO_2 factors for electricity generation from a given fuel type depending on the type of power plant and the specific country. A license is necessary to use Ecoinvent, whereas the IPCC report is available free of charge. CO_2 factors can differ between references mainly due to different allocations of emissions, especially for combined heat-and-power plants. More detailed information regarding emission allocations are given in [52–54]. Regarding annual average $CO_{2eq.}$ intensities of a country (see Table A1 in Appendix A), they can be calculated from Ecoinvent or taken from the website of the European Environment Agency [55].

For the sake of the simplicity, our case study considers a same CO_2 factor per EGT for every country. Therefore, it assumes that the CO_2 factor is independent of the country and the specific power plant as long as it uses the same EGT (disregarding the thermal efficiency or the age of the power plant). The proposed methodology is however more general. If a different $CO_{2eq.}$ factor should be considered for a same EGT but for a different plant efficiency, plant age, or country, a new EGT should be defined for each different $CO_{2eq.}$ factor considered.

In this study, data from the Ecoinvent database has been used. The phases that were considered in the CO_2 factor per EGT are the extraction of fuels, the construction of the power plant (including infrastructure and transport), its operation and maintenance as well as the end of use of the power plant. The CO_2 factor for hydro pumped storage is here assumed constant in time, 62 $gCO_{2eq.}$/kWh. In fact, it is dependent on the $CO_{2eq.}$ intensity of the electricity mix used when pumping water into the storage reservoir. Unlike Norway, this assumption can be critical for BZs that usually have a relatively high $CO_{2eq.}$ intensity. Strictly speaking, if the constant CO_2 factor considered for hydro pumped storage is much lower than the $CO_{2eq.}$ intensity of the electricity mix when water is pumped into the storage, it would correspond to a 'greenwashing' of the electricity mix. Furthermore, ENTSO-E defines an EGT category called 'other' with no further specifications. It is thus difficult to allocate a CO_2 factor for this production type and it could also differ among different countries. In this work, the factor is assumed to be the average of the fossil fuel technologies. Table A1 gives an overview of typical CO_2 factors for different fuel types.

3.2. Calculation Methodology

The electricity mix is assumed homogeneous in each BZ, meaning that a same $CO_{2eq.}$ intensity is used for the entire BZ at each hour of the year. For neighboring countries where the $CO_{2eq.}$ intensities are not evaluated (here called 'boundary BZ'), a yearly-averaged $CO_{2eq.}$ intensity is considered. In our case study, these countries are Great Britain, Belgium, Poland, Estonia, and Russia. It is nonetheless reasonable to assume that they have a limited impact on the Norwegian electricity mix. They are either 2nd tier countries (i.e., which do not have a direct grid connection to Norwegian BZs) or have limited electricity export to Norway (which is typically the case for Russia). By extension, BZs for which the average $CO_{2eq.}$ intensity is calculated for every hour of the year are hereafter called computed BZs.

Matrix T(t) (where 'T' stands for technology) includes the electricity generation from all EGTs in all BZs and is calculated for each hour of the year (t):

$$T(t) = \begin{bmatrix} P_{BZ_1,EGT_1}(t) & \cdots & P_{BZ_n,EGT_1}(t) \\ & \ddots & \\ \vdots & P_{BZ_j,EGT_i}(t) & \vdots \\ & & \ddots \\ P_{BZ_1,EGT_m}(t) & \cdots & P_{BZ_n,EGT_m}(t) \end{bmatrix} \quad (2)$$

where

- i is the "index of EGTs" ranging from 1 to m
- j is the "index of BZs" ranging from 1 to n

The size of matrix *T(t)* depends on the number of EGTs and number of BZs that are considered in a respective study.

The next step is a normalization to 1 MWh by dividing by the total hourly electricity generation (i.e., summing on all the EGT_i, also considering imports) in a bidding zone (BZ_j) during each hour (t) of the year. This step will be necessary to determine the $CO_{2eq.}$ intensity for 1 MWh of generated electricity in a respective BZ. Matrix *N(t)* (where 'N' stands for normalization) is set up as follows:

$$N(t) = \begin{bmatrix} \frac{1}{\sum_i P_{BZ_1,EGT_i}}(t) & 0 & 0 & 0 & 0 \\ 0 & \ddots & 0 & 0 & 0 \\ 0 & 0 & \frac{1}{\sum_i P_{BZ_j,EGT_i}}(t) & 0 & 0 \\ 0 & 0 & 0 & \ddots & 0 \\ 0 & 0 & 0 & 0 & \frac{1}{\sum_i P_{BZ_n,EGT_i}}(t) \end{bmatrix} \quad (3)$$

where

- i is the "index of EGTs" ranging from 1 to m
- j is the "index of a specific BZ" ranging from 1 to n

The matrix *P(t)* (where 'P' stands for production) is the share of each EGT on the total hourly electricity generation in a respective BZ, still considering electricity imports as an EGT. Regarding the electricity imports to a BZ, it is distinguished between imports from boundary BZs with a fixed $CO_{2eq.}$ intensity of the electricity mix ($P_{Import,fix,t}$) and imports from computed BZs with a variable electricity mix ($P_{Import,var,t}$). At this stage, *P(t)* only considers the share of each EGT in the electricity mix of a

specific BZ, but does not consider the share of each EGT in the imports. *P(t)* is calculated by multiplying *T(t)* and *N(t)*. The share of EGTs (located inside the BZ j) in the generation mix is called $P_{EGT,t}$.

$$P(t) = T(t) \cdot N(t) = \begin{bmatrix} P_{EGT,t} \\ P_{Import,fix,t} \\ P_{Import,var,t} \end{bmatrix} \quad (4)$$

$P_{EGT,t}$ and $P_{Import,fix,t}$ can be combined to define the matrix $P_{EGT,fix}$:

$$P_{EGT,fix} = \begin{bmatrix} P_{EGT,t} \\ P_{Import,fix,t} \end{bmatrix} \quad (5)$$

The next steps show how to include the share of each EGT in the electricity imports; in other words, how the electricity mix of a neighboring BZ influences the electricity mix of a BZ through imports. In general, the balance between electricity consumption and electricity generation has to be satisfied at all times for each BZ. This idea is further generalized in MRIO models, where interdependencies within the whole system can be captured, while preserving regional differences [56]. For each BZ, the sum of electricity import and generation by a specific EGT should be consumed in the BZ, or exported. This complies with the logic of MRIO models which can be used to calculate consumption-based emissions for an entire country or region [34]. The electricity balance can then be expressed as

$$M = P_{EGT,fix} + M \cdot P_{Import,var,t}, \quad (6)$$

with *M* (where '*M*' stands for mix) representing the share of each EGT on the electricity use of BZ_j and the exports from BZ_j. Solving Equation (6) for *M* is done by

$$M(i,j) = P_{EGT,fix} \cdot \left(I - P_{Import,var,t}\right)^{-1}. \quad (7)$$

where I is an identity matrix. Matrix *M(i,j)* contains the share of each EGT_i (and boundary BZ) on the electricity use and exports from BZ_j. A new matrix is computed for each hour of the year.

The average $CO_{2eq.}$ intensity of a BZ for every hour of the year is calculated by

$$e_j(t) = \sum_{i=1}^{m} ef_{EGT_i} \cdot M(i,j) \quad (8)$$

where *t* is the hour of the year, *i* is the index of the EGT ranging from 1 to m, *j* is the index of a specific BZ ranging from 1 to n and ef_{EGT_i} is the emission factor of the EGT of index i.

3.3. Applicability of the Methodology

Comparing the proposed methodology with the other existing methodologies presented in Table 1, its major advantage is its simplicity. Nevertheless, it also has limitations. As a decoupled approach, the method can be used as long as the number of buildings participating in DR schemes is low; in other words, as long as the level of the market penetration of DR in buildings is still limited. This limitation counts for all decoupled approaches, not only for the proposed method. Furthermore, this approach is representative for most simulation-based studies in building energy flexibility. Yearly average $CO_{2eq.}$ intensities of the electricity mix have been used extensively in the past to calculate the emission balance of buildings that export electricity to the grid [57]. Studies mostly focusing on the LCA of buildings often use average $CO_{2eq.}$ intensities rather than marginal intensities. The use of hourly average $CO_{2eq.}$ intensities as a control signal for DR is thus remaining coherent with that approach. Also, in the EPBD method, average primary energy factors are often used to evaluate the performance of buildings.

3.4. $CO_{2eq.}$ Intensities in Scandinavian Bidding Zones

As a case study, the hourly average $CO_{2eq.}$ intensities for all Norwegian BZs are evaluated for the year 2015. Results are plotted in Figure 2a. NO5 has the highest annual average $CO_{2eq.}$ intensity which is due to the electricity generation from the thermal power plant in Mongstad (see Figure 1 and Table 2). Furthermore, it is obvious that the highest $CO_{2eq.}$ intensity peaks occur in NO2. Figure 2b presents the average $CO_{2eq.}$ intensities for NO2, NO3, SE1, SE4, DK1, and FIN. It is clear that the Norwegian electricity mix has low average $CO_{2eq.}$ intensities compared to non-Norwegian BZs. Resulting from the large differences in $CO_{2eq.}$ intensity, the average $CO_{2eq.}$ intensity in NO2 usually increases when electricity is imported from DK1, which also explains the $CO_{2eq.}$ peaks in the BZ. The impact of fossil fuel-based electricity imports on the average $CO_{2eq.}$ intensity is particularly strong for the case of Norway because the electricity generation in Norway is almost entirely from hydropower. The impact of carbon-intensive electricity imports on the average $CO_{2eq.}$ intensity of other countries, like Finland or Denmark, is usually lower. A more detailed analysis of the correlation of the average $CO_{2eq.}$ intensity and electricity imports to Norway is provided in [39].

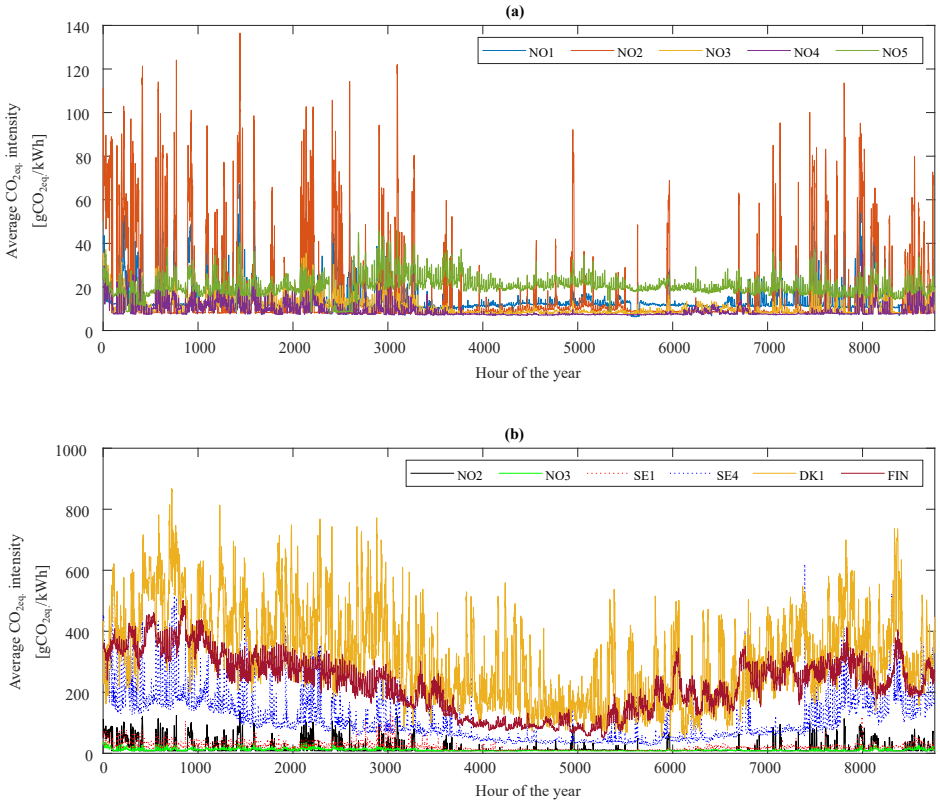

Figure 2. Hourly average $CO_{2eq.}$ intensity of the electricity mix for (**a**) the Norwegian bidding zones and (**b**) for several Scandinavian bidding zones.

Table 2. Comparison of the annual average $CO_{2eq.}$ intensities of the electricity mix for several Scandinavian bidding zones.

BZ	NO1	NO2	NO3	NO4	NO5	SE1	SE4	DK1	FIN
Average $CO_{2eq.}$ intensity ($gCO_{2eq.}$/kWh)	15	17	11	9	20	21	114	316	227
Average $CO_{2eq.}$ intensity without imports ($gCO_{2eq.}$/kWh)	7	8	8	7	20	21	259	461	241

An overview of the annual average $CO_{2eq.}$ intensities is provided in Table 2. DK1 has the highest annual average $CO_{2eq.}$ intensities, followed by FIN and SE4.

Figure 3 illustrates the relation between the average $CO_{2eq.}$ intensity and the electricity spot price for six Scandinavian BZs for an exemplary five-day period. For the Norwegian BZs NO2 and NO3 (see Figure 3a,b) it is shown that the average $CO_{2eq.}$ intensity is low, when the electricity spot price is high. In Norway, electricity is produced from hydropower in times of high demands. Electricity spot prices are high during high electricity demands, thus typically leading to low $CO_{2eq.}$ intensities. In general, the Norwegian hydropower reservoirs are operated in a cost-optimal way, so that electricity is imported during the night when electricity is cheap and exported to continental Europe during the day, when electricity is expensive [39]. This operation strategy can also be used to explain the $CO_{2eq.}$ intensities in the BZs shown in Figure 3. The correlation between the carbon intensity and the spot price for the Swedish BZs is similar to the Norwegian BZs.

SE1 (Figure 3c) is the northernmost Swedish BZ and relies primarily on electricity generation from hydro reservoirs and on-shore wind as well as on electricity imports from SE2. Thus, average $CO_{2eq.}$ intensities are generally rather low. Regarding the correlation with electricity spot prices, $CO_{2eq.}$ intensities are low when spot prices are high. This relation is also similar for SE4 (see Figure 3d) but to a lower extent. The average $CO_{2eq.}$ intensities in SE4 are several times higher compared to SE1 because SE4 trades a lot of electricity with Denmark, Poland, and Germany.

A rather weak correlation between the carbon intensity and the spot price can be seen for DK, which is in accordance with the findings from Knudsen et al. [24] who found that a low $CO_{2eq.}$ intensity does not necessarily occur concurrent with low costs. A difference between day and night is also visible for the $CO_{2eq.}$ intensity in DK1. A correlation between the carbon intensity and the spot price on an hour-by-hour basis is not obvious because the $CO_{2eq.}$ intensity varies much faster than the spot price. A clear relationship between the $CO_{2eq.}$ intensity and the spot price is not visible for FIN.

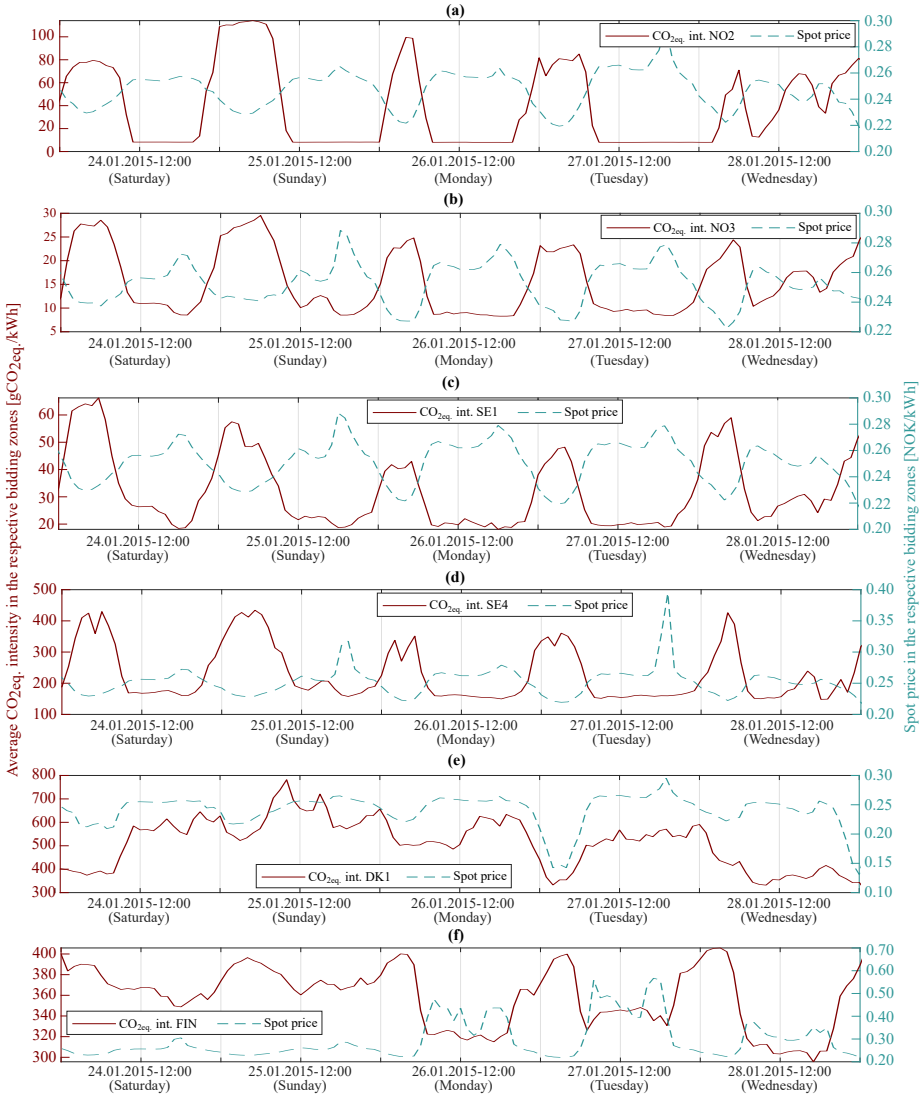

Figure 3. Average $CO_{2eq.}$ intensity and spot prices for five exemplary days in 2015 for six Scandinavian BZs: (**a**) NO2, (**b**) NO3, (**c**) SE1, (**d**) SE4, (**e**) DK1, and (**f**) FIN.

4. Case Study Using Demand Response for Heating

4.1. Case Building

To represent a large share of the Norwegian residential building stock, a single-family detached house built according to the building standard from the 1980s, TEK87, is chosen as a case [58]. The geometry of the building is based on the ZEB Living Lab which is a zero emission residential building located in Trondheim [59]. The envelope model of the real Living Lab has been calibrated with the help of dedicated experiments for the building performance simulation tool IDA ICE. However, the thermal properties of the building envelope for this case study comply with TEK87. The Living Lab has a heated floor area of 105 m^2, the floor plan being shown in Figure 4. An overview of the building properties is provided in Table 3. For the sake of the simplicity, natural ventilation, which

was usually applied in TEK87 buildings, is modeled as balanced mechanical ventilation with a heat recovery effectiveness η_{HR} of 0%. This study considers the U-values of the building walls, but it should be noted that the building insulation level [15] as well as the thermal capacity of a building [60–62] influences the flexibility potential. The climate of Trondheim is also relevant for Norway in general.

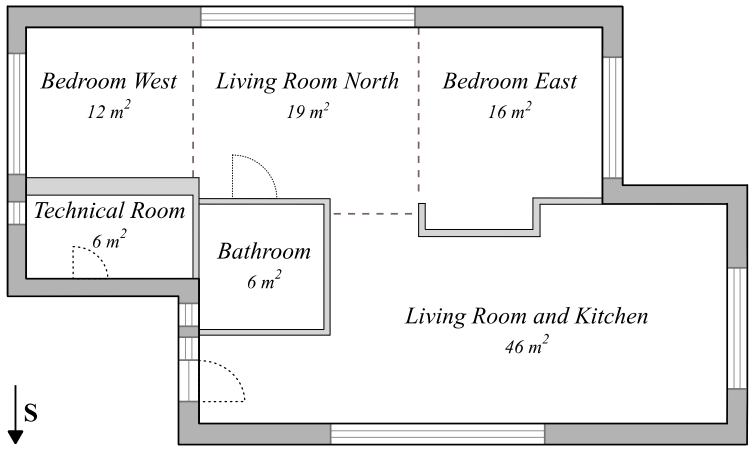

Figure 4. Floor plan of the studied building [15].

Table 3. Building envelope properties and energy system characteristics of the case study building (EW—external wall; IW—internal wall; n_{50}—air changes per hour at 50 Pa pressure difference; U_{Total}—the total U-value of the windows including the glazing and the frame; HR—heat recovery; ER—electric radiator; AHU—air handling unit; HDS—heat distribution system).

	Building Envelope				Thermal Bridges	Infiltration	Windows	AHU	HDS	SH Needs
Symbol	U_{EW}	U_{IW}	U_{Roof}	U_{Floor}			U_{Total}	η_{HR}	ER	
Unit	W/(m²·K)				W/(m²·K)	n_{50}	W/(m²·K)	%	W/m²	kWh/m²
	0.35	0.34	0.23	0.30	0.05	3.0	2.1	0	93	172

A detailed multi-zone model of the building is created using the software IDA ICE version 4.8, which is a dynamic building simulation software that applies equation-based modeling [63]. IDA ICE has been validated in several studies [64–68].

Electric radiators are used for SH as it is the most common space-heating system in Norwegian houses [69]. One electric radiator is placed in each room with a power equal to the nominal SH power of the room at design outdoor temperature (DOT) of −19 °C. DHW is produced in a storage tank. An electric resistance heater with a capacity of 3 kW is used for DHW heating and is installed in the lower third of the tank. IDA ICE has a one-dimensional model of a stratified water tank that accounts for the heat conduction and convection effects in the tank. The DHW storage tank is here divided into four horizontal layers to account for stratification effects. The DHW storage volume is calculated by

$$V_{DHW} \cong S{\cdot}65{\cdot}n_{people}^{0.7} \quad [\text{litre}] \tag{9}$$

where S is the safety margin and n_{people} the number of occupants. S is set to 125% for a low number of people [70]. The charging of the DHW storage tank is controlled by two temperature sensors that are installed in the bottom and the top of the tank. The electric resistance heater starts heating as soon as the temperature in the upper part of the tank drops below the set-point and it continues until the set-point for the temperature sensor in the lower part of the tank is reached. The DHW start

temperature is called the DHW TSP here. The DHW stop temperature is always taken 3 °C above to start temperature.

The internal heat gains from electrical appliances, occupants and lighting are defined according to the Norwegian technical standard, SN/TS 3031:2016 [71]. The daily DHW profiles are taken from the same standard. Schedules for electrical appliances are also based on SN/TS 3031:2016, whereas the schedules for occupancy and lighting are taken from prEN16798-1 and ISO/FDIS 17772-1 standards [72,73]. The internal heat gains are distributed uniformly in space. All profiles presented in Figure A1 have an hourly resolution and are applied for every day of the year.

The energy flexibility potential is evaluated for four different PRBCs by comparing them to the reference scenario that applies constant TSPs for SH (21 °C) and DHW (50 °C). The TSP for the bathroom is 24 °C. All doors are closed at all times. DR measures are applied to the common rooms only (meaning the living room, kitchen, and living room north). All cases use the weather data of 2015 (retrieved from [74]) for Trondheim, independent of the BZ considered. NordPool provides hourly day-ahead spot prices for each bidding zone [75]. They are used as an input signal for the price-based control and to calculate energy costs for heating. An electricity fee for the use of the distribution grid is not considered in the cost evaluation.

4.2. Demand Response Strategies

The reference scenario, termed BAU (for business as usual), maintains constant TSPs for SH and DHW heating at 21 °C and 50 °C respectively. Using constant TSP is the most common way to control the heating system in Norwegian residential buildings. These TSPs are varied for the DR strategies. The DHW TSP can be increased by 10 K or decreased by 5 K depending on the control signal. The limit for DHW temperature decrease is chosen with regards to Legionella protection. Regarding SH, the TSPs are increased by 3 K or decreased by 1 K. According to EN15251:2007 [76] indoor temperatures between 20 °C and 24 °C correspond to a predicted percentage dissatisfied (PPD) $< 10\%$ and $-0.5 < \text{PMV} < +0.5$ in residential buildings for an activity level of 1.2 MET and a clothing factor of 1.0 clo.

The control signal for the CO_2-based control is determined based on two principles. The first principle, hereafter called CSC-a, aims at operating the energy system in times of lowest $CO_{2eq.}$ intensities by increasing TSPs for SH and DHW during these periods. For Norway, this principle may in practice lead to extended periods with high TSPs because of the typical daily $CO_{2eq.}$ intensity profile (Figure 3a,b). This may lead to an unnecessary increase in annual energy use for heating. Therefore, the second principle—hereafter called CSC-b—does not aim at operating the heating system during periods with the lowest carbon intensities but rather charges the storages just before high-carbon periods in order to avoid the energy use during these critical periods. Using CSC-b, the TSPs are increased for shorter time periods compared to CSC-a, thus improving the energy efficiency.

The carbon-based PRBC uses a 24 h sliding horizon to determine a high-$CO_{2eq.}$ intensity threshold (HCT) and low-$CO_{2eq.}$ intensity threshold (LCT). At each hour, the current $CO_{2eq.}$ intensity (CI) is compared to these thresholds. Taking CI_{max} and CI_{min} as the maximum and minimum intensities for the next 24 h, LCT has been selected to $CI_{min} + 0.3$ (CI_{max}-CI_{min}) and HCT to $CI_{min} + 0.7$ (CI_{max}-CI_{min}). Regarding CSC-a, if the $CO_{2eq.}$ intensity of the current hour is below the LCT, the TSPs are increased. If the current $CO_{2eq.}$ intensity is above the HCT, the set-points are decreased to delay the start of the heating, whereas if the $CO_{2eq.}$ intensity of the current hour is between the LCT and HCT, the TSPs remain equal to the reference scenario. Regarding CSC-b, the control signal is also determined based on the three price segments, as defined for CSC-a, but, additionally, the control considers if the current $CO_{2eq.}$ intensity is increasing or decreasing with time. If the current $CO_{2eq.}$ intensity is between the LCT and HCT and the $CO_{2eq.}$ intensity increases in the next two hours, TSPs are increased. Both principles, CSC-a and CSC-b, are presented in Figure 5.

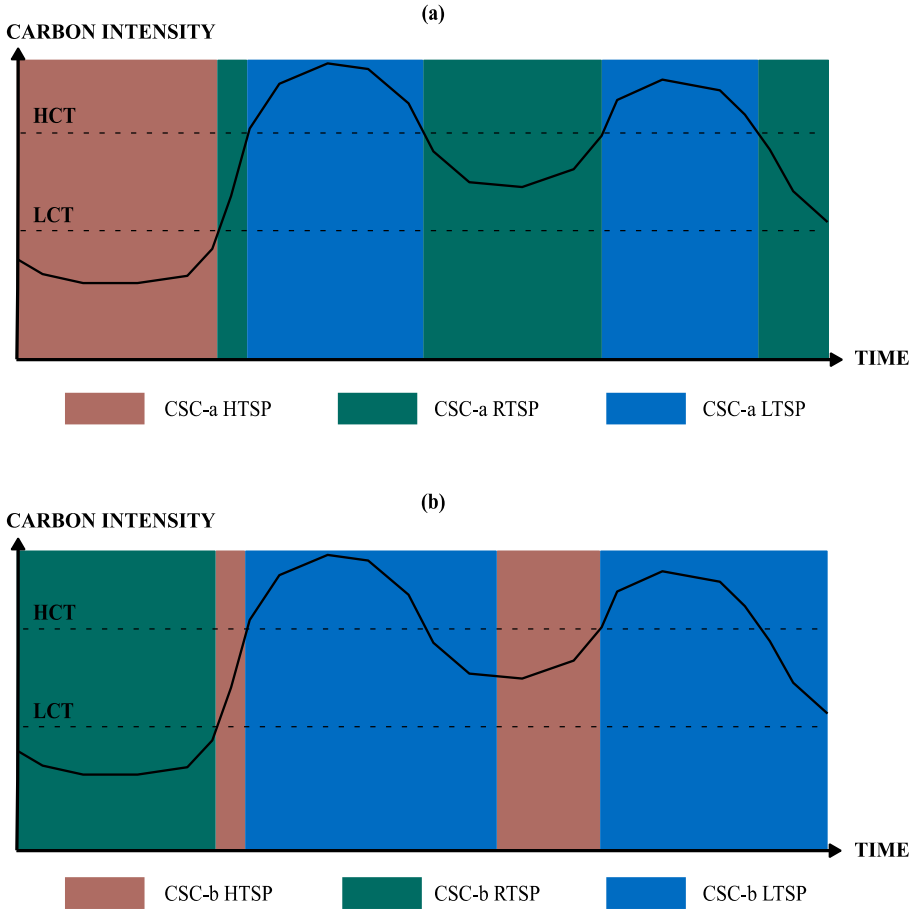

Figure 5. Principle of the determination of the carbon-based control signal according to (**a**) CSC-a and (**b**) CSC-b. (HTSP is high temperature set-points, RTSP is reference temperature set-points, LTSP is low temperature set-points).

The performance of the control with regards to emission savings is sensitive to the selection of thresholds, LCTs and HCTs. The influence of LCTs and HCTs on the number of hours per TSP-segment has been evaluated for BZ NO3. An LCT of 30% and an HCT of 70% have been chosen for calculating the control signal. The LCTs and HCTs for the other five BZs considered in the simulation study are chosen so that the number of hours in the three respective segments is equivalent to the case of NO3. An overview of the different scenarios is presented in Table 4. In fact, there is an optimum LCT and HCT for each BZ to minimize carbon emissions. However, in the case study, the two thresholds are rather chosen to have a similar number of hours in the respective TSP segments. This is done to investigate the influence of the $CO_{2eq.}$ intensity profile on the carbon emissions rather than optimizing the control principle thresholds.

Table 4. Influence of the low-carbon and high-carbon thresholds (LCT and HCT) on the number of hours per temperature set-point segment (LTSP—low-temperature set-points; RTSP—reference temperature set-points; HTSP—high temperature set-points).

	Thresholds Kept Constant						Adjusted Thresholds for Similar Segments					
	NO2	**NO3**	**SE1**	**SE4**	**DK1**	**FIN**	**NO2**	**NO3**	**SE1**	**SE4**	**DK1**	**FIN**
CSC-a												
LCT [%]	30	**30**	30	30	30	30	22	**30**	27	29.5	47	46
HCT [%]	70	**70**	70	70	70	70	68.5	**70**	66	68.5	81.5	82
LTSP [h]	1812	**1886**	1706	1814	2584	2439	1879	**1886**	1884	1878	1882	1881
RTSP [h]	1822	**2219**	2166	2236	2731	2930	2229	**2219**	2223	2223	2230	2245
HTSP [h]	5126	**4655**	4888	4710	3445	3391	4652	**4655**	4653	4659	4648	4634
CSC-b												
LCT [%]	30	**30**	30	30	30	30	22	**30**	27	29.5	21	16
HCT [%]	70	**70**	70	70	70	70	67	**70**	67.5	70	76	59
LTSP [h]	2624	**2924**	2758	2892	3954	3881	2912	**2924**	2925	2918	2933	2904
RTSP [h]	5125	**4654**	4487	4710	3445	3390	4651	**4654**	4652	4659	4648	4673
HTSP [h]	1011	**1182**	1115	1158	1361	1489	1191	**1182**	1183	1183	1179	1183

Price-based control signals, hereafter called CSP-a and CSP-b, are also determined similar to CSC-a and CSC-b, to also investigate DR measures based on the electricity spot price of each of the BZs. This means that the case study is performed for four DR signals applied to six Scandinavian BZs. In general, any form of penalty signal could be used for the control and optimization. If a proper penalty signal is chosen, a building can be controlled so that it is either energy efficient, cost efficient or CO_2 efficient. It would also be possible to select a combination of the different penalty signals for the building control [11].

4.3. Case Study Results

Figure 6 illustrates the principle of the CSC-a control during 48 h of the heating season exemplary for DK1. Figure 6a shows the $CO_{2eq.}$ intensity and both thresholds, LCT and HCT. Figure 6b presents the measured temperatures in the DHW tank and the start and stop TSPs of the DHW hysteresis control. These TSPs vary depending on the $CO_{2eq.}$ intensity signal. The same principle is shown for SH in Figure 6c. It is visible from Figure 6d that the electric radiators and the electric resistance heater for DHW heating are operated depending on the $CO_{2eq.}$ intensity signal and according to the proposed temperature hysteresis.

The energy use, $CO_{2eq.}$ emissions and costs are compared to the reference cases for each respective BZ. The relative difference in total annual emissions (Em.) for each BZ is calculated by

$$Em.(BZ_i) = \frac{Em._{BZ_i,PRBC}}{Em._{BZ_i,BAU}} * 100 - 100\ [\%] \quad (10)$$

Equation (10) can also be applied to determine the relative changes for annual energy use and annual costs, respectively. Results are presented in Table 5.

In general, the energy use increases for all DR cases. Regarding CSC, annual $CO_{2eq.}$ emissions decrease for NO2 while they remain rather close to the reference case for the other BZs. For NO3, the daily fluctuations in average $CO_{2eq.}$ intensity are too low to benefit from DR measures. Comparing results for NO2 and NO3 regarding overall emission savings, it demonstrates that electricity imports should be properly considered as they influence significantly the variations of $CO_{2eq.}$ intensities. These variations have shown to be important to make the CO_{2eq}-based DR effective.

Regarding CSP, costs increase slightly for NO2 and NO3 while they decrease for SE4, DK1, and FIN. For SE4, DK1, and FIN, cost savings can be achieved as daily price fluctuations are sufficient. High daily fluctuations of prices do usually not occur in Norway and northern Sweden. Therefore, for NO2, NO3, and SE1, consuming during slightly decreased electricity spot prices is outbalanced by

an increase in total energy use. Furthermore, using price-based control, overall emissions increase significantly for NO2, NO3, SE1, and SE4 as a result of typically high $CO_{2eq.}$ intensities at low-price periods (as shown Figure 3).

It is obvious, that reductions of $CO_{2eq.}$ emissions and costs are possible, but that they are very dependent on the characteristics of the $CO_{2eq.}$ intensity and the electricity spot price. Savings could be increased, if different thresholds (LCT and HCT) were applied, not taking NO3 as a reference regarding the number of hours per segment. Absolute savings depend on the LCT and HCT as well as the principle used to obtain the respective control signals. In addition, the maximum absolute savings should ideally be evaluated using MPC. Therefore, here, the performance of each control should be considered relative to each other rather than in absolute terms.

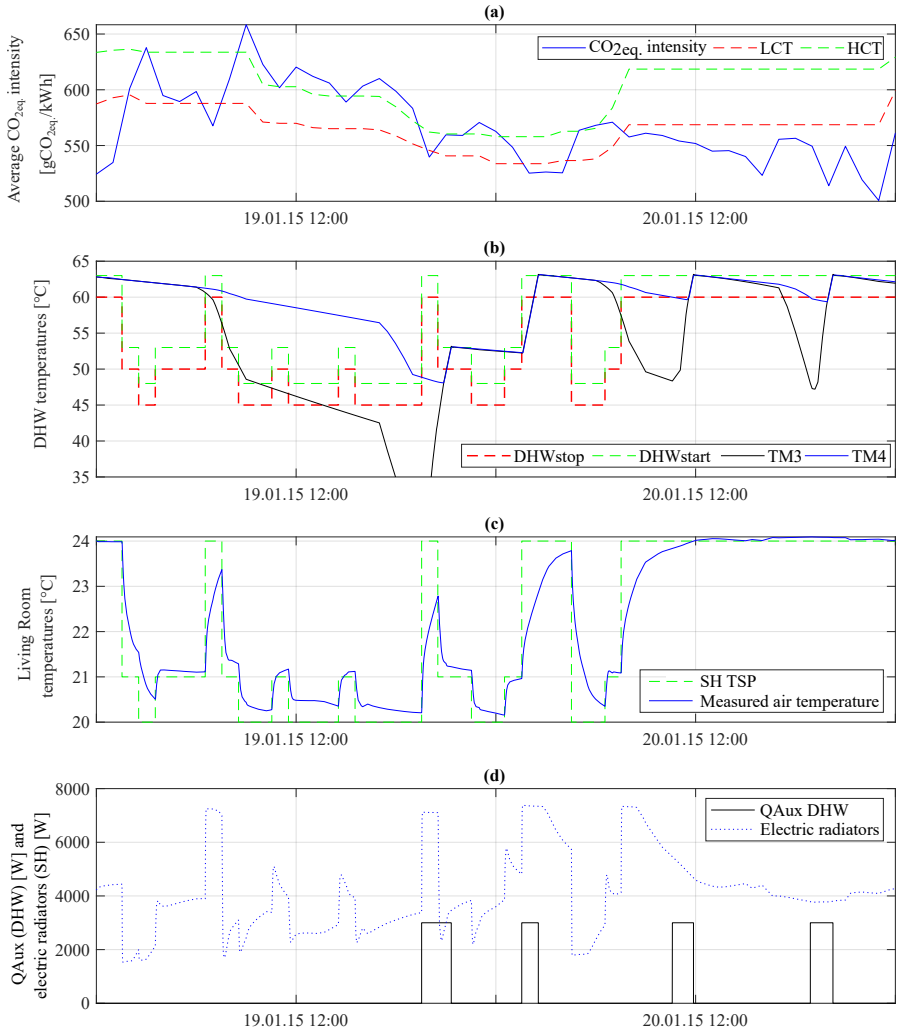

Figure 6. Illustration of the control principle for DK1 case CSC-a during a 48 h period, where (**a**) shows the $CO_{2eq.}$ intensity, (**b**) shows the DHW temperatures and hysteresis set-points, (**c**) shows the measured air temperature and the temperature set-point for space heating and (**d**) shows the power of the electric radiators and the electric auxiliary heater (DHWstart and DHWstop are the start and stop temperatures for DHW; TM is two temperature measurements in the water tank; SH TSP is space heating temperature set-point; QAux is the electric resistance heater).

Table 5. Cost and $CO_{2eq.}$ emission savings relative to the respective reference cases for all six bidding zones (E_{USe}—energy use; Em.—emissions; CSC—control strategy carbon; CSP—control strategy price).

	CSC-a			**CSC-b**			**CSP-a**			**CSP-b**		
	E_{Use}	**Em.**	**Costs**	**E_{Use}**	**Em.**	**Costs**	**E_{Use}**	**Em.**	**Costs**	**E_{Use}**	**Em.**	**Costs**
	%	%	%	%	%	%	%	%	%	%	%	%
NO2	+9	**−8**	+10	+3	-1	+2	+7	+21	**+2**	+4	+9	**+1**
NO3	+9	**+3**	+10	+3	+2	+2	+7	+13	**+2**	+4	+6	**+1**
SE1	+9	**+0**	+11	+3	+1	+2	+7	+14	**+1**	+4	+8	**+1**
SE4	+9	**+0**	+10	+3	+1	+1	+7	+11	**−3**	+4	+6	**−1**
DK1	+10	**+1**	+2	+3	+2	+1	+7	+1	**−6**	+4	+2	**−1**
FIN	+9	**+5**	+6	+3	+2	+1	+8	+8	**−9**	+4	+3	**−3**

Table 6 presents $CO_{2eq.}$ emission and cost savings for DHW heating and SH, separately. It can be seen that SH is the main contributor to total emission or cost savings because, for such a building with limited thermal insulation, the share of electricity use is much more significant for SH than for DHW heating. This will be different for buildings with better insulation levels. For example, regarding CSC-a in DK1, it can be seen that, even though DR measures for DHW heating lead to 12% emission savings, the overall emissions increase by 1% because the emissions resulting from SH increase by 3%.

Table 6. Cost and $CO_{2eq.}$ emission savings separated for DHW and SH (results are given in %).

	Emissions						**Costs**					
	CSC-a			**CSC-b**			**CSP-a**			**CSP-b**		
	Total	**DHW**	**SH**	**Total**	**DHW**	**SH**	**Total**	**DHW**	**SH**	**Total**	**DHW**	**SH**
NO2	**−8**	−17	−6	**−1**	+17	−3	**+2**	−5	+3	**+1**	−5	+2
NO3	**+3**	−3	+3	**+2**	+14	+0	**+2**	−7	+3	**+1**	−5	+2
SE1	**+0**	−3	+1	**+1**	+20	−1	**+1**	−9	+2	**+1**	−7	+2
SE4	**+0**	−7	+0	**+1**	+16	−1	**−3**	−20	+1	**−1**	−13	+2
DK1	**+1**	−12	+3	**+2**	−1	+2	**−6**	−27	−1	**−1**	−15	+2
FIN	**+5**	+0	+6	**+2**	+6	+2	**−9**	−32	−3	**−3**	−21	+1

Furthermore, $CO_{2eq.}$ emissions for DHW heating are decreased significantly in most of the zones using CSC-a. On the contrary, in the Norwegian and Swedish BZs, these emissions increase significantly using CSC-b. Using CSC-b, the water storage tanks are typically charged during late evenings whereas the next peak for DHW withdrawal only occurs the next morning. These peaks of DHW withdrawal happen when the $CO_{2eq.}$ intensities of the electricity mix are rather low. In other words, CSC-b shifts the operation from low $CO_{2eq.}$ intensities (meaning peaks of DHW withdrawal) to higher $CO_{2eq.}$ intensities (meaning late evenings). Regarding costs, these DR strategies applied to DHW heating are very promising to decrease the operational costs. Operational costs are decreased for all BZs for both CSP-a and CSP-b considering DHW heating. In conclusion, efficient DR measures using PRBC can be implemented for the DHW heating. However, the performance of these controls are moderate for SH. The price-based controls did not manage to decrease operational costs for SH for most cases. On the one hand, this can be due to the low daily fluctuations of the electricity spot prices. On the other hand, this can be due to the low insulation level and thermal mass of the building as well as the inherent limitations of PRBC compared to MPC.

5. Conclusions

This work consists of two distinct but complementary parts. Firstly, a generic methodology is proposed to determine the hourly average $CO_{2eq.}$ intensity of the electricity mix of a bidding zone (BZ) also considering time-varying $CO_{2eq.}$ intensities of electricity imports. Northern Europe is taken as a case. Secondly, this case study is extended to investigate the performance of demand response

measures based on the evaluated $CO_{2eq.}$ intensity. These measures aim at decreasing the environmental impact of the heating system operation of a typical Norwegian residential building.

The proposed methodology to evaluate the hourly average $CO_{2eq.}$ intensity of the electricity mix is an adaptation of multi-regional input–output models (MRIO). For each electricity generation technology (EGT), the method enforces the balance between electricity generation plus imports and electricity consumption plus exports. This balance is satisfied for both EGT and BZ at each hour of the year. Regarding the CO_2 factor for a specific EGT, it is shown that they can vary significantly among references depending on their respective assumptions. Among different possible applications, the average $CO_{2eq.}$ intensity that is determined using this methodology can be used as a control signal in predictive controls for building energy systems. The average $CO_{2eq.}$ intensity can actually be predicted using the forecast on hourly electricity generation provided by ENTSO-E.

Firstly, the methodology is applied to Northern Europe using CO_2 factors per EGT from the Ecoinvent database. It enables to highlight some important characteristics of this power market. Especially in Norway and northern Sweden, the electricity generation is characterized by a high share of hydropower in the electricity mix. These plants are typically operated when the price for electricity is high which happens during periods of high electricity demand. Therefore, the average $CO_{2eq.}$ intensities are usually low at times of high electricity demand. On the contrary, for countries where the electricity generation relies more on fossil fuels, average $CO_{2eq.}$ intensities are typically high at times of high electricity demand. In this respect, it is also important to consider electricity imports and their varying $CO_{2eq.}$ intensity when evaluating the average $CO_{2eq.}$ intensity. As soon as Norway imports electricity from neighboring BZs (typically in periods with low electricity demands), the $CO_{2eq.}$ intensity can increase significantly because electricity generation is usually more carbon-intensive in Norway's neighboring countries.

Secondly, the average $CO_{2eq.}$ intensity evaluated for Northern Europe is implemented into a predictive rule-based control (PRBC) to operate the electric heating system of a typical Norwegian residential building. The demand response measures based on the average $CO_{2eq.}$ intensity aim at decreasing the environmental impact of the heating system. Results prove that carbon-based controls can achieve emission reductions if daily fluctuations of the $CO_{2eq.}$ intensity are large enough to counterbalance for the increased electricity use generated by load shifting. As an example, the potential for emission reductions is higher in NO2 compared to NO3 because the daily fluctuations in the $CO_{2eq.}$ intensity in NO2 are much larger than in NO3. As these fluctuations in NO2 are mainly generated by imports, it further confirms the need to account for these imports in demand response analysis. If the heating system is controlled according to spot prices, results also confirm that price-based controls lead to increased emissions in the Scandinavian countries as operation is usually shifted towards night-time (for the case of Norway) when cheap but carbon-intensive electricity is indirectly imported from Germany, Poland, or the Netherlands (via Denmark and Sweden).

Demand response using PRBC applied to DHW heating show a strong potential for cost and emission savings. Conclusions regarding SH are more balanced. Depending on the control strategy and BZ, the PRBC manages to decreases the SH costs or the related $CO_{2eq.}$ emissions. The case building was taken representative for the Norwegian building stock and it results to a relatively low-level of thermal insulation. Energy use for SH is thus dominant over DHW. Consequently, the overall performance of DR using PRBC for heating (i.e., SH and DHW) is also balanced. Conclusions regarding SH may be different for buildings with better insulation as they have a higher storage efficiency. In addition, PRBC relies on predefined control rules which may not always be optimal. It should be explored whether advanced controls, such as model-predictive control (MPC), would lead to significant improvements regarding overall cost and emission savings.

Author Contributions: Regarding the methodology to evaluate the hourly average $CO_{2eq.}$ intensity, conceptualization was done by L.G. and J.C.; methodology and software were handled by C.S. and J.C.; validation, formal analysis, investigation, data curation, and visualization were the work of S.S. and J.C.; writing and original draft preparation was done by J.C. Regarding the case study on demand response using the $CO_{2eq.}$

intensity as a control signal, J.C. developed the building simulation model, implemented the control, ran the simulations, analyzed the data, visualized the results, and wrote the original draft of the article. Conceptualization and methodology were done by L.G. and J.C. All authors contributed to reviewing and editing the original article. The work was supervised by L.G.

Funding: This research received no external funding.

Acknowledgments: The authors would like to acknowledge IEA EBC Annex 67 "Energy Flexible Buildings", IEA HPT Annex 49 "Design and Integration of Heat Pumps for nZEBs" as well as the Research Centre on Zero Emission Neighbourhoods in Smart Cities (FME ZEN). Sebastian Stinner gratefully acknowledges that his contribution was supported by a research grant from E.ON Stipendienfonds im Stifterverband für die Deutsche Wissenschaft (project number T0087/29896/17).

Conflicts of Interest: The authors declare no conflict of interest.

Nomenclature

BZ	Bidding zone	LCA	Life-cycle assessment
CI	Carbon intensity	LCT	Low $CO_{2eq.}$ intensity threshold
CSC	Control strategy carbon	MPC	Model-predictive control
CSP	Control strategy price	MRIO	Multi-regional input–output
DHW	Domestic hot water	n_{50}	Air changes per hour at 50 Pa pressure difference
DR	Demand response		
EGT	Electricity generation technology	PRBC	Predictive rule-based control
Em.	Emissions	SH	Space heating
ENTSO-E	European Network of TSOs for Electricity	TSO	Transmission system operator
		TSP	Temperature set-point
HCT	High $CO_{2eq.}$ intensity threshold	ZEB	Zero Emission Building
HDS	Heat distribution system	η_{HR}	Heat recovery effectiveness
HVAC	Heating, ventilation, and air-conditioning	max	Maximum
		min	Minimum

Appendix A

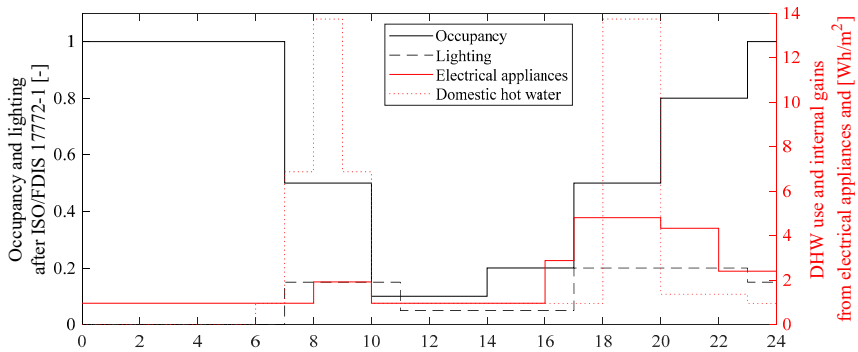

Figure A1. Daily profiles for DHW use and internal heat gains from electrical appliances, occupancy and lighting [15].

Table A1. Comparison of CO_2 factors per electricity generation technology (EGT) from different references [39].

Electricity Generation Technology (EGT)	Emission Factor [$gCO_{2eq.}/kWh_e$]		Name of EGT in Ecoinvent (for Reproduction Purposes)	Emission Factor ($gCO_{2eq.}/kWh_e$)
	IPCC	EEA		Ecoinvent (Applied Here)
Biomass	740	-	Electricity, high voltage {SE}| heat and power co-generation, wood chips, 6667 kW, state-of-the-art 2014 | Alloc Rec, U	60 [1]
Fossil brown coal/Lignite	820	-	Electricity, high voltage {DE}| electricity production, lignite | Alloc Rec, U	1240
Fossil coal-derived gas		-	Electricity, high voltage {DE}| treatment of coal gas, in power plant | Alloc Rec, U	1667
Fossil gas	490	-	Electricity, high voltage {DK}| heat and power co-generation, natural gas, conventional power plant, 100MW electrical | Alloc Rec, U	529
Fossil hard coal	1001	-	Electricity, high voltage {DK}| heat and power co-generation, hard coal | Alloc Rec, U	1266
Fossil oil		-	Electricity, high voltage {DK}| heat and power co-generation, oil | Alloc Rec, U	1000
Fossil oil shale		-	No data in Ecoinvent (assumed value)	1000
Fossil peat		-	Electricity, high voltage {FI}| electricity production, peat | Alloc Rec, U	1071
Geothermal	38	-	Electricity, high voltage {DE}| electricity production, deep geothermal | Alloc Rec, U	95
Hydro pumped storage	24	-	Electricity, high voltage {NO}| electricity production, hydro, pumped storage | Alloc Rec, U	62
Hydro run-of-river and poundage	24	-	Electricity, high voltage {SE}| electricity production, hydro, run-of-river | Alloc Rec, U	5
Hydro water reservoir	24	-	Electricity, high voltage {NO}| electricity production, hydro, reservoir, alpine region | Alloc Rec, U	8
Marine	24	-	No data in Ecoinvent (assumed value - as wind offshore)	18
Nuclear	12	-	Electricity, high voltage {SE}| electricity production, nuclear, pressure water reactor | Alloc Rec, U	13
Other		-	No data in Ecoinvent (assumed value - avg. fossil fuels)	979
Other RES		-	No data in Ecoinvent (assumed value - avg. RES)	46
Solar	45	-	Electricity, low voltage {DK}| electricity production, photovoltaic, 3kWp slanted-roof installation, single-Si, panel, mounted | Alloc Rec, U	144
Waste		-	Electricity, for reuse in municipal waste incineration only {DK}| treatment of municipal solid waste, incineration | Alloc Rec, U	500
Wind offshore	12	-	Electricity, high voltage {DK}| electricity production, wind, 1-3MW turbine, offshore | Alloc Rec, U	18
Wind onshore	11	-	Electricity, high voltage {DK}| electricity production, wind, 1-3MW turbine, onshore | Alloc Rec, U	14
Imports from all bidding zones with calculated hourly data	-	0		0
Imports from Russia	-	-	Electricity, high voltage {RU}| market for | Alloc Rec, U	862
Imports from Estonia	-	762	Electricity, high voltage {EE}| market for | Alloc Rec, U	1179
Imports from Poland	-	671	Electricity, high voltage {PL}| market for | Alloc Rec, U	1225
Imports from Belgium	-	212	Electricity, high voltage {BE}| market for | Alloc Rec, U	365
Imports from Great Britain	-	389	Electricity, high voltage {GB}| market for | Alloc Rec, U	762

[1] Assuming that biogenic CO_2 is climate neutral; 100-year spruce rotation assumption and dynamic GWP for climate impact of burning wood; does not consider climate impact from CO_2 from wood combustion.

References

1. Aduda, K.O.; Labeodan, T.; Zeiler, W.; Boxem, G.; Zhao, Y. Demand side flexibility: Potentials and building performance implications. *Sustain. Cities Soc.* **2016**, *22*, 146–163. [CrossRef]
2. Clauß, J.; Finck, C.; Vogler-Finck, P.; Beagon, P. Control strategies for building energy systems to unlock demand side flexibility—A review. In Proceedings of the 15th International Conference of the International Building Performance Simulation Association, San Francisco, CA, USA, 7–9 August 2017.
3. International Energy Agency (IEA). *Key World Energy Statistics*; International Energy Agency: Paris, France, 2015; Volume 82, p. 6. [CrossRef]

4. Arteconi, A.; Hewitt, N.J.; Polonara, F. State of the art of thermal storage for demand-side management. *Applied Energy* **2012**, *93*, 371–389. [CrossRef]
5. Chen, Y.; Xu, P.; Gu, J.; Schmidt, F.; Li, W. Measures to improve energy demand flexibility in buildings for demand response (DR): A review. *Energy Build.* **2018**, *177*, 125–139. [CrossRef]
6. Yin, R.; Kara, E.C.; Li, Y.; DeForest, N.; Wang, K.; Yong, T.; Stadler, M. Quantifying flexibility of commercial and residential loads for demand response using setpoint changes. *Appl. Energy* **2016**, *177*, 149–164. [CrossRef]
7. Haider, H.T.; See, O.H.; Elmenreich, W. A review of residential demand response of smart grid. *Renew. Sustain. Energy Rev.* **2016**, *59*, 166–178. [CrossRef]
8. Vandermeulen, A.; van der Heijde, B.; Helsen, L. Controlling district heating and cooling networks to unlock flexibility: A review. *Energy* **2018**, *151*, 103–115. [CrossRef]
9. Vandermeulen, A.; Vandeplas, L.; Patteeuw, D.; Sourbron, M.; Helsen, L. Flexibility offered by residential floor heating in a smart grid context: The role of heat pumps and renewable energy sources in optimization towards different objectives. In Proceedings of the 12th IEA Heat Pump Conference, Rotterdam, The Netherlands, 15–18 May 2017.
10. Lopes, R.A.; Chambel, A.; Neves, J.; Aelenei, D.; Martins, J. A literature review of methodologies used to assess the energy flexibility of buildings. *Energy Procedia* **2016**, *91*, 1053–1058. [CrossRef]
11. Junker, R.G.; Azar, A.G.; Lopes, R.A.; Lindberg, K.B.; Reynders, G.; Relan, R.; Madsen, H. Characterizing the energy flexibility of buildings and districts. *Appl. Energy* **2018**, *225*, 175–182. [CrossRef]
12. Finck, C.; Li, R.; Kramer, R.; Zeiler, W. Quantifying demand flexibility of power-to-heat and thermal energy storage in the control of building heating systems. *Appl. Energy* **2017**, *209*, 409–425. [CrossRef]
13. Péan, T.; Ortiz, J.; Salom, J. Impact of Demand-Side Management on Thermal Comfort and Energy Costs in a Residential nZEB. *Buildings* **2017**, *7*, 37. [CrossRef]
14. Lizana, J.; Friedrich, D.; Renaldi, R.; Chacartegui, R. Energy flexible building through smart demand-side management and latent heat storage. *Appl. Energy* **2018**, *230*, 471–485. [CrossRef]
15. Clauß, J.; Stinner, S.; Sartori, I.; Georges, L. Predictive rule-based control to activate the energy flexibility of Norwegian residential buildings: Case of an air-source heat pump and direct electric heating. *Appl. Energy* **2019**, *237*, 500–518. [CrossRef]
16. Fischer, D.; Bernhardt, J.; Madani, H.; Wittwer, C. Comparison of control approaches for variable speed air source heat pumps considering time variable electricity prices and PV. *Appl. Energy* **2017**, *204*, 93–105. [CrossRef]
17. Alimohammadisagvand, B.; Jokisalo, J.; Kilpeläinen, S.; Ali, M.; Sirén, K. Cost-optimal thermal energy storage system for a residential building with heat pump heating and demand response control. *Appl. Energy* **2016**, *174*, 275–287. [CrossRef]
18. Alimohammadisagvand, B.; Jokisalo, J.; Sirén, K. Comparison of four rule-based demand response control algorithms in an electrically and heat pump-heated residential building. *Appl. Energy* **2018**, *209*, 167–179. [CrossRef]
19. Le Dréau, J.; Heiselberg, P. Energy flexibility of residential buildings using short term heat storage in the thermal mass. *Energy* **2016**, *111*, 991–1002. [CrossRef]
20. Dar, U.I.; Sartori, I.; Georges, L.; Novakovic, V. Advanced control of heat pumps for improved flexibility of Net-ZEB towards the grid. *Energy Build.* **2014**, *69*, 74–84. [CrossRef]
21. Vogler-Finck, P.J.C.; Wisniewski, R.; Popovski, P. Reducing the carbon footprint of house heating through model predictive control—A simulation study in Danish conditions. *Sustain. Cities Soc.* **2018**, *42*, 558–573. [CrossRef]
22. Heidmann Pedersen, T.; Hedegaard, R.E.; Petersen, S. Space heating demand response potential of retrofitted residential apartment blocks. *Energy Build.* **2017**, *141*, 158–166. [CrossRef]
23. Hedegaard, R.E.; Pedersen, T.H.; Petersen, S. Multi-market demand response using economic model predictive control of space heating in residential buildings. *Energy Build.* **2017**, *150*, 253–261. [CrossRef]
24. Dahl Knudsen, M.; Petersen, S. Demand response potential of model predictive control of space heating based on price and carbon dioxide intensity signals. *Energy Build.* **2016**, *125*, 196–204. [CrossRef]
25. Péan, T.Q.; Salom, J.; Ortiz, J. Environmental and Economic Impact of Demand Response Strategies for Energy Flexible Buildings. *Proc. BSO* **2018**, *2018*, 277–283.

26. Patteeuw, D.; Bruninx, K.; Arteconi, A.; Delarue, E.; D'haeseleer, W.; Helsen, L. Integrated modeling of active demand response with electric heating systems coupled to thermal energy storage systems. *Appl. Energy* **2015**, *151*, 306–319. [CrossRef]
27. De Coninck, R.; Baetens, R.; Saelens, D.; Woyte, A.; Helsen, L. Rule-based demand-side management of domestic hot water production with heat pumps in zero energy neighbourhoods. *J. Build. Perform. Simul.* **2014**, *7*, 271–288. [CrossRef]
28. Killian, M.; Kozek, M. Ten questions concerning model predictive control for energy efficient buildings. *Build. Environ.* **2016**, *105*, 403–412. [CrossRef]
29. Fischer, D.; Madani, H. On heat pumps in smart grids: A review. *Renew. Sustain. Energy Rev.* **2017**, *70*, 342–357. [CrossRef]
30. IEA; Nordic Energy Research. *Nordic Energy Technology Perspectives 2016 Cities, Flexibility and Pathways to Carbon-Neutrality*; Nordic Energy Research: Oslo, Norway, 2016.
31. NordPoolGroup. NordPool 2018. Available online: https://www.nordpoolgroup.com/message-center-container/newsroom/exchange-message-list/2018/q2/nord-pool-key-statistics--may-2018/ (accessed on 13 June 2018).
32. NordPoolGroup. NordPool-About Us 2018. Available online: https://www.nordpoolgroup.com/About-us/ (accessed on 15 October 2018).
33. NordPoolGroup. NordPool Bidding Areas 2018. Available online: https://www.nordpoolgroup.com/the-power-market/Bidding-areas/ (accessed on 28 April 2018).
34. Wiebe, K.S. The impact of renewable energy diffusion on European consumption-based emissions. *Econ. Syst. Res.* **2016**, *28*, 133–150. [CrossRef]
35. Pan, L.; Liu, P.; Li, Z.; Wang, Y. A dynamic input–output method for energy system modeling and analysis. *Chem. Eng. Res. Des.* **2018**, *131*, 183–192. [CrossRef]
36. Guevara, Z.; Domingos, T. The multi-factor energy input–output model. *Energy Econ.* **2017**, *61*, 261–269. [CrossRef]
37. Palmer, G. An input–output based net-energy assessment of an electricity supply industry. *Energy* **2017**, *141*, 1504–1516. [CrossRef]
38. Arteconi, A.; Patteeuw, D.; Bruninx, K.; Delarue, E.; D'haeseleer, W.; Helsen, L. Active demand response with electric heating systems: Impact of market penetration. *Appl. Energy* **2016**, *177*, 636–648. [CrossRef]
39. Clauß, J.; Stinner, S.; Solli, C.; Lindberg, K.B.; Madsen, H.; Georges, L. A generic methodology to evaluate hourly average CO_2eq. intensities of the electricity mix to deploy the energy flexibility potential of Norwegian buildings. In Proceedings of the 10th International Conference on System Simulation in Buildings, Liege, Belgium, 10–12 December 2018. In Proceedings of the 10th International Conference on System Simulation in Buildings, Liege, Belgium, 10–12 December 2018.
40. Energinet. Retningslinjer for Miljødeklarationen for el 2017, 1–16. Available online: https://www.google.com.hk/url?sa=t&rct=j&q=&esrc=s&source=web&cd=1&cad=rja&uact=8&ved=2ahUKEwiFtdmLn8DhAhXsyIsBHUtOChwQFjAAegQIAxAC&url=https%3A%2F%2Fenerginet.dk%2F-%2Fmedia%2FEnerginet%2FEl-RGD%2FRetningslinjer-for-miljdeklarationen-for-el.pdf%3Fla%3Dda&usg=AOvVaw3lFa3nFoF1MpOpXtSk5pRa (accessed on 3 February 2019).
41. Milovanoff, A.; Dandres, T.; Gaudreault, C.; Cheriet, M.; Samson, R. Real-time environmental assessment of electricity use: A tool for sustainable demand-side management programs. *Int. J. Life Cycle Assess.* **2018**, *23*, 1981–1994. [CrossRef]
42. Roux, C.; Schalbart, P.; Peuportier, B. Accounting for temporal variation of electricity production and consumption in the LCA of an energy-efficient house. *J. Clean. Prod.* **2016**, *113*, 532–540. [CrossRef]
43. Tomorrow. CO2-equivalent Model Explanation 2018. Available online: https://github.com/tmrowco/electricitymap-contrib/blob/master/CO2eqModelExplanation.ipynb (accessed on 4 May 2018).
44. Bettle, R.; Pout, C.H.; Hitchin, E.R. Interactions between electricity-saving measures and carbon emissions from power generation in England and Wales. *Energy Policy* **2006**, *34*, 3434–3446. [CrossRef]
45. Hawkes, A.D. Estimating marginal CO_2 emissions rates for national electricity systems. *Energy Policy* **2010**, *38*, 5977–5987. [CrossRef]
46. Corradi, O. Estimating the Marginal Carbon Intensity of Electricity with Machine Learning 2018. Available online: https://medium.com/electricitymap/using-machine-learning-to-estimate-the-hourly-marginal-carbon-intensity-of-electricity-49eade43b421 (accessed on 28 February 2019).

47. Graabak, I.; Bakken, B.H.; Feilberg, N. Zero emission building and conversion factors between electricity consumption and emissions of greenhouse gases in a long term perspective. *Environ. Clim. Technol.* **2014**, *13*, 12–19. [CrossRef]
48. Askeland, M.; Jaehnert, S.; Mo, B.; Korpas, M. Demand response with shiftable volume in an equilibrium model of the power system. In Proceedings of the 2017 IEEE Manchester PowerTech, Manchester, UK, 18–22 June 2017. [CrossRef]
49. Quoilin, S.; Hidalgo Ganzalez, I.; Zucker, A. *Modelling Future EU Power Systems Under High Shares of Renewables The Dispa-SET 2.1 Open-Source Model*; Publications Office of the European Union: Luxembourg, LUXEMBOURG, 2017. [CrossRef]
50. Tomorrow. Electricity Map Europe 2016. Available online: https://www.electricitymap.org/?wind=false&solar=false&page=country&countryCode=NO (accessed on 13 April 2018).
51. Tranberg, B. Cost Allocation and Risk Management in Renewable Electricity Networks. PhD Dissertation, Department of Engineering, Aarhus University, Danske Commodities, Aarhus, Denmark, 2019.
52. IPCC. *Climate Change 2014: Mitigation of Climate Change. Contribution of Working Group III to the Fifth Assessment Report of the Intergovernmental Panel on Climate Change*; Edenhofer, O., Pichs-Madruga, R., Sokona, Y., Farahani, E., Kadner, S., Seyboth, K., Adler, A., Baum, I., Brunner, S., Eickemeier, P., et al., Eds.; Cambridge University Press: Cambridge, UK; New York, NY, USA, 2014.
53. Schlömer, S.; Bruckner, T.; Fulton, L.; Hertwich, E.; McKinnon, A.; Perczyk, D.; Roy, J.; Schaeffer, R.; Sims, R.; Smith, P.; et al. Annex III: Technology-specific cost and performance parameters. In *Climate Change 2014: Mitigation of Climate Change. Contribution of Working Group III to the Fifth Assessment Report of the Intergovernmental Panel on Climate Change*; Edenhofer, O., Pichs-Madruga, R., Sokona, Y., Farahani, E., Kadner, S., Seyboth, K., Adler, A., Baum, I., Brunner, S., Eickemeier, P., et al., Eds.; Cambridge University Press: Cambridge, UK; New York, NY, USA, 2014.
54. Ecoinvent. 2016. Available online: www.ecoinvent.org (accessed on 9 April 2018).
55. EEA. Overview of Electricity Production and Use in Europe 2018. Available online: https://www.eea.europa.eu/data-and-maps/indicators/overview-of-the-electricity-production-2/assessment (accessed on 12 April 2018).
56. Bachmann, C.; Roorda, M.J.; Kennedy, C. Developing a multi-scale multi-region input–output model developing a multi-scale multi-region input–output model. *Econ. Syst. Res.* **2015**, *27*, 172–193. [CrossRef]
57. Kristjansdottir, T.F.; Houlihan-Wiberg, A.; Andresen, I.; Georges, L.; Heeren, N.; Good, C.S.; Brattebø, H. Is a net life cycle balance for energy and materials achievable for a zero emission single-family building in Norway? *Energy Build.* **2018**, *168*, 457–469. [CrossRef]
58. Brattebø, H.; O'Born, R.; Sartori, I.; Klinski, M.; Nørstebø, B. Typologier for Norske Boligbygg—Eksempler på Tiltak for Energieffektivisering. Available online: https://brage.bibsys.no/xmlui/handle/11250/2456621 (accessed on 3 February 2019).
59. Goia, F.; Finocchiaro, L.; Gustavsen, A. Passivhus Norden|Sustainable Cities and Buildings The ZEB Living Laboratory at the Norwegian University of Science and Technology: A Zero Emission House for Engineering and Social science Experiments. In Proceedings of the 7th Nordic Passive House Conference, Copenhagen, Denmark, 20–21 August 2015.
60. Halvgaard, R.; Poulsen, N.; Madsen, H.; Jørgensen, J. Economic model predictive control for building climate control in a smart grid. In Proceedings of the 2012 IEEE PES Innovative Smart Grid Technologies (ISGT), Washington, DC, USA, 16–20 January 2012; pp. 1–6. [CrossRef]
61. Madsen, H.; Parvizi, J.; Halvgaard, R.; Sokoler, L.E.; Jørgensen, J.B.; Hansen, L.H.; Hilger, K.B. Control of Electricity Loads in Future Electric Energy Systems. In *Handbook of Clean Energy Systems*; Wiley: Hoboken, NJ, USA, 2015.
62. Johnsen, T.; Taksdal, K.; Clauß, J.; Georges, L. Influence of thermal zoning and electric radiator control on the energy flexibility potential of Norwegian detached houses. In Proceedings of the CLIMA 2019, Bucharest, Romania, 26–29 May 2019.
63. EQUA. EQUA Simulation AB 2015. Available online: http://www.equa.se/en/ida-ice (accessed on 16 October 2015).
64. EQUA Simulation AB; EQUA Simulation Finland Oy. *Validation of IDA Indoor Climate and Energy 4.0 with Respect to CEN Standards EN 15255-2007 and EN 15265-2007*; EQUA Simulation Technology Group: Solna, Sweden, 2010.

65. EQUA Simulation AB. *Validation of IDA Indoor Climate and Energy 4.0 build 4 with Respect to ANSI/ASHRAE Standard 140-2004*; EQUA Simulation Technology Group: Solna, Sweden, 2010.
66. Achermann, M.; Zweifel, G. *RADTEST—Radiant Heating and Cooling Test Cases Supporting Documents*; HTA Luzern: Luzern, Switzerland, 2003.
67. Bring, A.; Sahlin, P.; Vuolle, M. *Models for Building Indoor Climate and Energy Simulation Models for Building Indoor Climate and Energy Simulation 1. Executive Background and Summary*; Department of Building Sciences, KTH: Stockholm, Sweden, 1999.
68. Sahlin, P. *Modelling and Simulation Methods for Modular Continuous Systems in Buildings*; Royal Institute of Technology: Stockholm, Sweden, 1996.
69. Kipping, A.; Trømborg, E. Hourly electricity consumption in Norwegian households—Assessing the impacts of different heating systems. *Energy* **2015**, *93*, 655–671. [CrossRef]
70. Fischer, D.; Lindberg, K.B.; Madani, H.; Wittwer, C. Impact of PV and variable prices on optimal system sizing for heat pumps and thermal storage. *Energy Build.* **2017**, *128*, 723–733. [CrossRef]
71. SN/TS3031:2016. *Bygningers Energiytelse, Beregning av Energibehov og Energiforsyning*; Standard Norge: Oslo, Norway, 2016.
72. Ahmed, K.; Akhondzada, A.; Kurnitski, J.; Olesen, B. Occupancy schedules for energy simulation in new prEN16798-1 and ISO/FDIS 17772-1 standards. *Sustain. Cities Soc.* **2017**, *35*, 134–144. [CrossRef]
73. ISO17772-1. *Energy Performance of Buildings—Indoor Environmental Quality—Part1: Indoor Environmental Input Parameters for the Design and Assessment of Energy Performance of Buildings*; International Organization for Standardization: Geneva, Switzerland, 2017.
74. OpenStreetMap. Shiny Weather Data 2017. Available online: https://rokka.shinyapps.io/shinyweatherdata/ (accessed on 20 May 2017).
75. NordPoolGroup. NordPool Historical Market Data. Available online: https://www.nordpoolgroup.com/historical-market-data/ (accessed on 16 April 2018).
76. Standard Norge. *NS-EN 15251:2007 Indoor Environmental Input Parameters for Design and Assessment of Energy Performance of Buildings Addressing Indoor Air Quality, Thermal Environment, Lighting and Acoustics*; Standard Norge: Oslo, Norway, 2007.

PAPER 3

Predictive rule-based control to activate the energy flexibility of Norwegian residential buildings: Case of an air-source heat pump and direct electric heating

Clauß J[1], Stinner S[1], Sartori I[2], Georges L[1]

[1] Norwegian University of Science and Technology, Kolbjørn Hejes vei 1a, 7034 Trondheim, Norway

[2] SINTEF Building and Infrastructure, P.O. Box 124 Blindern, 0314 Oslo, Norway

This paper is published in *Applied Energy*, Volume 237, December 2018, Page 500–518.

Applied Energy 237 (2019) 500–518

Contents lists available at ScienceDirect

Applied Energy

journal homepage: www.elsevier.com/locate/apenergy

Predictive rule-based control to activate the energy flexibility of Norwegian residential buildings: Case of an air-source heat pump and direct electric heating

John Clauß[a,*], Sebastian Stinner[a], Igor Sartori[b], Laurent Georges[a]

[a] Norwegian University of Science and Technology, Kolbjørn Hejes vei 1a, 7034 Trondheim, Norway
[b] SINTEF Byggforsk, P.O. Box 124 Blindern, 0314 Oslo, Norway

HIGHLIGHTS

- Comparison of modulating and on-off air-source heat pump as well as direct electric heating.
- Demand response based on dynamic spot prices and $CO_{2eq.}$ intensities of the electricity mix.
- Sufficiently high daily fluctuations in spot prices and $CO_{2eq.}$ intensity necessary to benefit from demand response measures.
- Detailed modeling for both the heat pump system and the building.
- Described model complexity necessary to gain insight in real behavior of the energy system.

ARTICLE INFO

Keywords:
Building energy flexibility
Demand response
Heat pump
Predictive rule-based control
Direct electric heating
$CO_{2eq.}$ intensity

ABSTRACT

The building energy flexibility potential of a Norwegian single-family detached house is investigated using predictive rule-based control (PRBC) and building performance simulation (using IDA ICE). Norwegian timber buildings are lightweight and four different insulation levels are considered. Both on-off and modulating air-source heat pumps are analyzed and compared to direct electric heating which is the most common heating system for Norwegian residential buildings. A detailed model for both the heat pump system and the building is implemented, a level of detail not found in previous research on building energy flexibility. The three PRBC investigated have the following objectives: reduce energy costs for heating, reduce annual $CO_{2eq.}$ emissions and reduce energy use for heating during peak hours. This last objective is probably the most strategic in the Norwegian context where cheap electricity is mainly produced by hydropower. The results show that the price-based control does not generate cost savings because lower electricity prices are outweighed by the increase in electricity use for heating. The implemented price-based control would create cost savings in electricity markets with higher daily fluctuations in electricity prices, such as Denmark. For the same reasons, the carbon-based control cannot reduce the yearly $CO_{2eq.}$ emissions due to limited daily fluctuations in the average $CO_{2eq.}$ intensity of the Norwegian electricity mix. On the contrary, the PRBC that reduces the energy use for heating during peak hours turns out to be very efficient, especially for direct electric heating. For air-source heat pumps, the control of the heat pump system is complex and reduces the performance of the three PRBC. Therefore, results suggest that a heat pump system should be modeled with enough detail for a proper assessment of the building energy flexibility. First, by varying temperature set-points there is a clear interaction between the prioritization of domestic hot water and the control of auxiliary heaters which increases energy use significantly. Second, the hysteresis of the heat pump control and the minimum cycle duration prevent the heat pump from stopping immediately after the PRBC requires it. Finally, the paper shows that the influence of thermal zoning, investigated here by cold bedrooms with closed doors, has a limited impact on the building energy flexibility potential and the risk of opening bedroom windows.

* Corresponding author.
E-mail address: john.clauss@ntnu.no (J. Clauß).

https://doi.org/10.1016/j.apenergy.2018.12.074
Received 31 October 2018; Received in revised form 19 December 2018; Accepted 30 December 2018

Nomenclature

AHU	air handling unit
ASHP	air-source heat pump
BAU	baseline/business as usual
CBR	closed bedrooms
COP	coefficient of performance
CS	control strategy
CSC	control strategy carbon
CSP	control strategy price
CSS	control strategy schedule
DC	doors closed
DE	direct electric
DHW	domestic hot water
DOT	design outdoor temperature
DR	demand response
ER	electric radiator
FH	floor heating
HP	heat pump
HPT	high-price threshold
HTSP	high temperature set-point
LPT	low-price threshold
LTSP	low temperature set-point
MHP	modulating heat pump
MPC	model-predictive control
n_{people}	number of persons
Net-ZEB	Net-Zero Energy Building
OBR	open bedrooms
OHP	on/off heat pump
OTCC	outdoor temperature compensation curve
PH	passive house
PI	proportional-integral
PMV	predicted mean vote
PPD	predicted percentage of dissatisfied
PRBC	predictive rule-based control
PV	photovoltaic
Q_{Aux}	auxiliary heater
RTSP	reference temperature set-point
RBC	rule-based control
S	safety margin factor
SH	space heating
SP	spot price
T	temperature
TEK	Norwegian building regulation
TM	temperature measurement
TSP	temperature set-point
U_{Total}	total U-value of the windows including glazing and frame
V	volume
w/o	without
ZEB	Zero Emission Building
η_{HR}	heat recovery efficiency
φ_{max}	nominal space heating power, kW

Subscripts

EW	external wall
h	heating
IW	internal wall
max	maximum
min	minimum

1. Introduction

The transition to a sustainable energy system relies on the application of intermittent renewable energy sources. Demand side flexibility is essential to make full use of the electricity generated from intermittent renewable sources [1,2] and it can help balance the power grid and relieve it during grid peak hours [3]. Demand response measures can be applied to control the electricity use in a building depending on signals from the power grid and deploy demand side flexibility [4]. For heating systems in buildings, demand side flexibility can be seen as the margin by which a building can be operated while still fulfilling its functional requirements [5]. Numerous studies have been already conducted on building energy flexibility with focus on the heating system [2,5–22]. In these studies, heat pump systems play a major role and the electrification of heating using heat pumps in combination with thermal energy storage has been recognized as a promising measure for increasing the flexibility potential [3,4]. This potential for a heat pump system is dependent on the type of buildings, the type of heat pump and thermal storage as well as the applied control strategy [10]. In the introduction, references are analyzed with respect to building energy flexibility.

Regarding the thermal mass activation, Pedersen et al. [15] use an economic model-predictive control (MPC) to investigate the energy flexibility potential for different building insulation levels. Reynders et al. [6] make use of the structural thermal storage in residential buildings and quantify the energy flexibility in terms of available storage capacity, storage efficiency and power-shifting capacity. The thermal mass of a residential building is also used as short-term storage in the study by Le Dréau and Heiselberg [7]. They model two residential buildings with different insulation levels and quantify their flexibility potential. A flexibility factor is introduced to distinguish between electricity consumption during high-price and low-price hours.

Thermal zoning means that different indoor temperatures are applied to the various rooms in a building. The effect of thermal zoning on building energy flexibility has been investigated in a limited number of studies. In these studies, different temperature set-points (TSP) are defined for so-called day-zones and night-zones, where the TSP for the night zone is slightly lower than the TSP of the day zone [17,23,24]. Nevertheless, in other simulation studies, a single indoor temperature is considered for an entire dwelling. In Scandinavia, research nonetheless showed that many people prefer cold bedrooms which could limit the energy flexibility potential [25] with thermal mass activation. Berge et al. [26] conducted long-term measurements in highly-insulated apartments in Norway in combination with occupant surveys and found that extensive window opening was common to reach the desired lower temperatures in bedrooms. A limited number of papers has investigated the influence of the building insulation level (including partition walls), building thermal mass and the control of the heating and ventilation systems on the thermal zoning and the corresponding space heating (SH) needs [27–29].

The control of the heating system of a building is essential for deploying its energy flexibility potential. Even though MPC has been found to outperform non-optimal control strategies, MPC is more computationally expensive and more complex, essentially because a low-order model of the system to be controlled is required [10]. Compared to MPC, rule-based control (RBC) is based on a set of predefined rules to control the system. RBC is more straightforward to implement than MPC as it does not require a control model. Nevertheless, a careful design of the control rules is essential, which is not always obvious. RBC can be based on the prediction of the future boundary conditions, such as the hourly electricity price. It is then termed predictive rule-based control (PRBC). Fischer et al. [10] found that PRBC can be a promising alternative to MPC as it is simpler and still effective (providing the control rules are well defined). Several relevant studies confirmed that PRBC can decrease the energy costs for the building operation [18,30–35]. In order to define the PRBC rules, Georges et al. [36]

introduced a lower and upper price threshold so that energy is stored during low-price periods and energy use is lowered during high-price periods. Alimohammadisagvand et al. [30] successfully implemented a price-based PRBC to control the thermal energy storage of a residential building heated by a ground source heat pump. Fischer et al. [32] used PRBC for scheduling the heat pump operation depending on predictions of the electricity price, PV generation and thermal loads of the building. Here, the heat pump was either run at times of high PV generation to maximize the PV self-consumption or at times of minimum electricity prices to charge the storage tank of the heat pump system. Dar et al. [33] investigated the energy flexibility of a Net-ZEB heated by an air-source heat pump. They concluded that the peak power can be reduced significantly with a well-tuned RBC. Regarding modulating heat pumps, MPC and RBC are significantly different. Most studies using MPC assume that the compressor power can be directly controlled which ignores the details of the built-in PI control of the heat pump. RBC rather adjusts the set-point to this PI controller.

In general, different objectives can be targeted in the context of building energy flexibility (either by using MPC or RBC). Besides reducing the energy costs, maximizing the use of renewable energy sources, increasing the self-consumption of the on-site PV generation and limiting the peak power are frequently discussed [5]. De Coninck et al. [37] increased the use of on-site renewable energy by controlling a heat pump by means of the power injection to the grid or overvoltage at the grid connection of the buildings. Vanhoudt et al. [8] investigated an actively-controlled heat pump and successfully limited peak power demands and maximized self-consumption of the on-site electricity generation. Vandermeulen et al. [38] controlled the heat pump in a Belgian residential building to maximize the electricity when there was a high level of renewable energy generation in the power grid. Hedegaard et al. [16], Pedersen et al. [15] and Knudsen et al. [39] minimized the emissions of carbon dioxide ($CO_{2eq.}$) related to the SH in Danish residential buildings. Knudsen et al. [39] found that in Denmark the electricity spot price and $CO_{2eq.}$ intensity of the electricity mix (also called the $CO_{2eq.}$ factor) are not strongly correlated. Thus, a control focusing on minimizing the energy costs for SH would not automatically minimize the related $CO_{2eq.}$ emissions.

As already mentioned, many studies consider heat pump systems as key technology for building energy flexibility. Nevertheless, studies which resort to a detailed modeling of the heat pump system consider a simplified building model (such as low-order resistance capacitance models) or do not consider the thermal mass activation [21,32]. On the contrary, existing studies with a detailed building model resort to a simplified model for the heat pump system. To the authors' knowledge, no study considers a detailed modeling for both the heat pump system and the building, which is done in this work.

This study investigates the energy flexibility potential of Norwegian residential buildings by controlling their heating system using PRBC. It considers the activation of the building thermal mass and a water storage tank. The performance of an air-to-water heat pump and direct electric heating is compared. The paper answers four original research questions:

- Q1: *What is the energy flexibility potential of PRBC in the specific context of Norway?* To answer this question, this study considers different building insulation levels starting from old building standards to Norwegian Passive Houses (PH) and Zero Emission Buildings (ZEB). Norwegian houses are mostly heated using direct electricity, meaning electric radiators for SH and an electric resistance in a storage tank for the domestic hot water (DHW) production [40]. Nevertheless, for buildings with enough insulation, heat pumps are also a popular solution. In Norway, buildings are typically lightweight timber constructions and most of the electricity in the power grid is generated by hydropower [41].
- Q2: *How does the thermal zoning impact the energy flexibility potential?* This problem has been addressed in a very limited number of studies only [17,23,24], whereas most studies assume the same indoor temperature in all the rooms of the building, including bedrooms. Nevertheless, it has been proven that many Norwegians like cold bedrooms ($< 16\,^{\circ}C$) and may open windows for several hours a day to reach the desired bedroom temperature. The risk of flushing the heat stored in bedrooms is more important with increasing insulation levels. It is thus important to determine how the thermal mass activation using PRBC influences bedroom temperatures.
- Q3: How does the modeling complexity of the heat pump system influence the operation of the heating system and thus the energy flexibility potential? Most of the studies found in the literature are based on simulations using models that significantly simplify the heat pump system for one or several of the following aspects: (1) the heat pump is not able to modulate or, on the contrary, it modulates perfectly between 0 and 100%; (2) minimum cycle durations and pause times are not used with the heat pump; (3) the storage tank is simplified by neglecting either thermal stratification or the details of the connections to the tank as well as the exact location of the temperature sensors in the tank; (4) the control of the auxiliary heater is idealized.
  Here, a detailed modeling of the heat pump system has been implemented in the detailed dynamic simulation software IDA Indoor and Climate (IDA ICE) to answer this question. To the authors knowledge, this level of modeling detail for both the heat pump system and the building has not been proposed in the literature regarding building energy flexibility. Regarding the modeling of the heat pump system, the air-source heat pump (ASHP) is able to modulate continuously between 30% and 100%. It has an imposed minimum cycle and pause time and a realistic control to prioritize DHW over SH. The heat pump is connected to a detailed model of a storage tank with a realistic control of the auxiliary heaters. Even though the models for each component of the heat pump system (i.e. the heat pump, the tank or the SH distribution systems) are not the most sophisticated, the interaction between components and their control is particularly comprehensive.
- The proposed level of detail enables to answer a supplementary question. Q4: How does PRBC influence the operating conditions of the heat pump in terms of duration and frequency of cycles as well as the seasonal performance factor?

An indirect control is performed, meaning that a control (or penalty) signal from the grid is used as input to the PRBC to schedule the temperature set-point for the SH and DHW systems. These changes of temperature set-points enable heat to be stored in the thermal mass of the building or in the storage tank (for DHW but also for SH in the case of the ASHP). Three different control strategies are investigated to meet the specific objectives: (1) decrease the energy costs for heating using the day-ahead spot price for electricity as the input control signal [42], (2) decrease the $CO_{2eq.}$ emissions related to heating using the hourly $CO_{2eq.}$ intensity of the Norwegian electricity mix as input control signal and (3) decrease electricity use for heating during typical peak hours for Norwegian residential buildings [43].

The paper is organized as follows. Section 2 provides an overview of the methodology and a detailed description of the building as well as its heating and control systems. Demand response controls are defined in Section 3 while Section 4 introduces the key performance indicators. Results are presented and discussed in Section 5.

2. Methodology and test case

As this work involved detailed modeling a comprehensive description of the building and its heating system is necessary. Therefore, a real building is used as a test case for our investigations. Even though this case is specific, it has been selected as representative for Norway and provides enough technical information to build a reliable simulation model of the heat pump system.

The Living Lab is a ZEB residential building with a heated area of 105 m^2 located on the Gløshaugen campus in Trondheim (Norway). The building floor plan is shown in Fig. 1. Common rooms consist of the Living Room, Kitchen and the Living Room North. Detached single-family houses represent a large share of the Norwegian building stock. The building has a highly-insulated envelope and a lightweight timber construction [44]. SH and DHW production is performed by a heat pump and solar thermal collectors connected to a single storage tank. This is a common heating strategy applied in Norwegian ZEB, see e.g. [45]. The on-site electricity generation from photovoltaic panels is designed to compensate for the $CO_{2eq.}$ emissions embodied in the building materials as well as for emissions generated from the operational phase over the complete building lifetime. The climate of Trondheim is also relevant for Norway in general.

A detailed multi-zone model of the Living Lab has been created using the software IDA ICE version 4.8. IDA ICE is a dynamic building simulation software which applies equation-based modeling [46]. It allows investigation of the detailed dynamics of the components of the energy supply system and enables the user to evaluate the indoor climate as well as the energy use of a building. IDA ICE has been validated in several studies [47–51].

Starting from a detailed model of the ZEB Living Lab, a sensitivity analysis can be performed to investigate the impact of building parameters on the energy flexibility potential. First, the influence of the thermal performance of the building envelope is investigated, here by changing the insulation levels. Second, both on-off and modulating heat pumps are both considered as well as the use of direct electric heating. The potential of energy flexibility is investigated by comparing three different PRBC to the reference scenario which applies constant temperature set-points for SH and DHW.

As the weather- and grid-related data are correlated (such as the spot price and $CO_{2eq.}$ intensity), historical data from 2015 have been used for simulations.

2.1. Building envelope

Four different performance levels of the building envelope are investigated; here, these are termed the building insulation levels. In addition to the PH and ZEB levels, the requirements of two older Norwegian building regulations, TEK87 and TEK10, are considered. For each performance level, Table 1 provides an overview of their thermal characteristics taken from [52].

Except for the TEK87, all the building insulation levels require balanced mechanical ventilation. The air handling unit (AHU) has a rotary heat wheel with heat recovery effectiveness (η_{HR}). According to the building regulations, the constant air volume ventilation has a nominal airflow rate of 120 m^3/h. Natural ventilation was usually applied in TEK87 buildings. For the sake of the simplicity, natural ventilation is modeled as balanced mechanical ventilation with a η_{HR} of 0%.

Table 1
Summary of building envelope properties and energy system characteristics for different building insulation levels (EW – external wall, IW – internal wall, HR – heat recovery, U_{Total} is the total U-value of the windows including the glazing and the frame).

Component	Parameter	Unit	Building insulation type			
			PH	ZEB	TEK10	TEK87
Building envelope	U_{EW}	W/(m^2·K)	0.10	0.16	0.22	0.35
	U_{IW}	W/(m^2·K)	0.34	0.34	0.34	0.34
	U_{Roof}	W/(m^2·K)	0.09	0.11	0.18	0.23
	U_{Floor}	W/(m^2·K)	0.09	0.10	0.18	0.30
Infiltration		ACH	0.6	0.7	2.5	3.0
Thermal bridges		W/(m^2·K)	0.03	0.045	0.03	0.05
Windows	U_{Total}	W/(m^2·K)	0.8	0.8	1.2	2.1
AHU	η_{HR}	%	85	85	70	0
Heat pump	Q_h (A7/W35)	kW	5.1	5.1	5.1	–
	COP	–	4.57	4.57	4.57	–
Water tank	DHW	l	215	215	215	215
	SH	l	243	275	382	–
	$Q_{Aux,DHW}$	kW	3	3	3	–
	$Q_{Aux,SH}$	kW	9	9	9	–
Heat distribution system	FH	W/m^2	40	45	78	–
	El. Radiator	W/m^2	40	45	78	93
Solar thermal SH needs	Collector Area	m^2	–	4	–	–
		kWh/m^2	34	48	91	172

For the ZEB insulation level, the multi-zone IDA ICE model of the building envelope heated by an electric radiator has been calibrated with measurement data from a dedicated experiment conducted in April and May 2017 [53]. It was found that the model correctly predicted the short-term thermal dynamics of the building and the temperature differences between rooms [54].

2.2. Heating system

Two different heating systems have been considered. First, an ASHP is connected to a water storage tank used for both SH and DHW. For the

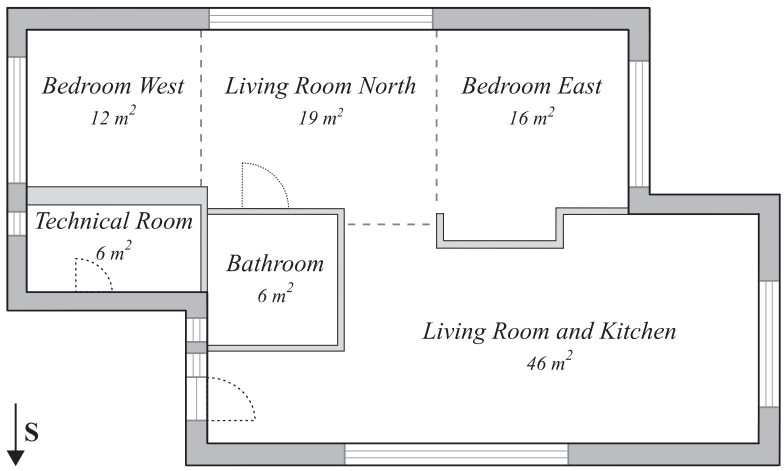

Fig. 1. Floor plan of the studied building.

ZEB insulation level, the heat pump is assisted by 4 m^2 of solar thermal collectors (in line with the most common concepts of Norwegian ZEB). With the ASHP, the SH distribution is performed using floor heating (FH). The peak and back-up heating is done by electric resistances. The layout of the heat pump system is presented in Fig. 2. Second, the building is heated by direct electricity, meaning electric radiators for SH and a resistance in a storage tank for DHW.

2.2.1. Power sizing

The heat pump is sized according to "bivalence point" principle, which is recommended by heat pump manufacturers [55–57]. For a design outdoor temperature (DOT) of −19 °C, the ZEB has a nominal SH power (φ_{max}) of 3.6 kW, whereas the DHW heating power is 1.4 kW. The selected heat pump is a Hoval Belaria SRM 4 [58] working in bivalent mono-energetic mode at low outdoor temperatures [55]. The heat pump power has been selected for a bivalence outdoor temperature of about −9 °C. In that way, the heat pump is able to modulate between 30% and 100% for outdoor air temperatures between 5 °C and −9 °C. This temperature range represents most of the SH season in Trondheim. This leads to a nominal capacity (A7/W35) of 5.1 kW (COP 4.57) for the ZEB case. As smaller heat pumps are difficult to find on the market, the same heat pump capacity is used for the PH case. For the sake of the simplicity, the same power is also applied for the heat pump in the TEK10 case. Even though the φ_{max} of the TEK10 building is 5.6 kW, it can still be supplied by the selected heat pump, the ASHP is just operated more often at a full speed. On/off auxiliary heaters are installed at the top layer of the SH and DHW parts of the tank to ensure that the required water distribution temperatures are always met. The auxiliary heater in the DHW tank has a capacity of 3 kW, whereas the auxiliary heater for the SH tank has a capacity of 9 kW [59]. The capacities of both auxiliary heaters are chosen according to the manufacturer data of the storage tank which is installed in the ZEB Living Lab.

2.2.2. Heat pump system

The heat pump system is introduced first. The FH system consists of seven circuits with at least one circuit per room. The nominal SH power of each room is calculated for a DOT of −19 °C in order to determine the nominal power of each floor heating circuit. This power is adjusted for each building insulation level. The FH supply temperature is adapted using an outdoor temperature compensation curve (OTCC).

The modeling of the components is not the most detailed but the modeling of the interaction between components and their control is particularly comprehensive. Several studies [60–62] provide detailed descriptions of the heat pump model which is embedded in IDA ICE. The heat pump model is steady-state with a heat exchanger model for the condenser and evaporator as well as a correction for part load operation. The model parameters are calibrated using manufacturer data at full load [63] according to the methodology reported by Niemelä et al. [61]. The water in the SH tank is heated when flowing through the heat pump condenser (i.e. a direct connection). The heat pump can reach a desired supply temperature either by (1) running the heat pump at full load and adjusting the water flow rate of the circulation pump or by (2) running the circulation pump at nominal speed and adjusting the heat pump compressor speed. In SH mode, the mass flow is constant and a PI control adjusts the compressor power to reach a temperature set-point measured in the SH storage tank. Parameters of the PI control are tuned using SIMC tuning rules (Skogestad Internal Model Control) [64]. Regarding DHW, the heat pump is first operated at full load and the mass flow is adjusted by a P-controller in order to meet a given temperature set-point at the outlet of the condenser. As soon as the circulation pump runs at full speed, the heat pump compressor speed is adjusted. The heat pump is connected to the DHW tank through a heat exchanger. Then, the supply temperature of the heat pump is slightly higher than the temperature set-point in the DHW storage tank. In this study, the default heat pump model in IDA ICE (called ESBO plant) has been extended in to order to account for additional physical

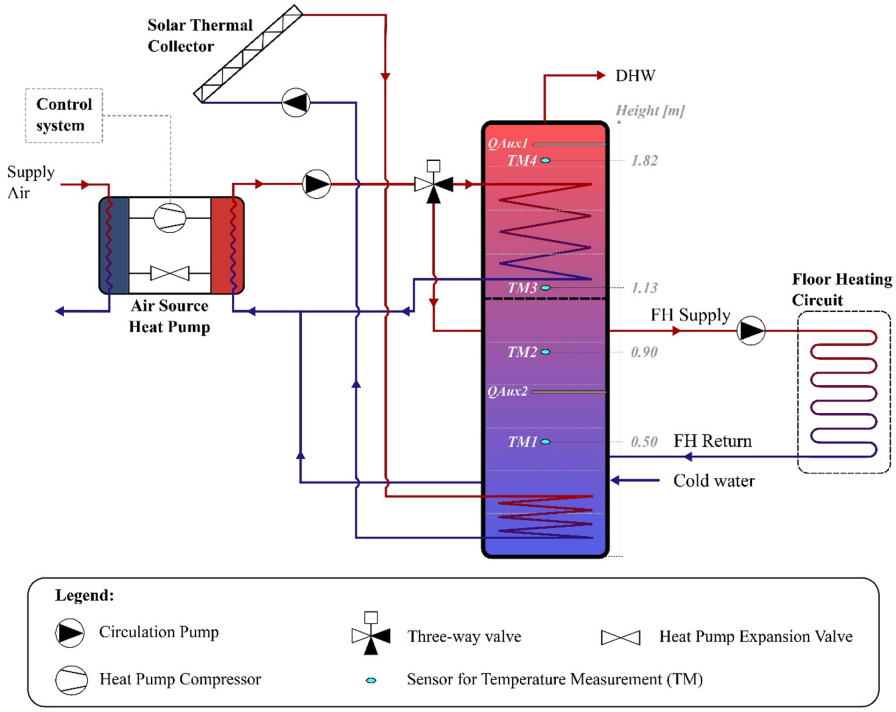

Fig. 2. Configuration of the heating system in the ZEB case.

phenomena. First, the heat pump modulates continuously between 30% and 100% of the nominal compressor capacity while it cycles on-off below 30%. Second, a minimum run and pause time has been implemented (here taken at 10 min) in order to prevent on-off cycling from occurring too frequently. Third, a realistic prioritization of the DHW over the SH production is implemented so that the heat pump cannot support SH when producing DHW. Few studies about building energy flexibility considered DHW prioritization (e.g. [17]). All these three actions require supplementing an anti-windup to the PI control in order to prevent the saturation of the integral action.

Furthermore, it is worth mentioning that the DHW prioritization and the minimum run and stop times may lead to the violation of the temperature set-points for SH. Then, auxiliary heaters have to compensate. To the author's knowledge, these physical effects have hardly been taken into account in other studies.

IDA ICE has a one-dimensional model of a stratified tank that accounts for the heat conduction and convection effects in the tank. The storage tank is divided into ten horizontal layers: the DHW part consists of the four upper layers and the SH part of the six lower layers. The required DHW storage volume is dependent on the number of people and on a safety margin S, which is set to 125% for a low number of people [65]. The storage volume for DHW is calculated by:

$$V_{DHW} \cong S \cdot 65 \cdot n_{people}^{0.7} \quad [l] \tag{1}$$

The dimensioning of the SH buffer tank is not only dependent on the type of heat pump and its power but also on the temperature of the heat distribution system as well as the thermal inertia of the building. According to [65], the recommended storage volume for SH is:

$$V_{SH} \cong 81.54 + 53.8 \cdot \varphi_{max} \quad [l] \tag{2}$$

Following Eqs. (1) and (2), the storage volume for DHW tank is kept constant for all building insulation levels while the volume for SH is adapted for each case (as φ_{max} changes). Even though the overall tank volume changes, the same aspect ratio of the water storage tank is kept as well as the relative position of the connection to the tank in order to maintain similar stratification effects.

The operation of the heat pump as well as both auxiliary heaters is based on measured water temperatures in the tank. The principle of heat pump control is presented in Fig. 3. There are four temperature sensors in the water tank. Each part of the tank (i.e. the DHW and SH parts) has two sensors to control their charging. The heat pump is started as soon as the temperature in the upper layer of the respective tank part drops below a certain set-point. It runs until the set-point for the sensor in the lower layer of the tank part is reached. For the reference control scenario, called BAU (business-as-usual), the temperature set-points to start and stop DHW heating are set to 50 °C and 53 °C, respectively. The temperature set-points for the SH tank vary as a function of the OTCC. The stop criterion of the SH hysteresis is set to OTCC + 8 K. A hysteresis of 8 K gives enough storage to prevent the heat pump from cycling too frequently, even during mild outdoor temperatures (and thus low OTCC), but a large dead-band leads to reduced energy efficiency.

With a bivalent heat pump system, the control of the auxiliary heaters should be clearly defined as the auxiliary heater operation can have a strong impact on the total electricity use for heating [21,66]. The temperature set-points of both electric auxiliary heaters are set 3 K below the start temperature of the heat pump. In that way, the heat pump is started when the temperature drops below a certain threshold. If the heat pump cannot cover the heat demand and the tank temperature continues to decrease, the auxiliary heater eventually starts. The auxiliary heaters are controlled by a thermostat with a dead band of 4 K.

2.2.3. Direct electric heating

An electric resistance heater with a power of 3 kW is used for DHW heating whereas electric radiators are used for SH. One electric radiator is placed in each room with a power equal to the nominal SH power of the room.

2.3. Boundary conditions

The heat gains from electrical appliances, occupants and lighting are 17.5, 13.1 and 11.4 kWh/(m^2·year) respectively, according to Norwegian technical standard, SN/TS 3031:2016 [67]. Schedules for electrical appliances are based on SN/TS 3031:2016, whereas the schedules for occupancy and lighting are taken from prEN16798-1 and ISO/FDIS 17772-1 standards [68,69]. The internal gains are uniform in space. The hourly profiles over a day are presented in Fig. 4. The occupancy profiles are treated as deterministic daily profiles [68], where

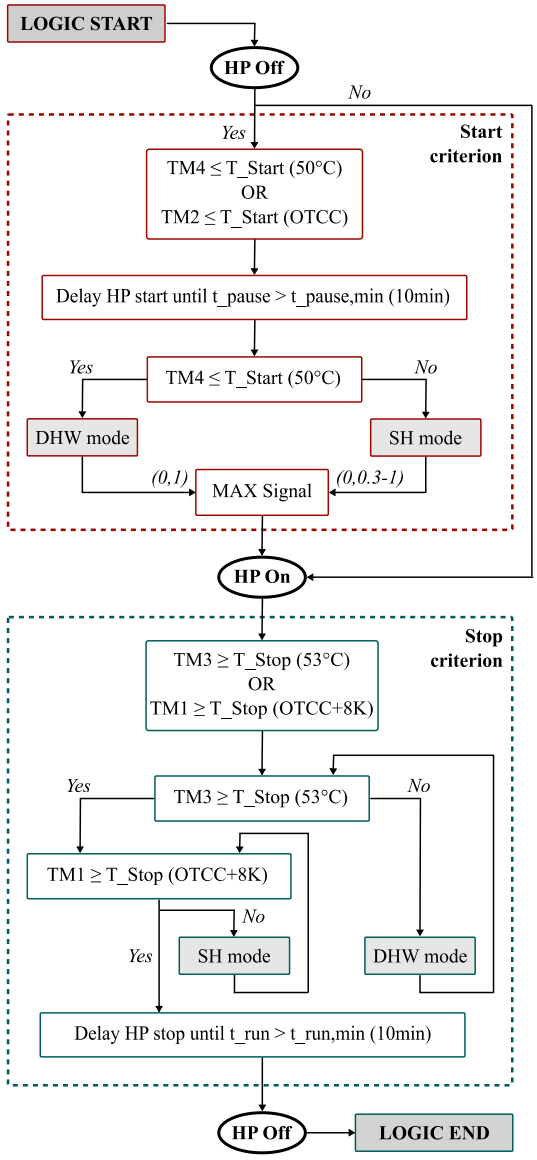

Fig. 3. Principle of the temperature-based heat pump control.

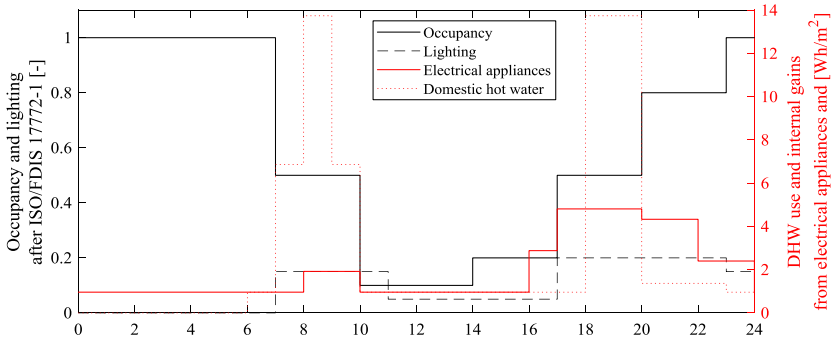

Fig. 4. Daily profiles for DHW use and internal heat gains from electrical appliances, occupancy and lighting.

0 means absence and 1 full presence. A fraction of 0.5 means that the building reaches 50% of full occupancy. The daily profile for DHW consumption is taken from SN/TS 3031:2016 [67], see Fig. 4., with an annual energy use of 25 kWh/(m^2·year). All profiles have an hourly resolution and are applied for every day of the year.

Using the Predicted Mean Vote (PMV) method, indoor operative temperature set-points can be defined depending on the activity and clothing level of the occupants [70]. According to EN15251:2007 [71], a minimum and maximum indoor operative temperature of 20 °C and 24 °C correspond to a Predicted Percentage Dissatisfied (PPD) $<$ 10% and $-0.5 < \text{PMV} < +0.5$ in residential buildings for an activity level of 1.2 MET and a clothing factor of 1.0 clo. With thermal activation, indoor operative temperatures are varied between 20 °C and 24 °C. When thermal zoning is investigated, a temperature set point of 16 °C is used in bedrooms to account for the temperature preferences of many Norwegians.

Hourly weather data is taken from [72] and includes dry-bulb air temperature, relative humidity, wind direction and speed as well as direct and diffuse solar radiation on a horizontal plane. NordPool provides hourly day-ahead spot prices for each bidding zone, including the bidding zone of the Trondheim area (NO3) [42]. It is used as an input signal for the price-based control and to calculate energy costs for heating. The hourly average $CO_{2eq.}$ intensity is determined according to the methodology proposed in [41] based on the hourly generation from each generation technology. The method considers the electricity imports to the bidding zone. The hourly $CO_{2eq.}$ intensity of the electricity mix is used as control signal to decrease annual $CO_{2eq.}$ emissions. Weather data, spot prices and $CO_{2eq.}$ intensity of the electricity mix in NO3 are correlated so that historical data from 2015 for the city of Trondheim is applied.

3. Simulation scenarios

3.1. Demand response control scenarios

The baseline scenario (called BAU), maintains a constant indoor temperature of 21 °C and constant temperature set-points for the heating system throughout the whole year. The start and stop temperatures for DHW heating are 50 °C and 53 °C, respectively. These constant set-points are chosen as the baseline scenario because this is the most common way to control heating systems in Norwegian residential buildings. For the three demand response (DR) control strategies, all the set-points for SH are either increased by 3 K or decreased by 1 K whereas the set-points for DHW heating are either increased by 10 K or decreased by 5 K. Regarding the DR for DHW heating, increasing the TSP by 10 K leads to an upper temperature boundary of 63 °C, which is just below the maximum supply temperature that the heat pump is able to deliver. Temperature set-points that are related to DHW heating are the start and stop temperatures (of the hysteresis), as well as the supply temperature of the heat pump. Temperature set-points that are related to SH are the room temperature, the start and stop temperatures of the hysteresis as well as the FH supply temperature. With DR, annual energy savings could occur if temperature set-points are frequently lower than values of the BAU control. The first DR control scenario is based on the time-varying spot price. Electricity prices vary throughout a day so that energy costs could be reduced if the heating system is operated outside high-price periods. Two different algorithms can be applied for the price-based control. The second DR scenario considers the dynamic $CO_{2eq.}$ intensity of the electricity mix in the NO3 bidding zone. The $CO_{2eq.}$ intensity gives an indication of the carbon intensity in the fuel type which has been used for electricity generation. It can thus be used to maximize the consumption of electricity generated from non-fossil fuels. The rules for the control strategies based on the spot price and $CO_{2eq.}$ intensity are similar. In the Norwegian electricity grid, a major concern regarding residential buildings is the maximum power and electricity use during peak hours. In the last DR scenario, the control reduces the energy use for heating during peak hours and flattens the consumption profile.

3.2. PRBC using the spot price (Control Strategy Price, CSP)

The price-based control signal is calculated in two different ways (a) the spot price for the next 24 h is divided into three price segments, where the set-points are adjusted depending on the spot price of the current hour, or (b) additionally to the three price segments, the control checks whether the spot price is increasing or decreasing with time.

3.2.1. Version a (CSP-a)

This price-based PRBC uses a 24-hour sliding horizon to determine a high-price threshold (HPT) and low-price threshold (LPT). At each hour, the current spot price is compared to these thresholds. Taking SP_{max} and SP_{min} as the maximum and minimum prices for the next 24 h, LPT has been selected to $SP_{min} + 0.3\ (SP_{max}\text{-}SP_{min})$ and HPT to $SP_{min} + 0.75\ (SP_{max}\text{-}SP_{min})$. The temperature set-points for DHW and SH are adjusted depending on the current spot price. If the price of the current hour is below the LPT, the temperature set-points are increased. If the current spot price is above the HPT, the set-points are decreased to delay the start of the heating, whereas if the spot price of the current hour is between the LPT and HPT, the temperature set-points remain equal to BAU. The performance of the control is sensitive to the selection of LPTs and HPTs. Table 2 shows the influence of the thresholds on the number of hours at a respective temperature set-point. Generally, the higher the LPT, the more hours with an increased temperature set-point occur during a year. On the contrary, the lower the HPT, the more hours with decreased temperature set-points occur. An analysis of the price thresholds found that this control strategy may charge

Table 2
Influence of the low-price and high-price thresholds on the control signal in terms of number of hours per set-point segment (LTSP is low temperature set-point, RTSP is reference temperature set-point, HTSP is high temperature set-point).

LPT&HPT [%]	CSP-a			CSP-b		
	t_{LTSP} [h]	t_{RTSP} [h]	t_{HTSP} [h]	t_{LTSP} [h]	t_{RTSP} [h]	t_{HTSP} [h]
20&75	2728	3690	2342	4805	2341	1614
25&75	2728	3350	2682	4607	2681	1472
30&75	**2728**	**3020**	**3012**	**4423**	**3011**	**1326**
35&75	2728	2695	3337	4242	3336	1182
40&75	2728	2334	3698	4043	3697	1020
30&60	3765	1984	3011	4879	3010	871
30&65	3433	2316	3011	4737	3010	1013
30&70	3098	2651	3011	4585	3010	1165
30&80	2369	3380	3011	4256	3010	1494
30&85	2030	3719	3011	4112	3010	1638

the thermal storage many hours before the next high-price period. Therefore this leads to an unnecessary increase in annual heating energy use.

3.2.2. Version b (CSP-b)

The control signal is here determined based on the three price segments, as defined in CSP-a, but, additionally, the control checks if the spot price is increasing or decreasing with time. If the current spot price is between the LPT and HPT and the spot price is increasing in the next two hours, the temperature set-point is increased (Fig. 5).

If the current spot price is between the LPT and HPT and the price is decreasing in the next two hours, the TSPs are decreased. Contrary, if the current spot price is between LPT and HPT and the price is increasing in the next two hours, the TSPs are increased. Unlike CSP-a, this logic aims at charging the thermal storages right before high-price periods. The duration for an increased temperature set-point depends on the difference between the two price thresholds. The larger the difference between the thresholds, the longer the period for charging a thermal storage. An LPT of 30% and an HPT of 75% are chosen for determining the CSP-b control signal. Comparing CSP-a and CSP-b in Table 2, it is obvious that the temperature set-points are decreased for more hours during a year (2728 vs. 4423) and increased less often (3012 vs. 1326) using CSP-b.

3.3. PRBC using $CO_{2eq.}$ intensity (Control Strategy Carbon, CSC)

The principle of the $CO_{2eq.}$-based control strategy is similar to the price-based control strategy CSP-b, but aims at reducing $CO_{2eq.}$ emissions. A high-carbon threshold of 70% and a low-carbon threshold of 30% are chosen based on a sensitivity analysis. It can be seen from Fig. 6 that low spot prices occur at times of high average $CO_{2eq.}$ intensity, thus leading to contradictory control objectives. Norway usually imports electricity during the night, giving a higher $CO_{2eq.}$ intensity, whereas the hydropower plants run during the day to balance supply and demand, leading to a lower $CO_{2eq.}$ intensity.

A control scenario which makes use of the lowest $CO_{2eq.}$ intensity of the electricity mix (corresponding to CSC-a) would therefore lead to increased heating electricity use during peak periods. This situation is specific to Norway because $CO_{2eq.}$ intensity and peak power are usually highly correlated in other European countries, such as Germany. To prevent increased energy use during peak hours, the implemented $CO_{2eq.}$-based control signal is also determined according to version b of CSP, here corresponding to CSC-b.

3.4. Schedule-based control (Control Strategy Schedule, CSS)

The temperature set-points are changed based on a schedule. Knowing the hourly profile of typical electricity use for Norwegian households [43], peak hours can be defined and electricity use during these hours decreased by charging the heat storages before the daily peak periods. Typical peak hours occur between 7 a.m. and 10 a.m. and between 5 p.m. and 8 p.m. Temperature set-points are increased three hours before a defined peak period and decreased during peak periods. Three hours of pre-heating are chosen to make sure that the time period is sufficiently long to charge both the storage tank and the building thermal mass, even during the coldest outdoor temperatures.

3.5. Consequences of DR on the heating system

When changing temperature set-points during DR control, it should be ensured that the use of the heat pump is prioritized over auxiliary heaters. Therefore, auxiliary heaters should be controlled carefully. First, the temperature set-point for auxiliary heaters is not increased when the temperature set-points for the heat pump are increased. Second, the SH-related set-points are increased only if the heat pump is not heating DHW. Otherwise, when the heat pump heats DHW, higher

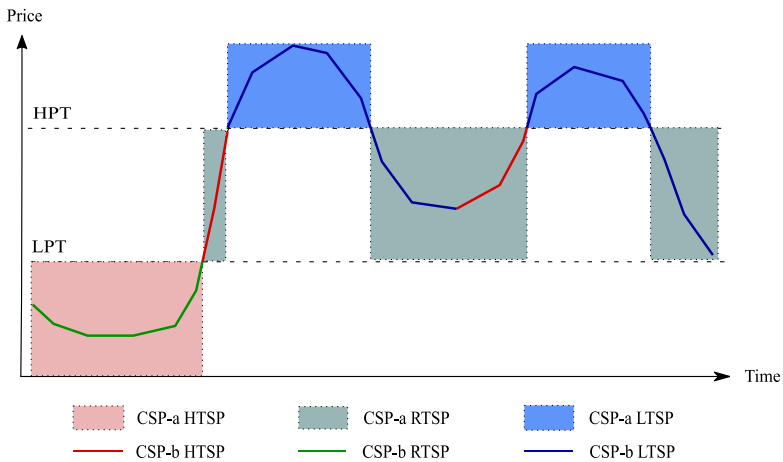

Fig. 5. Principle of the determination of the price-based control signal after CSP-a and CSP-b (HTSP is high temperature set-point, RTSP is reference temperature set-point, LTSP is low temperature set-point).

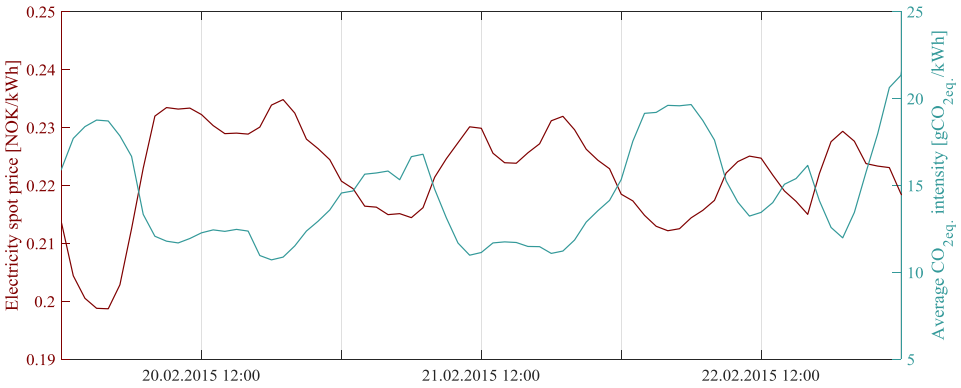

Fig. 6. Spot price [42] and average $CO_{2eq.}$ intensity [41] in bidding zone NO3 during an exemplary period in 2015.

SH-related set-points would lead to a faster cooling down of the SH tank, eventually leading the auxiliary heater to start before the heat pump has finished producing DHW.

Fig. 7 illustrates the principle of the CSP-b control during 48 h of the heating season. Fig. 7(a) presents the spot price signal as well as the LPT and HPT. Fig. 7(b) illustrates the temperatures in the DHW tank as well as the start and stop temperatures of the hysteresis. It can be seen that the set-points are changing depending on the price signal. It is clear from Fig. 7(c) and (d) that the SH-related set-points are increased only if the heat pump is not in DHW mode. For example, in the morning of 20 February, the DHW set-point is increased as soon as the spot price is increasing and is between LPT and HPT, whereas the SH-related set-points are not increased during that period. The modulation of the heat pump compressor is presented in Fig. 7(e) together with the heat emitted to the rooms and the power of the auxiliary heater. The compressor speed increases up to nominal capacity as soon as DHW heating is required. The temperature in the SH tank decreases when there is DHW heating because the heat pump cannot contribute to the heating of the SH tank at the same time. If the temperature in the SH tank drops too low, the electric auxiliary heater starts running. A combination of several design parameters influences the duration of the DHW mode and consequently determines whether the SH auxiliary heater has to be started: the capacity of the heat pump, the water volume to be heated up as well as the start and stop temperatures for DHW. Another reason for the SH auxiliary heater to operate when the heat pump is in DHW mode is related to the tank layout. The DHW is preheated by the SH

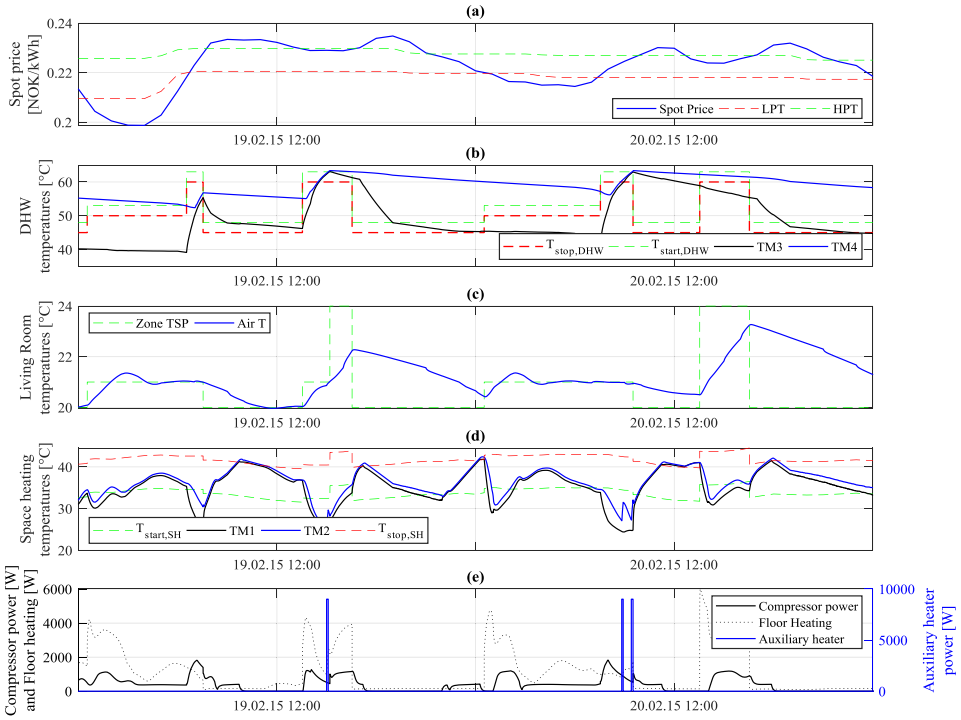

Fig. 7. Illustration of the control principle using the CSP-b during a period of 48 h: $T_{start,SH}$ and $T_{stop,SH}$ are the start and stop temperatures for SH.

tank so that the temperature in the SH tank is decreased by the fresh DHW inlet during a draw-off.

At the start of a DHW mode (e.g. afternoon of 19 February), the compressor speed increases to full load and the water circulates through the condenser at a low flow rate in order to reach the supply temperature set-point at the condenser outlet. When the maximum supply temperature allowed by the heat pump is reached, the water flow rate is increased whereas the compressor capacity is reduced. When the stop criteria for DHW is met, the heat pump switches to the SH mode and the compressor modulates continuously to keep the required FH supply temperature. As soon as the SH-related set-points are decreased, no more heat is emitted to the rooms and the SH tank is heated up until the stop criteria for the SH hysteresis is reached.

3.6. Thermal zoning

In the baseline case, all internal doors are open and the same indoor temperature set-point is applied to all rooms. Thermal zoning is achieved by closing internal doors to bedrooms. In this scenario, a constant heating temperature set-point of 16 °C is applied to both bedrooms, while the temperature set-point in the other rooms is controlled as in the baseline cases. Thermal zoning with cold bedrooms should lead to a reduction in electricity use for heating and a decreased load shifting potential. The heat storage capacity is decreased because the thermal mass of colder bedrooms does not contribute to thermal mass activation. All the simulation cases investigated are summarized in Fig. 8.

4. Introduction of performance indicators

Several performance indicators are evaluated and compared to quantify the effect of the different control strategies and construction types.

4.1. Energy related indicators

- *Electricity use for heating:* The electricity use for heating covers both SH and DHW. It includes the heat pump compressor (if applied), the electric resistances and electric radiators (if applied) and excludes the circulation pumps
- *Load shifting:* Load shifting from peak hours to off-peak hours can be expressed in terms of energy. The electricity use for heating is investigated for pre-peak, peak and after-peak hours where pre-peak hours are the three hours before each respective peak period and the after-peak hours are defined as the two hours after each respective peak period.
- *Annual heating costs:* The annual electricity costs for heating consist of hourly spot prices and additional fees, which depend on the size of the installed fuse as well as the energy use in the building. A single-family building usually has a 63A fuse with 230 V. For this fuse, the price that has to be paid on top of the spot price is 0.40 NOK/kWh (in 2015) [73]. Two cost-scenarios are evaluated: (1) annual costs for heating including the electricity fee, and (2) annual costs for heating without considering the electricity fee.
- *Annual $CO_{2eq.}$ emissions:* The annual $CO_{2eq.}$ emissions due to the operation of the heating system are evaluated using $CO_{2eq.}$ intensity.

4.2. Heat pump-related indicators

- *Number of heat pump cycles per year or per month:* A low number of heat pump cycles is preferred as unnecessary on/off cycling reduces the lifetime of the compressor.
- *Seasonal coefficient of performance (SCOP):* This indicator characterizes the heat pump and does not consider the electricity use for circulation pumps.

5. Results and discussion

Results are presented first for the ZEB case and the generalization to other insulation levels is discussed later on. If not defined explicitly in the text, the price-based and carbon-based control scenarios correspond to CSP-b and CSC-b, respectively.

5.1. Power

The hourly averaged compressor power is shown in Fig. 9 for the modulating heat pump in a ZEB. Even though this single case is discussed here, it is representative and supports the main conclusions. In general, the heat pump hardly runs at full load for long periods but rather modulates at low compressor speeds. In the BAU scenario (Fig. 9(a)), the heat pump is often run during peak hours because these hours also coincide with peak DHW demand. The CSP-b strategy (Fig. 9(c)), enforces heat pump operation in early morning and early afternoon because spot prices are usually increasing at these times. The CSC-b strategy (Fig. 9(b)) amplifies the heat pump operation during late evening and peak hours in the morning in close accordance with the typical daily fluctuations of the $CO_{2eq.}$ intensity.

The CSS strategy (Fig. 9(d)) enforces the heat pump operation during pre-defined periods. The heat pump operates not only during the hours of increased temperature set-points, but also continues its operation during the first hour of the peak periods. This is due to the hysteresis control of the SH tank which allows the heat pump to stop only if the stop temperature is reached, see e.g. Fig. 7(d) and (e). This creates a delay between the decision to reduce the SH temperature set-points and the time where the heat pump can actually be stopped. This effect cannot be captured by simplified models, which neglect the

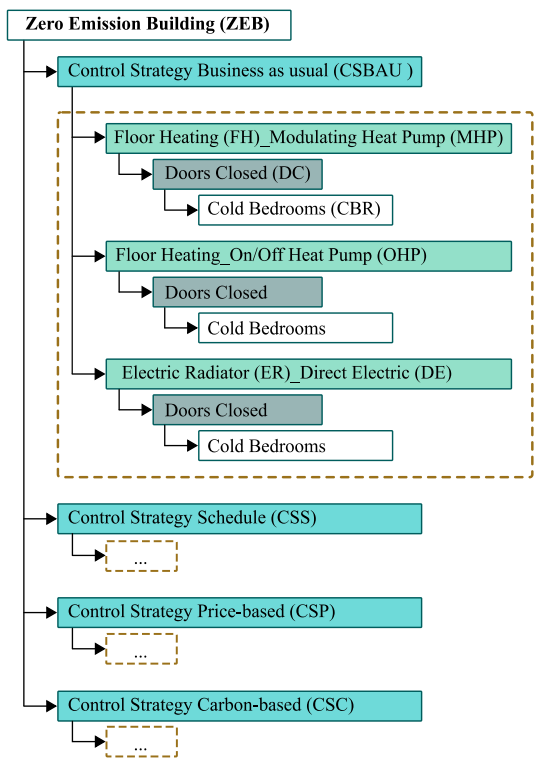

Fig. 8. Structure of the different simulation cases.

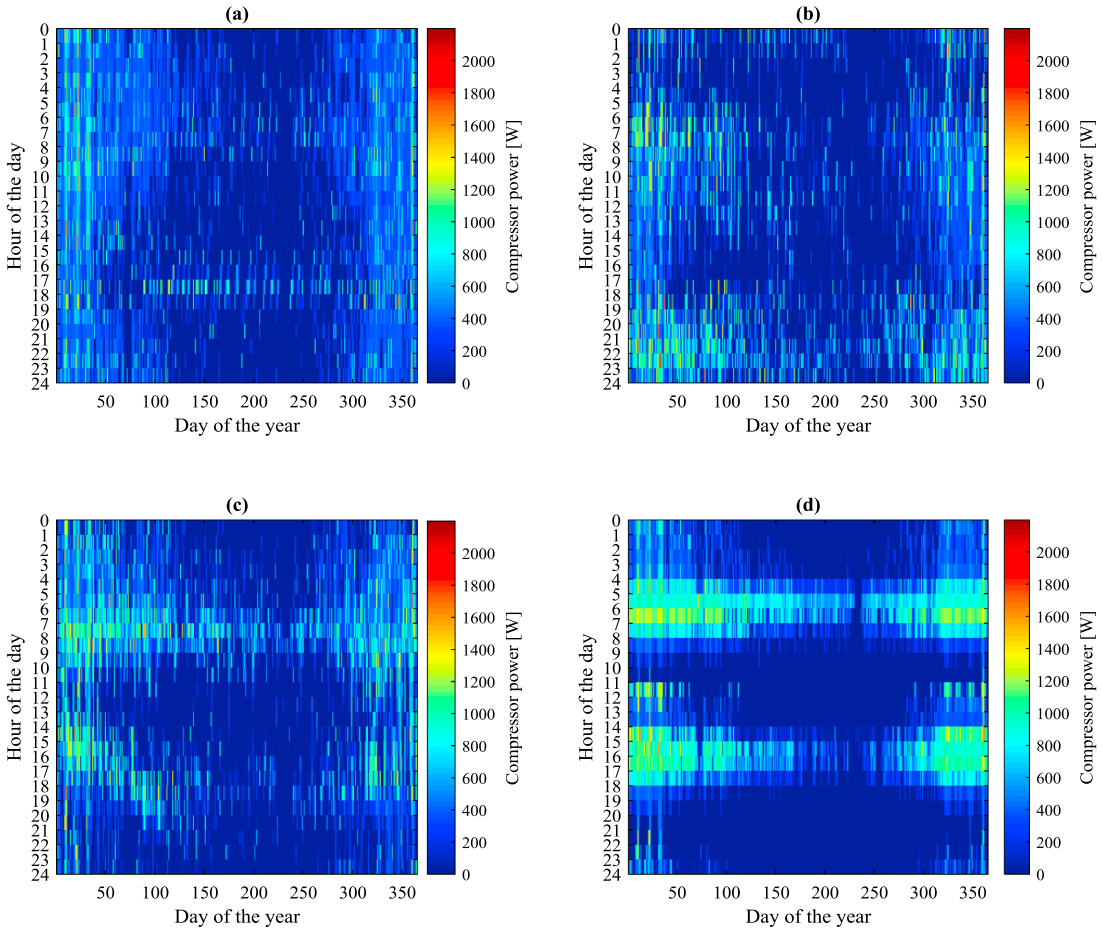

Fig. 9. Carpet plot of the hourly averaged compressor power of the modulating heat pump in the ZEB: (a) BAU, (b) CSC-b, (c) CSP-b and (d) CSS.

hysteresis. Compared to the BAU scenario, the heat pump modulates more often at higher compressor powers for CSC, CSP and CSS due to the higher temperature set-points.

The hourly averaged power of the heat pump system is illustrated in Fig. 10 for an entire year. The operation of the auxiliary heaters increases for all DR control strategies compared to BAU. It can be seen that the daily peak power occurs at different times of the day during the year for the different control strategies. Especially for the CSS, the auxiliary heaters operate just before the peak period starts.

5.2. Load shifting potential

Fig. 11 illustrates the influence of the control scenarios on the annual electricity use for heating during pre-peak, peak and after-peak hours for the different PRBC scenarios applied in the ZEB. Fig. 11(a) and (b) correspond to the modulating heat pump system whereas Fig. 11(c) and (d) correspond to the direct electric heating.

The case of direct electric heating is discussed first. The CSS control leads to a higher increase in electricity use during pre-peak hours compared to the CSP-b and CSC-b control scenarios. The CSS is extremely effective to reduce energy use during peak hours but may generate new peaks during pre-peak periods. CSC-b leads to increased electricity use during after-peak hours, but decreased use in pre-peak and peak periods. CSP-b leads to increased heating during pre-peak periods and reduced electricity use during peak periods. In conclusion, all controls reduce the energy use during peak hours, especially CSS. CSC-a on the contrary, would lead to increased electricity use during peak hours as well as after-peak hours. The annual electricity use for heating is increased slightly for the CSP-b and CSS controls compared to the references (BAU), whereas it is decreased for the CSC-b strategy (Fig. 11(d)).

For the case of a modulating ASHP, the CSS control is much less effective to reduce electricity use during peak hours. CSC-b has almost unchanged energy use during that time period while CSP-b has increased energy use during peak hours. Regarding CSP-b, an increased use of the auxiliary heater during peak hours, which is due to the strict prioritization of DHW heating for the heat pump, is indicated in Fig. 10(c). Furthermore, Fig. 10(d) shows a more frequent use of the auxiliary heater between 4 a.m. and 6 a.m. for CSS, thus leading to a strong increase in electricity use for heating during pre-peak hours (Fig. 11(a)).

There is an increase in the annual electricity use for heating for all three control scenarios. The reasons for increased electricity use for heating are the TSP variations for DHW heating and SH, hence increased thermal losses from the water storage tank and through the walls as well as the DHW prioritization for the heat pump. Because of

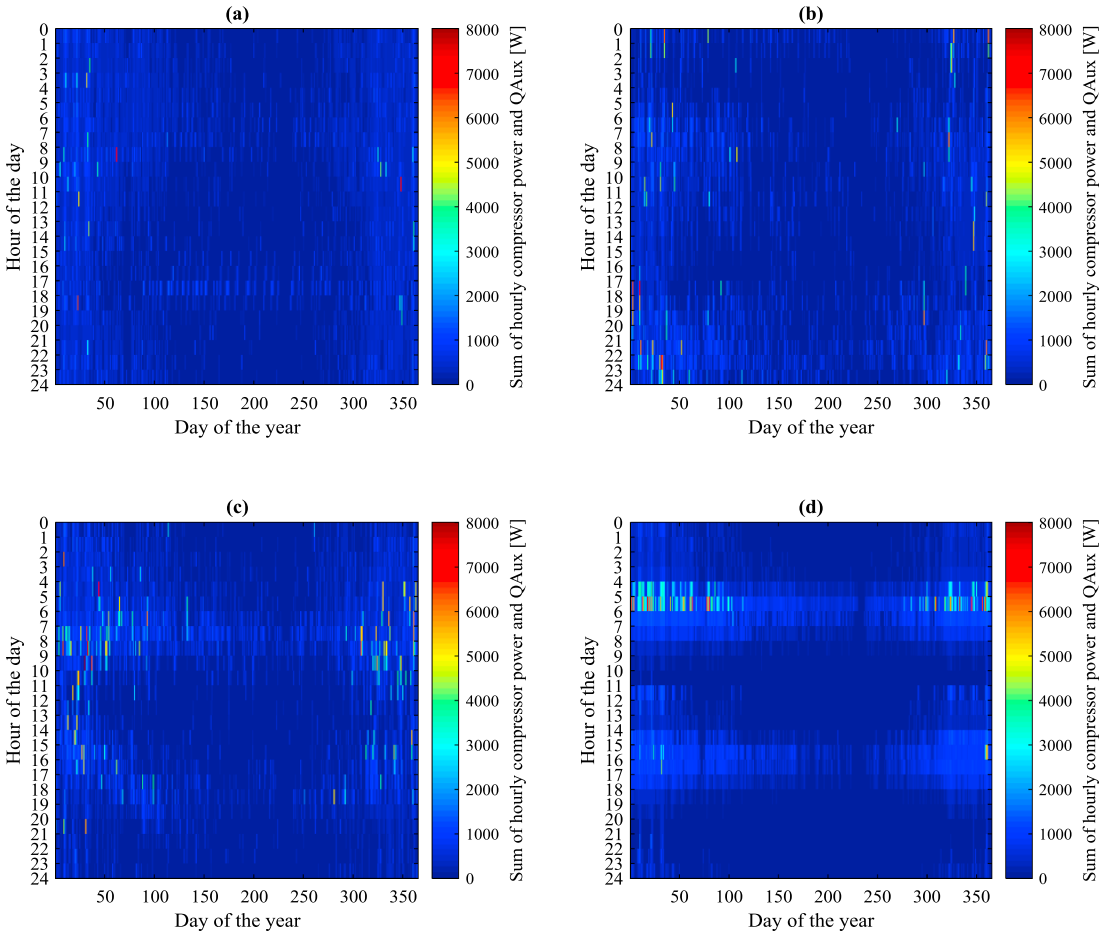

Fig. 10. Carpet plot of the hourly averaged electrical power for heating including the modulating heat pump and electric auxiliary heaters (ZEB): (a) BAU, (b) CSC-b, (c) CSP-b and (d) CSS.

the prioritization of DHW heating, the SH tank is less frequently charged to higher temperatures by the heat pump. Thus, the auxiliary heater is used more often for the CSC-b, CSP-b and CSS cases as the water temperature in the SH tank drops below the respective set-point for the auxiliary heater more frequently. It is obvious from Fig. 11 that a more regular use of the auxiliary heater will increase the amount of electricity used for heating. Better control for switching between the two heating modes is necessary considering the state-of-charge for the two parts of the tank. The increase in energy use for heating is not due to the complexity of the power modulation control: the results for the on-off heat pump have a similar trend regarding load shifting.

Fig. 12 presents the duration curves for the mean air temperature in the common rooms (Fig. 12(a)) and the upper half of the DHW tank (Fig. 12(b)). Generally, all three DR scenarios lead to higher mean indoor air temperatures.

Fig. 12 shows an increasing trend for temperature duration curves starting with the lowest value at hour zero. This figure is used to show the number of hours that a temperature is below a certain value. For example, the mean indoor air temperature in the common rooms for CSS (red line in Fig. 12(a)) is below 24 °C for about 7000 h. The TSP increases for a longer period for CSS, whereas CSC-b and CSP-b have shorter periods with increased set-points. The room temperature set-points are at 24 °C for 440 h for CSC-b, 750 h for CSP-b and 1250 h for CSS. The DHW duration curves for the three DR control scenarios are more similar, especially the duration curves for CSC-b and CSP-b. For both strategies, the control signals are determined using the same approach and the input signals (i.e. spot price and $CO_{2eq.}$ intensity) have similar trends (Fig. 6).

5.2.1. Annual heating costs

Table 3 presents the annual heating costs. Regarding the ASHP, the annual heating costs are increased by up to 25% for the CSS. The CSP-b leads to 21% increase in electricity costs. The effect of a lower spot price is outweighed by the increased electricity use. Regarding the direct electric heating case, the CSP-b leads to slightly higher heating costs (+5%), even though the electricity use is increased by 13%. Cost savings are influenced by the fee for the grid connection. The cost savings are higher when the grid connection fee is not included in the cost analysis. The price-based control strategy CSP-a leads to much higher heating electricity use and annual heating costs than CSP-b. Even though CSP-a makes use of the lowest spot prices, it leads to higher energy costs because it also involves longer periods with increased temperature set-points. On the contrary, the temperature set-points are increased for shorter periods using CSP-b which charges the

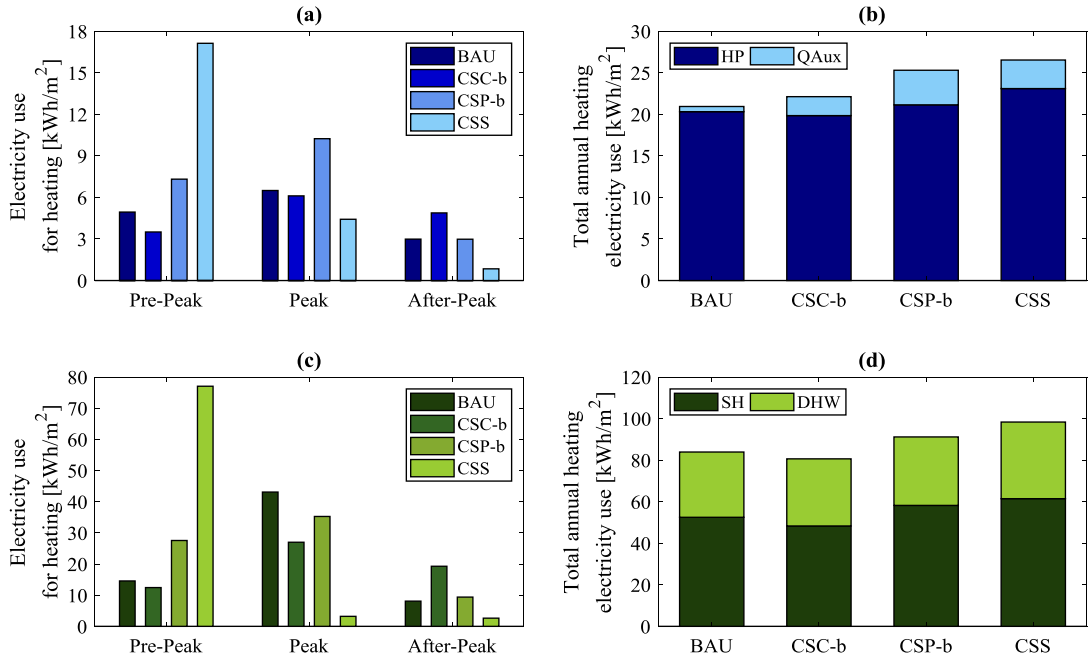

Fig. 11. Electricity use for heating of the ZEB using a modulating heat pump (a, b) or direct electric heating (c, d).

thermal storages right before high-price periods. In other words, the averaged electricity price consumed by CSP-a is lower (NOK/kWh) whereas energy costs are lower for CSP-b (NOK).

This suggests that applying a PRBC to reduce energy costs for heating does not work in Norway. In fact, spot prices do not fluctuate as much during the day as in other countries. A price-based control is more favorable in countries with greater price fluctuations. For instance, the same building and price-based controls have been tested for Denmark, using actual weather data, hourly spot prices and $CO_{2eq.}$ intensities for Aarhus in 2015. Using direct electric heating, it has been found that the electricity use increased by 19%, whereas the cost was lowered by 9% for the CSP-a case. CSP-b increases the electricity use by 8%, while annual heating costs remained the same. This emphasizes that the applied control has to be adjusted for the respective region and its spot price fluctuations. In comparison, other studies suggest that applying an MPC could reduce energy costs for SH by 14% for a residential building heated by electric radiators and located in Aarhus [39].

5.2.2. Annual $CO_{2eq.}$ emissions for heating

Table 4 presents a comparison for the carbon emissions for all control strategies for the ZEB case. CSC-b leads to slightly reduced annual carbon emissions for direct electric heating, whereas it does not reduce the carbon emissions for the ASHP. Compared to the spot price, the fluctuations in $CO_{2eq.}$ intensities are rather small compared to other European countries. Thus, the emission savings of CSC-b reported for direct electric heating are closely related to the decreased electricity

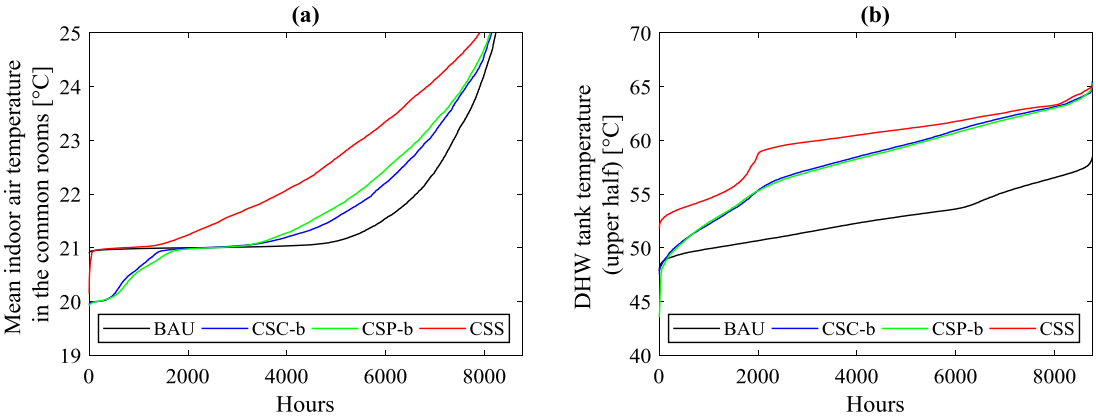

Fig. 12. Duration curve for the mean indoor air temperature of the common rooms (a) and the upper half of the DHW tank (b) using the modulating heat pump in the ZEB.

Table 3
Annual heating costs for the modulating ASHP and direct electric heating for the ZEB case.

	ASHP						Direct electric heating					
	Heating E_{Use}		Costs with el. fee		w/o el. fee		Heating E_{Use}		Costs with el. Fee		w/o el. Fee	
	kWh	%	NOK	%	NOK	%	kWh	%	NOK	%	NOK	%
BAU	2199	–	1364	–	484	–	8809	–	5393	–	1869	–
CSC-b	2323	+6	1442	+6	513	+6	8464	−4	5183	−4	1797	−4
CSP-a	3057	+39	1828	+34	605	+25	10,659	+21	6310	+17	2046	+9
CSP-b	2657	+21	1648	+21	585	+21	9572	+13	5796	+7	1967	+5
CSS	2786	+27	1704	+25	590	+22	10,324	+17	6172	+14	2042	+9

Table 4
Annual carbon emissions for the tested control strategies for the ZEB case.

	ASHP					Direct electric heating				
	BAU	CSC-a	CSC-b	CSP-b	CSS	BAU	CSC-a	CSC-b	CSP-b	CSS
Emissions kg]	27	30	28	31	33	101	101	96	109	120
Emissions [%]	–	+11	+4	+15	+22	–	0	−5	+8	+19
Emissions per $kWh_{heating}$ [g/kWh]	12.1	10.2	12.1	11.5	11.8	11.5	10.1	11.4	11.4	11.6

use. CSC-a leads to higher $CO_{2eq.}$ emissions than CSC-b. CSC-a consumes electricity with lower emissions per $kWh_{heating}$ but this gain is outweighed by the increased electricity use during low-carbon hours.

5.2.3. Influence of insulation levels

The electricity use for heating during pre-peak, peak and after-peak hours for different insulation levels is illustrated in Fig. 13. The results are shown for the cases with direct electric heating.

It is obvious that there will be increased electricity use with decreased insulation level. In absolute terms, Fig. 13 shows that the reduction of energy use during peak hours is larger for buildings with poorer insulation when using the CSS control. For other controls, this reduction is almost left unchanged. On the contrary, in relative terms, the energy use during peak hours is slightly increased with poorer insulation for all DR controls compared to BAU, see Table 5. This can be explained by the better storage efficiency with higher insulation levels. This storage efficiency is defined as the relative increase in energy use when storage is activated compared to BAU [6,74].

Table 5
Influence of the control strategy (CS) on the reduction of electricity use for heating during pre-peak, peak and after-peak periods for the four building insulation levels and direct electric heating.

	Building	Control strategy			
		BAU	CSC-b	CSP-b	CSS
$E_{PrePeak,CS}/E_{PrePeak,BAU}$ [–]	PH	1	0.84	1.89	6.17
	ZEB	1	0.85	1.89	5.29
	TEK10	1	0.98	1.56	4.18
	TEK87	1	0.98	1.34	3.19
$E_{Peak,CS}/E_{Peak,BAU}$ [–]	PH	1	0.60	0.62	0.07
	ZEB	1	0.63	0.82	0.07
	TEK10	1	0.77	0.73	0.10
	TEK87	1	0.83	0.73	0.12
$E_{AfterPeak,CS}/E_{AfterPeak,BAU}$ [–]	PH	1	2.78	1.14	0.28
	ZEB	1	2.38	1.16	0.32
	TEK10	1	1.87	0.99	0.41
	TEK87	1	1.49	0.84	0.71

5.3. Influence on energy system performance indicators

For the ZEB insulation level, Fig. 14 presents the number of heat pump cycles per month for the modulating and the on/off ASHP. The calculation of the cycle length only considers when the heat pump is turned on. The year can be typically divided into two periods. From October to April, both SH and DHW are important while, between May

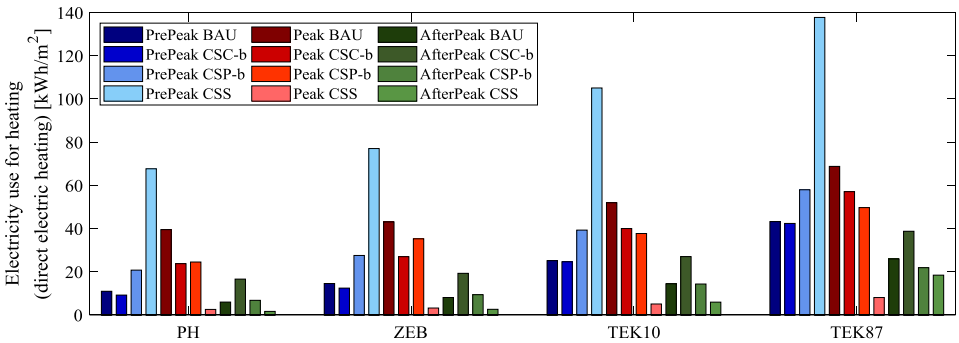

Fig. 13. Heating electricity use for the cases with direct electric heating and different insulation levels.

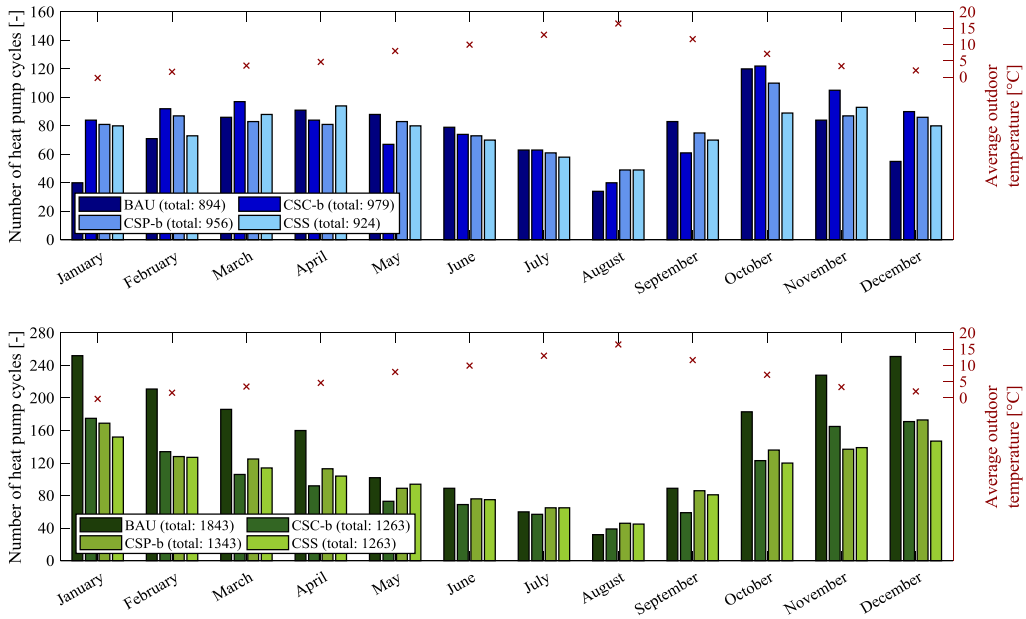

Fig. 14. Influence of the control strategies on the number of heat pump cycles for a modulating and an on/off ASHP and the ZEB case.

and September, the DHW needs are dominant. In this last period, the number of heat pump cycles is similar between the DR control strategies as well as between the on-off and modulating heat pumps (i.e. in the range of 40 to 100 cycles per month). On the contrary during the period when SH needs are significant, the number of heat pump cycles differs between cases. The trend is analyzed below and is partly explained by the outdoor temperature.

Regarding the BAU control, the number of heat pump cycles for the modulating heat pump increases with the rising outdoor temperature from January to April, whereas an opposite trend can be seen for the

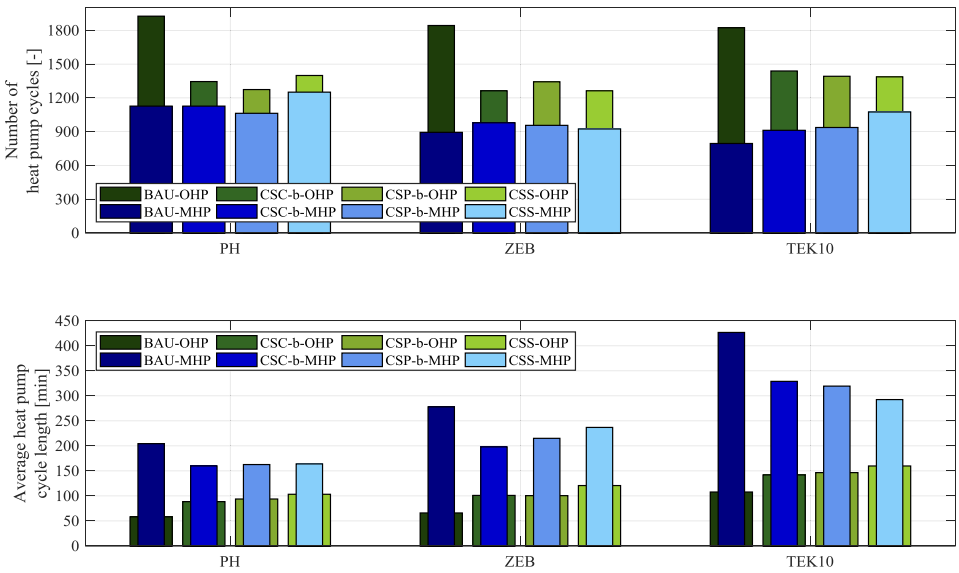

Fig. 15. Influence of the building insulation level on the total number of heat pump cycles per year for a modulating (MHP) and an on/off ASHP (OHP).

on/off heat pump. The modulating heat pump cycles less often with colder outdoor temperatures due to the power sizing procedure. The heat pump is sized in order to operate continuously for outdoor temperatures that are typical for winter. Above these temperatures, the modulating heat pump behaves more like an on/off heat pump and has shorter cycles for heating the storage tanks. For the BAU case, the benefit of a modulating heat pump compared to an on-off heat pump is clear in terms of heat pump cycles.

For the three DR controls, they lead to a decreased number of cycles for the on-off heat pump compared to the BAU control. The DR controls with fluctuating temperature set-points lead to less frequent and longer cycles. For the modulating heat pump, DR controls do not significantly change the number of cycles except in the colder months of the year (i.e. January and December) when the number of cycles is increased compared to BAU. During these months, the heat pump is sized to operate continuously so that the DR controls interrupt this continuous operation. For an entire year, the DR controls do not significantly alter the number of cycles of the modulating heat pump.

Fig. 15 compares the total number of heat pump cycles and the average heat pump cycle length for one year between the different building insulation levels. Following the conclusions in the last paragraph, the advantage of the modulating compared to the on-off heat pump is less important when using DR controls than when using the BAU. Comparing building insulation levels, the total number of heat pump cycles is similar, but the average duration of a cycle is different. The SH tank volume is smaller for higher insulation levels because of lower nominal SH power, see Eq. (2). As the heat pump capacity is the same for all three cases, the average cycle length is shorter for higher levels of insulation. It is obvious that proper sizing of the heat pump system (i.e. both the heat pump and storage tank) is essential.

For the same heat pump control and building insulation level, DR controls do not alter the SCOP more than 20% taking the BAU control as a reference (Appendix, Table A1). It confirms that the increase in the electricity use when applying DR control is mostly due to the operation of the auxiliary heaters and not the degradation of performance of the heat pump.

5.3.1. Effect of thermal zoning

Fig. 16 illustrates the duration curve for the mean indoor air temperature of bedrooms for two building insulation levels, the PH and TEK87 cases. A longer heating season for TEK87 compared to PH is obvious. Comparing the PH and TEK87 buildings, the bedroom temperature is evidently colder for the less insulated building. Furthermore, the bedroom temperature in the PH is always above 16 °C meaning that no SH is required in these rooms, whereas SH is applied in the TEK87 building to keep a minimum temperature of 16 °C. For the PH, a highly-insulated external wall, effective heat recovery of the ventilation air in combination with the internal heat gains may lead to bedroom temperatures above 16 °C during winter.

Using the thermal zoning strategy, duration curves show that the temperature of bedrooms is independent of the DR control strategy applied in the common rooms (such as the living room). It means that DR controls will not increase the risk that occupants open windows to reduce temperature of bedrooms and thus flush out the heat stored in the building. For the baseline strategy with open internal doors, there is efficient heat exchange between rooms. In addition, the same temperature set-point is applied for all rooms. Therefore, the temperature in the building is almost uniform. For instance, the dashed lines in Fig. 16(a) are similar to the mean temperature of the common rooms shown in Fig. 12(a).

Table 6 presents the influence of thermal zoning on selected performance indicators for the ZEB case. The electricity use for heating is decreased by roughly 10% for all control scenarios. This leads to a similar reduction in the energy costs for heating and the $CO_{2eq.}$ emissions. Nevertheless, the influence of thermal zoning on the energy use during peak periods differs among the control scenarios. For the CSS, the thermal zoning strategy does not change the energy use during peak hours: this quantity is reduced by 93% with open and closed internal doors. On the contrary, the thermal zoning strategy slightly reduces the load shifting potential for the other DR controls. In conclusion, the thermal zoning strategy is a way to investigate the influence of the users' behavior. Results show that thermal zoning generally has an impact on the building energy flexibility, but these variations are relatively limited (up to 10% reductions).

6. Conclusions

This work investigates three types of predictive rule-based control (PRBC) to perform the demand response for heating a Norwegian residential building. The single-family detached house has a lightweight timber construction and four different insulation levels are evaluated. Unlike other studies, a detailed model of an air-source heat pump (ASHP) system has been implemented to obtain realistic operation of the system. There is a comparison of an ASHP modulating between 30% and 100% of the compressor power and an on-off ASHP. Furthermore, direct electric heating is investigated as this is the most common

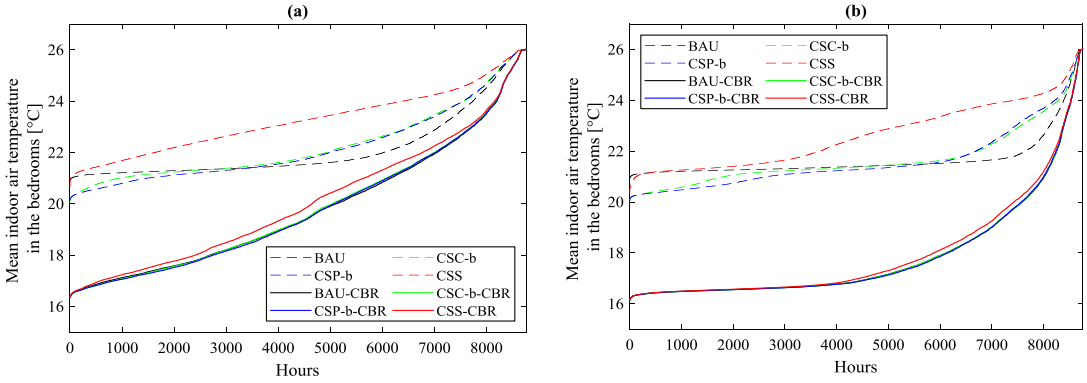

Fig. 16. Duration curve for the indoor air temperature in bedrooms for the (a) PH and (b) TEK87 buildings with direct electric heating: dashed lines show the reference case with open bedroom doors; solid lines show the cases with closed bedroom doors (CBR) and 16 °C as the temperature set-point.

Table 6
Influence of thermal zoning with cold bedrooms on selected key performance indicators for the ZEB and electric radiator cases (OBR means open bedroom doors, CBR means closed bedroom doors and CS means control strategy).

	BAU		CSC-b		CSP-b		CSS	
	OBR	CBR	OBR	CBR	OBR	CBR	OBR	CBR
E_{Use} [kWh]	8809	8169	8464	7744	9572	8620	10,324	9357
Costs [NOK]	5393	5000	5183	4742	5796	5216	6172	5598
$CO_{2eq.}$ [kg]	101	93	96	88	109	99	120	109
$E_{Peak,CS}/E_{Peak,BAU,OBR}$	1	0.97	0.63	0.59	0.82	0.72	0.07	0.07

heating system for residential buildings in Norway. The three PRBC strategies are designed to reduce (a) energy costs for heating using the hourly spot prices as input, (b) the annual $CO_{2eq.}$ emissions for heating using the hourly $CO_{2eq.}$ intensity of the electricity mix in Norway and (c) the energy use during peak-load hours using a pre-defined schedule. In the Norwegian context, reducing the energy use during peak-load hours is probably the most important objective for control, as bottlenecks in the distribution grids are expected in the near future. On the contrary, Norwegian electricity currently has a relatively low price and $CO_{2eq.}$ intensity compared to other European countries.

The first research question (Q1) evaluated the energy flexibility potential of PRBC in the specific context of Norway. The price-based PRBC leads to increased heating costs even though it aims to avoid heating during high-price periods. The potential cost savings for the tested PRBC are outweighed by the increase in electricity use for heating. Generally, price-based PRBC is more profitable in electricity markets such as Denmark with greater daily fluctuations in the electricity price. It has been shown that the investigated price-based controls, which do not lead to cost savings in the Norwegian context, result in cost savings if they were applied to the same building in Denmark. The carbon-based PRBC is associated with higher electricity use during early mornings and late evenings. As for the price-based control, increased energy use and limited daily fluctuations of the $CO_{2eq.}$ intensities (compared to other European bidding zones) limit the reduction of the annual $CO_{2eq.}$ emissions. Reductions can only be achieved when there is direct electric heating, not the ASHP. The schedule-based control proved to be very efficient to reduce the energy use for heating during peak hours, especially for the direct electric heating. In the case of the heat pump, the reduction is significantly lowered due to the complexity of the heat pump control (see Q3 below). In the Norwegian context, the schedule-based control manages to significantly reduce the energy use during peak hours, which is a main goal. By definition, PRBC is based on predefined control rules that may not be optimal. For energy costs and $CO_{2eq.}$ emissions, it should therefore be investigated whether model-predictive control could generate significant benefit even though the price and $CO_{2eq.}$ signals have limited fluctuations in Norway.

The second research question (Q2) investigates the influence of thermal zoning on the energy flexibility potential. Energy flexibility has been evaluated for warm and cold bedrooms with open and closed doors, respectively. Lower temperature in bedrooms reduces the annual electricity use for heating (typically by 10%) compared to a uniform temperature in the building. It leads to a similar reduction in the energy costs for heating and annual $CO_{2eq.}$ emissions. For DR controls, the results found that thermal zoning has a limited effect on the reduction of energy use during peak periods. For colder bedrooms with closed doors, it is shown that the bedroom temperatures are not strongly dependent on the heating control strategies applied in the other rooms. These are important conclusions because it suggests that energy flexibility potential is moderately impacted by thermal zoning which is an important aspect of user behavior. In addition, the risk of open bedroom windows to keep bedroom cold will not be increased by the different DR controls. In Norway, buildings are often constructed in wood which leads to thermal insulation in partition walls to limit the sound propagation. The conclusion may be different for construction modes with non-insulated partition walls, such as concrete.

The third research question (Q3) investigates the impact of the modeling complexity of the heat pump system on the energy flexibility potential. With DR controls using time-varying set-points, results show that the domestic hot water (DHW) prioritization, the minimum cycle length as well as the hysteresis between the start and stop temperatures (when the heat pump operates below its minimum power modulation capabilities) prevent the heat pump stopping immediately after it is required by the PRBC. This may also trigger the operation of the auxiliary heater too frequently and significantly increase the energy use for heating. These phenomena have a major impact on the performance of the DR controls. Compared to a simpler heating system, direct electric heating, the performance of DR controls with the ASHP is systematically lower. Modeling these details in a heat pump system are most often neglected in the literature but are important to predict the realistic energy flexibility potential. Finally, such detailed heat pump models can be used to optimize PRBC. For instance, improving the prioritization control strategy between DHW and SH should be considered to make maximum use of the heat pump and minimize the use of auxiliary heaters while respecting the temperature set-points.

The influence of the PRBC on the operating conditions of the heat pump in terms of duration and frequency of cycles is also addressed (Q4). The study confirms the advantages of a modulating heat pump over an on-off heat pump. For the reference case (BAU) with constant heating set-points, the modulating heat pump leads to roughly half the number of heat pump cycles throughout the year. Compared to BAU, the DR controls lead to a comparable number cycles for the modulating heat pump whereas an on-off heat pump will have fewer cycles with longer durations. As the number of cycles is related to the mechanical wear and the lifetime of the heat pump, an increased (or decreased) number of cycles correspond to a cost (or a saving) that needs to be investigated in future work.

Acknowledgements

The authors would like to acknowledge IEA EBC Annex 67 “Energy Flexible Buildings”, IEA HPT Annex 49 “Design and Integration of Heat Pumps for nZEBs” as well as the Research Centre on Zero Emission Neighbourhoods in Smart Cities (FME ZEN). The contribution of Sebastian Stinner for this research was supported by a research grant from E.ON Stipendienfonds im Stifterverband für die Deutsche Wissenschaft (project number T0087/29896/17).

Appendix A

See Table A1.

Table A1
SCOP for both heat pump cases for four investigated control strategies and all building insulation levels.

Building	Control strategy	SCOP	
		Modulating heat pump	On-off heat pump
PH	BAU	2.42	2.33
	CSC-b	2.32	2.12
	CSP-b	2.40	2.12
	CSS	2.12	1.91
ZEB	BAU	2.25	2.30
	CSC-b	2.35	2.15
	CSP-b	2.31	2.08
	CSS	1.97	1.84
TEK10	BAU	2.80	2.60
	CSC-b	2.75	2.39
	CSP-b	2.79	2.44
	CSS	2.55	2.02

References

[1] Jensen SØ, Marszal-Pomianowska A, Lollini R, Pasut W, Knotzer A, Engelmann P, et al. IEA EBC Annex 67 energy flexible buildings. Energy Build 2017;155:25–34. https://doi.org/10.1016/j.enbuild.2017.08.044.

[2] Aduda KO, Labeodan T, Zeiler W, Boxem G, Zhao Y. Demand side flexibility: Potentials and building performance implications. Sustain Cities Soc 2016;22:146–63. https://doi.org/10.1016/j.scs.2016.02.011.

[3] IEA, Nordic Energy Research. Nordic Energy Technology Perspectives 2016 Cities, flexibility and pathways to carbon-neutrality. Oslo: 2016.

[4] Finck C, Li R, Kramer R, Zeiler W. Quantifying demand flexibility of power-to-heat and thermal energy storage in the control of building heating systems. Appl Energy 2017;209:409–25. https://doi.org/10.1016/j.apenergy.2017.11.036.

[5] Clauß J, Finck C, Vogler-Finck P, Beagon P. Control strategies for building energy systems to unlock demand side flexibility – A review. 15th Int. Conf. Int. Build. Perform. Simul. Assoc. San Fr. USA, San Francisco. 2017.

[6] Reynders G, Diriken J, Saelens D. Generic characterization method for energy flexibility: Applied to structural thermal storage in residential buildings. Appl Energy 2017;198:192–202. https://doi.org/10.1016/j.apenergy.2017.04.061.

[7] Le Dréau J, Heiselberg P. Energy flexibility of residential buildings using short term heat storage in the thermal mass. Energy 2016;111:991–1002. https://doi.org/10.1016/j.energy.2016.05.076.

[8] Vanhoudt D, Geysen D, Claessens B, Leemans F, Jespers L, Van Bael J. An actively controlled residential heat pump: Potential on peak shaving and maximization of self-consumption of renewable energy. Renew Energy 2014;63:531–43. https://doi.org/10.1016/j.renene.2013.10.021.

[9] Georges E, Cornélusse B, Ernst D, Lemort V, Mathieu S. Residential heat pump as flexible load for direct control service with parametrized duration and rebound effect. Appl Energy 2017;187:140–53. https://doi.org/10.1016/j.apenergy.2016.11.012.

[10] Fischer D, Madani H. On heat pumps in smart grids: A review. Renew Sustain Energy Rev 2017;70:342–57. https://doi.org/10.1016/j.rser.2016.11.182.

[11] Fischer D, Wolf T, Wapler J, Hollinger R, Madani H. Model-based flexibility assessment of a residential heat pump pool. Energy 2017;118:853–64. https://doi.org/10.1016/j.energy.2016.10.111.

[12] Lopes RA, Chambel A, Neves J, Aelenei D, Martins J. A literature review of methodologies used to assess the energy flexibility of buildings. Energy Procedia 2016;91:1053–8. https://doi.org/10.1016/j.egypro.2016.06.274.

[13] Halvgaard R, Poulsen N, Madsen H, Jørgensen J. Economic model predictive control for building climate control in a smart grid. 2012 IEEE PES Innov. Smart Grid Technol. 2012. p. 1–6. https://doi.org/10.1109/ISGT.2012.6175631.

[14] Masy G, Georges E, Verhelst C, Lemort V. Smart grid energy flexible buildings through the use of heat pumps and building thermal mass as energy storage in the Belgian context. Sci Technol Built Environ 2015;21(6):800–11. https://doi.org/10.1080/23744731.2015.1035590.

[15] Heidmann Pedersen T, Hedegaard RE, Petersen S. Space heating demand response potential of retrofitted residential apartment blocks. Energy Build 2017;141:158–66. https://doi.org/10.1016/j.enbuild.2017.02.035.

[16] Hedegaard RE, Pedersen TH, Petersen S. Multi-market demand response using economic model predictive control of space heating in residential buildings. Energy Build 2017;150:253–61. https://doi.org/10.1016/j.enbuild.2017.05.059.

[17] Péan T, Ortiz J, Salom J. Impact of demand-side management on thermal comfort and energy costs in a residential nZEB. Buildings 2017;7:37. https://doi.org/10.3390/buildings7020037.

[18] Stinner S, Huchtemann K, Müller D. Quantifying the operational flexibility of building energy systems with thermal energy storages. Appl Energy 2016;181:140–54. https://doi.org/10.1016/j.apenergy.2016.08.055.

[19] Lund PD, Lindgren J, Mikkola J, Salpakari J. Review of energy system flexibility measures to enable high levels of variable renewable electricity. Renew Sustain Energy Rev 2015;45:785–807. https://doi.org/10.1016/j.rser.2015.01.057.

[20] Oldewurtel F. Stochastic model predictive control for energy efficient building climate control. ETH Zurich; 2011.

[21] Salpakari J, Lund P. Optimal and rule-based control strategies for energy flexibility in buildings with PV. Appl Energy 2016;161:425–36. https://doi.org/10.1016/j.apenergy.2015.10.036.

[22] D'hulst R, Labeeuw W, Beusen B, Claessens S, Deconinck G, Vanthournout K. Demand response flexibility and flexibility potential of residential smart appliances: Experiences from large pilot test inBelgium. Appl Energy 2015;155:79–90. https://doi.org/10.1016/j.apenergy.2015.05.101.

[23] Reynders G, Nuytten T, Saelens D. Potential of structural thermal mass for demand-side management in dwellings. Build Environ 2013;64:187–99. https://doi.org/10.1016/j.buildenv.2013.03.010.

[24] Arteconi A, Patteeuw D, Bruninx K, Delarue E, D'haeseleer W, Helsen L. Active demand response with electric heating systems: Impact of market penetration. Appl Energy 2016;177:636–48. https://doi.org/10.1016/j.apenergy.2016.05.146.

[25] Georges L, Alonso MJ, Woods R, Wen K, Håheim F, Liu P, et al. Evaluation of simplified space-heating hydronic distribution for Norwegian passive houses. Trondheim; 2017.

[26] Berge M, Georges L, Mathisen HM. On the oversupply of heat to bedrooms during winter in highly insulated dwellings with heat recovery ventilation. Elsevier Ltd; 2016https://doi.org/10.1016/j.buildenv.2016.07.011.

[27] Georges L, Wen K, Alonso MJ, Berge M, Thomsen J, Wang R. Simplified space-heating distribution using radiators in super-insulated apartment buildings. Energy Procedia 2016;96:455–66. https://doi.org/10.1016/j.egypro.2016.09.177.

[28] Georges L, Håheim F, Alonso MJ. Simplified space-heating distribution using radiators in super-insulated terraced houses. Energy Procedia 2017;132:604–9. https://doi.org/10.1016/j.egypro.2017.09.677.

[29] Selvnes E. Thermal zoning during winter in super-insulated residential buildings. Norwegian University of Science and Technology; 2017.

[30] Alimohammadisagvand B, Jokisalo J, Kilpeläinen S, Ali M, Sirén K. Cost-optimal thermal energy storage system for a residential building with heat pump heating and demand response control. Appl Energy 2016;174:275–87. https://doi.org/10.1016/j.apenergy.2016.04.013.

[31] Alimohammadisagvand B, Jokisalo J, Sirén K. Comparison of four rule-based demand response control algorithms in an electrically and heat pump-heated residential building. Appl Energy 2018;209:167–79. https://doi.org/10.1016/j.apenergy.2017.10.088.

[32] Fischer D, Bernhardt J, Madani H, Wittwer C. Comparison of control approaches for variable speed air source heat pumps considering time variable electricity prices and PV. Appl Energy 2017;204:93–105. https://doi.org/10.1016/j.apenergy.2017.06.110.

[33] Dar UI, Sartori I, Georges L, Novakovic V. Advanced control of heat pumps for improved flexibility of Net-ZEB towards the grid. Energy Build 2014;69:74–84. https://doi.org/10.1016/j.enbuild.2013.10.019.

[34] Kandler C, Wimmer P, Honold J. Predictive control and regulation strategies of air-to-water heat pumps. Energy Procedia 2015;78:2088–93. https://doi.org/10.1016/j.egypro.2015.11.239.

[35] Pallonetto F, Oxizidis S, Milano F, Finn D. The effect of time-of-use tariffs on the demand response flexibility of an all-electric smart-grid-ready dwelling. Energy Build 2016;128:56–67. https://doi.org/10.1016/j.enbuild.2016.06.041.

[36] Georges E, Garsoux P, Masy G, DeMaere D'Aetrycke G, Lemort V. Analysis of the

flexibility of Belgian residential buildings equipped with Heat Pumps and Thermal Energy Storages. CLIMA 2016 - Proc. 12th REHVA World Congr., Aalborg. 2016.
[37] De Coninck R, Baetens R, Saelens D, Woyte A, Helsen L. Rule-based demand-side management of domestic hot water production with heat pumps in zero energy neighbourhoods. J Build Perform Simul 2014;7:271–88. https://doi.org/10.1080/19401493.2013.801518.
[38] Vandermeulen A, Vandeplas L, Patteeuw D, Sourbron M, Helsen L. Flexibility offered by residential floor heating in a smart grid context : the role of heat pumps and renewable energy sources in optimization towards different objectives. 12th IEA Heat Pump Conf. 2017, Rotterdam, Netherlands. 2017.
[39] Dahl Knudsen M, Petersen S. Demand response potential of model predictive control of space heating based on price and carbon dioxide intensity signals. Energy Build 2016;125:196–204. https://doi.org/10.1016/j.enbuild.2016.04.053.
[40] Brattebø H, O'Born R, Sartori I, Klinski M, Nørstebø B. Typologier for norske boligbygg - Eksempler på tiltak for energieffektivisering; 2014.
[41] Clauß J, Stinner S, Solli C, Lindberg KB, Madsen H, Georges L. A generic methodology to evaluate hourly average CO_2 intensities of the electricity mix to deploy the energy flexibility potential of Norwegian buildings. Proc. 10th Int. Conf. Syst. Simul. Build., Liege, Belgium. 2018. p. 1–19.
[42] Nord Pool Spot. http://www.nordpoolspot.com/historical-market-data 2016. http://www.nordpoolspot.com/historical-market-data.
[43] Rendum J, Vik AL, Knutsen AS. Innføring av AMS i norske husstander, og mulighetene dette gir for nettfleksibilitet. Norwegian University of Science and Technology; 2016.
[44] Goia F, Finocchiaro L, Gustavsen A. 7. Passivhus Norden | Sustainable Cities and Buildings The ZEB Living Laboratory at the Norwegian University of Science and Technology : a zero emission house for engineering and social science experiments, Copenhagen; 2015.
[45] Kristjansdottir TF, Houlihan-Wiberg A, Andresen I, Georges L, Heeren N, Good CS, et al. Is a net life cycle balance for energy and materials achievable for a zero emission single-family building in Norway? Energy Build 2018;168:457–69. https://doi.org/10.1016/j.enbuild.2018.02.046.
[46] EQUA. EQUA Simulation AB 2015. http://www.equa.se/en/ida-ice.
[47] EQUA Simulation AB, EQUA Simulation Finland Oy. Validation of IDA Indoor Climate and Energy 4.0 with respect to CEN Standards EN 15255-2007 and EN 15265-2007; 2010.
[48] EQUA Simulation AB. Validation of IDA indoor climate and energy 4.0 build 4 with respect to ANSI/ASHRAE Standard 140-2004. Stockholm; 2010.
[49] Achermann M, Zweifel G. RADTEST – Radiant heating and cooling test cases supporting documents. Luzern; 2003.
[50] Bring A, Sahlin P, Vuolle M. Models for building indoor climate and energy simulation models for building indoor climate and energy simulation 1. Executive background and summary; 1999.
[51] Sahlin P. Modelling and simulation methods for modular continuous systems in buildings; 1996.
[52] Georges L, Iwanek T, Thalfeldt M. Energy efficiency of hydronic space-heating distribution systems in super-insulated residential buildings. Proc. 15th IBPSA Conf. 2017. p. 1852–61.
[53] Vogler-Finck P, Clauß J, Georges L, Sartori I, Wisniewski R. Inverse model identification of the thermal dynamics of a Norwegian zero emission house. In: Johansson D, editor. Springer Proc. Energy, Cold Clim. HVAC 2018 Conf.,. Springer Nature Switzerland AG 2019; 2018.
[54] Clauß J, Vogler-Finck P, Georges L. Calibration of a high-resolution dynamic model for detailed investigation of the energy flexibility of a zero emission residential building. In: Johansson D, editor. Springer Proc. Energy, Cold Clim. HVAC 2018 Conf., Kiruna Sweden: Springer Nature Switzerland AG 2019; 2018. https://doi.org/10.1007/978-3-030-00662-4_61.
[55] Stiebel Eltron. Planung und Installation: Wärmepumpen; 2013.
[56] Vaillant. Innovativ Heizen und Kühlen mit Wärmepumpen; 2017.
[57] Viessmann. Planungshandbuch Wärmepumpen; 2011.
[58] HOVAL. Dimensionierungshilfe für Wärmepumpenanlagen 2017; 2017.
[59] OSOHotwater. OSO Hotwater, "OSO Optima EPC series". Patent 328503, 02 2014; 2014.
[60] Niemelä T, Kosonen R, Jokisalo J. Comparison of energy performance of simulated and measured heat pump systems in existing multi-family residential buildings. 12th IEA Heat Pump Conf. 2017, Rotterdam, Netherlands. 2017.
[61] Niemelä T, Vuolle M, Kosonen R, Jokisalo J, Salmi W, Nisula M. Dynamic simulation methods of heat pump systems as a part of dynamic energy simulation of buildings. Proc. 3rd Ibpsa-engl. Conf. BSO 2016, Newcastle. 2016.
[62] Fadejev J, Kurnitski J. Geothermal energy piles and boreholes design with heat pump in a whole building simulation software. Energy Build 2015;106:23–34. https://doi.org/10.1016/j.enbuild.2015.06.014.
[63] Hoval. Luft/Wasser-Wärmepumpen; 2018.
[64] Skogestad S. PID-tuning using the SIMC rules; 2017.
[65] Fischer D, Lindberg KB, Madani H, Wittwer C. Impact of PV and variable prices on optimal system sizing for heat pumps and thermal storage. Energy Build 2017;128:723–33.
[66] Renaldi R, Kiprakis A, Friedrich D. An optimisation framework for thermal energy storage integration in a residential heat pump heating system. Appl Energy 2017;186:520–9. https://doi.org/10.1016/j.apenergy.2016.02.067.
[67] SN/TS3031:2016. Bygningers energiytelse, Beregning av energibehov og energiforsyning 2016.
[68] Ahmed K, Akhondzada A, Kurnitski J, Olesen B. Occupancy schedules for energy simulation in new prEN16798-1 and ISO/FDIS 17772–1 standards. Sustain Cities Soc 2017;35:134–44. https://doi.org/10.1016/j.scs.2017.07.010.
[69] ISO17772-1. Energy performance of buildings - Indoor environmental quality - Part1: Indoor environmental input parameters for the design and assessment of energy performance of buildings; 2017.
[70] ISO7730:2005. Ergonomics of the thermal environment – Analytical determination and interpretation of thermal comfort using calculation of the PMV and PPD indices and local thermal comfort criteria; 2005.
[71] Standard Norge. NS-EN 15251:2007 Indoor environmental input parameters for design and assessment of energy performance of buildings addressing indoor air quality, thermal environment, lighting and acoustics; 2007.
[72] OpenStreetMap. Shiny weather data 2017. https://rokka.shinyapps.io/shinyweatherdata/ [accessed May 20, 2017].
[73] TrønderEnergi. Nettleie privat 2016. https://tronderenerginett.no/nettleie/privat/priser-fra-1.jan-2016 [accessed October 31, 2016].
[74] Reynders G, Diriken J, Saelens D. A generic quantification method for the active demand response potential of structural storage in buildings. 14th Int Conf Int Build Perform Simul Assoc. 2015.

PAPER 4

Influence of thermal zoning and electric radiator control on the energy flexibility potential of Norwegian detached houses

Johnsen T[1], Taksdal K[1], Clauß J[1], Yu X[1], Georges L[1]

[1] Norwegian University of Science and Technology, Kolbjørn Hejes vei 1a, 7034 Trondheim, Norway

This paper is accepted at *13th REHVA Congress CLIMA 2019* held in Bucharest, Romania, 26-29 May 2019.

Influence of thermal zoning and electric radiator control on the energy flexibility potential of Norwegian detached houses

Thea Johnsen[1,*], *Katrine Taksdal*[1], *John Clauß*[1], *Xingji Yu*[1] *and Laurent Georges*[1]

[1]Energy and Process Engineering Department, Norwegian University of Science and Technology (NTNU)

Abstract. Energy flexibility of buildings can be used to reduce energy use and costs, peak power, CO_{2eq}-emissions or to increase self-consumption of on-site electricity generation. Thermal mass activation proved to have a large potential for energy flexible operation. The indoor temperature is then allowed to fluctuate between a minimum and maximum value. Many studies investigating thermal mass activation consider electric radiators. Nevertheless, these studies most often assume that radiators modulate their emitted power, while, in reality, they are typically operated using thermostat (on-off) control. Firstly, this article aims at comparing the energy flexibility potential of thermostat and P-controls for Norwegian detached houses using detailed dynamic simulations (here IDA ICE). It is evaluated whether the thermostat converges to a P-control for a large number of identical buildings. As the buildings are getting better insulated, the impact of internal heat gains (IHG) becomes increasingly important. Therefore, the influence of different IHG profiles has been evaluated in the context of energy flexibility. Secondly, most studies about energy flexibility consider a single indoor temperature. This is questionable in residential buildings where people may want different temperature zones. This is critical in Norway where many occupants want cold bedrooms (~16°C) during winter time and open bedroom windows for this purpose. This article answers to these questions for two different building insulation levels and two construction modes (heavy and lightweight).

1 Introduction

Energy consumption needs to be more flexible. Firstly, the use of power demanding electric appliances is increasing which means that consumers are demanding more power from the distribution grid than before and often at the same time. The power grid is dimensioned to accommodate the highest possible load that can occur. Since the consumption of electricity varies significantly over hours, days and years, the grid will only experience this dimensioning load for short periods [1]. During an average weekday, the electricity consumption in Norwegian residential buildings peaks between 07:00 and 10:00 and between 16:00 and 21:00 [2]. Secondly, to make the transition to a sustainable energy system, more of the electricity must be produced from renewable energy sources. However, an increasing production from intermittent energy sources such as solar and wind may have serious adverse effects on the stability of the electricity grid. Therefore, it will become increasingly important to shift from a system based on generation-on-demand to a system where the energy use is flexible and controlled according to grid requirements or intermittent energy production.

In the recent years, there has been an increasing focus on energy flexibility on the demand side. Demand side management (DSM) adapts the consumption according to the needs of the surrounding electricity grid [3]. When the electricity use for heating and cooling is considered for DSM, a thermal storage is necessary [4]. For buildings, DSM can be achieved in several ways, for example using heat storage in hot-water tanks or in the thermal mass and by shifting the use of plug loads in time [5]. Storage in the building structure, i.e. the building thermal mass, has been identified as a promising and cost-effective way for buildings to offer flexibility [6, 7]. The available storage capacity in the building structure is not only dependent on the material properties but also on the geometry of the building, the distribution of thermal mass inside the building and the interaction with the heating system. In addition, the performance of structural thermal storage will vary with time, as weather conditions and occupant behavior affect the available storage capacity [8].

To activate the thermal mass of the building, a suitable control strategy is necessary. Rule Based Control (RBC) is a common control approach for energy systems in buildings. Even though simpler than Model Predictive Control (MPC), RBC can still be used to deploy the building energy flexibility [4]. For instance, RBC has been investigated for Norwegian residential buildings using either time-scheduled or day-ahead electricity prices to control the set-point indoor temperature [9, 10].

Key performance indicators (KPIs) can be used to evaluate the performance of a system with respect to a specific desired result. A KPI is a parameter (or value) that provides simplified information about a complex system, to show the general state or trend [11]. For instance, KPIs

* Corresponding author: thea.john@stud.ntnu.no

are necessary to quantify the energy flexibility generated by different control strategies. Typical KPIs of building energy flexibility can describe physical features of the building, such as the storage capacity, or quantify the magnitude of the building's response to external signals, e.g. the electricity price [4].

Simplifications of modelling the occupant behavior is a main reason for the gap between the predicted and actual energy performance of a building. For buildings with better insulation levels, internal heat gains (IHG) have an increasing contribution to the space-heating demand [12]. It is common practice in the building industry to dimension the power of the space-heating system without accounting for IHGs. This often leads to oversizing of the space-heating system in highly-insulated buildings. In addition, it is important to use realistic IHG profiles in energy simulations to get reliable predictions of the actual energy performance. For instance, a bottom-up stochastic model to generate realistic electricity load profiles can be used to create realistic IHG profiles [13].

Several studies have identified occupant dissatisfaction with too high bedroom temperatures in Norwegian highly-insulated buildings during winter time. Low temperature in bedrooms is difficult to achieve without window opening which eventually leads to a significant increase of the space-heating needs. This is especially true when there is a desire for higher temperatures in the rest of the building [14-18]. One key characteristic of DSM is user acceptability, i.e. the occupant's willingness to accept that the building is controlled depending on the needs of the electricity grid [3]. For example, a compromise could be a cheaper electricity bill at the sacrifice of thermal comfort (within certain limits). Storing heat using the building thermal mass typically leads to relatively high indoor temperatures which can prevent reaching cold temperatures in bedrooms. Only a limited number of studies investigated the effect of thermal zoning on building energy flexibility. Different temperature set-points (TSP) are defined for so-called day-zones and night-zones, with the TSP for the day zone is slightly higher than the TSP of the night zone [6, 19, 20]. However, most studies assume a single temperature for the entire building.

The Norwegian building stock is dominated by single-family houses (SFH). The interest in high-performance buildings is rapidly increasing but they still represent a small fraction of the building stock. In 2013, only 31 % of the inhabited building stock were built after 1980 [21]. In Norwegian residential buildings, the most common space-heating system is electric radiators, however, the number of heat pump installations is increasing [21, 22]. According to electric radiator manufacturers, the most common control of these radiators is thermostatic control (meaning that the radiator is operated at full power between a start and stop temperature). Nevertheless, the studies on energy flexibility are usually done assuming a continuous power modulation. This can for example be a proportional (P) controller or a proportional-integral (PI) controller.

The objectives of this study is to identify the flexibility potential of Norwegian detached houses heated by electric radiators. More specifically, this energy flexibility potential is compared between a thermostatic and a proportional control of the radiators. Furthermore, the influence of the thermal mass activation on internal thermal zoning is investigated as well as the impact of such a zoning on the flexibility potential. These questions are investigated using detailed dynamic simulations in IDA ICE. A detached house controlled with two simple RBC strategies for heating is simulated. Since IHGs are expected to have an influence on the building thermal dynamics, different scenarios of IHG profiles are evaluated. This includes fixed IHG profiles defined from standards but also stochastic IHG profiles. Stochastic IHG profiles enable to investigate whether the thermostat control converges to a P-control when energy flexibility is evaluated for a large number of identical buildings, at a so-called aggregated level.

2 Methodology

2.1. Definition of the case building

A two-storey detached house with a heated floor area of 160 m^2 located in Oslo is used as a case study. An illustration of the building geometry from IDA ICE is shown in **Fig. 1**.

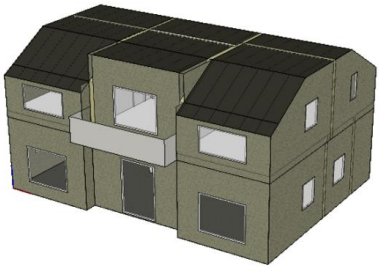

Fig. 1*. 3D geometry of the building model implemented in IDA ICE (showing the southwest façade).*

Two different construction modes are investigated, one lightweight timber construction (LCM) and one heavy masonry construction (HCM). The heat storage capacity and the average U-values of the internal structures for the two construction modes are listed in **Table 1**.

Table 1. *Heat storage capacity and average U-value of the internal walls and floors for the lightweight construction mode (LCM) and the heavy construction mode (HCM).*

Construction mode	Heat storage capacity [MJ/K]	$U_{int.wall}$ [W/m^{2}K]	$U_{int.floor}$ [W/m^{2}K]
HCM	86	2.84	1.60
LCM	14	0.25	0.21

Furthermore, two levels of insulation are investigated, one corresponding to the Norwegian passive house (PH) standard and the other is set in accordance with the example building of the TABULA project in the age segment 1981-1990 (TB building) [23, 24]. This results in a total of four investigated building types; passive house

standard with heavy construction (PHH) and lightweight construction (PHL), and an insulation level typical for a building built in the 1980s with heavy construction (TBH) and lightweight construction (TBL). The building envelope specifications for the PH and TB insulation levels are listed in Table 2. The PH buildings are modeled with a balanced mechanical ventilation system with heat recovery and an air temperature of 20 °C for the supply ventilation air. The ventilation airflow rates are in accordance with the Norwegian building code [25]. Natural ventilation is usually applied to old buildings. For the sake of simplicity the TB buildings are modelled with a balanced mechanical ventilation without heat recovery.

Table 2. *U-values for external constructions (W/m^2K), infiltration rate (n_{50}), normalized thermal bridge factor (Ψ'') and heat recovery effectiveness (η_{HR}) for the PH and TB insulation levels.*

Construction element	PH	TB
U_{roof} [W/m^2K]	0.10	0.36
$U_{ext.wall}$ [W/m^2K]	0.10	0.32
$U_{ext.floor}$ [W/m^2K]	0.09	0.20
$U_{windows}$ [W/m^2K]	0.8	2.80
n_{50} [h^{-1}]	0.6	4
Ψ''[W/m^2K]	0.03	0.05
η_{HR} [%]	85	0

The space-heating system consists of electric radiators in every room except for the two bathrooms and the laundry room which are equipped with floor heating. The nominal space-heating power of each room is evaluated using IDA ICE simulations with ideal heaters, no IHG and a constant design outdoor temperature (DOT) of Oslo (i.e. -19.8 °C). The dimensioning of the radiator is done according to the current practice: the nominal power of the radiators and floor heating equals the nominal power of the respective room they are located in. The radiator control has a dead-band (Δ) and P-band of 1 °C. The thermostat control starts at TSP – Δ/2 and stops at TSP + Δ/2.

2.2 Rule-based control strategies

To evaluate the energy flexibility potential, two different RBC strategies are applied: an off-peak hour control strategy (OPCS) and a spot price control strategy (SPCS). Both adjust the TSP of the space-heating system.

The OPCS aims at reducing the electricity use for space-heating during peak hours. This objective is critical for Norway as the distribution grid is expected to face bottlenecks in the near future [26]. Peak hours are based on the average electricity consumption of Norwegian residential buildings on a weekday. Based on this daily profile, peak hours for electricity consumption are defined between 07:00 and 09:00 as well as between 17:00 and 19:00 [2]. With OPCS, the TSP is 21 °C in all rooms. Nevertheless, this temperature is reduced by 2 K in the defined peak hours while it is increased by 2 K one hour before peak hours to store energy in the thermal mass.

The SPCS aims at reducing energy costs for space-heating. It is based on the day-ahead hourly spot price for electricity, retrieved from NordPool [27]. The TSP is here controlled using two thresholds for the electricity price. The low and high thresholds are set to the minimum spot price plus 25 % and 75 % of the difference between the minimum and maximum day-ahead spot prices, respectively. Therefore, thresholds are updated every day. These two thresholds define periods of low, medium and high electricity prices. The SPCS decreases the TSP by 2K in high-price periods, keeps the TSP at 21°C in medium-price periods and increases the TSP by 2K in low price periods. Since the nighttime is characterized with a low electricity demand, the spot price is relatively low. The SPCS would initially exploit this low price to increase the TSP. This is expected to lead to a higher energy consumption and cost, as concluded in a previous study [9]. Therefore, the SPCS only operates between 06:00 and 23:00. Otherwise it is overruled to 21 °C.

2.3 Internal heat gain profiles

Four different IHG profiles are investigated. Two are based on Norwegian standards and are uniform in space. Nevertheless, one of these profiles is static (NS) and the other one is distributed in time with a fixed daily profile (TS). The two other IHG profiles are stochastic, with variations from day to day and between the seasons. The magnitude of these stochastic profiles is the same, but one profile contains IHGs distributed in time (SM_t) while the second has IHGs varying in both time and space (SM_{ts}).

The annual profile for lighting and electric appliances is generated using the bottom-up model developed by Richardson et. al. [13] which has been adjusted to Norwegian households by Rangøy [28]. However, there is currently no stochastic occupancy model compatible with the available Norwegian statistical data. Therefore, a fixed occupancy profile with an hourly resolution was created artificially.

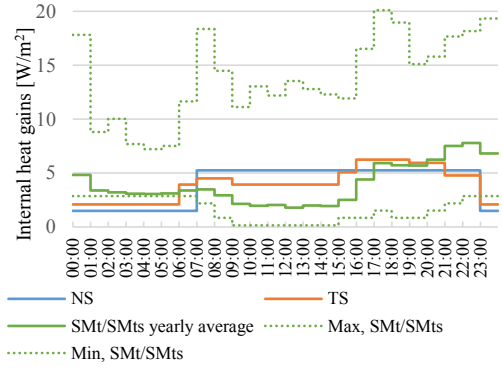

Fig. 2. *Yearly-averaged internal heat gains from the four investigated profiles.*

This occupancy profile does not contain as many fluctuations as the profiles for lighting and electric appliances. However, a separation is made between weekdays and weekends. In addition, variations in the occupancy have been considered for the summer, winter

and spring/autumn months. The occupancy, appliance and lighting profiles are generated for a household of four persons. Finally, the stochastic profiles are scaled so that the yearly-averaged IHGs in W/m^2 is the same as in the two Norwegian standards (NS and TS). The daily IHG profiles are illustrated in Fig. 2, where the yearly average of the stochastic profile is shown along with the maximum and minimum values.

2.4 Summary of simulation scenarios

Table 3 summarizes the control scenarios investigated. All simulations are carried out with both thermostatic and P-control. To evaluate the influence of internal thermal zoning, the RBCs either impose the changes of the TSP to the bedrooms or not. This last scenario, here called "decoupled" bedrooms, applies a constant TSP in bedrooms, of either 16 °C or 21 °C. The internal doors are always closed for all scenarios. Furthermore, the effects of overruling the SPCS during nighttime is evaluated, also in combination with decoupled bedrooms.

Table 3. *Summary of control strategy scenarios: the flexibility is also evaluated with the bedrooms decoupled (bdc) from the control strategy with a constant TSP of 21 °C or 16 °C; SPCS is also evaluated with no overruling at nighttime (nor).*

Control Strategies	Overruling nighttime	Bedrooms Decoupled
OPCS	-	No
$OPCS_{bdc21}$	-	Yes (TSP 21 °C)
$OPCS_{bdc16}$	-	Yes (TSP 16 °C)
SPCS	Yes	No
$SPCS_{nor}$	No	No
$SPCS_{bdc21}$	Yes	Yes (TSP 21 °C)
$SPCS_{bdc16}$	Yes	Yes (TSP 16 °C)
$SPCS_{nor+bdc16}$	No	Yes (TSP 16 °C)

To be able to evaluate the effects of the RBC strategies, each of the simulation scenarios is compared with a reference case with a constant TSP of 21 °C. Each investigated scenario has its own reference case. The only difference between the investigated scenario and its respective reference case is the implementation of RBC strategy. This means that the effects of the RBC strategy are compared with a simulation of the same building type with the same radiator controller and IHG profile. For the $OPCS_{bdc16}$ and $SPCS_{bdc16}$, the reference case has a constant TSP of 16 °C in the bedrooms. In conclusion, there are separate reference simulations for the different building types, IHG profiles and radiator controls. Based on the performance of the respective reference simulation, the energy flexibility potential of each simulation case is here evaluated using a single KPI. The KPI, called q_{ph}, is the ratio between the energy use in peak hours for the simulation with a implemented control strategy ($Q_{ph,RBC}$) and the energy use in the peak hours with the reference simulation with constant TSP ($Q_{ph,ref}$). This KPI is defined by equation 1:

$$q_{ph} = \frac{Q_{ph,RBC}}{Q_{ph,ref}} \quad (1)$$

For clarity this means that a q_{ph} of 1 means that no energy is shifted in the peak hours, i.e. the energy consumption in the peak hours is the same as the reference case without the implemented RBC. A low value for q_{ph} indicates more energy shifted and a value of 0 means that the energy use is fully shifted away from peak hours.

3 Results

This section successively shows the effect of the radiator control type, the IHG profile and the temperature zoning on the flexibility potential.

3.1 Controller type and internal heat gains

Table 4 shows the relative change in energy use during the peak hours (q_{ph}) with OPCS and SPCS for both controller types using SM_{ts} IHGs. Both RBC strategies successfully shift energy and power use from the defined peak hours to off-peak hours. The share of shifted energy and power is much more significant for the PH buildings than the TB buildings. In PH buildings, the OPCS leads to zero energy and power consumption during the four defined peak hours of the day throughout the year.

Table 4 *KPI for energy use during peak hours (q_{ph}) with OPCS and SPCS: results are given for both proportional and thermostatic control and using SM_{ts} IHG profile.*

RBC	PHL	PHH	TBL	TBH
	Proportional control (PC)			
OPCS	0.000	0.000	0.139	0.078
SPCS	0.557	0.586	0.663	0.570
	Thermostatic control (TC)			
OPCS	0.000	0.000	0.086	0.028
SPCS	0.525	0.582	0.629	0.515

Fig. 3(a) shows the absolute change in yearly energy use during the peak hours compared to the reference cases, for the OPCS and SPCS and for the PHL and PHH. This is given for both radiator controls and all four IHG profiles. Stochastic profiles always result in the largest amount of energy shifted from peak hours, the SM_{ts} is the profile with the highest amount of shifted energy. Furthermore, with stochastic IHG profiles the magnitude of energy shifted is relatively similar with thermostatic and proportional control. For standard static IHGs the magnitude of energy shifted is much more significant with proportional control. The same is illustrated for the TB buildings in Fig. 3(b). The magnitude of energy reduced during peak hours for these TB buildings is almost ten times higher than for the PH buildings. Unlike the PH buildings, the difference of energy shifted between the different control types and IHG profiles is limited.

The space-heating power given in Fig. 4(a) is the average of the 20 equivalent PHL buildings, but with different SM_{ts} profiles. This is given for 22nd January. The average space-heating power is compared for the reference and the RBC, with thermostatic and proportional control. Fig. 4 shows that the aggregated space-heating power of a neighborhood is very similar with thermostatic control and with P-control. It is assumed that with more buildings with different SM_{ts} IHG

profiles, the results with the thermostatic controller would be smoother. The most significant difference with a thermostatic controller compared to the P-controller is the rebound peak with OPCS. The aggregation with a P-controller results in a more distinct rebound peak after the pre-defined peak hours. This is because in some of the building zones, especially the ones with floor heating (technical room, bathrooms), the air temperature will not drop below 20.5 °C during the peak hours. If the temperature in these zones is between 20.5 °C and 21 °C, the P-controller will start to operate while the thermostatic controller will wait until the temperature is below 20.5 °C. Therefore, the selection of the start and stop temperatures (or dead-band) of the thermostatic control or the constant of the P-control will also have an impact on the rebound effect.

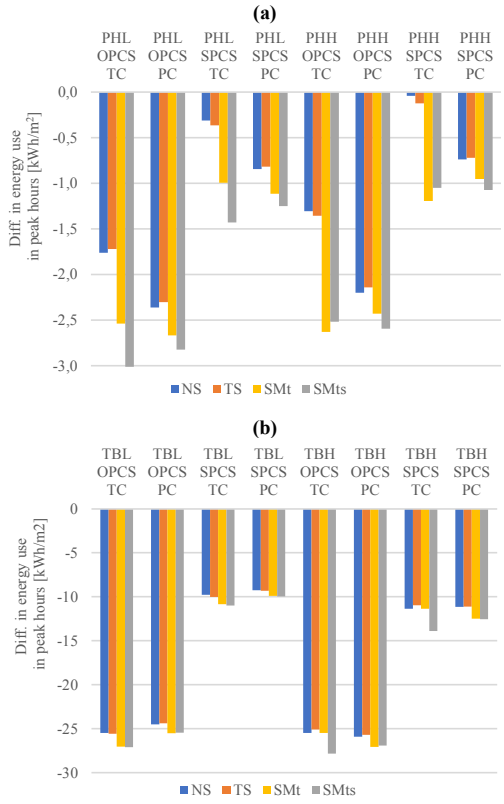

Fig. 3. *Difference in annual specific energy use during peak hours between the reference and the OPCS or SPCS for (a) the PHL and PHH and (b) for the TBL and TBH (for thermostatic control (TC) and proportional control (PC)).*

The results for TBL, shown in Fig. 4(b), have the same trend as the PHL regarding the difference between radiator controls. However, unlike the PHL, the difference in rebound peak between the thermostatic and proportional controls is insignificant. As the temperature drop during peak hours is higher for the TB buildings, both the thermostatic and proportional controls will operate at full power right after the peak period and lead to the same magnitude of the rebound peak. Again, in terms of modeling, higher insulation levels require a more careful definition of the radiator control.

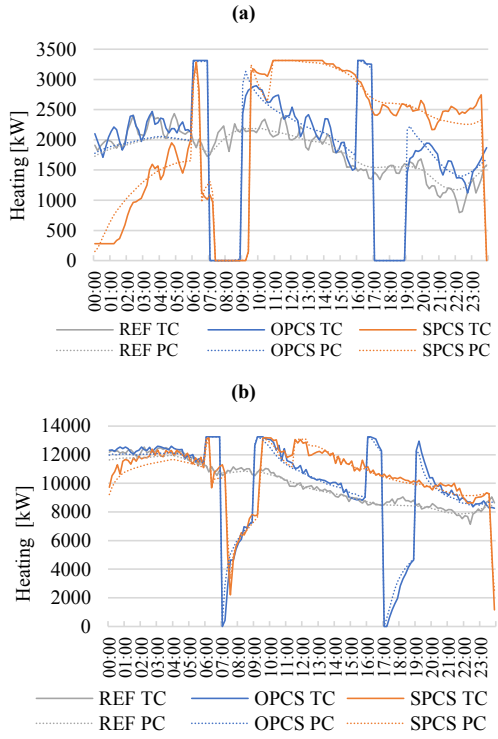

Fig. 4. *Average space-heating power of (a) 20 PHL buildings and (b) 20 TBL buildings with different SM_{ts} profiles for thermostatic and P control (given for one cold day for the reference case, OPCS and SPCS).*

3.2 Internal thermal zoning

The effects of decoupling the bedrooms from the RBC strategies are investigated for the bedroom in the South-East corner of the building (bedroom SE). The operative temperature in bedroom SE is studied during nighttime during the heating season considering the SM_{ts} profile. Based on simulations, the heating season is defined between October and April. Fig**.** 5(a) shows the time distribution of the operative temperature for the TB buildings with a constant bedroom TSP of 21 °C. A stable temperature for the reference case is obvious. OPCS and SPCS result in a temperature above 22 °C for almost 20% of the time. However, when the bedrooms are decoupled ($OPCS_{bdc21}$ and $SPCS_{bdc21}$), the temperatures are similar to the reference cases. The bedroom temperature is not significantly affected by the two DSM controls whatever the construction mode, if decoupled.

It is difficult to achieve low bedroom temperatures in PH buildings due to the balanced mechanical ventilation with a centralized heat recovery, relatively low heat losses through the envelope and solar gains. Fig. 5(b) shows the percentage of time for different temperature intervals in bedroom SE in the PH during nighttime and the heating season. The analysis of the reference cases shows that the

operative temperature is already above 22°C for about 30% of the time without any activation of the thermal mass using RBCs. The SPCS leads to a higher increase of bedroom temperatures than OPCS, especially for the lightweight PH building (PHL): the operative temperature is then above 22 °C for more than 50 % of the night-time during the heating season. As for the TB buildings, decoupling the bedrooms from the RBC strategies has a positive effect on reducing the bedroom temperatures. The $SPCS_{bdc21}$ results in a noticeable improvement: with this strategy, the share of time over 22 °C is reduced significantly. A difference can be noticed between the construction modes. Compared to PHL, PHH has less hours at high temperatures when RBC strategies are applied to bedrooms. However, the decoupling of the bedrooms is not as effective for PHH as for PHL. This is reasonable as internal walls of lightweight buildings are insulated, thus having a lower U-value than in heavyweight buildings. The heat transfer in internal constructions is significant in heavyweight buildings so that the bedroom temperature is influenced by temperature fluctuations generated by the RBCs in the neighboring rooms.

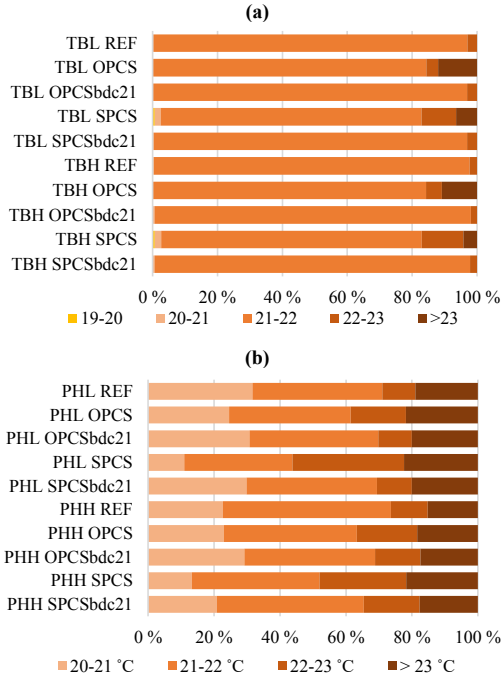

Fig. 5. *Breakdown of the operative temperature into intervals in bedroom SE during night-time and the heating season: reference case TSP, the original RBCs and the RBCs with decoupled bedrooms with TSP of 21 °C for (a) TB and (b) PH.*

Fig. 6 is similar to Fig. 5, but shows the cases for a TSP of 16 °C in the bedrooms. Regarding the TB buildings, Fig. 6(a) shows that these buildings. achieve temperatures close to this low TSP for most of the heating season TSP. With $OPCS_{bdc16}$ and $SPCS_{bdc16}$, the bedroom temperature in TBL is below 17 °C almost 100 % of the time. For the reference control, the temperature is higher in the TBH, but the temperature remains below 17 °C for 70 % of the time. $OPCS_{bdc16}$ and $SPCS_{bdc16}$ do not modify this trend. In addition, SPCS without overruling during nighttime ($SPCS_{bdc16+nor}$) is also studied. $SPCS_{bdc16+nor}$ leads to a lot of hours with a TSP of 23 °C in the rest of the building (i.e. not bedrooms) but it only slightly increases the bedroom temperature. For the TB buildings, the thermal mass activation in the common rooms does not increase the resulting bedroom temperatures. Therefore, the risk to open windows to decrease bedroom temperatures is not expected to be higher with the thermal mass activation.

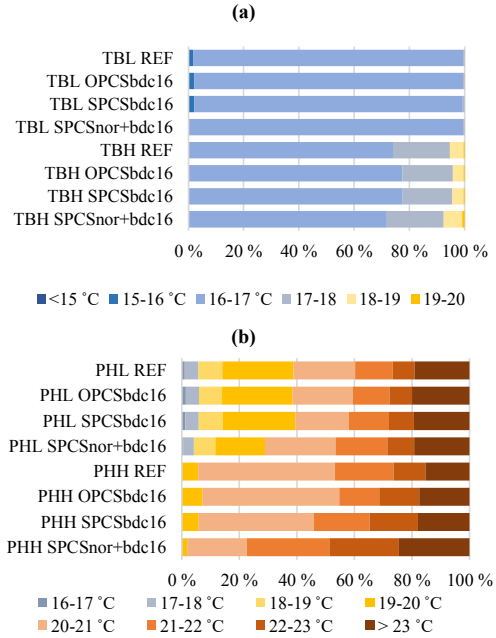

Fig. 6. *Breakdown of the operative temperature into intervals in bedroom SE during night-time in the heating season: reference case TSP, the original RBCs and the RBCs with decoupled bedrooms with TSP of 16 °C with and without overruling for (a) TB and (b) PH.*

Fig. 6(b) shows the time distribution of the operative temperature for the PH buildings. The reference for these cases is taken with a constant TSP of 16 °C in the bedrooms and 21 °C in the rest of the zones. In general, the reduction of the TSP to 16 °C in the bedrooms does not contribute to a reduction of the highest temperatures for the PH buildings. This indicates that the temperature of 23 °C is not due to the TSP, but rather due to internal and solar heat gains. With a TSP of 16 °C, the bedroom radiators are off during the entire year for the PHH. Only the PHL achieves bedroom temperatures close to the TSP, leading to small space-heating needs for a low share of the time. One main reason for this, especially for the colder months, is that the ventilation supply air TSP is 20 °C (which is a common set-point). Thus, even with no heat from local heating units, the heat from the supply air and other zones will keep bedrooms warm. The implementation of the RBCs leads to limited changes of the bedroom temperature except for the $SPCS_{bdc16+nor}$ in the PHH building. Besides this single case, the

temperature in bedrooms is not affected by the RBCs suggesting that the risk of window opening is not increased.

By decoupling the bedrooms from the RBC strategies, the amount of energy and power shifted is reduced, as the radiators in the bedrooms will operate with a constant TSP of 21 °C or 16 °C. The energy flexibility potential with the bedrooms decoupled from the RBC strategies is evaluated using the energy use during peak hours (q_{ph}) for the reference case and for the RBC strategies. Again, $OPCS_{bdc16}$ and $SPCS_{bdc16}$ are evaluated against a reference case with a constant TSP of 16 °C in the bedrooms and 21 °C in the other zones. In general, the indicator q_{ph} is higher when bedrooms are decoupled (bdc) from the RBC compared to the scenario with coupled bedrooms. This is illustrated in Fig. 7.

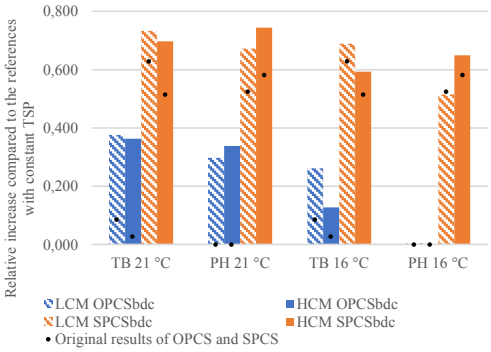

Fig. 7. *Energy use relative to the respective reference case during peak hours with $OPCS_{bdc21/bdc16}$ and $SPCS_{bdc21/bdc16}$: original results of the OPCS and SPCS without decoupling are illustrated with black marks.*

4 Conclusions

This work evaluated the energy flexibility that Norwegian residential buildings can provide to the electricity grid. This has been done using rule-based controls (RBC) that adjust the temperature set-point (TSP) of a direct electric space-heating system. Physical aspects which may influence the energy flexibility are investigated, including internal heat gains (IHG), the type of radiator control and the occupant preference for cold or warm bedrooms.

Two RBC strategies activating the building energy flexibility are applied: one with a pre-defined schedule (OPCS) that aims at reducing electricity use during peak hours and one that aims at decreasing energy costs using time-variable spot prices (SPCS). These RBCs have been evaluated using simulations for a detached house with two different insulation levels and two construction modes. The main focus was the load shifting away from peak hours (which is a main concern in Norway). Results showed that all building types have potential to shift their energy and power use. The buildings with a higher insulation level achieve a higher relative share of energy and power shifted. Although less insulated buildings have a lower relative peak shaving potential, the magnitude of the energy and power shifted is significantly higher.

With highly-insulated buildings, the largest potential for energy and power shifting was found for stochastic IHG profiles, which are assumed to be the most realistic representations of occupant behaviour. However, the influence of the internal gains on the energy shifted is small for the less-insulated buildings. This indicates that the flexibility potential using thermal mass can be dependent on the timing of the IHGs, especially in highly-insulated buildings. Thus, modelling IHGs using standard fixed profiles may underestimate the load-shifting.

It was found that the type of radiator control has an impact on the energy and load shifting potential of highly-insulated buildings, whereas this effect is almost negligible for low insulation levels. The two RBCs were also evaluated for 20 identical buildings but with different stochastic IHG profiles. Considering aggregated results, the performance of the thermostatic control converges to a proportional control. Proportional control can thus reasonably be used to evaluate the energy flexibility of several buildings. However, for highly-insulated buildings, the rebound peak right after the peak hours was found to be higher with proportional control compared to thermostatic control.

With low insulation levels, cold bedrooms can be easily created by applying a low temperature set-point in these rooms (e.g. ~16 °C). If the two RBCs are not applied to bedrooms (but only to the rest of the building), bedroom temperatures do not increase significantly. With high insulation levels including a centralized heat recovery of the ventilation air, it is intrinsically difficult to create cold bedrooms. Periods with moderate to high bedroom temperatures will be found systematically during the space-heating season (as long as bedroom windows are not open). If the two RBCs are not applied to bedrooms (but only to the rest of the building), they do not amplify this phenomenon. Consequently, these results suggest that the activation of the building thermal mass, if not applied in bedrooms, will not further increase the risk of window opening or user dissatisfaction in bedrooms. The window opening should be avoided as it would lead to a noticeable increase of the space-heating needs. In addition, the thermal mass activation without considering bedrooms leads to a moderate reduction of the load-shifting potential compared to the activation of the entire building.

As a general comment, higher insulation levels require more complexity for all the physical phenomena investigated (i.e. IHG definition, radiator control and temperature zoning). Results are relatively insensitive to this modelling complexity for low insulation levels. As most of the Norwegian building stock is composed of low-insulated buildings, this is an important conclusion.

5. Acknowledgements

The authors would like to acknowledge IEA EBC Annex 67 and the Norwegian Research Center on Zero Emission Neighborhoods in Smart Cities, ZEN, as this work has been carried out under these frameworks. The authors would like to thanks Dr. Igor Sartori (Senior Researcher at SINTEF Building and Infrastructure) for his explanations and support regarding stochastic internal heat gains.

References

1. Norges vassdrags- og energidirektorat. *Ny teknologi og forbrukerfleksibilitet*. 2015 Updated: 04.05.2017 [cited 2018 25.01]; Available from: https://www.nve.no/elmarkedstilsynet-marked-og-monopol/sluttbrukermarkedet/ny-teknologi-og-forbrukerfleksibilitet/.
2. Langseth, B., I.H. Magnussen, and D. Spilde, *Energibruksrapporten 2013*, NVE, Editor. 2014.
3. Aduda, K.O., et al., *Demand side flexibility: Potentials and building performance implications.* Sustainable Cities and Society, 2016. **22**: p. 146-163.
4. Clauß, J., et al., *Control strategies for building energy systems to unlock demand side flexibility – A review*, in *12th International Conference of IBPSA*. 2017: San Francisco, US.
5. Jensen, S.Ø., et al., *IEA EBC Annex 67 Energy Flexible Buildings.* Energy & Buildings, 2017. **155**: p. 25-34.
6. Reynders, G., et al., *Potential of structural thermal mass for demand-side management in dwellings.* Building and Environment, 2013. **64**: p. 187-199.
7. Le Dréau, J. and P. Heiselberg, *Energy flexibility of residential buildings using short term heat storage in the thermal mass.* Energy, 2016. **111**: p. 991-1002.
8. Reynders, G., J. Diriken, and D. Saelens, *A Generic Quantification Method for the Active Demand Response Potential of Structural Storage in Buildings*, in *14th Conference of International Building Performance Simulation Association*. 2015.
9. Clauß, J., et al. *Investigations of Different Control Strategies for Heat Pump Systems in a Residential nZEB in the Nordic Climate*. in *12th IEA Heat Pump Conference*. 2017. Rotterdam, Netherlands.
10. Dar, U.I., et al., *Advanced control of heat pumps for improved flexibility of Net-ZEB towards the grid.* Energy & Buildings, 2014. **69**: p. 74-84.
11. Deru, M. and P. Torcellini, *Performance Metrics Research Project - Final Report*. 2005.
12. Yan, D., et al., *IEA EBC Annex 66: Definition and simulation of occupant behavior in buildings.* Energy and Buildings, 2017. **156**: p. 258-270.
13. Richardson, I., et al., *Domestic electricity use: A high-resolution energy demand model.* Energy and Buildings, 2010. **42**(10): p. 1878-1887.
14. Berge, M., J. Thomsen, and H.M. Mathisen, *The need for temperature zoning in high-performance residential buildings.* Journal of Housing and the Built Environment, 2017. **32**(2): p. 211-230.
15. Georges, L., et al., *Simplified Space-heating Distribution Using Radiators in Super-insulated Apartment Buildings.* Energy Procedia, 2016. **96**: p. 455-466.
16. Thomsen, J., et al., *Evaluering av boliger med lavt energibehov (EBLE) (Evaluation of housing with low energy needs)*. 2017.
17. Georges, L., et al., *Evaluation of Simplified Space-Heating Hydronic Distribution for Norwegian Passive Houses*. 2017, SINTEF akademisk forlag.
18. Georges, L., F. Håheim, and M.J. Alonso, *Simplified Space-Heating Distribution using Radiators in Super-Insulated Terraced Houses.* Energy Procedia, 2017. **132**(C): p. 604-609.
19. Thibault, Q.P., O. Joana, and S. Jaume, *Impact of Demand-Side Management on Thermal Comfort and Energy Costs in a Residential nZEB.* Buildings, 2017. **7**(2): p. 37.
20. Arteconi, A., et al., *Active demand response with electric heating systems: Impact of market penetration.* Applied Energy, 2016. **177**(C): p. 636-648.
21. Brattebø, H., et al., *Fremtidig utvikling i energiforbruk og CO2-utslipp for Norges boligmasse*. 2016.
22. Ericson, T., et al., *Varmepumper i energisystemet*. 2016, NVE.
23. Standard Norge, *NS3700:2013 Criteria for passive houses and low energy buildings, Residential buildings.* 2013.
24. Brattebø, H., et al., *Typologier for norske boligbygg - Eksempler på tiltak for energieffektivisering*. 2016.
25. Direktoratet for byggkvalitet, *Technical Building Works Regulations - TEK17*. 2017.
26. Benjamin Donald Smith, et al., *Nordic Energy Technology Perspectives 2016: Cities, flexibility and pathways to carbon-neutrality*. 2016: International Energy Agency (IEA).
27. Nord Pool AS. *Day-ahead prices*. 2016 [cited 2018 05.02]; Available from: https://www.nordpoolgroup.com/Market-data1/Dayahead/Area-Prices/ALL1/Hourly/?view=table.
28. Rangøy, E., *Master Thesis: Validation of user profiles for building energy simulations*. 2013, Norwegian University of Science and Technology.

PAPER 5

Model complexity of heat pump systems to investigate the building energy flexibility and guidelines for model implementation

Clauß J[1], Georges L[1]

[1] Norwegian University of Science and Technology, Kolbjørn Hejes vei 1a, 7034 Trondheim, Norway

A revised version of this paper is submitted to *Applied Energy* in July 2019.

Model complexity of heat pump systems to investigate the building energy flexibility and guidelines for model implementation

John Clauß[a]* and Laurent Georges[a]

[a]Department of Energy and Process Engineering, Norwegian University of Science and Technology, Trondheim, Norway

Norwegian University of Science and Technology, Kolbjørn Hejes vei 1a, 7034 Trondheim, Norway

*john.clauss@ntnu.no

Abstract

Building performance simulation (BPS) is a powerful tool for engineers working in building design and heating, ventilation and air-conditioning. Many case studies using BPS investigate the potential of demand response (DR) measures with heat pumps. However, the models are often simplified for the components of the heat pump system (i.e. heat pump, electric auxiliary heater and storage tank) and for their interactions. These simplifications may lead to significant differences in terms of DR performance so that more comprehensive models for a heat pump system may be necessary. The contribution of this work is twofold. Firstly, this work investigates the influence of the modeling complexity of the heat pump control on different key performance indicators for the energy efficiency, the DR potential and the heat pump operation. To this end, the performance of six different heat pump controls is compared. Secondly, it describes the implementation of a comprehensive control for a heat pump system in BPS tools. This control is not often documented in the BPS literature and is error-prone. Generic pseudo-codes are provided, whereas IDA ICE is taken as an example in the case study. A predictive rule-based control is implemented to study price-based DR of residential heating. It is shown that a realistic operation of the heat pump system can be achieved using the proposed modeling approach. The results prove that the modeling complexity of the system control has a significant impact on the performance indicators, meaning that this aspect should not be overlooked. For some performance indicators, e.g. the annual energy use for heating and average water tank temperature, it is shown that a proportional (P-) and proportional-integral (PI-) control can lead to similar results. If the heat pump operation is investigated in detail and a short-time resolution is required, the difference between P- and PI-controls and their tuning is important. As long as the heat pump operation and electrical power at short timescales are not of importance, the choice of controller (P or PI) is not crucial. However, the use of P-control significantly simplifies the modeling work compared to PI-control. If DR is performed for domestic hot water, it is also demonstrated that the prioritization of domestic hot water can indirectly influence the operation of auxiliary heaters for space-heating, significantly increasing the use of electricity. However, the electricity use is only slightly increased if DR control is only used for space heating.

Keywords: heat pump system; system modeling; demand response; energy flexibility; model complexity

Nomenclature

ASHP	Air-source heat pump	*OTCC*	Outdoor temperature compensation curve
BAU	Business as usual	*P*	Proportional
BPS	Building performance simulation	*PI*	Proportional integral
COP	Coefficient of performance	*PMV*	Predicted mean vote
CP	Circulation pump	*PPD*	Predicted percentage dissatisfied
CSP	Control strategy price	*PRBC*	Predictive rule-based control
DE	Direct electric	*PV*	Photovoltaic
DHW	Domestic hot water	*RTSP*	Reference temperature set-point
DOT	Design outdoor temperature	*SH*	Space heating
DR	Demand response	*SCOP*	Seasonal coefficient of performance
HP	Heat pump	*SP*	Spot price
HPT	High-price threshold	T_i	Integral time
HTSP	High temperature set-point	*TM*	Temperature measurement
k	Gain parameter	*TSP*	Temperature set-point
LPT	Low-price threshold	τ_c	Tuning parameter for PI-controller tuning
LTSP	Low temperature set-point	*ZEB*	Zero emission building
max	Maximum		
MHP	Modulating heat pump		
min	Minimum		
MPC	Model-predictive control		
OHP	On-off heat pump		

1 Introduction

Demand response (DR) measures can be applied to building energy systems to achieve load shifting and peak power reductions, according to reviews on demand side flexibility [1] and demand response [2] [3]. DR measures can deploy building energy flexibility by making use of available thermal energy storages [4], such as the thermal mass of a building [5] or hot water storage tanks [6]. Several studies consider the activation of the building energy flexibility using (predictive) rule-based control ((P)RBC), e.g. [7] [8]. These controls are frequently implemented into building performance simulation (BPS) tools. Heat pump systems can be used to perform DR measures to deploy the demand side flexibility of buildings. A *heat pump system* refers to a heat pump unit combined with auxiliary heaters and (potentially) thermal storage as well as the system control. Typically, a heat pump is connected to a water tank to store domestic hot water (DHW) or provide space heating (SH).

1.1 Model complexity and simplifications

An overview of simulation-based studies of DR using heat pumps and applying RBC is presented in Table 1, focusing especially on the model simplifications applied to the respective heating systems. From this overview in Table *1*, it appears that there is a lack of detailed information of the heat pump system and that modeling simplifications are introduced. These studies typically combine one or several of the following simplifications for the modeling of the heat pump system:

(1) *The heat pump modulates perfectly between 0% and 100%, or is on/off*. These assumptions make the operation of the heat pump continuous or discrete which considerably simplifies the modeling when considered separately. Obviously, with a perfect modulation, the number of heat pump cycles throughout the year cannot be studied.
(2) *Minimum duration and pause times in the heat pump cycle are not considered*. Without these constraints, frequent on-off cycling could occur.
(3) *The water storage tank is simplified.*

(a) *Thermal stratification is neglected.* Thermal stratification in a water tank results from complex heat transfer phenomena. The use of stratification is part of the working principle in many heat pump systems. To model the stratification, detailed information about the tank construction is required such as the location of the connections to the tank. Regarding control, the location of the temperature sensors inside the tank is also important.

(b) On the contrary*, the tank may be idealized in order to maximize stratification.* In this idealized framework, the physical heights of the tank connections vary continuously depending on the temperature to be supplied. The height of the connections to the tank do not need to be known.

A *realistic tank model* should be used for detailed analysis of DR measures. Here, a *realistic tank model* means that the tank connections are at fixed heights, where the exact height of connections has to be defined in the model. In addition, a reasonable number of horizontal layers in the tank should be chosen to account for stratification inside the tank. Furthermore, the location of temperature sensors inside the tank for controlling the heat pump operation also has to be defined. Manufacturers of water tanks usually provide a detailed technical description of their products.

(4) *DHW prioritization over SH is not considered.* Heat pumps usually prioritize DHW production. Detailed knowledge of this control is required for realistic modeling of the operation of the heat pump and auxiliary heaters. DHW prioritization has been considered in some studies, e.g. [9] and [10].

(5) *There is no temperature limit for the condenser and evaporator temperatures.* Heat pumps have a maximum supply temperature which should be considered as well as a minimum temperature at the evaporator side. In addition, *defrosting cycles* of air-source heat pumps are usually not taken into account in a consistent way.

(6) The *control strategy of the auxiliary heater(s) is idealized*. It is sometimes assumed that auxiliary heaters exactly compensate for the lack of power from the base load to meet the heating needs. In reality, the control of auxiliary heaters is not perfect. In addition, the heating required for the legionella protection may involve the auxiliary heater (due to the maximum temperature limit of the heat pump).

(7) The *heat pump model only considers steady-state operation at full load measured during standard rating conditions according to EN 14511*. The influence of cycling losses (meaning transient losses) or the change of the coefficient of performance (COP) at part load are not considered even though these are key phenomena as explained in Section 2. In general, performance data during part load operation are often not communicated by heat pump manufacturers [3].

Ideally, knowledge about the short-time dynamics of heat pump systems is required when DR measures for heating are performed to study the energy flexibility potential of these systems. These short-time dynamics depend to a great extent on the tuning of the heat pump controller, which usually is a proportional-integral (PI) controller. The controller tuning is often overlooked in studies regarding DR and energy flexibility using BPS and cannot be captured in detail by strongly simplified models for heat pump systems. Regarding these DR applications, the specific level of modeling complexity of the heat pump (system) control has not yet been addressed in the literature. In this paper, *modeling complexity* of the heat pump system refers to the models for the water storage tank, the heat pump control, the auxiliary heater control and the heat pump system control. The required modeling complexity of a heat pump system depends on the objectives of the respective study. For example, simplified models may be sufficient to analyze the annual energy use whereas a more detailed model of the heat pump system is required if the detailed operating conditions of the heat pump system are of interest. Madani et al. [11] address the question of the required model complexity for complex heat pump systems. Their aim is to find

the minimum level of detail to capture the behavior of the heat pump system with satisfactory accuracy. As shown in Figure 1, they suggest a roadmap to select the necessary level of model complexity for a given type of analysis considering both the heat pump unit and the heat sources or sinks. The current work focuses on Zone D in Figure 1 where both a detailed modeling of the heat pump system and the heat sinks are required. As a detailed building model is needed, BPS packages, such as IDA ICE or TRNSYS, are assumed to be used as simulation environment.

Table 1. Typical model simplifications for heat pump systems to perform demand response using rule-based controls.

Reference	Control aim	Heat pump	Water tank	Software tool
De Coninck et al. [12]	- Reducing non-renewable energy use	- Air-to-water - Based on performance maps - No minimum run time	- For DHW only - Calibrated and validated DHW tank model	Modelica
Dar et al. [13]	- Increasing PV self-consumption	- Air-to-water - Based on performance maps - No minimum run time	- For SH and DHW - 20 stratification layers	MATLAB
Esfehani et al. [14]	- Using surplus electricity generation from wind power	- Ground-source - On-off heat pump - Monovalent operation - No minimum run time	- For SH and DHW - 4 stratification layers	TRNSYS
Alimohammadisagvand et al. [15]	- Reducing operational costs	- Ground-source - Perfect modulation (0-100 %) - DHW prioritized over SH - No minimum run time	- For SH and DHW - 10 stratification layers - Model validated with measurement data	IDA ICE
Masy et al. [16]	- Reducing operational costs	- Air-to-water - Simplified empirical model - Calibrated on manufacturer data - No minimum run time	- Fully mixed	-
Georges et al. [17]	- Reducing operational costs	- Air-to-water - Based on performance maps - DHW prioritized over SH - On-off and modulating heat pump - No minimum run time	- Two separate tanks used for SH and DH - DHW tank: two-node model with homogeneous temperature in each zone - SH tank: fully mixed	-
Salpakari and Lund [18]	- Increasing PV self-consumption	- Ground-source - Perfect modulation (0-100 %) - No minimum run time	- Fully mixed	-
Psimopoulos et al. [19]	- Increasing PV self-consumption	- Exhaust air heat pump - Based on performance maps - Modulating heat pump	- Two separate tanks used for SH and DH - DHW tank (180 liters): 5 stratification layers - SH tank (25 liters): fully mixed	TRNSYS
Lizana et al. [9]	- Reducing operational costs - Reducing environmental footprint	- Air-to-water - Based on performance maps (use of correction functions to correct rated operation data to nominal conditions)	- For DHW only (200 liters) - 3 stratification layers	TRNSYS

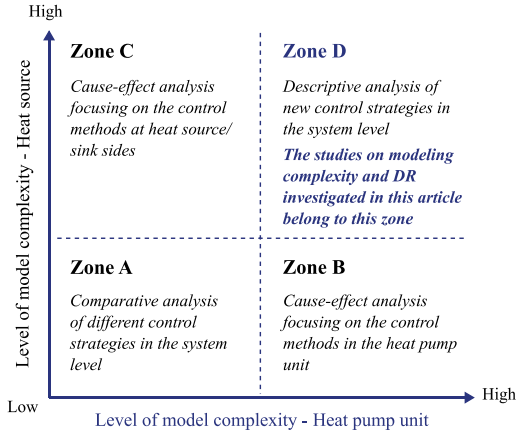

Figure 1. Roadmap for required model complexity depending on the type of study (adapted from [11]): the work carried out in the current paper is in Zone D.

1.2 Physical characteristics of heat pumps

The responsiveness of the heat pump to an external penalty signal for DR influences the short-time behavior of the heat pump system. Therefore, it is essential to carefully consider the heat pump characteristics when developing the respective component models of the heat pump system and its control. The heat pump characteristics that are also of interest for studies of DR are described in the remainder of this section.

A vast number of studies focus on the design and operation of heat pump systems in residential buildings. Specifically, many studies compare the energy performance of on-off heat pumps (OHP) and modulating/inverter-driven heat pumps (MHP), e.g. [11] [20] [21]. The run-time performance of heat pump systems depends on several conditions, such as the choice of heat pump system sizing (monovalent vs. bivalent), the heat distribution system, the thermal mass of the building and insulation level, ambient climate conditions, the occupant behavior, the choice and integration of thermal energy storages as well as the control to operate all the components of the heat pump system [11] [22].

The importance of heat pump sizing is addressed by several studies, e.g. [11] [21] [23]. Using a monovalent heat pump system, the heat pump is sized to fully cover the heating needs of the building, even for its nominal heating power evaluated for the design outdoor temperature (DOT). As cold outdoor temperatures similar to DOT do not occur frequently during a heating season, the heat pump behavior in part load should be considered carefully. In particular, the use of inverter-driven heat pumps offers the possibility to modulate the heat pump capacity to meet the heating loads of the building [21] during periods with higher outdoor temperatures (and thus lower SH demands in the building). As pointed out by Dongellini et al. [23] and Bettanini et al. [24], the seasonal performance of heat pumps depends strongly on their COP during part load operation. On the contrary, using a bivalent heat pump system, the heat pump covers the heating load above the so-called bivalent temperature. Below this temperature, auxiliary heaters support SH or DHW demands. Therefore, the heat pump is sized to only cover a fraction of the nominal heating power of the building. For on-off heat pumps that are sized to meet a high fraction of the nominal building power, this will eventually lead to shorter cycles so that the impact of losses due to frequent on-off cycling would be increased.

Cycling losses occur during the start-up of each cycle because the compressor has to re-establish the pressure difference between the evaporator and the condenser. The heating capacity of the heat pump unit is lower until steady-state conditions are reached [22]. Dongellini et al. [22] [23],

Bagarella et al. [20] and Uhlmann and Bertsch [25] investigate energy losses due to on-off cycling. Based on experimental data provided by a heat pump manufacturer, Dongellini et al. [22] reported that the steady-state condition for a small residential heat pump is reached after approximately 150 s and that the heating capacity of the heat pump unit is 42% lower during transient periods compared to steady-state conditions. Bagarella et al. [26] also found that steady-state condition was reached after 100 to 200 s and that the average COP during the start-up period was about 50% lower than during steady-state operation. They also found that cycling losses should not be neglected if an on-off heat pump is sized to cover a high fraction of the building nominal demand as this would lead to a high number of cycles throughout the year [20]. Uhlmann and Bertsch [25] performed field and laboratory measurements of the start-up and shut-down behavior of residential heat pumps. They concluded that the loss of efficiency is less than 2%, if a minimum heat pump run time of 15 min can be ensured.

Several studies found that the performance is improved for modulating heat pumps compared to on-off heat pumps [20] [22] [27]. For example, Madani et al. [28] investigate the operation of an on-off heat pump and a modulating heat pump system for a single-family residential building in Sweden. They found that there is no significant difference between the performance of the two heat pumps, if the on-off heat pump is sized to cover more than 65% of the peak heating demand of the building and if an electric auxiliary heater was used as a peak load system. In addition to cycling losses, this is due a second physical effect. Many modulating heat pumps have a higher COP at part load compared to nominal load. In Dongellini et al. [22], the COP is ~20% higher between 40 Hz and 60 Hz compared the nominal frequency of 120 Hz. For a same nominal frequency of 120 Hz, the minimum capacity is limited to 20-30 Hz according to Bagarella et al. [20]. Below this minimum frequency, the volumetric efficiency of the compressor decreases significantly as the lubrication cannot ensure a sufficient tightness against the return of the refrigerant to the suction.

Furthermore, a modulating heat pump is typically controlled by PI-control. The tuning of the two control parameters (i.e. the gain parameter k and integral time T_i) is important for the time response of the controller. A very reactive controller usually oscillates until it reaches the required compressor frequency that satisfies the heat load. If the heating load is too low and the amplitude of the oscillations is too high, the compressor frequency may drop below the minimum compressor frequency set by the manufacturer and thus the heat pump may be switched off to protect the compressor. Oscillations usually occur for high (proportional) gains k and low integral times T_i. If the controller is less reactive, it has less or even no oscillations and is thus more stable, but it takes more time for the heat pump to match the required heating load [20]. As an example, Dongellini et al. [22] use a PI-controller to modulate an inverter-driven heat pump where the parameters of the PI-controller are chosen according to manufacturer data: the values of the proportional gain k_p and the integral time T_i have been set equal to 10 and 300 s. If manufacturer data are not available, commonly used tuning rules for PID-controllers are Ziegler-Nichols [29] or Skogestad tuning rules (SIMC) [30]. On top of the PI-controller tuning, an anti-windup control should be established.

1.3 Main contribution of the study

This paper addresses two questions. Firstly, it investigates the model complexity of the heat pump system control required to study the behavior of heat pump systems in detail, with a special focus on DR. Secondly, the paper documents generically how to implement temperature-based control of heat pump systems into a BPS tool in order to investigate DR. An overview of the main contributions of this paper is given in Figure 2.

As this paper deals with detailed modeling, different model complexities should be compared using a specific case study where the technical specifications of all the components and their

interconnections are known in detail. As a case study, the heating of a detached house using an air-to-water heat pump (ASHP) is simulated in IDA ICE. Although the layout of an HVAC system can differ from building to building, the presented approach and conclusions remain generic. In this work, the heat pump modulates continuously between 30% and 100% of its nominal compressor capacity using a PI control. A minimum modulation of 30% is chosen as it is a typical lower modulation capability of heat pump compressors, e.g for the Hoval Belaria SRM 4 heat pump [31]. Below 30%, the heat pump cycles on-off. Minimum run and pause times have been implemented to prevent too frequent heat pump cycles. In addition, a realistic prioritization of DHW heating over SH is implemented so that the heat pump cannot support SH when producing DHW. All these three actions require supplementing an anti-windup to the PI control (to prevent the saturation of the integral action). To the authors` knowledge, the proposed level of modeling complexity with detailed models for the building and the heat pump system is hardly found in other studies of DR. The models taken for the different components of the heat pump system are not always the most sophisticated. For instance, the model for the heat pump unit is steady-state. However, the interaction between these components is comprehensive.

It is worth mentioning that most of the commercial BPS tools do not propose this level of modeling complexity in their default library of heating systems. In other words, the modeling complexity can be investigated using these tools but this requires the user to create the system based on the available library of components, including the control. This implementation is time-consuming and error-prone. However, comprehensive descriptions of detailed models for heat pump systems and their control are not often available in the literature. Therefore, this paper documents the implementation of a heat pump system in BPS tools. In addition, this description makes the interpretation of our simulation results transparent. In order to be generic and not specific to IDA ICE, the control logic (or algorithm) is defined as pseudo-codes.

Using the proposed comprehensive model of a heat pump system, the influence of the modeling complexity is investigated for two key components that are overlooked in the literature. Firstly, the controller for the heat pump unit is analyzed. Secondly, the influence of the DHW prioritization on the auxiliary heater operation is analyzed when DR measures are applied. This paper demonstrates that the model complexity affects the short-time behavior of a heat pump system when performing DR. Furthermore, it is recommended to consider controller tuning for studies of heat pump systems with focus on DR regardless of the applied control strategies, e.g. PRBC or model-predictive control.

The heat pump controller model is progressively simplified to evaluate the influence of the modeling assumptions on some main key performance indicators (KPIs). Typically, these KPIs are the energy use of the heat pump, the yearly-averaged tank temperatures, seasonal performance factor (SCOP), the number of heat pump cycles per year, average heat pump run time, and the short-time dynamics of the compressor (i.e. with a 3-minute time step). To investigate the influence of the controller complexity, six different cases are compared: (1) an MHP with a tuned PI-controller, (2) an MHP with a PI-controller with a higher integral time (relative to the tuned integral time), (3) an MHP with a proportional (P-) controller, (4) an OHP, (5) an MHP without a minimum run time and (6) an MHP modulating continuously from 0% and 100%. The main reason to specifically focus on the heat pump controller is that these six investigated controls lead to very different levels of modeling complexity, and thus model development time and tuning. In addition, these scenarios are common approximations in existing studies on DR and building energy flexibility.

The remainder of the paper is structured as followed. Section 2 documents the detailed implementation of the temperature-controlled heat pump system into BPS tools. It also presents how price-based DR control using PRBC can be implemented. Section 3 presents the results and shows the influence of the heat pump controller and its modeling complexity on different KPIs.

Furthermore, it illustrates how the influence of the DHW prioritization becomes critical when DR controls are introduced. The implementation of the control logics in Section 2 and the presented study in Section 3 are coupled (see also Figure 2). The conclusions are presented in Section 4.

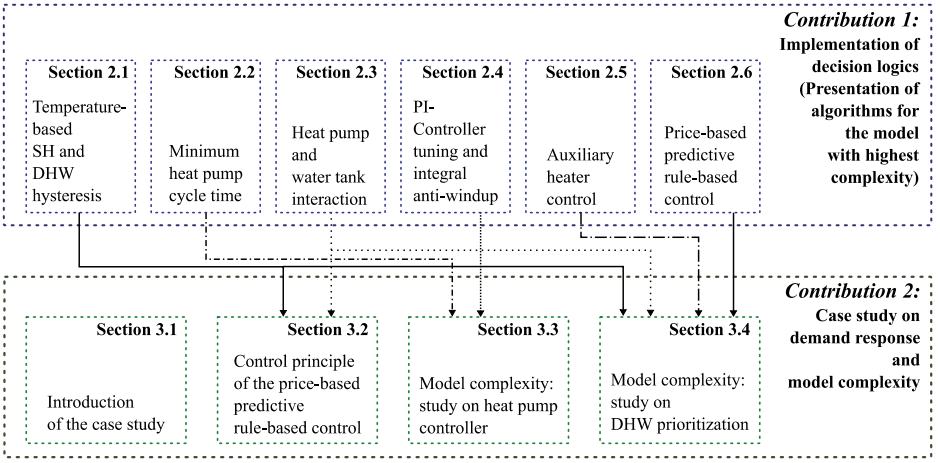

Figure 2. Overview and coherence of the main contributions.

2 Implementation of a detailed heat pump system model

This section provides a detailed description of a temperature-based control of a heat pump system. The presented control logic is generic and can be implemented in other BPS software tools. However, in the case of this paper the BPS software IDA ICE is used. The overall control logic is divided into modules that are presented in form of pseudo-codes in the different sections. The combination of all the algorithms that creates the overall control is illustrated in Figure 6.

The parameters of the realistic tank model are based on the EPTRC 400 water tank [32]. The tank is divided into ten horizontal layers, where the lower six layers represent the SH tank, and the upper four layers the DHW tank respectively. Even though the tank is modeled as one unit, it behaves like two physically-separated tanks. Four temperature sensors, two in the DHW tank and two in the SH tank, control the tank charging. Different possibilities for the integration of a water tank into a system exist, such as four-pipe, two-pipe, serial and parallel connections [33], but not all of these are considered in this paper. The configuration of the energy system is illustrated in Figure 3, where it can be seen that the SH tank has a four-pipe connection.

In general, two different strategies can be applied to a heat pump in order to load a storage tank. The circulation pump (CP) that circulates water between the generator and the tank can have a constant mass flow. The compressor power of the heat pump is then controlled according to the needs of the tank. This is typically done using a PI-control for a modulating heat pump. Alternatively, the compressor power of the heat pump can be kept at full load while the mass flow of the CP is controlled according to the needs of the tank. In our case study, the compressor power is controlled using a PI in SH mode while the CP mass flow is controlled using P-control in DHW mode. The mass flow is controlled so that the heat pump heats up water at the DHW temperature.

To investigate DR measures, temperature-based controls for the heat pump as well as the auxiliary heaters are implemented. Both the thermal storage in the thermal mass of the building and the hot water storage tank are used for DR.

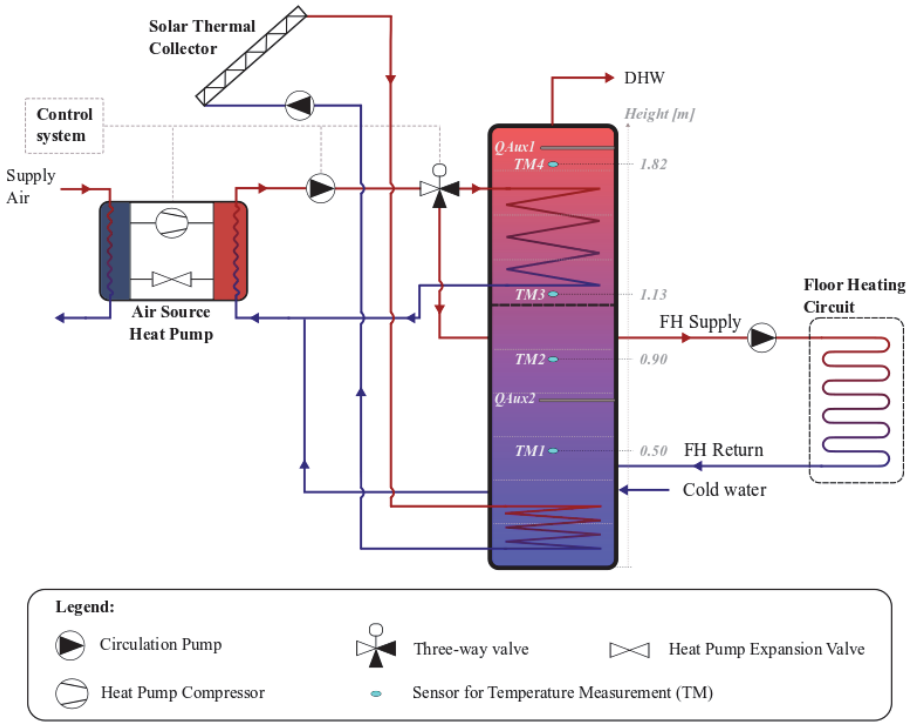

Figure 3. Configuration of the energy system in a residential building (adapted from [34]).

2.1 Tank: detecting DHW heating and SH requirements

As a starting point, the control should check whether the DHW and SH tanks require heating. In principle, the hysteresis for DHW heating and SH works as follows:

- As soon as the temperature in the upper layer of the respective tank part (DHW or SH) drops below a certain temperature set-point (TSP), the tank heating is started.
- The tank heating keeps working until the TSP of the sensor in the lower part of the respective tank is reached.

Algorithm 1 shows the pseudo-code to detect the need for DHW heating. This is based on an hysteresis function using the start and stop temperatures, $T_{start,DHW}$ and $T_{stop,DHW}$. The $T_{start,\ DHW}$ and $T_{stop,\ DHW}$ can be varied by the DR control, see Algorithm 7 in Section 2.6. However, unlike a standard hysteresis, the control is based on two measured temperatures. Therefore, the measurements from the temperature sensors in the water tank, TM3 and TM4, are compared to their respective set-points using a *Comparator* to determine if start or stop conditions have been reached. This signal then enters the hysteresis component. If the heat pump is in the DHW heating mode and the hysteresis input is a stop, the DHW heating should stop. If the heat pump is not in DHW heating and the hysteresis input is a start, the DHW heating should start. Otherwise, the DHW mode signal is unchanged.

Algorithm 1. Pseudo-code for the implementation of a DHW hysteresis.

Algorithm 1: Detect the need for DHW heating

```
% Comparator lower part of DHW tank
Input Hysteresis = 1
if (TM3 > T_stop, DHW)
    Input Hysteresis = 0
end
% Comparator upper part of DHW tank
if (TM4 < T_start, DHW)
    Input Hysteresis = 2
end
% Hysteresis component with DHW Signal in memory and output:
if (DHW Signal = true) & (Input Hysteresis <=0)
    DHW Signal = false % DHW mode off
end
if (DHW Signal = false) & (Input Hysteresis >= 2)
    DHW Signal = true % DHW mode on
end
% Algorithm output is DHW Signal
```

The pseudo-code for the SH hysteresis is illustrated in Algorithm 2. The logic of the SH hysteresis is similar to the DHW hysteresis. Here, the measured temperatures TM1 and TM2, are compared to the set-points $T_{stop,SH}$ and $T_{start,SH}$. These two set-points depend on the outdoor temperature compensation curve (OTCC) of the heat distribution system. To provide enough heat storage even during milder outdoor temperatures, $T_{start,SH}$ is set to OTCC while $T_{stop,SH}$ is set to OTCC + a differential ΔT, here taken at 8K. This last measure prevents too frequent cycling of the heat pump but this large temperature differential generates a loss of energy efficiency. Again, $T_{start,SH}$ and $T_{stop,SH}$ can depend on price signals because of DR measures. The *SH Signal* is the output from Algorithm 2.

Algorithm 2. Pseudo-code for the implementation of a SH hysteresis.

Algorithm 2: Detect the need for SH

```
% Comparator lower part of SH tank
Input Hysteresis = 1
if (TM1 > T_stop,SH)
    Input Hysteresis = 0
end
% Comparator upper part of SH tank
if (TM2 < T_start,SH)
    Input Hysteresis = 2
end
% Hysteresis component with SH Signal in memory and output:
if (SH Signal = true) & (Input Hysteresis <=0)
    SH Signal = false % SH mode off
end
if (SH Signal = false) & (Input Hysteresis >= 2)
    SH Signal = true % SH mode on
end
% Algorithm output is SH Signal
```

2.2 Heat pump: minimum heat pump cycle time

The pseudo-code for the determination of the minimum heat pump run and pause time is presented in Algorithm 3. The *minimum HP cycle time* is implemented via a timer component.

If the duration of a heat pump cycle is above the minimum run time, the SH and DHW signals of Algorithms 1 and 2 are left unchanged. If the minimum run time has not been reached and no more heating is required according to Algorithms 1 and 2, the heating is forced to continue by changing the SH signal from 0 to 1. The temperature in the SH tank will then exceed the stop temperature, $T_{stop,SH,}$ and keep increasing until the minimum run time is reached. As it will be explained in Section 2.4, the minimum modulation capability of the heat pump is modeled by a saturation of the PI-control output (here taken at 0.3). During this period where the heat pump is forced to continue, the heat pump will therefore be operated at this minimum modulation capability.

Algorithm 3. Considering the requirement of a minimum heat pump run and pause time.

Algorithm 3: Minimum heat pump run and pause time

```
% Timer component integrates the run/stop time
Input Timer = (DHW signal or SH signal)
% Heat pump run time requirement considered in Output Timer
% SH Signal overridden if run time too short
if HP run time < minimum HP cycle time
    if (DHW Signal = 0) or (SH Signal = 0)
        SH Signal = 1
    end
end
% Algorithm output is SH and DHW Signal
```

A minimum run time could also be achieved by sizing the heat pump system considering the volume of water in the tank that has to be heated as well as the choice of the differential between the start and stop temperatures for both SH and DHW hysteresis. For some heat pumps, the start and stop temperatures are replaced by a control based on degrees-minutes. The control error for the temperature is integrated over time and the heat pump is started or stopped if this integral exceeds some thresholds.

2.3 Heat pump and tank interaction

Once the need for SH or DHW heating has been detected (see Section 2.1), the control should prioritize these two needs and control the heat pump accordingly. In this work, a realistic prioritization of DHW heating over SH is implemented so that the heat pump cannot support SH when producing DHW.

Regarding the charging of the tank, if the heat pump is in DHW mode, the mass flow through the condenser is adapted by a proportional control (P-control) to control the condenser outlet temperature to a given TSP. The heat pump compressor is then operated at full load. This TSP is set to a slightly higher temperature than the $T_{stop,DHW}$ of the DHW tank (here taken 5K higher). This ensures that the heat pump supply temperature is always sufficient for DHW heating. If the heat pump is in SH mode, the mass flow through the condenser is kept constant and the compressor power is adapted using a PI-control and the SH temperature set-point from the tank, $T_{start,SH}$. The pseudo-code is shown in Algorithm 4.

Algorithm 4. Pseudo-code of the heat pump and tank interaction.

Algorithm 4: Heat pump and tank interaction

```
% DHW prioritization and charging the tank
if DHW Signal = 1 (prioritization)
    % heat pump in DHW mode
    TSP = T_stop,DHW + 5K
    CP_DHW = P-control of mass flow comparing HP outlet temperature to TSP
    CP_SH = 0.0
    HP control = 1.0
else
    if SH Signal = 1
        % heat pump in SH mode
        TSP = T_start_SH
        CP_SH = 1.0
        CP_DHW = 0.0
        HP control = PI-control comparing TSP to TM2
    else % no heating mode
        CP_SH = 0
        CP_DHW = 0
        HP control = 0.0
    end
end
```

2.4 Heat pump: PI modulation and anti-windup control

The PI-control is implemented here using a PID where the derivative action is set to zero. This does not limit the scope of these explanations. A flow chart of a typical PID-controller is presented in Figure 4. A heat pump modulation between 30% and 100% is implemented by a limiter component placed right after the output of the PI-control and with a lower limit of 0.3 and an upper limit of 1.0. The implementations of (1) a heat pump modulation limited between 30% and 100%, (2) a prioritization of DHW over SH (Algorithm 4) as well as (3) a minimum run time (Algorithm 3) require supplementing an anti-windup to the PI control. These actions can lead to the tank temperature TM2 deviating from its TSP over a relatively long period of time which can saturate the integral action.

The integral anti-windup ensures that the control error (i.e. temperature difference between TM2 and the TSP) is not integrated when one of the three above actions prevents the TSP from being continuously tracked by the PI-controller. Firstly, a standard anti-windup is directly embedded inside the PI-control to take the effect of the saturation into account, see the dotted green box in Figure 4. In our implementation in IDA ICE, this is done using the *LimPID* component from the IDA ICE component library, combining a PID-controller with limited output and an anti-windup compensation. The *LimPID* component works similar to the PI-controller presented in Figure 4. The default PI-controller in the IDA ICE thermal plant does not have integral anti-windup. The *LimPID* should therefore replace the default PI-controller. The *LimPID* component is not adapted here but the input should be adjusted to account for the "reset". The *LimPID* compares the PI output signal before and after the saturation (i.e. the *limiter* in Figure 4). The difference between both signals is used to adapt the control error at the input of the integral action and thus limit its saturation. Secondly, the PI-controller should be reset every time the controller is not used. The reset aims to keep the PI-controller input close to 0. In other words, if not reset, the PI-controller would try to take action to keep the measurement signal (here TM2) close to the TSP even though the PI-controller output is not used anymore. This happens if the heat pump is either heating DHW (i.e. *DHW Signal* is 1) or if no SH is required according to Algorithm 2 (i.e. *SH Signal* is 0). Algorithm 5 shows the pseudo-code for the logic of a PI-controller reset.

As mentioned in Section 1.2, the gain parameter k and integral time T_i are usually not given by heat pump manufacturers. Among existing PI tuning rules, Skogestad`s method [30] can be applied to adjust the gain parameter k and the integral time T_i. SIMC tuning rules rely on one tuning parameter, τ_c. A small τ_c leads to a fast response (more oscillations) and a large τ_c leads to a slower response (less or no oscillations). The tuning is case-dependent and thus k and T_i differ for each system.

Algorithm 5. Pseudo-code for the reset of the PI-controller.

Algorithm 5: PI-controller anti-windup and reset

```
if SH Signal is 1
    Standard use of the limited PI-control with embedded anti-windup
else
    % SH Signal is 0 or DHW Signal is 1
    Control error at the input of the PI control forced to 0
end
```

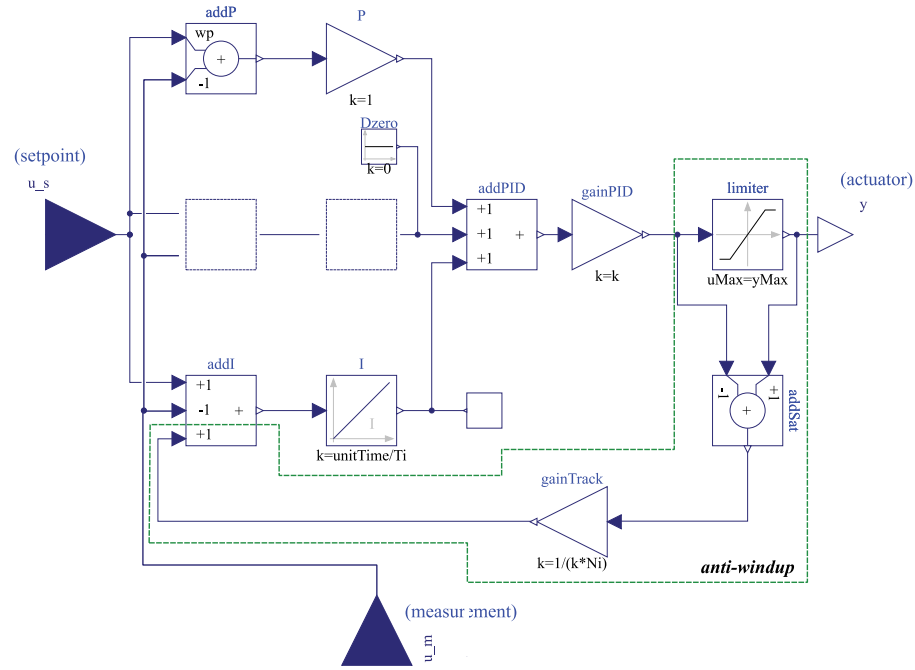

Figure 4. Flow chart of the PI-controller with integral anti-windup control (which is marked in the green box) [35].

2.5 Tank: control of the auxiliary heaters

The pseudo-code for the control of the auxiliary heater in the SH tank is presented in Algorithm 6. The auxiliary heater is controlled by a thermostat, which has a differential of 4K in this study. The start temperature of this thermostat, $T_{start,aux}$, is related to the $T_{start,SH}$ of the heat pump, which can change if DR measures are applied. Generally, $T_{start,aux}$ is taken slightly lower than the $T_{start,SH}$ (here 3K lower) so that the auxiliary heater only starts to operate if the heat pump cannot cover the SH demand. However, using this control strategy, the auxiliary heater may start when the heat pump is heating DHW (and thus cannot heat the SH tank).

Regarding DR measures, the $T_{start,aux}$ is kept at its reference set-point even though the heat pump set-point $T_{start,SH}$ might be increased. The $T_{start,aux}$ is decreased if the $T_{start,SH}$ is decreased.

Algorithm 6. Pseudo-code for the implementation of the control for the electric auxiliary heater in the SH tank.

Algorithm 6: Auxiliary heater control

```
% TM2 as measurement input to thermostat of auxiliary heater
if (SH Signal = 1)
    if (DHW Signal = 1)
        % SH Signal is 1 and DHW Signal is 1
        T_start,aux = T_start,SH
    else
        % SH Signal is 1 and DHW Signal is 0
        if (no DR)
        T_start,aux = T_start,SH − ΔT % here, ΔT = 3 K (in the case of no DR)
        if (DR)
        T_start,aux = T_start,SH − ΔT % here, ΔT = 3 K (for reference and low TSPs (see Section 3.6))
    end
end
```

2.6 Price-based demand response measures

Thermal energy can be stored in the building using time-variable TSPs for heating. For indirect DR measures, these TSPs are adapted as a function of a penalty signal such as a time-varying electricity price or the dynamic $CO_{2eq.}$ intensity of the electricity mix [36] [37]. For the sake of the clarity, this paper only reports a price-based control using the day-ahead electricity spot price (SP). However, the conclusions of this paper remain valid using other types of penalty signal or even using direct controls.

With PRBC, a typical way to create a control signal to perform DR is to divide the spot price time profile into three price segments as shown in Figure 5. A similar approach has been reported in [17] and [9]. In this work, the PRBC makes use of a 24h sliding horizon to determine a low-price threshold (LPT) and a high-price threshold (HPT) which are used to define the three price segments of low, moderate and high prices. The LPT has been selected to SP_{min} + 0.3 (SP_{max}-SP_{min}) and the HPT to SP_{min} + 0.75 (SP_{max}-SP_{min}), where SP_{max} and SP_{min} are taken as the maximum and minimum spot prices for the next 24h. 30% and 75% have been chosen for the thresholds based on a sensitivity analysis evaluating the influence of the LPTs and HPTs on the control signal in terms of the number of hours per set-point segment [34]. The PRBC compares the spot price to the HPT and LPT at each hour of the day and adjusts the TSPs for both DHW and SH accordingly.

The following control rules and the choice of thresholds are not trivial and based on the user experience. This tuning of a PRBC may be time consuming as reported in [7]. Algorithm 7 illustrates the pseudo-code for the PRBC logic of a price-based TSP variation. The same logic is applied for DHW heating and SH. Figure 5 illustrates this principle of the determination of the price-based control signal. TSPs are increased to a higher temperature set-point (HTSP) for pre-loading before periods of high prices. Therefore, the HTSP is used if the current spot price is between the LPT and HPT and if it will increase during the next 2 hours. On the contrary, the TSPs are decreased to a lower temperature set-point (LTSP) if the current spot price is above the LPT and is decreasing or, alternatively, during period of high prices, meaning if the spot price is above the HPT. The reference temperature set-point (RTSP) is kept for low-price periods, i.e. spot prices below the LPT.

TSP for SH can be applied to the SH storage tank ($T_{start,SH}$) and the room temperature ($T_{room,SH}$). This set-point for the room temperature is typically chosen based on the predicted mean vote (PMV) and predicted percentage dissatisfied (PPD) method. According to EN15251:2007 [38], a LTSP of 20 °C and HTSP of 24 °C for $T_{room,SH}$ corresponds to a PMV between -0.5 and +0.5 or a

PPD lower than 10%, assuming a residential building, a clothing factor of 1.0 clo and an activity level of 1.2 MET.

Algorithm 7. Pseudo-code for the implementation of a price-based temperature set-point variation.

Algorithm 7: Price-based temperature set-point variation (same routine for SH and DHW)

```
% RTSP:
    for DHW: RTSP = 50 °C
    for SH tank: RTSP = OTCC
    For SH room: RTSP = 21°C
% LTSP:
    for DHW: LTSP = RTSP – 5°C
    for SH tank: LTSP = RTSP – 1°C
    for SH room: LTSP = 20°C
% HTSP:
    for DHW: HTSP = RTSP + 10°C
    for SH tank: HTSP = RTSP + 3°C
    for SH room: HTSP = 24°C
% Price-based temperature set-point variation:
    if (LPT < SP < HPT) & (SP increases during the next 2 hours)
        T_start,SH, T_room,SH and T_start,DHW = HTSP
    else
        if (SP > HPT) or ((SP > LPT) & SP decreases during next 2 hours)
            T_start,SH, T_room,SH and T_start,DHW = LTSP
        else
            if (SP < LPT)
                T_start,SH, T_room,SH and T_start,DHW = RTSP
        end
    end
% Algorithm output is TSP
```

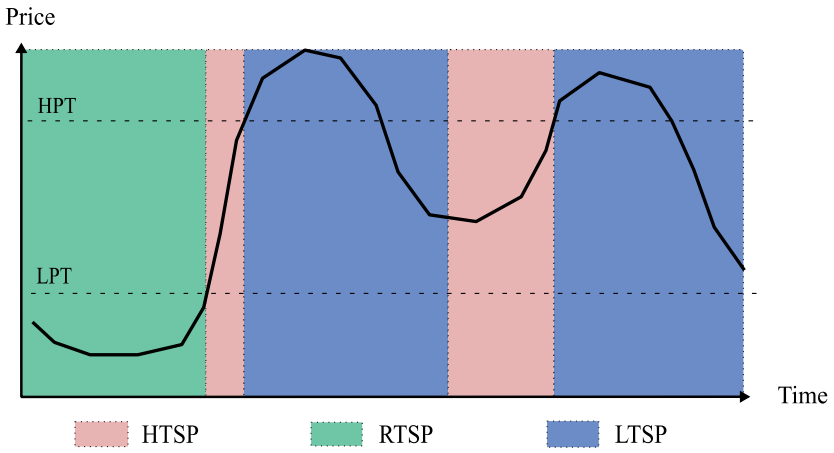

Figure 5. Principle of the determination of the price-based control signal (HTSP is high temperature set-point, RTSP is reference temperature set-point, LTSP is low temperature set-point).

As shown in the principle sketch in Figure 6, the algorithms are combined together to form the overall control of the heat pump system. The algorithms have been presented in a generic form that does not depend on a specific heat pump system or BPS software. However, the combination of these algorithms will always be case-specific. For instance, the combination of algorithms here follows the system layout of Figure 3.

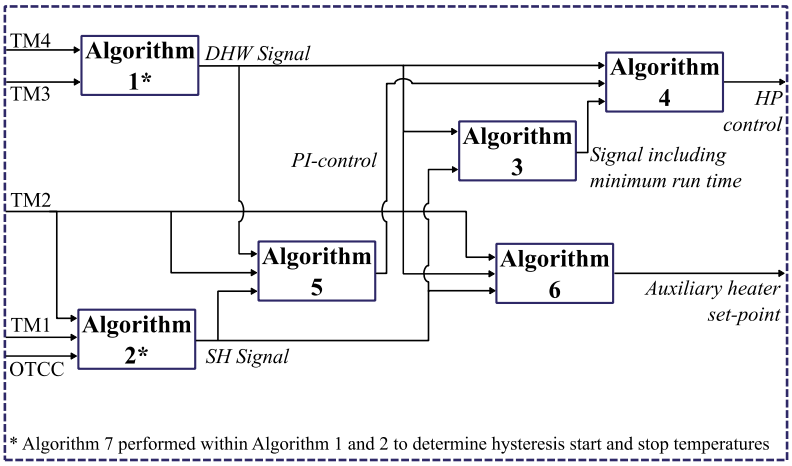

Figure 6. Simplified sketch of the algorithm combination for the heat pump system control.

3 Case study on demand response and model complexity

A case study of a building heated by either an MHP, an OHP or direct electric (DE) heating is simulated in IDA ICE using the previously described algorithms. To illustrate the control principle of the price-based PRBC, the results for the case with an MHP are shown in Section 3.2. The influence of the modeling complexity of the heat pump control on chosen KPIs is presented in Section 3.3, while Section 3.4 focuses on the DHW prioritization of the heat pump.

3.1 Description of the case study

DR measures have been investigated for the case of a Norwegian detached single-family house with a heated floor area of 105 m^2. The building is located in Trondheim, Norway. As shown in Figure *7*, it has two bedrooms, one bathroom and two living rooms [39]. It is a zero-emission residential building (ZEB) with a lightweight timber construction. The electricity generation from on-site photovoltaic (PV) is designed to compensate for embodied emissions as well as emissions from the operational phase during the lifetime of the building [39]. The IDA ICE model of the building envelope, which is used in this paper, has been calibrated using dedicated experiments. During these experiments, the building was excited using a specified pre-defined heating sequence with sub-hourly resolution and the air temperatures and operative temperatures were measured as a response to this excitation [40]. The short-term dynamics of the building were predicted correctly by the model.

Internal heat gains from occupants, electrical appliances and lighting are chosen according to the Norwegian technical standard SN/TS 3031:2016 [41]. Schedules for lighting and occupancy are based on prEN16798-1 and ISO/FDIS 17772-1 standards whereas the schedule for electrical appliances is taken from SN/TS 3031:2016. Also the DHW consumption profile is based on SN/TS 3031:2016. All schedules have hourly resolution. Additional information is provided in [34].

The modeled heat pump is based on the Hoval Belaria SRM 4 [31] which has a nominal capacity (with standard test conditions A7/W35) of 5.1 kW and a COP of 4.57 using EN 14511. The parameters of the heat pump model are calibrated with the manufacturer data based on the calibration procedure explained in [42]. The heat pump is dimensioned as a bivalent/mono-energetic system with a bivalence outdoor temperature of -9 °C. The heat pump is able to operate continuously using power modulation for outdoor temperatures of up to 5 °C. This temperature

range (i.e. -9 °C to 5 °C) represents most of the SH season in Trondheim. Furthermore, a heat pump supply temperature of 65 °C can be achieved with this kind of state-of-the-art heat pump technology, e.g. [43]. In accordance with common concepts of Norwegian ZEBs, a solar thermal collector (4 m^2) assists the heat pump to provide DHW heating and SH [44].

It should be mentioned that IDA ICE has a steady-state grey-box heat pump model which is explained in detail in [42]. In this framework, it is impossible to take cycling losses into account, and neither the increase of the COP at part load for the modulating heat pump. Our investigations of the OHP and MHP exclude these phenomena even though they would be important if the objective of the paper was to compare both technologies. However, this does not impact the conclusions of this work about the modeling complexity of the heat pump controller. In addition, these cycling losses and variations of COP at part load can be integrated in other BPS tools, such as TRNSYS [22] while these properties are currently not available in the current IDA ICE heat pump model.

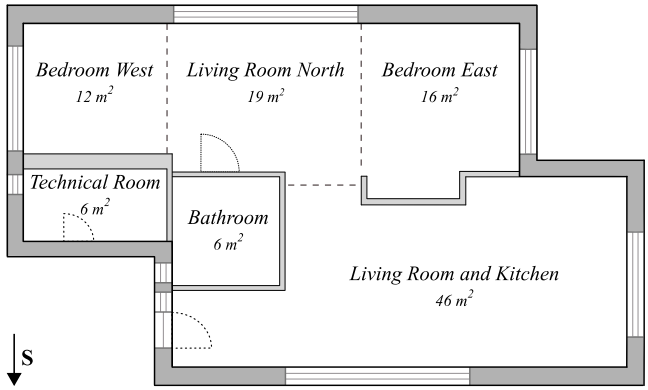

Figure 7. Floor plan of the case study building [34].

Regarding load shifting, peak periods are defined to be between 7 a.m. and 10 a.m. as well as between 5 p.m. and 8 p.m. based on a typical hourly profile for the electricity use in Norwegian households [45]. Pre-peak and after-peak hours are defined as the three hours before and two hours after a peak period, respectively. The analysis is performed using the historical measurements of 2015 for electricity prices and weather data so that their correlation is taken into account. Weather data are taken from [46] and spot prices are available at [47].

3.2 Control principle of a price-based PRBC for demand response

Simulations show that a realistic operation of the MHP system can be reached. Results presented in Figure 8 illustrate the working principle of the control. It is evident from Figure 8 that DHW heating is prioritized over SH because the TSPs for DHW heating are increased as soon as the spot price signal allows it (Figure 8 (b)). The SH-related TSPs are increased after the DHW tank has been charged (Figure 8 (c)), for example, as in the early afternoon of 19 February.

In general, the heat pump modulates to keep TM2 close to the $T_{start,SH}$. This principle can be seen in Figure 8 (d) and (e) from midnight to 10 a.m. on 19 February. The heat pump modulates down to 30% of the nominal compressor capacity if the heating demand in the rooms is low and the temperatures in the SH tank are sufficiently high. When no more SH is required in the rooms, the compressor continues to operate until the stop criteria of the SH hysteresis, $T_{stop,SH}$, is reached. In this way, the SH tank is charged as well. Regarding the operation of the electric auxiliary heaters, Figure 8 (b), (d) and (e) show that the SH tank cools down when DHW heating is prioritized as warm water is continuously supplied to the floor heating system. This temperature decrease

eventually leads the electric back-up heater in the SH tank to start operating. This happens in the morning of 20 February.

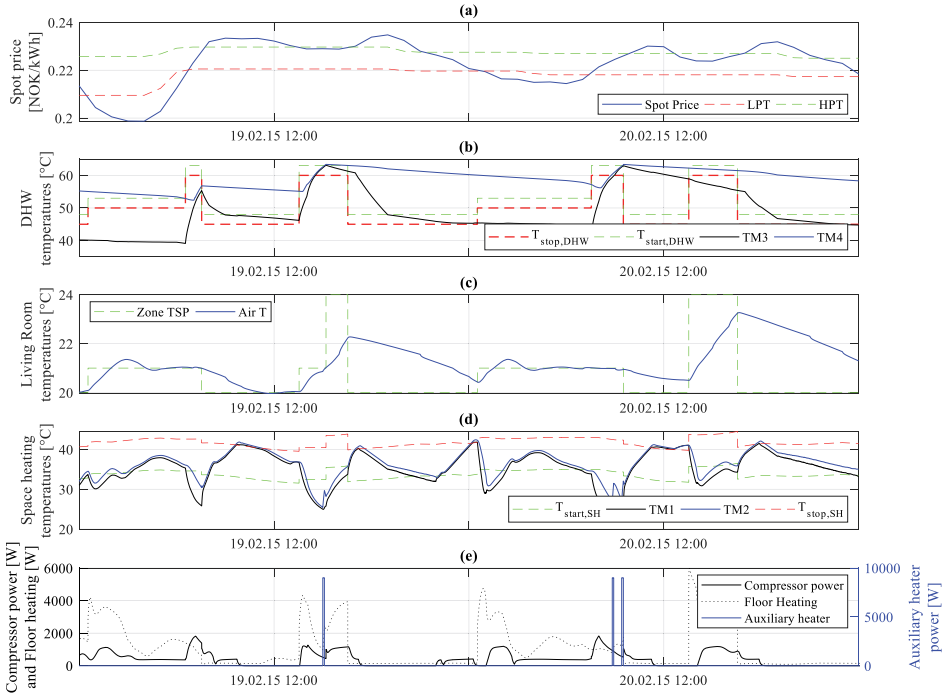

Figure 8. Control principle of a price-based control for the MHP during an exemplified period of two days [34].

3.3 Modeling complexity: the heat pump control

This section investigates the control of the heat pump unit and how its modeling complexity influences some important KPIs: (1) energy-related KPIs, such as energy use for heating and the average tank temperature during the heating season and (2) KPIs related to the heat pump unit, such as the seasonal coefficient of performance (SCOP), the number of heat pump cycles per year and the average heat pump run time.

Six different cases are investigated: (1) an MHP with a tuned PI-controller (called MHP-PI-tuned), (2) an MHP with a PI-controller with a high integral time compared to the tuned integral time (called MHP-PI-highTi), (3) an MHP with a P-controller (called MHP-P), (4) an OHP, (5) an MHP as defined in case (1) but without a minimum run time (called MHP-noCT, with noCT meaning no cycling time) and (6) an MHP modulating between 0% and 100% (called MHP-PM, with PM meaning perfect modulation). If not mentioned, the cases include a minimum heat pump run time and a heat pump that is able to modulate between 30% and 100%. Table 2 presents the influence of these different heat pump controls on the chosen KPIs.

The electricity use for heating is rather similar for all studied cases, except for the perfect modulation (MHP-PM). The heat pump with a perfect modulation (MHP-PM) performs best whereas the OHP has the highest electricity use for heating. The MHPs with different P- or PI-controls have very similar electricity use for heating. Therefore, it can be concluded that the perfectly modulating heat pump idealizes the performance of the system and thus overestimates the potential for cost or emissions savings.

The tank temperatures for the SH and the DHW tanks are the average temperature of the uppermost two layers of each tank. These temperatures are averaged over the SH season which is assumed to be from 1 September to 15 May. Indeed, during summer time, only DHW heating is required so that all the investigated heat pumps behave in the same way, namely like an OHP. Regarding the DHW tank, the temperature differences in all the cases are within 1.1 K. The differences are small because DHW heating is always controlled by a hysteresis.

Regarding the SH tank, the maximum temperature difference between the studied cases is 4.5 K. The OHP has the highest average temperature in the SH tank because it charges the tank to higher temperatures for each cycle based on the hysteresis. For the MHP cases, the compressor speed is controlled to keep the temperature in the tank close to the $T_{start,SH}$. On average, this leads to a lower tank temperature during the heating season and thus to lower heat losses from the tank. Due to higher condenser temperatures and thermal losses from the tank, the OHP has the lowest SCOP. On the contrary, the MHP-PM the highest SCOP.

Table 2. Definition of the heat pump controls including their parameters as well as their influence on the chosen KPIs for an evaluation period of one year.

Case	**Controller parameters**		**E_{Use} [kWh]**		**Average tank temperature [°C]**		**No. of HP cycles [-]**	**Average HP run time [min]**	**SCOP**
	k [-]	T_i [s]	HP	Q_{Aux}	SH	DHW			
MHP-PI-tuned	0.1	300	2025	8	36.7	52.5	983	260	3.72
MHP-P	1	-	2028	9	36.8	52.6	808	322	3.73
MHP-PI-highTi	0.1	3300	2035	9	36.8	52.5	1059	239	3.69
OHP	-	-	2197	2	38.2	53.0	1988	59	3.41
MHP-noCT	0.1	300	2033	8	36.8	52.6	870	297	3.71
MHP-PM	0.1	300	1891	17	33.7	51.9	438	767	4.43

Even though the electricity use and average tank temperatures are relatively similar for all cases, there are significant differences for the number of cycles and the average run time of the heat pump. The OHP has approximately twice the number of cycles compared to the MHP with a tuned PI-controller. The average run time is lowest for the OHP while it increases with a decreasing number of heat pump cycles. This confirms the advantage of MHPs over OHPs. The number of cycles is influenced by the choice of control (i.e. P- or PI-control) and the tuning of the control parameters.

Figure 9 compares the output control signal to the heat pump for the P-control (MHP-P) and two PI-controls (MHP-PI-tuned and MHP-PI-highTi) for different time resolutions. The resolutions of 15 and 60 minutes are evaluated by averaging the original time series of 1 minute over the last 15 and 60 minutes, respectively. Generally, the output of the PI-controls is smoother than the P-control which can have sudden variations in the signal. If the aim is to achieve a smooth operation of the heat pump, a PI-controller should be preferred to a P-controller. As it can be seen in Figure 9 (a) between minutes 420 and 545, the tuned PI-control leads to larger oscillations. The PI-controller with a higher integral time has weaker oscillations. These differences are directly related to the PI tuning rules applied in this work. Regarding the SIMC tuning parameter, a τ_c could be chosen so that a P-controller and a PI-controller would give a very similar behavior. The large difference in output signals between the three controllers will lead to different electricity use in the short-term. These differences would be even larger if transient effects (such as cycling losses) were accounted for in the heat pump model. These differences between controllers almost disappear for a resolution time of 60 minutes. Actually, Figure 9 shows that the control signals for the P- and PI-controls are under-resolved above an averaging time of 15 minutes. Therefore, a time resolution lower than 15 minutes should be chosen if the aim is to investigate the dynamics of the heat pump in detail. The choice of controller is also important when power is investigated.

The maximum power required during a year is very similar for a P- and a PI-controller as a controller output signal of 1 leads to the heat pump operating at full load. However, for time intervals lower than 15 minutes, the controllers will lead to different electrical powers.

In summary, the most appropriate modeling complexity depends on the type of investigation. Is the focus solely on energy and operational costs or is the detailed behavior of the heat pump or power of interest? The KPIs in Table 2 show that a P-controller and a PI-controller can lead to similar results as long as the heat pump operation and power are not investigated for short time scales. A P-controller has the advantage of significantly simplifying the modeling setup. Its tuning is easier and the problem of integral windup avoided. On the contrary, if the heat pump operation is investigated for short time scales, the heat pump control and tuning cannot be simplified. To conclude, it is worth mentioning that the conclusions regarding the controller modeling and tuning are not only valid for PRBC. For instance, model predictive control (MPC) would also adapt the TSPs and not directly control the compressor power.

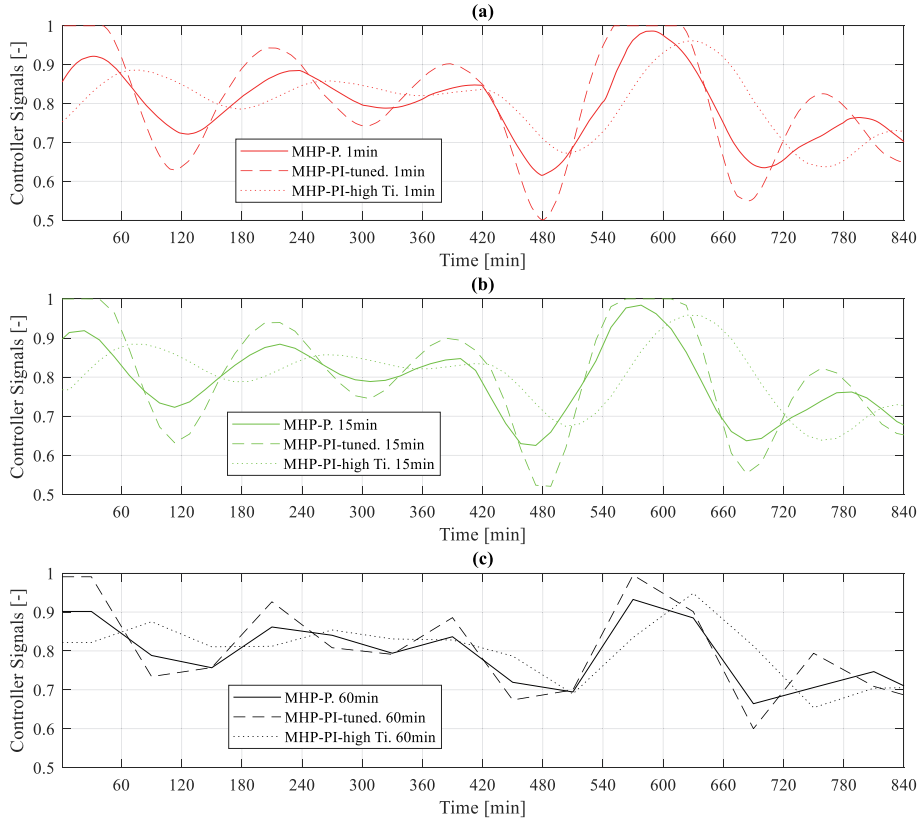

Figure 9. Comparison of P-controller and two PI-controller output signals to the heat pump for (a) time resolution of 1min, (b) 15 min and (c) 60 min during an exemplified period of 14h.

3.4 Modeling complexity: influence of DHW prioritization

As it will be shown, the DHW prioritization can strongly influence the auxiliary heater operation. This influence is more pronounced for the periods when DR events are performed and significantly impact the system performance such as the energy use for heating and energy costs. Therefore, this aspect should not be overlooked for bivalent heat pump systems. To demonstrate this, the price-based DR scenario (CSP), introduced in Section 2.6, is compared to a reference

case (called BAU for business-as-usual) where all the set-points are constantly at RTSP. However, it is distinguished whether the CSP is applied to both SH and DHW, to DHW only (then termed CSP-DHW) or to SH only (then termed CSP-SH).

3.4.1 Influence on energy use

The performance of the different control scenarios is compared in terms of annual electricity use for heating, see Figure 10 (b). The share of the heat pump and the auxiliary heaters in the electricity use is shown in order to emphasize the operation of auxiliary heaters. In addition, it is also worth comparing the CSP if applied to direct electric heating (DE). In this case, SH and DHW have two distinct systems so that no DHW prioritization is required. Finally, it is instructive to present results at shorter timescales, especially during periods where the price-based control applies sudden variations of the TSPs. In Norway, prices are higher during peak hours and a price-based control should adapt TSPs accordingly. Therefore, the electricity use for heating is analyzed for pre-peak, peak and after-peak periods, see Figure 10 (a).

Regarding DE heating, it can be seen in Figure 10 (a) that the CSP leads to reduced electricity use during peak periods, whereas the electricity use increases during pre-peak and after-peak periods. This conclusion does not hold for the MHP and OHP systems. Unlike DE, the electricity use for heating increases for all HP cases during peak hours. Given the DHW draw-off profiles, DHW heating is required during peak hours for all test cases. During the SH season, SH needs are usually present when DHW is produced by the heat pump. This leads to a temperature decrease in the SH tank that ultimately triggers the operation of the auxiliary heater. As the duration of DHW mode is prolonged by DR compared to BAU, the resulting increase in electricity use is larger when DR is applied to DHW. This confirms that the primary cause of increased electricity use for heating is the prioritization of DHW. This is especially true for the MHP but significantly less pronounced for the OHP. Unlike MHP, the OHP control is exclusively based on a hysteresis and thus, somehow, on a charging of the SH tank. Therefore, with OHP, the SH tank has a larger autonomy when the HP is in DHW mode before the SH auxiliary heater has to be triggered. The auxiliary heater is then used less frequently by the OHP compared to the MHP.

To further confirm these conclusions, Figure 10 (b) illustrates the annual electricity use for heating. When the CSP is applied, it leads to increased annual electricity use for heating compared to BAU. This is due to the energy storage in the water tanks or the building thermal mass at a temperature higher than in the BAU scenario. All these storages have thermal losses which may eventually lead to a decrease of the energy efficiency compared to the reference scenario. Nonetheless, a decrease in energy use is possible if the TSP for SH (here with a LTSP of 20 °C) is often below the RTSP (here 21 °C) using the DR scenarios. These conclusions will be further discussed in the next section but were needed here to explain the order of magnitude in Figure 10 (b). The share of electricity use from the auxiliary heater is most significant for CSP when DR is applied to both DHW and SH. If only applied to DHW, the auxiliary heater is still operated frequently. Even though DHW is prioritized in the CSP-SH case, the auxiliary heater does not contribute significantly to the electricity use for heating.

This case study is used to demonstrate the importance of the DHW prioritization in relation with the auxiliary heater control. However, the specific values for the energy use are case-dependent and should not be considered universal (unless further research proves that they are). For instance, the power sizing of the heat pump and the choice of system design (monovalent or bivalent) are essential. If the heat pump was oversized, the DHW tank would be charged faster thus reducing the risk of using the auxiliary heater for SH. Furthermore, it was possible to use additional set-points for DHW heating along lower electricity spot prices to operate the heat pump more frequently and to avoid a too frequent operation of the electric auxiliary heater.

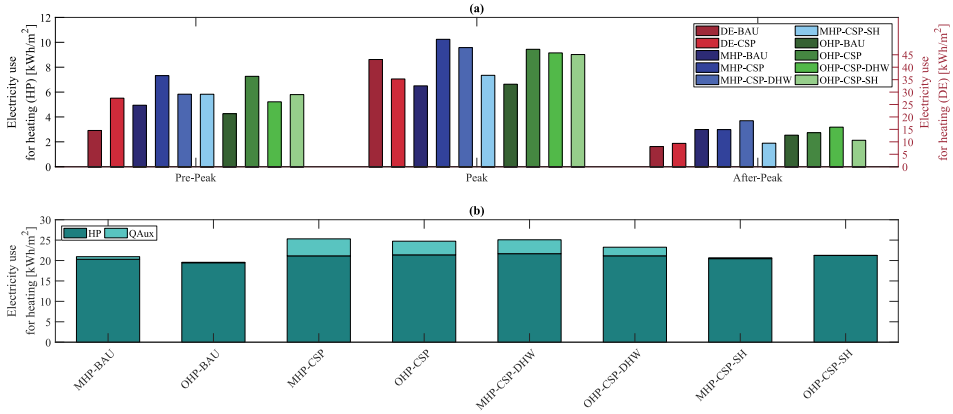

Figure 10. (a) Electricity use for heating using direct electric heating (DE) (right axis), a modulating heat pump (MHP) and an on-off heat pump (OHP) (both left axis) and (b) annual electricity use for heating for the MHP and OHP for the different DR scenarios.

3.4.2 Annual heating costs for the heat pump systems

Table 3 presents a comparison of the annual heating costs for both DHW heating and SH. Heating costs are calculated by multiplying the hourly electricity use with the current spot price for each hour of the year. The electricity fee for the grid connection of the building is not considered in the cost calculation.

As energy costs are directly related to the energy use, the annual energy use for heating is analyzed first. If the CSP is only applied to SH, the annual energy use for heating is slightly decreased for the MHP and slightly increased for the OHP. If CSP is applied to DHW, this annual energy use is significantly increased due to the auxiliary heater operation. Even though the CSP operates the heating system during periods with favorable electricity prices, energy costs are not decreased if the energy use has increased considerably. This explains that the annual heating costs using the MHP are increased up to 21% when CSP is applied to DHW whereas costs are slightly decreased if CSP is applied to SH only. Regarding the OHP, annual heating costs are increased by up to 27%. Even for the DR scenario which only considers SH, costs are still increased by almost 10%.

It should not be concluded that the CSP control introduced in Section 2.6 always fails at reducing costs. In this case study, the daily fluctuations in the Norwegian spot prices are too small to counterbalance the increase of energy use generated by the CSP and to eventually obtain reasonable costs savings. For example, the use of model predictive control (MPC) instead of PRBC may give different conclusions as this optimal control is in a better position to limit this increase in energy use and to benefit from price fluctuations.

Table 3. Annual heating costs for the two heat pump systems.

		MHP				**OHP**			
		BAU	CSP	CSP-DHW	CSP-SH	BAU	CSP	CSP-DHW	CSP-SH
Heating energy use	**kWh/m²**	20.94	25.30	25.08	20.67	19.57	24.74	23.26	21.27
	%	-	+21	+20	-1	-	+26	+19	+9
Costs w/o el. fee	**NOK**	484	585	583	470	451	571	541	490
	%	-	+21	+20	-3	-	+27	+20	+9

4 Conclusions

This paper investigates the influence of the modeling complexity of the heat pump control in the context of demand response (DR) and building energy flexibility. Based on a summary of typical modeling simplifications for heat pump systems, the paper analyses two key components: the heat pump controller and the DHW prioritization of the heat pump.

To investigate the model complexity of the heat pump controller, the performance of six different controls are compared: on-off control, power modulation using a P-control or different PI-controls, perfect power modulation between 0% and 100% of the compressor power, and the inclusion of a minimum heat pump cycle time. The case of a detached single-family house heated using an air-source heat pump is analyzed with a price-based predictive rule-based control (PRBC).

The results demonstrate that the modeling complexity of the system control has a significant impact on the key performance indicators, proving that this aspect should not be overlooked:

- (1) The model complexity affects the short-time behavior of a heat pump system when performing DR. It is recommended to consider controller tuning for studies on heat pump systems with focus on DR regardless of the applied control strategies, e.g. PRBC or model-predictive control (MPC).
- (2) The annual electricity use for heating is rather similar for all cases, expect for the perfect modulation. In fact, the perfectly modulating and on-off heat pumps lead to the lowest and highest average tank temperatures, respectively. The on-off heat pump charges the tank using a hysteresis with a temperature differential, whereas modulating heat pumps (MHP) modulate to keep the temperature in the tank close to a set-point (corresponding to the starting temperature of the hysteresis). Hence, average tank temperatures and heat losses are lower for MHPs leading to higher SCOPs compared to on-off heat pumps. Therefore, it can be concluded that the perfectly modulating heat pump idealizes the performance of the system and thus overestimates the potential for cost or emissions savings.
- (3) The MHP using P- and PI-controls have a similar number of heat pump cycles while these numbers are significantly different for on-off and perfectly modulating heat pumps. The average run time per cycle is therefore different.
- (4) The controller type (i.e. P- or PI-control) and tuning are important when heat pump operation is investigated at short time scales. In practice, a PI-controller would be preferred to achieve a smoother operation of the heat pump. The controller tuning is often overlooked in studies on DR and energy flexibility using building performance simulation (BPS) and cannot be captured in detail by strongly simplified models for heat pump systems.

For short time scales, the modeling of the heat pump controller and the transient effects of the heat pump, such as cycling losses during start-up, are important. The difference between P- and PI-controllers and their parameter tuning should be considered in a realistic way if the heat pump operation is investigated at short time scales. Besides PRBC, these conclusions are also valid for other controls, such as MPC, where typically temperature set-points are controlled and not the compressor power directly. The choice of MHP controller (i.e. P- or PI-control) and its tuning is not crucial if the heat pump operation and electric power are not investigated at short time scales. A P-controller can be advantageous as it significantly simplifies the modeling setup. Its tuning is easier and the problem of integral windup is avoided.

Regarding the DHW prioritization, the results demonstrate a strong influence of this prioritization on the control of the electric auxiliary heaters. Electricity use increases significantly when the DR is applied to DHW as this increases the use of the auxiliary heater for space-heating. With price-based control applied to DHW, the annual heating costs increase because the advantage of consuming during lower electricity prices is outweighed by the large increase in electricity use. The use of additional set-points for DHW heating along lower electricity spot prices to operate the heat pump more frequently should be considered in future studies to avoid a too frequent operation of the electric auxiliary heater.

Furthermore, this paper describes the control for a detailed model of a heat pump system in a BPS tool. The system is equipped with an MHP and applies PRBC to perform DR. The approach is presented in a generic way using pseudo-codes, whereas the BPS tool IDA ICE is taken as an example. Results show that the presented modeling approach leads to a realistic operation of the heat pump system.

Acknowledgements

The authors would like to gratefully acknowledge IEA EBC Annex 67 on Energy Flexible Buildings as well as IEA HPT Annex 49 on the Design and Integration of Heat Pumps for nearly Zero Energy Buildings. Furthermore, we would like to thank EQUA Solutions AG and EQUA Finland Oy for their support in IDA ICE and Research Scientist Maria Justo Alonso from SINTEF Byggforsk Trondheim for valuable discussions and feedback.

References

[1] Aduda KO, Labeodan T, Zeiler W, Boxem G, Zhao Y. Demand side flexibility: Potentials and building performance implications. Sustain Cities Soc 2016;22:146–63. doi:10.1016/j.scs.2016.02.011.

[2] Chen Y, Xu P, Gu J, Schmidt F, Li W. Measures to improve energy demand flexibility in buildings for demand response (DR): A review. Energy Build 2018;177. doi:10.1016/j.enbuild.2018.08.003.

[3] Haider HT, See OH, Elmenreich W. A review of residential demand response of smart grid. Renew Sustain Energy Rev 2016;59:166–78. doi:10.1016/j.rser.2016.01.016.

[4] Arteconi A, Hewitt NJ, Polonara F. State of the art of thermal storage for demand-side management. Appl Energy 2012;93:371–89. doi:10.1016/j.apenergy.2011.12.045.

[5] Reynders G, Diriken J, Saelens D. Generic characterization method for energy flexibility: Applied to structural thermal storage in residential buildings. Appl Energy 2017;198:192–202. doi:10.1016/j.apenergy.2017.04.061.

[6] Finck C, Li R, Kramer R, Zeiler W. Quantifying demand flexibility of power-to-heat and thermal energy storage in the control of building heating systems. Appl Energy 2017;209:409–25. doi:10.1016/j.apenergy.2017.11.036.

[7] Fischer D, Bernhardt J, Madani H, Wittwer C. Comparison of control approaches for variable speed air source heat pumps considering time variable electricity prices and PV. Appl Energy 2017;204:93–105. doi:10.1016/j.apenergy.2017.06.110.

[8] Alimohammadisagvand B, Jokisalo J, Kilpeläinen S, Ali M, Sirén K. Cost-optimal thermal energy storage system for a residential building with heat pump heating and demand response control. Appl Energy 2016;174:275–87. doi:10.1016/j.apenergy.2016.04.013.

[9] Lizana J, Friedrich D, Renaldi R, Chacartegui R. Energy flexible building through smart demand-side management and latent heat storage. Appl Energy 2018;230:471–85. doi:10.1016/j.apenergy.2018.08.065.

[10] Péan T, Ortiz J, Salom J. Impact of Demand-Side Management on Thermal Comfort and Energy Costs in a Residential nZEB. Buildings 2017;7:37. doi:10.3390/buildings7020037.

[11] Madani H, Claesson J, Lundqvist P. Capacity control in ground source heat pump systems: Part I: modeling and simulation. Int J Refrig 2011;34:1338–47. doi:10.1016/J.IJREFRIG.2011.05.007.

[12] De Coninck R, Baetens R, Saelens D, Woyte A, Helsen L. Rule-based demand-side management of domestic hot water production with heat pumps in zero energy neighbourhoods. J Build Perform Simul 2014;7:271–88. doi:10.1080/19401493.2013.801518.

[13] Dar UI, Sartori I, Georges L, Novakovic V. Advanced control of heat pumps for improved flexibility of Net-ZEB towards the grid. Energy Build 2014;69:74–84. doi:10.1016/j.enbuild.2013.10.019.

[14] Esfehani HH, Kriegel M, Madani H. Load Balancing Potential of Ground Source Heat Pump System Coupled with Thermal Energy Storage : A Case Study for. CLIMA2016 - Proc. 12th REHVA World Congr., 2016.

[15] Alimohammadisagvand B, Jokisalo J, Sirén K. Comparison of four rule-based demand response control algorithms in an electrically and heat pump-heated residential building. Appl Energy 2018;209:167–79. doi:10.1016/j.apenergy.2017.10.088.

[16] Masy G, Georges E, Verhelst C, Lemort V. Smart grid energy flexible buildings through the use of heat pumps and building thermal mass as energy storage in the Belgian context. Sci Technol Built Environ 2015;21:6:800–11. doi:10.1080/23744731.2015.1035590.

[17] Georges E, Garsoux P, Masy G, DeMaere D`Aetrycke G, Lemort V. Analysis of the flexibility of Belgian residential buildings equipped with Heat Pumps and Thermal Energy Storages. CLIMA 2016 - Proc. 12th REHVA World Congr., Aalborg: 2016.

[18] Salpakari J, Lund P. Optimal and rule-based control strategies for energy flexibility in buildings with PV. Appl Energy 2016;161:425–36. doi:10.1016/j.apenergy.2015.10.036.

[19] Psimopoulos E, Bee E, Widén J, Bales C. Techno-economic analysis of control algorithms for an exhaust air heat pump system for detached houses coupled to a photovoltaic system. Appl Energy 2019;249:355–67. doi:10.1016/j.apenergy.2019.04.080.

[20] Bagarella G, Lazzarin R, Noro M. Sizing strategy of on–off and modulating heat pump systems based on annual energy analysis. Int J Refrig 2016;65:183–93. doi:10.1016/J.IJREFRIG.2016.02.015.

[21] Lee CK. Dynamic performance of ground-source heat pumps fitted with frequency inverters for part-load control. Appl Energy 2010;87:3507–13. doi:10.1016/J.APENERGY.2010.04.029.

[22] Dongellini M, Abbenante M, Morini GL. A strategy for the optimal control logic of heat pump systems: impact on the energy consumptions of a residential building. Proc. 12th IEA Heat Pump Conf. 2017, 2017.

[23] Dongellini M, Naldi C, Morini GL. Seasonal performance evaluation of electric air-to-water heat pump systems. Appl Therm Eng 2015;90:1072–81. doi:10.1016/J.APPLTHERMALENG.2015.03.026.

[24] Bettanini E, Gastaldello A, Schibuola L. Simplified models to simulate part load performances of air conditioning equipments. Proc. 8th Int. IBPSA Conf., Eindhoven, Netherlands: 2003.

[25] Uhlmann M, Bertsch SS. Theoretical and experimental investigation of startup and shutdown behavior of residential heat pumps. Int J Refrig 2012;35:2138–49. doi:10.1016/j.ijrefrig.2012.08.008.

[26] Bagarella G, Lazzarin RM, Lamanna B. Cycling losses in refrigeration equipment: An experimental evaluation. Int J Refrig 2013;36:2111–8. doi:10.1016/J.IJREFRIG.2013.07.020.

[27] Cheung H, Braun JE. Performance comparisons for variable-speed ductless and single-speed ducted residential heat pumps. Int J Refrig 2014;47:15–25. doi:10.1016/J.IJREFRIG.2014.07.019.

[28] Madani H, Claesson J, Lundqvist P. Capacity control in ground source heat pump systems part II: Comparative analysis between on/off controlled and variable capacity systems. Int J Refrig 2011;34:1934–42. doi:10.1016/J.IJREFRIG.2011.05.012.

[29] Åström KJ, Hägglund T. Revisiting the Ziegler–Nichols step response method for PID control. J Process Control 2004;14:635–50. doi:10.1016/J.JPROCONT.2004.01.002.

[30] Skogestad S, Grimholt C. The SIMC Method for Smooth PID Controller Tuning, Springer, London; 2012, p. 147–75. doi:10.1007/978-1-4471-2425-2_5.

[31] HOVAL. Dimensionierungshilfe für Wärmepumpenanlagen 2017. 2017.

[32] OSOHotwater. OSO Hotwater, "OSO Optima EPC series". Patent 328503, 02 2014, 2014.

[33] Floss A, Hofmann S. Optimized integration of storage tanks in heat pump systems and adapted control strategies. Energy Build 2015;100:10–5. doi:10.1016/j.enbuild.2015.01.009.

[34] Clauß J, Stinner S, Sartori I, Georges L. Predictive rule-based control to activate the energy flexibility of Norwegian residential buildings: Case of an air-source heat pump and direct electric heating. Appl Energy 2019;237:500–18. doi:10.1016/J.APENERGY.2018.12.074.

[35] Modelica. ModelicaStandardLibrary 2018. https://modelica.org/libraries.

[36] Clauß J, Stinner S, Solli C, Lindberg KB, Madsen H, Georges L. Evaluation Method for the Hourly Average CO2eq. Intensity of the Electricity Mix and Its Application to the Demand Response of Residential Heating. Energies 2019;12:1345. doi:10.3390/en12071345.

[37] Péan TQ, Salom J, Ortiz J. Environmental and Economic Impact of Demand Response Strategies for Energy Flexible Buildings. Proc BSO 2018 2018:277–83.

[38] Standard Norge. NS-EN 15251:2007 Indoor environmental input parameters for design and assessment of energy performance of buildings addressing indoor air quality, thermal environment, lighting and acoustics 2007.

[39] Goia F, Finocchiaro L, Gustavsen A. The ZEB Living Laboratory at the Norwegian University of Science and Technology : a zero emission house for engineering and social science experiments. 7 . Passiv. Nord. - Sustain. Cities Build., Copenhagen: 2015.

[40] Clauß J, Vogler-Finck P, Georges L. Calibration of a high-resolution dynamic model for detailed investigation of the energy flexibility of a zero emission residential building. In: Johansson D, editor. Springer Proc. Energy, Cold Clim. HVAC 2018 Conf., Kiruna, Sweden: Springer Nature Switzerland AG 2019; 2018. doi:https://doi.org/10.1007/978-3-030-00662-4_61.

[41] SN/TS3031:2016. Bygningers energiytelse, Beregning av energibehov og energiforsyning 2016.

[42] Niemelä T, Kosonen R, Jokisalo J. Comparison of energy performance of simulated and measured heat pump systems in existing multi-family residential buildings. 12th IEA Heat Pump Conf. 2017, Rotterdam, Netherlands: 2017.

[43] NIBE. Luft / vann-varmepumpe Slik fungerer NIBE F2120 Installasjonsprinsipp. 2013.

[44] Kristjansdottir TF, Houlihan-Wiberg A, Andresen I, Georges L, Heeren N, Good CS, et al. Is a net life cycle balance for energy and materials achievable for a zero emission single-family building in Norway? Energy Build 2018;168:457–69. doi:10.1016/j.enbuild.2018.02.046.

[45] Rendum J, Vik AL, Knutsen AS. Innføring av AMS i norske husstander, og mulighetene dette gir for nettfleksibilitet. Norwegian University of Science and Technology, 2016.

[46] OpenStreetMap. Shiny weather data 2017. https://rokka.shinyapps.io/shinyweatherdata/ (accessed May 20, 2017).

[47] Nord Pool Spot. www.nordpoolspot.com/historical-market-data 2016. www.nordpoolspot.com/historical-market-data.

PAPER 6

Control strategies for building energy systems to unlock demand side flexibility – A review

Clauß J[1], Finck C[2], Vogler-Finck P[3], Beagon P[4]

[1] Norwegian University of Science and Technology, Trondheim, Norway

[2] Eindhoven University of Technology, Eindhoven, Netherlands

[3] Neogrid Technologies ApS / Aalborg University, Aalborg, Denmark

[4] Energy Institute, School of Mechanical Engineering, UCD, Dublin, Ireland

This paper is published in *Proceedings of the 15th IBPSA Conference* held in San Francisco, USA in August 2017, Pages 1750-1759.

BUILDING SIMULATION 2017
INTERNATIONAL BUILDING PERFORMANCE SIMULATION ASSOCIATION

Control strategies for building energy systems to unlock demand side flexibility – A review

John Clauß[1,*], Christian Finck[2], Pierre Vogler-Finck[3], Paul Beagon[4]
[1]Norwegian University of Science and Technology, Trondheim, Norway
[2]Eindhoven University of Technology, Eindhoven, Netherlands
[3]Neogrid Technologies ApS / Aalborg University, Aalborg, Denmark
[4]Energy Institute, School of Mechanical Engineering, UCD, Dublin, Ireland
[*]email: john.clauss@ntnu.no

Abstract

Conventional key performance indicators (KPI) assessed in building simulation lack specific measures of how the building interacts with the grid and its energy flexibility. This paper aims to provide an overview of specific energy flexibility performance indicators, together with supporting control strategies. If applied correctly, the indicators help improving the building performance in terms of energy flexibility and can enable minimization of operational energy costs. Price-based load shifting, self-generation and self-consumption are among the most commonly used performance indicators that quantify energy flexibility and grid interaction. It has been found that the majority of performance indicators, specific to energy flexibility, are combined with rule-based control. Only a limited amount of specific energy flexibility KPIs are used in combination with optimal control or model predictive control. Both of these advanced control approaches often have a couple of economic or comfort objectives that do not take into account an energy flexibility KPI. There is evidence that recent model predictive control approaches incorporate some aspects of building energy flexibility to minimize operational cost in conjunction with time varying pricing.

Introduction

The transition to a sustainable energy system requires a shift to intermittent renewable energy sources, which call for increased flexibility in the energy system. There is therefore a need for consumers to adopt a more holistic approach to energy use beyond the traditional single building management. Generally, building energy flexibility can be understood as the margin in which the building can be operated while respecting its functional requirements.

Demand side management (DSM) in power systems is a way to overcome potential challenges of the electricity grid, such as balancing the generation and consumption, voltage regulation or high peak loads. Demand response (DR) has been implemented into power grids for decades, with forms ranging from load shedding for blackout prevention, to time-of-use (ToU) rates to reduce system peak load (O´Connell et al., 2014).

According to the Building Performance Institute Europe, future buildings, e.g. termed nZEBs 2.0, should play a significant role in transforming the European energy market, as they become interactive players in balancing the grid by DSM (D´Angiolella et al., 2016). Steadily decreasing prices for communication, sensing and computing devices will make future management systems more affordable and thus open up possibilities of improved controls for DR. The choice or design of an appropriate control strategy can be a challenging task, thus it is important to focus on the appropriate KPIs to ensure desired performance results.

Common control strategies are rule-based controls (RBCs) or model-predictive controls (MPCs). In order to operate the energy system in an efficient way, RBCs typically apply pre-defined set points for temperatures (heating) or CO_2 levels (ventilation system). A MPC often makes use of a simplified model of the building for predicting future states of the system and optimizes the schedule over a sliding horizon according to an objective function, such as the total energy consumption (Ma et al., 2012). More details about MPC theory and applications to building HVAC and comfort/energy management are provided in the extensive reviews by Afram and Janabi-Sharifi (2014), Dounis and Caraiscos (2009), Shaikh et al. (2014) and Li and Wen (2014).

This paper aims to review and classify the control strategies to provide demand side flexibility (DSF). The authors give an overview of applied KPIs and present control strategies for deploying energy flexibility in heating and cooling systems of buildings.

This review includes 45 articles. Major keywords during the literature search were: demand side flexibility, energy flexibility, energy flexible buildings, advanced control, demand response control in buildings. Firstly, the need for energy flexibility and its indicators will be discussed. Secondly, an overview of conventional and specific energy flexibility KPIs is presented. Thirdly, a summary of control strategies aiming to deploy DSF is given and associated KPIs in applications are shown. On top of this, building simulation tools used for specific energy flexibility KPIs are presented considering RBC, optimal control (OC), and MPC.

Background concepts

Introduction to performance data

An effective KPI provides an accurate measure of overall system status, thus facilitating decision making, by

https://doi.org/10.26868/25222708.2017.462

quantification and prioritization of resource allocation. A building KPI must be applicable throughout the system's operational lifespan; during all seasons and occupancy levels. KPIs differentiate themselves as both "predictive" and "persistent" (Mauboussin, 2012). Deru and Torcellini (2005) define an indicator as "a high-level performance metric that is used to simplify complex information and point to the general state or trends of a phenomenon." Different performance metric address different audiences:

- Indicators: Policy makers
- Tier 2 metrics: Designers, suppliers & owners
- Tier 1 metrics: Designers, operators & researchers
- Monitor data: Operators & researchers

Monitoring procedures display data, followed by further procedures and analysis to produce higher metrics and indicators. Higher level metrics fit over longer timescales.

Performance *goals* should drive the design of a building to operate towards a desired result. Performance *metrics* measure and track performance towards the performance goals. Effective control maintains or even increases the value of performance metrics despite the abundance of possible monitoring data.

Conventional KPIs of energy efficiency at building level

KPIs for individual building energy efficiency are well covered in the literature. Common performance indicators during operational stage are:

- Final energy use
- Energy needs
- Cost of energy
- Primary energy use
- CO_2 emissions

These conventional KPIs can be however complemented by specific energy flexibility indicators related to services that a building can offer to the grid, as discussed in the following parts.

Demand side flexibility

Energy system flexibility is proposed as one enabler for high levels of renewable energy penetration (Lund et al., 2015). This builds upon the well-established concept of DSM described in seminal work by Gellings and Smith (1989).

Introduction to demand side flexibility

In a literature review by Lopes et al. (2016) several definitions of "flexibility" and methodologies used to quantify the energy flexibility in buildings have been proposed.

The building-to-grid energy flexibility is often reduced to the electricity consumption for heating and cooling. For example, in a cooling regime (such as in California) HVAC systems are a leading demand response resource (Watson, 2013). Some form of storage (typically thermal mass or water storage tanks) is required to exploit the full flexibility potential. As this storage gets activated, it is temporarily loaded to higher (or lower) temperatures. As a result, the total energy consumption is often increased, while operational costs can be actively reduced and a service to the electricity grid can be provided. Common demand management services are load shifting, peak shaving or load balancing. If responsive and reliable at short notice, DSM may potentially support other grid ancillary services, such as spinning reserves, frequency stability or voltage regulation, but often requires electrical or battery energy storage. A battery discharge time has an upper limit and further depends on its charge state at the time when it is directed to discharge. The uncertainty of a battery's charge state disqualifies it from capacity and grid ancillary services according to its detractors (Huntoon, 2016). In terms of load balancing and non-spinning reserves the electricity grid can benefit from an advanced DSM in order to increase renewable generation integration. DSM supports renewable integration primarily by load following and grid frequency regulation; especially if its ramping rates are high (Watson, 2013).

The flexibility potential often depends on the size of the storage. For building engineers and designers, this is crucial because the storage size directly influences the required capacity of the HVAC system as well as the investment costs. As foreseen by Strbac (2008), the economic analysis of energy flexibility is still challenging.

The economic benefits of energy flexibility vary over time and stage in a heating or cooling season. Increased flexibility during winter is quantified in the second example of Stinner et al. (2016) similarly by Pallonetto et al. (2016). Garnier et al. (2015) analyze different seasons of HVAC operation, noting that one source of energy flexibility, building thermal inertia, is low during the summer. That work also found that seasonal variability is one of the reasons that MPC optimizes energy costs compared to RBC.

Practitioners of building simulation tools already use time varying inputs such as weather, outside air temperature and irradiance. Daily energy markets and real time (i.e. hourly or half hourly) pricing introduces electricity pricing as another time varying input to a simulation of a grid integrated building or district. High grid penetration by renewables causes uncertainty in electricity generation due to the weather, especially solar irradiance and wind speed. The predominant uncertainty means that real-time electricity pricing may be analyzed as a stochastic process (Kitapbayev et al., 2013).

Mathematical finance techniques process stochastic inputs in order to quantify the flexibility of a possible investment. One technique, *real options*, is a way to make a business decision. Applied to a demand site equipped with a CHP, the high level control decision is to operate or idle the local power plant in favor of utility supplied energy based on dynamic energy (Kienzle and Andersson, 2009). The decisions rely on Monte Carlo simulation of stochastic energy price inputs into an Energy Hub model.

The "Real options" method exceeds the discounted cash flow valuations, by modelling uncertainty and operational flexibility. Use of simulation requires a time-step,

enabling its re-calibration to influence short-term operational control. As shown by Kitapbayev et al. (2015) "short term flexibility can change the long term business case, while the long term investment plan can enable short term flexibility".

KPIs of energy flexibility

Table 1 provides an overview of KPIs related to energy flexibility. A number of KPIs is presented, together with their formal mathematical definition and context of application. Notations are introduced in the nomenclature at the end of the paper.

Indicators for load matching and grid interaction are gaining importance, particularly for net zero energy buildings. Such buildings produce electricity from on-site renewable energy sources in order to meet the annual zero energy balance. Electricity grids are usually designed to cover the peak demands of the connected buildings, but not for handling peaks from on-site electricity generation. Therefore, considerations about self-consumption of on-site generated electricity is becoming increasingly important (both at design and operation level), especially in countries with a large share of on-site renewable energy sources (Salom et al., 2014a).

Table 1. Overview of the KPIs related to energy flexibility

KPI	Mathematical definition of the KPI	Characteristics	Reference
Self-generation (also known as load cover factor)	Proportion of electrical demand met by on-site generation. $$\gamma_l = \frac{\int_0^T min[g(t) - S(t) - \zeta(t), l(t)]dt}{\int_0^T l(t)dt} \quad (1)$$ The time resolution often is one hour, often over an annual period.	- Displays daily and seasonal effects caused by different generator types such as PV, CHP. - Comparing control strategies is possible - Accepted by several research groups, such as Annex 52. - Independent of any energy or emission savings by the whole energy system.	(Salom et al., 2014a) (Baetens et al., 2010) (De Coninck et al., 2014) (Vanhoudt et al., 2014) (Salom et al., 2014b) (Klein et al., 2015)
Self-consumption (also supply cover factor)	Proportion of on-site generation consumed by building. $$\gamma_s = \frac{\int_0^T min[g(t) - S(t) - \zeta(t), l(t)]dt}{\int_0^T g(t)dt} \quad (2)$$		
Peak power generation	Peak value of the on-site generation normalized by the designed grid connection capacity (E_{des}). $$\bar{G} = \frac{max[g(t)]}{E_{des}} \quad (3)$$	- Provide boundaries to load duration curves and carpet plots. - Identify the load or generation peak periods. - Comparisons to the net export and net imports respectively.	(Salom et al., 2014a)
Peak power load	Peak value of the demand normalized to the nominal designed grid connection capacity (E_{des}). $$\bar{L} = \frac{max[l(t)]}{E_{des}} \quad (4)$$		(Salom et al., 2014a)
Flexibility (optimum cost)	The maximum reachable load is sum of all controllable loads. Maximum and minimum load (l), lead to a positive or negative flexibility (Φ) (possibility of increased or decreased power consumption, respectively) during an interval (t). $$\Phi_{pos} = l(t)_{max} - l(t)_{ref} \geq 0 \quad (5)$$ $$\Phi_{neg} = l(t)_{min} - l(t)_{ref} \leq 0 \quad (6)$$ Relative costs (Γ) vary due to total cost J_c. $$\Gamma_{max} = J_{c,max} - J_{c,ref} \geq 0 \quad (7)$$ $$\Gamma_{min} = J_{c,min} - J_{c,ref} \geq 0 \quad (8)$$	- Solves several optimal control problems - Reference scenario optimally controls for thermal comfort and operational costs - Aggregatable and comparable to various buildings, climates and energy systems (incl. renewables) - Instantaneous cost curves vary over time-steps and boundaries.	(De Coninck and Helsen, 2016)
Flexibility factor FF_{PC} (costs)	In terms of procurement costs (PC) avoided. $$FF_{PC} = \frac{PC_{max} - PC}{PC_{max} - PC_{min}} \quad (9)$$ Dar et al. (2014) call it relative import bill (RIB).	- Annual PC varies due to electricity time of use (ToU) tariffs. - FF maximizes as PC → PC_{min} if all heating is done during cheapest ToU.	(Dar et al., 2014) (Masy et al., 2015)
Flexibility factor FF_{shift} (volume)	In terms of energy shifted compared to a reference profile. $$FF_{shift} = \frac{FF_{PC} - FF_{PC,ref}}{FF_{PC,ref}} \quad (10)$$	- $FF_{PC,ref}$: flexibility in terms of PC for a flat tariff reference case	(Masy et al., 2015)
Flexibility factor (FF)	Ability to shift the energy use from high to low price periods: $$FF = \frac{\int_{LPT} l_{heating}\,dt - \int_{HPT} l_{heating}\,dt}{\int_{LPT} l_{heating}\,dt + \int_{HPT} l_{heating}\,dt} \quad (11)$$	- Gives a quick indication of when heating energy is consumed - FF = 0 if demand is similar during both price periods - FF = 1 (max) or -1 (min), if demand in single pricing period	(Le Dréau and Heiselberg, 2016)
Load shift for CO_2	Optimization value function to minimizing carbon emissions: $$V = \int_0^T C_{CO_2}(t) \cdot l(t)dt \quad (12)$$	- Requires carbon emissions per kWh for time-steps *t*	(Favre and Peuportier, 2014)

KPI	Mathematical definition of the KPI	Characteristics	Reference
Energy flexibility ε	Amount of flexible energy that could be delivered. $\varepsilon_{forced}(t) = \int_0^{T_{forced}} l_{flex.forced}\, dt$ (13) $\varepsilon_{delayed}(t) = \int_0^{T_{delayed}} l_{flex.delayed}\, dt$ (14)	- *"Forced flexibility"*: charging or heating the TES by a grid connected heater. - *Negative flexibility*: increase generation - *"Delayed flexibility"*: discharging TES, while grid connected heater is off - *Positive flexibility:* reduce generation - Two other metrics: ramp-up capability (MW/min) and power capacity (MW)	(Stinner et al., 2016)
Available structure storage capacity	Amount of heat that can be added to a building's thermal mass during a predefined charging event, while constrained by thermal comfort. $C_{ADR} = \int_0^T (l_{ADR} - l_{ref})\, dt$ (15)	- A characteristic property of a building, but time varying. - C_{ADR} varies due to boundary conditions of climate, occupant behavior and heating system. - The ADR event starts at a minimum comfort temperature	(Reynders et al., 2015)
Storage efficiency	Fraction of heat that is stored during an ADR event, later used to reduce heating load power to maintain the thermal comfort. $\eta_{ADR} = 1 - \frac{\int_o^{\infty}(l_{ADR} - l_{ref})dt}{\int_0^T (l_{ADR} - l_{ref})\, dt}$ (16)	- Can be seen as a characteristic property of a building - The integral in the denominator equals the heat stored in the storage event or the C_{ADR}	(Reynders et al., 2015)
Shifting efficiency	Heating energy shifted compared to a reference case: $\eta_{shift} = \frac{-\Delta l_{heat\ discharged}}{\Delta l_{heat\ charged}}$ (17)	- Used to characterize the thermal mass as a storage medium - Methodology can also be used for water storage tanks	(Le Dréau and Heiselberg, 2016)
Loss of load probability (LOLP)	Time (%) when on-site generation is less than local demand. $LOLP_b = \frac{\int_0^T f(t)dt}{T}$ $\begin{cases} f(t) = 1, if\ ne(t) < 0 \\ f(t) = 0, if\ ne(t) \geq 0 \end{cases}$ (18) Energy autonomy: $A_b = 1 - LOLP_b$ (19)	- Measures proportion of the year requiring grid electricity imports - Omits the volume of grid imports - Can be used for designing the control of the PV / energy system - Links to energy autonomy (A_b)	(Salom et al., 2014a)
Power shifting capability	Difference between heating power during the ADR event and the reference heating power during normal operation. $l_{shift} = l_{ADR} - l_{ref}$ (20)	- Load/power flexibility of building - Associated metric "power shifting capability" combines l_{shift} and its duration t_{shift}	(Reynders et al., 2015)
Grid feed-in	$Grid\ feed\ in = \int_0^T ne(t)dt$ (21)	- Minimizing grid feed-in increases self-consumption - More efficient than curtailment to achieve grid integration regulation	(Salpakari and Lund, 2016)
Demand recovery ratio	$DRR = \frac{\int_0^T l_{heating}(t)dt}{\int_0^T \min[l_{heating}(t)]\, dt}$ (22)	- Quantifies the increase in energy use due to load shifting at the demand side - If ADR = 0, then DDR = 1 (min) - Indicates reduced thermal losses with increasing number of flexible buildings - System level: different temperature set points and storage technologies	(Arteconi et al., 2016)

Flexibility indicators can describe physical characteristics of a building (e.g. storage capacity) or quantify the magnitude of the building´s reaction to external signals (e.g. electricity price) within the context of the power grid. Load matching and grid interaction indicators (e.g. equations 1-4, 18, 21) give a coarse overview of the ratio of the building energy load vs. on-site electricity generation as well as identify the load and generation peak periods. Energy flexibility indicators (e.g. equations 9-11) are often price-based and show whether energy/electricity is consumed during high- or low-price periods. Their generic nature allows their application to various building types, climates and energy systems. All the presented parameters can be used for determining the energy flexibility (or related characteristics) of a building and can either be calculated during post processing of the building simulation results or be included into a model-based control algorithm directly. Limitations of the indicators include the availability of the data used to compute them, so that the simulation software must be able to provide the data.

Control strategies for deploying energy flexibility

RBC strategies are a common approach for controlling energy systems of buildings. They use pre-defined conditions (or decision rules) to change the current state of a system and can easily be implemented into dynamic building simulation tools. Depending on the decision criteria of the RBC (e.g. weather, price, occupancy), it can aim at activating the energy flexibility of the building to improve grid interaction, lower energy costs, perform load shifting or reduce energy needs by varying the temperature set points of the buildings zones or the water

storage tanks. RBCs mainly fulfill a certain control objective, but are not designed to achieve optimization of the overall system behavior. Therefore, a balance between different control objectives, such as a low energy consumption and reduced energy costs, but a high load shifting potential has to be found, for instance by advanced control strategies, such as MPC.

Afram and Janabi-Sharifi (2014) point out that advanced control systems (OC, fuzzy logic, MPC) in combination with thermal storages show a great opportunity for peak shaving, hence reducing infrastructure and operational costs. These controls can use external information for minimizing the energy consumption and therefore have a higher potential to fully deploy the flexibility of a building compared to rule-based control. Classical control strategies, such as thermostatic on/off control, PI or PID control are state-of-the-art for HVAC applications and are not able to adapt to time-varying disturbances or changes in environmental conditions (Afram and Janabi-Sharifi, 2014) and thus may fail to provide flexibility in a dynamic manner. A control strategy that enables the flexibility of the HVAC system operation, such as MPC, permits optimization of the energy consumption while preserving or even improving thermal comfort (Afram and Janabi-Sharifi, 2014). Predictive and optimal controls show a great potential for deploying DSF because they can deal with time-varying operating conditions and can interact with the energy system and the grid (De Coninck and Helsen, 2016). In this manner, they have a potential to contribute to peak shaving and load shifting of the electricity consumption (Haghighi, 2013). MPC is seen as one of the most promising developments as it can take into account future weather, electricity price forecasts (including their uncertainties (Oldewurtel, 2011)) as well as occupant behavior when computing an optimal consumption decision. Research at a district scale argues that the value of building energy flexibility depends on time varying energy prices (Kitapbayev et al., 2015).

Energy price data sources are publicly available in a number of countries seeking to improve transparency on the market, which facilitates the use of real world data for building simulations. In particular, data for the Scandinavian markets and neighboring countries is provided by NordPool (Nord Pool Spot, 2016), Energinet for Denmark (Energinet, 2016) and Statnett for Norway (Statnett, 2016). For Ireland, data is available on the single electricity market platform (Single Electricity Market Operator, 2016), and for Britain and the Netherlands data is provided by power exchange (Apx Power Spot Exchange, 2016). Estimations of time-varying CO_2 intensity of the power due to electricity generation are available from the Eco-Invent database (Ecoinvent, 2016).

Compared to RBCs, which are often designed to improve one control objective, MPCs allow the computation of an optimum schedule that can compromise between different control objectives. Several software tools were used in the reviewed articles to assess building energy flexibility. Commonly used tools for building simulation are EnergyPlus (Le Dréau and Heiselberg, 2016), IDA ICE (Alimohammadisagvand et al., 2016) or TRNSYS (Esfehani et al., 2016). These tools apply detailed numerical models for modelling the building energy performance, where RBCs can be implemented easily. If MPC is to be tested in combination with these tools, the optimization problem of the MPC is to be solved in another software, such as MATLAB. Furthermore, an interface, which couples the optimization software and the building simulation software, is required. The BCVTB and MLE+ interfaces were used by Ma et al. (2011) and Garnier et al. (2015), respectively. MATLAB and Modelica can be used for both, modelling the building performance and running the optimization. In Modelica, RC-models (used by Klein et al. (2015)) or component models from different libraries (De Coninck and Helsen, 2016; Reynders et al., 2015) can be applied for building simulation. RC-models lead to simplified building models which express the building properties properly. Halvgaard et al. (2012) used RC-models in MATLAB in order to test an economic MPC.

Table 2 provides an overview of control strategies that have been implemented in building performance simulations to deploy demand side flexibility. All the control strategies are either a RBC, an optimal control or a MPC. The characteristics of each strategy are shown for easier reproduction.

Table 2. Summary of control strategies to deploy demand side flexibility

Building energy control	**Control design consideration**		**Characteristics**	**References**
	LS[1]	ORM[2]	[1]LS – Load shaping, [2]ORM – On-site renewable energy maximization	
RBC (1)	x	x	Increase of 12K in DHW set point caused by three triggers - RBC 1a: time based at 12:00 every day, activating the heat pump - RBC 1b: if the power injection to the grid exceeds a threshold - RBC 1c: if voltage of buildings grid connection exceeds a threshold	(De Coninck et al., 2014)
RBC (2)	x	x	Load shifting takes place if either local PV surplus generation or high proportion of RE in grid electricity - Zone heating curve heating increases by 3K, compared to reference - Zone cooling curves cooling decreases by 3K, compared to reference	(Klein et al., 2015)
RBC (3)	x		Set point of zone temperature responds to ToU pricing - Decreases by 2K during high price period (maximum duration 4-24h) - Increases by 2K during low price period (maximum duration 4-24h)	(Le Dréau and Heiselberg, 2016)

Building energy control	Control design consideration		Characteristics	References
	LS[1]	ORM[2]	[1]LS – Load shaping, [2]ORM – On-site renewable energy maximization	
RBC (4)	x	x	While comfort constrained, a TES coupled heat pump activates for, - *Self-consumption*: If surplus PV electricity generation - *Power-exchange*: PV surplus > limit & TES or space heating possible - *Price based control*: If hourly tariff < specified threshold	(Dar et al., 2014)
RBC (5)	x		- Temperature set point increased by dT_{comf} [K], a set of (1, 2, 3, 4), for a period that ranges from 15 min to 6 h. - Heating load subsequently reduced but minimum comfort maintained.	(Reynders et al., 2015)
RBC (6)	x	x	*Surplus (off peak) scenario*: heat pump consumes surplus grid electricity - DHW and space heating set point deadband of ±2K, 15min time-step - Minimize peak time consumption by 5K DHW set point reduction	(Esfehani et al., 2016)
RBC (7)	x		Price based control called *"Momentary control algorithm"*: - Hourly tariff ≤ limit: normal set points of DHW (55°C) and space heating (21°C). TES maximum set point experimented over 55-95°C - Hourly tariff > limit: minimum set points of DHW & space heating. - If heating off, available TES energy heats DHW and space	(Alimohammad isagvand et al., 2016)
RBC (8)	x		- 1) Occupancy set points: 21°C (24°C bathroom), else 18°C - 2) Constant set points: 21°C (24°C bathroom) - 3) Occupancy set points from 1) and overnight TES heating to 55°C for use during peak time of 10:00 - 12:00	(Masy et al., 2015)
RBC (9)		x	- If PV generation surplus, self-consumed by shiftable (inside 24 h) appliances, battery or TES. - PV generation insufficient, battery discharged and deficit from grid	(Salpakari and Lund, 2016)
Optimal control (OC) (1)	x		- Heat pump operation scheduled over 24 h horizon for cost-optimality - Challenging due to heat pump COP non-linearity with temperature - Computation time depends on flexibility (TES, battery or appliances).	(Salpakari and Lund, 2016)
OC (2)	x		- Heat pump operation is optimized by model predictive control for two tariff structures: day/night and ToU spot pricing. - Zone temperatures set point 20-22°C either i) continuously or ii) daily time interval 08:00-12:00. - Control objective is operational costs minimization of the heat pump	(Masy et al., 2015)
OC (3)	x		- Comfort constrained, cost minimization produces a reference plan - Electricity ToU tariffs stimulate consumption deviation from the reference plan during specific intervals in order to minimize cost. - Discomfort cost calculated during occupancy and outside 21.8-23.5°C - Special case of temperature reference tracking about set point	(De Coninck and Helsen, 2016)
Economic MPC (1)	x		- Comfort constrained, electricity cost minimization by heat pump - Heat energy storage of floor shifts consumption to lower tariff periods	(Halvgaard et al., 2012)
Economic MPC (2)	x		- Comfort constrained, energy minimization by HVAC system - Potential for grid frequency regulation by exports of active power - Parameter adaptive building model contains four flexibility variables: air flow and power, both increase and decrease flexibility. - Novel proposal to co-design the control algorithm and HVAC system	(Haghighi, 2013)
Economic MPC (3)	x		- Minimization and shaping of aggregated building electricity demand, by scheduling of residential cooling set points. - Energy systems integration of aggregated building demand with grid	(Corbin and Henze, 2016a)
Economic MPC (4)	x	x	- Shape residential demand profile from grid feeder - Minimization of the deviation from reference demand curves by steps - (1) Compute a reference demand curve aggregated at the feeder level - (2) Disaggregate to a reference demand curve per residence; then modify for renewables generation. - (3) Minimize the difference between the actual residence demand curve and the modified reference demand curve - MPC controllers of each residence adjust the cooling set points depending on their pre-defined boundaries	(Corbin and Henze, 2016b)
MPC (5)	x		- Balances energy consumption and, when applicable, discomfort - Output is an optimal sequence of heating supply temperatures - Patented	(Lindelöf et al., 2015)
MPC (6)	x		- Minimization of energy consumption by a multi-zone HVAC system - Thermal comfort constraints are indicated by predicted mean vote - Artificial neural network schedules both cooling and heating	(Garnier et al., 2015)
Economic predictive control	x	x	- Minimization of heat pump energy costs by shifting its operation to times that match high on-site PV generation	(Kandler et al., 2015)

In order to see the aims of each control strategy, they are distinguished between two control design considerations: load shaping (LS) and maximum use of on-site renewable energy (ORM). Load shaping includes peak shaving and load shifting to off-peak hours.

It can be seen from Table 2, that among the investigated literature, RBC and MPC are both used for load shifting. However, RBC is more often used for achieving a maximization of the use of on-site renewable energy than MPC. This may be due to the easier implementation of RBC into building performance simulations.

Mapping of KPIs with control strategies

Table 3 provides an overview of the reviewed references focusing on combinations of investigated control strategies and KPIs. For most of the respective studies, MPC is used with conventional KPIs, whereas flexibility indicators are used with RBC. This can be due to the greater ease of implementation of RBC strategies in building performance simulations, compared to MPC which is still a relatively new field of research. KPIs can be calculated based on output data available from building performance simulation, thus MPC could easily be used together with specific energy flexibility KPIs.

Conclusion

Key performance indicators measuring energy flexibility are becoming increasingly important for building performance simulations, especially with the inclusion of DSM or time-varying energy pricing. The authors are convinced that model-based control applied to energy flexibility improves a building´s sustainable design and operation. Generally, RBCs as well as OCs and MPCs can have energy flexibility embedded in the control objectives.

The main findings from this paper are:

- Multiple specific energy flexibility KPIs exist, which allow quantifying different aspects of DSF.
- Services covered by energy flexibility KPIs (mainly focusing on the building) do not cover all possible services for DSM such as grid integration or grid ancillary services.
- Most KPIs specific to energy flexibility are found in RBC studies, whereas OC or MPC studies focus mainly on conventional KPIs.
- RBCs are reported as effective, if focused on a single KPI (including conventional and specific energy flexibility KPIs).

Table 3. Overview of KPIs used in control ([1] rule-based control, [2] optimal control, [3] (economic) model-predictive control)

		Controller	
		RBC[1]	**OC[2] and MPC[3]**
KPIs for energy flexibility	Self-generation	RBC (1) (De Coninck et al., 2014) RBC (2) (Klein et al., 2015)	
	Self-consumption	RBC (1) (De Coninck et al., 2014) RBC (2) (Klein et al., 2015) RBC (4) (Dar et al., 2014) RBC (9) (Salpakari and Lund, 2016)	
	Flexibility factor FF	RBC (3) (Le Dréau and Heiselberg, 2016)	
	FF_{PC} and FF_{shift}	RBC (4) (Dar et al., 2014) RBC (8) (Masy et al., 2015)	OC (2) (Masy et al., 2015)
	Flexibility (optimum cost)		OC (3) (De Coninck and Helsen, 2016)
	Grid feed-in		OC (1) (Salpakari and Lund, 2016)
	Available structure storage capacity	RBC (5) (Reynders et al., 2015)	
	Storage efficiency	RBC (5) (Reynders et al., 2015)	
	Shifting efficiency	RBC (3) (Le Dréau and Heiselberg, 2016)	
	Power shifting capability	RBC (5) (Reynders et al., 2015)	
Conventional KPIs	Energy consumption	RBC (6) (Esfehani et al., 2016) RBC (7) (Alimohammadisagvand et al., 2016)	E-MPC (3) (Corbin and Henze, 2016a) E-MPC (4) (Corbin and Henze, 2016b) MPC (5) (Lindelöf et al., 2015) MPC (6) (Garnier et al., 2015)
	Energy costs	RBC (7) (Alimohammadisagvand et al., 2016)	E-MPC (1) (Halvgaard et al., 2012) E-MPC (2) (Haghighi, 2013) OC (1) (Salpakari and Lund, 2016)

- OC and MPC can consider different "objective functions" that optimize the system behavior by taking into account energy flexibility. Moreover, they can be assessed with a broader variety of KPIs beyond the sole objective they focus on.
- Energy flexibility KPIs relying on RBC can be derived rather easily from simulation tools, such as EnergyPlus, TRNSYS or IDA ICE.
- Advanced control strategies including optimization procedures (MPC and OC) typically use simulations in MATLAB and Modelica.

Furthermore, information on grid energy data sources were provided to encourage the use of realistic data in future simulation work. Future research should concentrate on the limitations and robustness of existing energy flexibility KPIs as well as their implementation in OCs and MPCs. Furthermore, development of additional KPIs addressing DSM services towards the power grid is also expected to provide valuable contribution.

Acknowledgement

The authors would like to gratefully acknowledge IEA EBC Annex 67 Energy Flexible Buildings and IEA HPT Annex 49 Design and Integration of Heat Pumps for nZEB which have been the framework of this work.

The Ph.D. position of Pierre J.C. Vogler-Finck within the ADVANTAGE project is funded by the European Community's 7th Framework Programme (FP7-PEOPLE-2013-ITN) under grant agreement no 607774.

Paul Beagon gratefully acknowledges that his contribution has emanated from research supported in part by a research grant from Science Foundation Ireland (SFI) under the SFI Strategic Partnership Programme Grant Number SFI/15/SPP/E3125.

Nomenclature

A_b	Energy autonomy
ADR	Active demand response
C	Capacity
C_{CO_2}	CO_2 intensity of power [$kgCO_2/kWh$]
$e(t)$	Electricity exported to the grid
E_{des}	Nominal design connection capacity between the building and the grid
$f(t)$	Binary function indicating net import
$g(t)$	On-site electricity generation
$\bar{G}$	Maximum electricity generation normalized to E_{des}
$i(t)$	Electricity imported from the grid
J_c	Energy costs
$l(t)$	Energy load, e.g. heating power. Optional time step (t)
$\bar{L}$	Maximum electricity load normalized to E_{des}
$LOLP_b$	Loss of load probability of the building
$ne(t)$	Net exported energy to the grid
$S(t)$	Energy storage balance
t	Index of observation time-step
T	Time interval under consideration (e.g. year)
V	Objective function for CO_2 emissions

Greek

γ_l	Self-generation / load cover factor
γ_s	Self-consumption / supply cover factor
Φ_{neg}	Negative flexibility
Φ_{pos}	Positive flexibility
Γ_{max}	Maximum relative costs
Γ_{min}	Minimum relative costs
$\zeta(t)$	Energy losses
ε	Energy flexibility
Δl	Load difference

Subscripts

b	Building
des	Design
l	Load
neg	Negative
pos	Positive
ref	Reference
shift	Shifting
s	Supply

Acronyms

COP	Coefficient of performance
DHW	Domestic hot water
DR	Demand response
DSF	Demand side flexibility
DSM	Demand side management
EMPC	Economic model-predictive control
FF	Flexibility factor
HPT	High price time
KPI	Key performance indicator
LPT	Low price time
LS	Load shaping
max	Maximum
min	Minimum
MPC	Model-predictive control
OC	Optimal control
ORM	On-site renewable energy maximization
PC	Procurement costs
RBC	Rule-based control
RE	Renewable energy
TES	Thermal energy storage
ToU	Time-of-use

References

Afram, A., and Janabi-Sharifi, F. (2014). Theory and applications of HVAC control systems - A review of model predictive control (MPC). Build. Environ. *72*, 343–355.

Alimohammadisagvand, B., Jokisalo, J., Kilpeläinen, S., Ali, M., and Sirén, K. (2016). Cost-optimal thermal energy storage system for a residential building with heat pump heating and demand response control. Appl. Energy *174*, 275–287.

Apx Power Spot Exchange (2016). www.apxgroup.com/market-results/apx-power-uk/ukpx-rpd-historical-data/.

Arteconi, A., Patteeuw, D., Bruninx, K., Delarue, E., D'haeseleer, W., and Helsen, L. (2016). Active demand response with electric heating systems: Impact of market penetration. Appl. Energy *177*, 636–648.

Baetens, R., De Coninck, R., Helsen, L., and Saelens, D. (2010). The Impact of Load Profile on the Grid-Interaction of Building Integrated Photovoltaic (BIPV) Systems in Low-Energy Dwellings. J. Green Build. *5*, 137–147.

De Coninck, R., and Helsen, L. (2016). Quantification of flexibility in buildings by cost curves - Methodology and application. Appl. Energy *162*, 653–665.

De Coninck, R., Baetens, R., Saelens, D., Woyte, A., and Helsen, L. (2014). Rule-based demand-side management of domestic hot water production with heat pumps in zero energy neighbourhoods. J. Build. Perform. Simul. *7*, 271–288.

Corbin, C.D., and Henze, G.P. (2016a). Predictive control of residential HVAC and its impact on the grid. Part I: simulation framework and models. J. Build. Perform. Simul. 1–19.

Corbin, C.D., and Henze, G.P. (2016b). Predictive control of residential HVAC and its impact on the grid. Part II: simulation studies of residential HVAC as a supply following resource. J. Build. Perform. Simul. 1–13.

D´Angiolella, R., De Groote, M., and Fabbri, M. (2016). Buildings as micro energy hubs. REHVA J. 52–55.

Dar, U.I., Sartori, I., Georges, L., and Novakovic, V. (2014). Advanced control of heat pumps for improved flexibility of Net-ZEB towards the grid. Energy Build. *69*, 74–84.

Deru, M., and Torcellini, P. (2005). Performance Metrics Research Project - Final Report.

Dounis, A.I., and Caraiscos, C. (2009). Advanced control systems engineering for energy and comfort management in a building environment-A review. Renew. Sustain. Energy Rev. *13*, 1246–1261.

Le Dréau, J., and Heiselberg, P. (2016). Energy flexibility of residential buildings using short term heat storage in the thermal mass. Energy *111*, 991–1002.

Ecoinvent (2016). www.ecoinvent.org.

Energinet (2016). www.energinet.dk/EN/El/Engrosmarked/Udtraek-af-markedsdata/Sider/default.aspx.

Esfehani, H.H., Kriegel, M., and Madani, H. (2016). Load Balancing Potential of Ground Source Heat Pump System Coupled with Thermal Energy Storage : A Case Study for. In CLIMA2016 - Proceedings of the 12th REHVA World Congress.

Favre, B., and Peuportier, B. (2014). Application of dynamic programming to study load shifting in buildings. Energy Build. *82*, 57–64.

Garnier, A., Eynard, J., Caussanel, M., and Grieu, S. (2015). Predictive control of multizone heating, ventilation and air-conditioning systems in non-residential buildings. Appl. Soft Comput. J. *37*, 847–862.

Gellings, C.W.; Smith, W.M. (1989). Integrating Demand-Side Management into Utility Planning. Proc. IEEE *77*, 908–918.

Haghighi, M.M. (2013). Controlling Energy-Efficient Buildings in the Context of Smart Grid : A Cyber Physical System Approach. University of California at Berkeley.

Halvgaard, R., Poulsen, N., Madsen, H., and Jørgensen, J. (2012). Economic model predictive control for building climate control in a smart grid. Innov. Smart Grid … 1–6.

Huntoon, S. (2016). Battery Storage : Drinking the Electric Kool-Aid. Public Util. Fortn. *36*.

Kandler, C., Wimmer, P., and Honold, J. (2015). Predictive control and regulation strategies of air-to-water heat pumps. Energy Procedia *78*, 2088–2093.

Kienzle, F., and Andersson, G. (2009). Valuing Investments in Multi-Energy Generation Plants under Uncertainty : A Real Options Analysis by. IAEE Eur. Conf. 1–17.

Kitapbayev, Y., Moriarty, J., Mancarella, P., and Blochle, M. (2013). A real options assessment of operational flexibility in district energy systems. Int. Conf. Eur. Energy Mark. EEM.

Kitapbayev, Y., Moriarty, J., and Mancarella, P. (2015). Stochastic control and real options valuation of thermal storage-enabled demand response from flexible district energy systems. Appl. Energy *137*, 823–831.

Klein, K., Kalz, D., and Herkel, S. (2015). Grid Impact of a Net-Zero Energy Building With BIPV Using Different Energy Management Strategies. In CISBAT 2015, (Lausanne, Switzerland), pp. 579–584.

Li, X., and Wen, J. (2014). Review of building energy modeling for control and operation. Renew. Sustain. Energy Rev. *37*, 517–537.

Lindelöf, D., Afshari, H., Alisafaee, M., Biswas, J., Caban, M., Mocellin, X., and Viaene, J. (2015). Field tests of an adaptive, model-predictive heating controller for residential buildings. Energy Build.

99, 292–302.

Lopes, R.A., Chambel, A., Neves, J., Aelenei, D., and Martins, J. (2016). ScienceDirect A literature review of methodologies used to assess the energy flexibility of buildings. Energy Procedia *91*, 1053–1058.

Lund, P.D., Lindgren, J., Mikkola, J., and Salpakari, J. (2015). Review of energy system flexibility measures to enable high levels of variable renewable electricity. Renew. Sustain. Energy Rev. *45*, 785–807.

Ma, J., Qin, S.J., Li, B., and Salsbury, T. (2011). Economic model predictive control for building energy systems. BT - 2011 IEEE PES Innov. Smart Grid Technol. ISGT 2011, January 17, 2011 - January 19, 2011 1–6.

Ma, Y., Kelman, A., Daly, A., and Borrelli, F. (2012). Predictive Control for Energy Efficient Buildings with Thermal Storage. IEEE Control Syst. Mag.

Masy, G., Georges, E., Verhelst, C., and Lemort, V. (2015). Smart grid energy flexible buildings through the use of heat pumps and building thermal mass as energy storage in the Belgian context. Sci. Technol. Built Environ. *21:6*, 800–811.

Mauboussin, M.J. (2012). The true measures of success. Harvard Bus. Rev. 90(10) 46–56.

Nord Pool Spot (2016). www.nordpoolspot.com/historical-market-data.

O´Connell, N., Pinson, P., Madsen, H., and O´Malley, M. (2014). Benefits and challenges of electrical demand response: A critical review. Renew. Sustain. Energy Rev. *39*, 686–699.

Oldewurtel, F. (2011). Stochastic Model Predictive Control for Energy Efficient Building Climate Control. ETH Zurich.

Pallonetto, F., Oxizidis, S., Milano, F., and Finn, D. (2016). The effect of time-of-use tariffs on the demand response flexibility of an all-electric smart-grid-ready dwelling. Energy Build. *128*, 56–67.

Reynders, G., Diriken, J., and Saelens, D. (2015). A generic quantification method for the active demand response potential of structural storage in buildings. 14th Int. Conf. Int. Build. Perform. Simul. Assoc.

Salom, J., Marszal, A.J., Widén, J., Candanedo, J., and Lindberg, K.B. (2014a). Analysis of load match and grid interaction indicators in net zero energy buildings with simulated and monitored data. Appl. Energy *136*, 119–131.

Salom, J., Marszal, A.J., Candanedo, J., Widén, J., Lindberg, K.B., and Sartori, I. (2014b). Analysis of load match and grid interaction indicators in net zero energy buildings with high-resolution data A report of Subtask A IEA Task 40 / Annex 52 Towards Net Zero Energy Solar Buildings.

Salpakari, J., and Lund, P. (2016). Optimal and rule-based control strategies for energy flexibility in buildings with PV. Appl. Energy *161*, 425–436.

Shaikh, P.H., Nor, N.B.M., Nallagownden, P., Elamvazuthi, I., and Ibrahim, T. (2014). A review on optimized control systems for building energy and comfort management of smart sustainable buildings. Renew. Sustain. Energy Rev. *34*, 409–429.

Single Electricity Market Operator (2016). www.sem-o.com.

Statnett (2016). www.statnett.no/en/Market-and-operations/Data-from-the-power-system/Production-and-consumption.

Stinner, S., Huchtemann, K., and Müller, D. (2016). Quantifying the operational flexibility of building energy systems with thermal energy storages. Appl. Energy *181*, 140–154.

Strbac, G. (2008). Demand side management: Benefits and challenges. Energy Policy *36*, 4419–4426.

Vanhoudt, D., Geysen, D., Claessens, B., Leemans, F., Jespers, L., and Van Bael, J. (2014). An actively controlled residential heat pump: Potential on peak shaving and maximization of self-consumption of renewable energy. Renew. Energy *63*, 531–543.

Watson, D.S. (2013). Fast Automated Demand Response to Enable the Integration of Renewable Resources. Lawrence Berkeley Natuional Lab Rep. *LBNL-5555E*.

PAPER 7

Calibration of a High-Resolution Dynamic Model for Detailed Investigation of the Energy Flexibility of a Zero Emission Residential Building

Clauß J[1], Vogler-Finck P[2], Georges L[1]

[1] Norwegian University of Science and Technology, Kolbjørn Hejes vei 1a, 7034 Trondheim, Norway

[2] Neogrid Technologies ApS / Aalborg University, Aalborg, Denmark

This paper is published in *Springer Proceedings in Energy "Cold Climate HVAC Conference 2018"* held in Kiruna, Sweden, in March 2018, Pages 725-736.

Calibration of a high-resolution dynamic model for detailed investigation of the energy flexibility of a zero emission residential building

John Clauß[1], Pierre Vogler-Finck[2] [0000-0002-3893-8956], Laurent Georges[1] [0000-0001-7135-3565]

[1] Norwegian University of Science and Technology, K. Hejes vei 1b, 7034 Trondheim, Norway
[2] Neogrid Technologies ApS, Niels Jernes Vej 10, 9220 Aalborg Ø, Denmark
john.clauss@ntnu.no

Abstract. A detailed multi-zone building model of an existing zero emission residential building (ZEB) has been created using the software IDA Indoor Climate and Energy (IDA ICE). The model will later be used for investigating control strategies for the heating system to activate the building energy flexibility. The main purpose of this paper is to show how reliable the model reproduces the short-term thermal dynamics and the temperature zoning of the building. This is of particular interest for the control of heating, ventilation and air conditioning (HVAC) systems in order to provide meaningful insights of active demand response (ADR) measures. The model has been validated using data sets from seven experiments. Two dimensionless indicators, the normalized mean bias error (NMBE) and the coefficient of variation of the root mean square error (CVRMSE) were applied in order to evaluate the trend of the average indoor temperatures. The first approach considered standard operating conditions, where the measured indoor air temperature was used as input for the control of the electrical radiator and the total electricity use of the radiator as an output. Excitation sequences have been used in the second approach, where the electric power of the radiator has been imposed and the operative temperature taken as the output. The model shows good agreement between the temperature profiles from the measurements and the simulations based on the NMBE and CVRMSE remaining below 5 % for most cases.

Keywords: detailed building model, model validation, zero emission building, energy flexibility, active demand response

1 Introduction

1.1 Context of the work

Calibration of a building model is an essential step to ensure simulation accuracy and thus to increase confidence in simulation results. Calibration can be achieved using monitoring data from the respective building [1]. This is of particular interest for ZEBs which contain advanced technologies that can be challenging to simulate. Model calibration often has, among others, two limitations: model complexity (use of single-zone

models) and the use of hourly aggregated data of the energy consumption for space heating [1]. The ASHRAE 14 guideline defines acceptance criteria based on the energy consumption, whereas no standards exist that determine acceptance criteria for model calibration based on indoor temperatures [2, 3]. Nevertheless, several studies use a threshold for the CVRMSE of 5 % when calibrating a building model with respect to hourly indoor temperatures [2, 4–6].

A detailed multi-zone numerical model of an existing residential ZEB, the Living Laboratory in Trondheim (Norway) [7], has been created using the software IDA ICE. The calibrated model will later be used to investigate the influence of different control strategies for space heating to activate the energy flexibility using structural energy storage. Knowing the short-term thermal dynamics and thermal zoning of the building envelope as a response to time-varying space heating set-point temperatures is of importance for active demand response measures as well as for the development of resulting control strategies for heat pumps. During structural energy storage, the indoor temperatures should fluctuate within the thermal comfort levels. Therefore, this study aims at investigating the indoor air temperature and operative temperature in different zones of the building.

1.2 Contribution

A multi-zone approach is used to evaluate the differences of the thermal environment between the bedrooms and the living spaces. Monitoring of the indoor thermal environment has been carried out during two periods, in February/March 2017 and April/May 2017. During the experiments in April and May 2017 the dynamics of the indoor thermal environment have been measured as a response to an excitation using a specified pre-defined heating sequence (with sub-hourly resolution). A first qualitative validation of the building model is carried out by a direct visual comparison of the measured building thermal behavior with the predictions from simulations in IDA ICE using identical boundary conditions. In a second step, a quantitative validation against experimental data is conveyed. Two dimensionless indicators, the NMBE and CVRMSE are used to evaluate the accuracy of the calibration based on the average indoor air temperature and operative temperature.

2 The Living Laboratory – A residential ZEB in Norway

2.1 Short description of the building

The case study building (Fig. 2a) is a Norwegian residential zero emission building [7] which is located at the Gløshaugen Campus of the Norwegian University of Science and Technology (NTNU) in Trondheim, Norway.

The on-site electricity generation from the photovoltaic panels is designed to compensate for the building CO_{2eq} emissions from the operational phase as well as for embodied emissions over the lifetime of the building. The floor area is approximately 105 m^2 [8] and the specifications for the building envelope follow the requirements

from the Norwegian standard for residential passive houses NS3700. The building has a highly-insulated envelope with a lightweight wooden construction [7] as well as energy efficient windows with low emissivity. Furthermore, it contains 90 m^2 of phase change material (PCM) in the roof construction. The PCM is active between 18 and 26 °C [9] and thus mitigates indoor temperature fluctuations in the building. The Living Laboratory consists of five heated zones (see Fig. 1): two bedrooms, one bathroom, one working room and one large room combining a kitchen, a living room and an entrance.

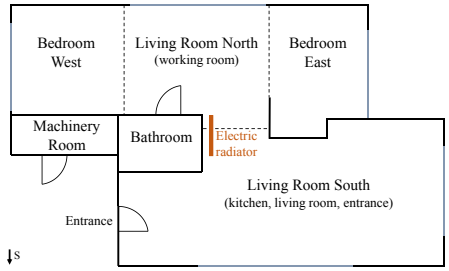

Fig. 1. Floor plan of the ZEB Living Laboratory (dashed lines show borderlines of the zones; moving doors between bedrooms and Living Room North can be opened)

A single heat emitter is placed between the two living rooms, since such a passive house can theoretically be heated using a single heat emitter [10]. The other rooms are without active heating, except for the bathroom equipped with floor heating. Temperature differences between the rooms are thus expected.

2.2 Building model in IDA ICE

The building simulation is done in IDA ICE 4.7.1 which is a dynamic multi-zone simulation software. The software applies equation-based modelling [11] and enables the user to evaluate the energy use and the indoor thermal climate of a building. A sketch of the 3-D virtual model is presented in Fig. 2b. The roof overhang at the entrance of the real building was not considered in the building model, as this was originally done to increase the roof area for PV installation. It does not affect the heating needs nor the indoor temperatures of the building because this part of the building is not heated up.

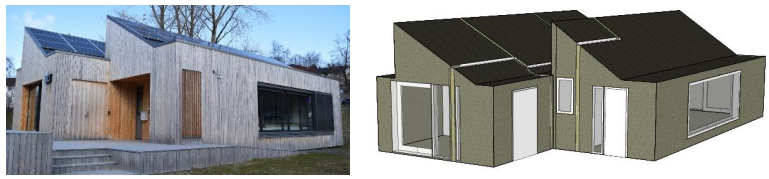

(a) (b)

Fig. 2. (a) Photo of the Living Laboratory at the Gløshaugen Campus at NTNU and (b) sketch of the modelled building

3 Experiments

The building model is validated on the basis of two sets of experiments where the first four experiments were conducted between the 16th of February 2017 and the 24th of March 2017, whereas three other experiments were carried out from the 18th of April 2017 to the 15th of May 2017. During the second set of experiments, the indoor air temperatures and operative temperatures (at 0.7m from the floor) were measured every 5 minutes in all heated zones, whereas during the first set of experiments the indoor temperatures were measured every minute. The air temperature was measured by Pt100 sensors, whereas the operative temperature was measured using Pt100 sensors enclosed in black globes. Vertical stratification of the air temperature was measured in the two living rooms. The bathroom door was always closed and the building was not occupied, although dummies with incandescent lamps were placed to mimic internal gains according to NS3031 using predefined on/off schedules for the first set of experiments.

3.1 Experiments 1 to 4 from February and March 2017

The aim of these measurements was the investigation of the temperature zoning by closing and opening the bedroom doors and to analyze the thermal dynamics of the Living Lab. An overview of the settings for these four experiments is given in Table 1.

The electricity use of the 1.6 kW electric radiator (with thermostatic on/off control) was logged every 30 seconds. The constant air volume (CAV) ventilation system continuously supplied air with a temperature of ca. 19 °C. All windows were always fully blinded to limit the influence of solar radiation. Weather data was taken from [12], which uses data from major weather stations close to a respective location as well as satellite data to construct the weather conditions with a grid size of 11x11 km [13].

Table 1. Overview of the test settings for Experiments 1 to 7 (E1–E7) where "Night setback" means that no electric heating is allowed between 23:00–07:00

Experiment	Time period	Bedroom doors	Night setback	Indoor Temperature variation [°C]	Sky condition
E1	17.2. 00:00–20.2. 00:00	Closed	No	15.7–19.9	Overcast
E2	20.2. 09:00–25.2. 00:00	Open	No	17.6–20.1	Clear on 21.2.
E3	16.3. 00:00–20.3. 12:00	Open	Yes	16.9–20.7	Clear on 19.3.
E4	20.3. 12:00–24.3. 12:00	Closed	Yes	14.5–21.6	Clear on 21.3.
E5	18.4. 20:00–24.4. 20:00	Open	No	16.8–24.5	Mostly clear
E6	29.4. 00:00–08.5. 09:00	Closed	No	15.9–26.8	Mostly clear
E7	09.5. 00:00–15.5. 06:00	Open	No	19.0–28.0	Mostly clear

3.2 Experiments 5 to 7 from April and May 2017

Electrical radiators with on/off control and a capacity of 0.8 kW (Experiment 7) and 1 kW (Experiment 5 and 6) were operated according to a pseudo random binary sequence (PRBS) [14, 15] in order to investigate the thermal dynamics of the building

over a wide range of frequencies. This excitation sequence is typically applied for inverse modelling. A PRBS does not necessarily ensure comfortable thermal conditions inside a building. A more detailed description of these experiments can be found in [16], whereas an overview of the test settings is provided in Table 1.

The ventilation supply air temperature was set to 30 °C for the first experiment (E5) and changed to 18 °C in the beginning of the second experiment (E6). Ventilation heating was deactivated for the last days of Experiment 7. Windows were not blinded. Weather data was measured using the building embedded weather station. The Skartveit-Olsen method has been used to split the global horizontal radiation data (measured on-site) into direct horizontal and diffuse radiation [17].

4 Validation results

The calibration of the building model was done based on the data set of Experiment 6 and with respect to the operative temperature aiming for a high correlation between the modelled and the measured temperatures. The model parameters (Table 2) were adjusted manually in an iterative manner, starting from their design values. The calibrated model has been validated using the data sets of six other experiments.

Table 2. Overview of tuned model parameters during calibration

Parameter	Starting value	Final tuned value	Range
U-value of external walls [W/(K· m^2)]	0.1	0.1591	0.1–0.1591
g-value of windows [-]	0.2	0.3	0.1–0.5
Solar transmittance [-]	0.17	0.24	0.17–0.47
Internal emissivity of windows [-]	0.837	0.6	0.5–0.9
External emissivity of windows [-]	0.837	0.05	0.03–0.837
Thermal bridges [W/(K·m^{2}floor area)]	0.03	0.045	0.025–0.06
Infiltration rates [ACH]	0.3	0.7	0.3, 0.7
C_d flow coefficient for internal openings [-]	0.65	0.80	0.6–0.8

Two approaches have been applied to carry out the validation. For Experiments 1 to 4, the space-average of the measured indoor air temperature of the Living Room North and the Living Room South has been used as a set point for the electric radiator and the time-averaged measured electric power of the radiator was compared to the simulation results ("closed-loop" approach). In Experiments 5 to 7, the operative temperature of the rooms has been measured as a response to a pre-defined heating schedule ("open-loop" approach).

4.1 Dimensionless indicators for model calibration

Two indicators for evaluating the model accuracy are the NMBE and the CVRMSE. The NMBE gives an indication of the total difference (percent error) between the measured and the predicted value from the simulations [18] and is calculated by

$$MBE = \frac{\sum_{i=1}^{n}(y_i - \hat{y}_i)}{n} \quad (1)$$

$$NMBE = \frac{MBE}{\bar{y}} \cdot 100 \quad (2)$$

where y_i and $\hat{y}_i$ are the measured and simulated value at instance i, $\bar{y}$ is the average of the measured data and n is the number of instances used in the calibration. The CVRMSE is a measure for the goodness-of-fit of a model showing the variability between simulated and monitored data [1]. It is calculated by

$$RMSE = \sqrt{\frac{\sum_{i=1}^{n}(y_i - \hat{y}_i)^2}{n}} \quad (3)$$

$$CV\ RMSE = \frac{RMSE}{\bar{y}} \cdot 100 \quad (4)$$

The model is considered calibrated with NMBE < 10% and CVRMSE < 30%, if the model is calibrated with respect to hourly energy use for space heating [19]. Since there is no approved guideline that determines acceptance criteria for model calibration with respect to indoor temperatures, the same thresholds were applied in this study, even though the calibration was aiming for a NMBE and CVRMSE < 5 %. A threshold of 5 % has also been applied in other studies [2, 4–6] and is thus used as a benchmark.

4.2 Calibration data set: Experiment 6 (closed bedroom doors)

During that experiment, the ambient temperature varied between -2.9 °C and 17.2 °C, whereas the global solar radiation varied between 0 W/m^2 and 834 W/m^2. An on/off-controlled electric radiator was operated according to a specified PRBS signal (Fig. 3). The bedroom doors were closed during this experiment.

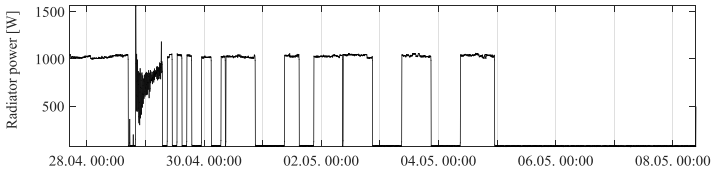

Fig. 3. Power supplied to the radiator during Experiment 6

Fig. 4 shows the trend of the operative temperature for Living Room South and Bedroom West at the end of the calibration. It can be seen that the model is reliable for predicting the temperature trend for cases with intermittent heating. If the electric radiator is turned off for a longer time (such as in the end of this experiment), the model predicts a faster temperature drop.

The overall UA-value of the building model is 83 W/K and is thus in the range of the values (70–100 W/K) identified during experiments conducted by Vogler-Finck et

al. using inverse modelling [20]. If the UA-value of the model was increased, the predicted temperature fluctuations would be even larger. The temperature fit for periods without any heating can be improved by considering the thermal mass of technical equipment (white goods) and by adjusting the properties of the PCM. Both will be investigated in further studies. The final NMBE and CVRMSE of Experiment 6 are shown in Table 3.

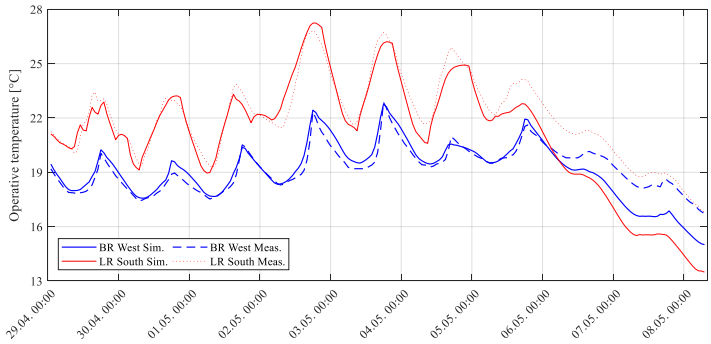

Fig. 4. Operative temperature trend in the Living Room South and Bedroom West at the end of the calibration

4.3 Example of a validation case: Experiment 7 (open bedroom doors)

The model is also reliable for predicting the thermal dynamics of the building, if bedroom doors are opened. Fig. 5 shows the trend of the operative temperatures in Living Room South and Bedroom West for the validation of Experiment 7. The temperature trend is similar for both Living Rooms as well as for both Bedrooms.

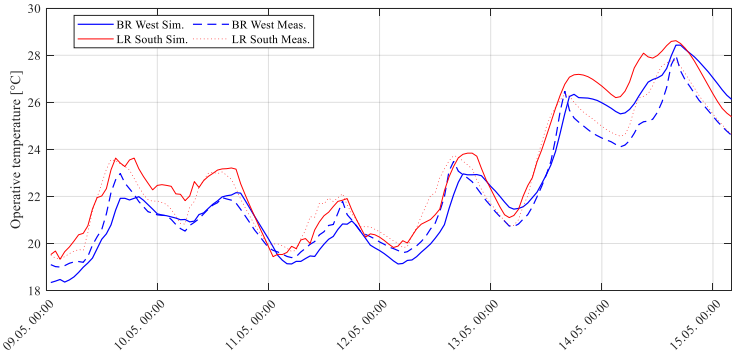

Fig. 5. Operative temperature trend in the Living Room South and the Bedroom West during Experiment 7

The model predicts the temperature fluctuations well for both rooms up to a temperature of 25 °C. It seems to slightly overpredict the maximum room temperature. This can be improved by tuning the thermal properties of the PCM. A summary of the results of all validation cases is given in Table 3.

The calibrated model predicts the temperature trend for all studied cases reliably, based on the NMBE and CVRMSE. Both indicators are below 8 % for all studied cases, for most of the cases even below 5 %. These results are in good agreement with other validation studies on residential buildings, where the building model was calibrated with respect to indoor temperatures [5, 6]. For experiments E2 and E3, the model predicts a slightly higher electricity use for keeping the indoor air temperature.

Table 3. Summary of the NMBE and CVRMSE (for indoor air temperatures and operative temperatures) for all validation cases

Experiment	Room	NMBE	MBE	CVRMSE	RMSE	Energy use [kWh]	
		[%]	[°C]	[%]	[°C]	Measurement	Simulation
E1	BR East	5.57	0.94	6.05	1.02	51	42
	BR West	5.95	1.04	6.34	1.11		
	LR North	0.00	0.00	0.18	0.04		
	LR South	-0.56	-0.11	0.62	0.12		
E2	BR East	3.49	0.65	3.67	0.68	112	124
	BR West	2.56	0.47	2.72	0.50		
	LR North	-0.39	-0.07	0.75	0.14		
	LR South	0.74	0.14	1.26	0.24		
E3	BR East	3.47	0.64	3.92	0.72	65	73
	BR West	4.87	0.91	5.16	0.97		
	LR North	1.67	0.31	2.57	0.48		
	LR South	1.93	0.36	3.32	0.62		
E4	BR East	3.10	0.51	3.71	0.61	51	51
	BR West	6.76	1.20	7.00	1.24		
	LR North	1.11	0.21	2.67	0.51		
	LR South	1.60	0.30	2.99	0.57		
E5	BR East	-1.06	-0.22	3.61	0.74	PRBS signal given as model input and thus identical radiator power	
	BR West	0.14	0.03	3.23	0.67		
	LR North	-2.31	-0.47	4.59	0.93		
	LR South	-0.74	-0.15	5.23	1.07		
E6 (used for calibration)	BR East	-0.20	-0.04	3.82	0.71	PRBS signal given as model input and thus identical radiator power	
	BR West	0.80	0.15	4.17	0.80		
	LR North	3.54	0.77	6.46	1.40		
	LR South	4.56	1.01	7.61	1.68		
E7	BR East	-0.85	-0.19	3.71	0.83	PRBS signal given as model input and thus identical radiator power	
	BR West	-0.96	-0.21	3.81	0.84		
	LR North	-3.33	-0.74	4.49	0.99		
	LR South	-1.66	-0.38	3.47	0.79		

Only for Experiment 1, the model uses less electricity to keep the temperature set-point in the two living rooms. This discrepancy will be investigated in further studies.

5 Conclusion

The aim of this study was the calibration of a dynamic multi-zone building model of a super-insulated residential building located in Trondheim, Norway. Seven experiments have been used for the validation of the building envelope model (one for calibration and six for validation). The building model was calibrated on measurement results of a 9-day long experiment with respect to the operative temperature trend in different rooms. An on/off-controlled electric radiator with a capacity of 1 kW heated the building according to a pre-determined excitation sequence.

The calibrated model was validated against measurement data from six other experiments, where the validation was based on the NMBE and CVRMSE, revealing that both indicators are below 8 % for all seven cases. The temperature trend of the calibrated model has been studied for cases with opened as well as closed internal doors. The model predicts the temperature trend for the different rooms reliably. The NMBE ranges between -3.33 % (MBE is -0.74 °C) and 6.76 % (MBE is 1.20 °C), whereas the CVRMSE is in a range of 0.18 % (RMSE is 0.04 °C) to 7.61 % (RMSE is 1.68 °C). Both indicators are 5 % or lower for cases with open bedroom doors (E2, E3, E5, E7), which is in good agreement with other studies on calibrations with respect to indoor temperatures [2, 5, 6].

Compared to the measurements, the model predicts a faster temperature decrease, if the building is not heated (Fig. 4) even though the overall UA-value of the building model (83 W/K) is within the range of 70–100 W/K, which has been determined by Vogler-Finck et al. [20].

Therefore, further work will investigate the impact of additional thermal mass inside the building as well as the influence of the PCM on the indoor temperature trend. Furthermore, the impact of solar radiation on the indoor temperatures will be studied. A similar temperature trend for model predictions and measurements as response to intermittent heating will be important for the evaluation of ADR measures in future studies. The calibrated model will be used for testing different heating control strategies with regards to the energy flexibility potential that residential buildings can provide to the electricity grid.

Acknowledgements
The authors would like to acknowledge IEA EBC Annex 67 “Energy Flexible Buildings” which was the platform of this collaboration. Access to the Living Laboratory was provided and funded by the *Research Centre on Zero Emission Buildings* project and its follow-up project *Research Centre on Zero Emission Neighborhoods in Smart Cities*. The PhD position of Pierre Vogler-Finck within the ADVANTAGE project is funded by the European Community´s 7th Framework Programme (FP7-PEOPLE-2013-ITN) under grant agreement no 607774.

References

1. E. Fabrizio and V. Monetti, “Methodologies and Advancements in the Calibration of Building Energy Models,” *energies*, vol. 8, pp. 2548–2574, 2015.
2. N. Zibin, R. Zmeureanu, and J. A. Love, “A Bottom-up Method to Calibrate Building Energy Models Using Building Automation System (BAS) Trend Data,” in *Aalborg Universitet CLIMA 2016 - proceedings of the 12th REHVA World Congress*, 2016.
3. F. Roberti, U. F. Oberegger, and A. Gasparella, “Calibrating historic building energy models to hourly indoor air and surface temperatures : Methodology and case study,” *Energy Build.*, vol. 108, pp. 236–243, 2015.
4. M. Taheri, F. Tahmasebi, A. Mahdavi, and B. Ecology, “Two case studies in optimization-based thermal building performance model calibration,” in *Central European Symposium on Building Physics*, 2013.
5. P. Paliouras, N. Matzaflaras, R. H. Peuhkuri, and J. Kolarik, “Using measured indoor environment parameters for calibration of building simulation model- a passive house case study,” *Energy Procedia*, vol. 78, pp. 1227–1232, 2015.
6. R. Simson, J. Kurnitski, and K. Kuusk, “Experimental validation of simulation and measurement-based overheating assessment approaches for residential buildings,” *Archit. Sci. Rev.*, vol. 60, pp. 192–204, 2017.
7. F. Goia, L. Finocchiaro, and A. Gustavsen, “7 . Passivhus Norden | Sustainable Cities and Buildings The ZEB Living Laboratory at the Norwegian University of Science and Technology : a zero emission house for engineering and social science experiments,” 2015.
8. J. Clauß, I. Sartori, M. J. Alonso, M. Thalfeldt, and L. Georges, “Investigations of different control strategies for heat pump systems in a residential nZEB in the nordic climate,” in *12th IEA Heat Pump Conference 2017*, 2017.
9. F. Kuznik and J. Virgone, “Experimental investigation of wallboard containing phase change material : Data for validation of numerical modeling,” *Energy Build.*, vol. 41, pp. 561–570, 2009.
10. L. Georges *et al.*, *Evaluation of Simplified Space-Heating Hydronic Distribution for Norwegian Passive Houses*. Trondheim, 2017.
11. EQUA, “EQUA Simulation AB,” 2015. [Online]. Available: http://www.equa.se/en/ida-ice.
12. OpenStreetMap, “Shiny weather data.” [Online]. Available: https://rokka.shinyapps.io/shinyweatherdata/. [Accessed: 20-May-2017].
13. L. Lundström, “Mesoscale Climate Datasets for Building Modelling and Simulation,” in *CLIMA 2016 - proceedings of the 12th REHVA World Congress*, 2016.
14. P. Bacher and H. Madsen, “Identifying suitable models for the heat dynamics of buildings,” *Energy Build.*, vol. 43, no. 7, pp. 1511–1522, 2011.
15. H. Madsen *et al.*, “Thermal performance characterization using time series data - IEA EBC Annex 58 Guidelines,” 2015.
16. P. Vogler-Finck, J. Clauß, and L. Georges, “A dataset to support dynamical modelling of the thermal dynamics of a super-insulated building,” Publication in progress, 2017.
17. P. Schild, “Personal communication,” 2017.
18. J. Granderson, S. Touzani, and D. Jump, “Assessment of Automated Measurement and Verification (M & V) Methods,” 2015.
19. ASHRAE, “Measurement of energy and demand savings,” *ASHARE Guidel. 14-2002*, vol. 8400, pp. 1–165, 2002.
20. P. Vogler-Finck, J. Clauß, L. Georges, I. Sartori, and R. Wisniewski, “Inverse model identification of the thermal dynamics of a Norwegian zero emission house,” 2017.

PAPER 8

Investigations of different control strategies for heat pump systems in a residential nZEB in the Nordic climate

Clauß J[1], Sartori I[2], Alonso M J[3], Thalfeldt M[1], Georges L[1]

[1] Norwegian University of Science and Technology, Kolbjørn Hejes vei 1b, 7034 Trondheim, Norway

[2] SINTEF Building and Infrastructure, P.O. Box 124 Blindern, 0314 Oslo, Norway

[3] SINTEF Building and Infrastructure, Høgskoleringen 7B, 7034 Trondheim, Norway

This paper is published in *Proceedings of the 12th IEA Heat Pump Conference* held in Rotterdam, Netherlands in May 2017.

12th IEA Heat Pump Conference 2017

Investigations of Different Control Strategies for Heat Pump Systems in a Residential nZEB in the Nordic Climate

John Clauß[a]*, Igor Sartori[b], Maria Justo Alonso[c], Martin Thalfeldt[a], Laurent Georges[a]

[a]Norwegian University of Science and Technology, Kolbjørn Hejes vei 1b, 7034 Trondheim, Norway
[b]SINTEF Byggforsk, P.O. Box 124 Blindern, 0314 Oslo, Norway
[c]SINTEF Byggforsk, Høgskoleringen 7B, 7034 Trondheim, Norway

Abstract

The paper investigates different control strategies for a ground source heat pump of a Norwegian residential zero emission building, with detailed dynamic simulations (here using IDA ICE). These rule-based controls aim at activating the energy flexibility of the building to improve grid interaction, lower energy costs, perform load shifting and reduce energy needs. Three load shifting controls load the building before pre-defined peak hours based on the electricity grid, whereas three other control strategies are based on hourly electricity spot prices. One additional control promotes the PV self-consumption in order to improve the grid interaction. Investigations showed that none of the proposed controls was able to maximize all objectives at the same time. The controls for peak load shifting were able to activate the water storage tank, but did not manage to activate the thermal mass of the building. Price-based heating control strategies for temperature set-points for space heating and domestic hot water heating led to an increased energy consumption of up to 25% as well as increased operational costs for the heat pump, but also decreased the total annual heat pump run time above 30% part load ratio by 13%. The controls were able to shift the electricity consumption to low-price hours, but failed to achieve savings for annual operational costs. A control for improving the PV self-consumption increased the building´s self-generation by 9% (up to 61%) and the building´s self-consumption by 5% (to up to 28%).

Selection and/or peer-review under responsibility of the organizers of the 12th IEA Heat Pump Conference 2017.

Keywords: nZEB, heat pumps systems, rule-based control, control strategies, grid interaction

1. Introduction

National building standards vary among European countries, partly due to different climate conditions. In cold climate countries like Norway, space heating needs are dominant over space cooling demands. According to the EPBD recast, all new buildings built after 2020 have to be nearly zero energy buildings [1]. The Norwegian Research Centre on Zero Emission Buildings (ZEB) focuses on the balance of CO_2 emissions rather than on primary energy. In Norway, the CO_{2eq} balance is typically promoted by (1) highly-insulated building envelopes in order to decrease space heating (SH) needs, (2) energy efficient thermal systems, as well as (3) covering the final energy use by renewable energy sources. A common approach for harvesting renewable energy is the use of heat pumps in combination with a geothermal energy storage and solar energy, solar thermal as well as photovoltaic.

The common approach for determining the energy needs of an nZEB applies fixed set-point temperatures for

* Corresponding author. Tel.: +4794284156.
E-mail address: john.clauss@ntnu.no.

AHU	Air handling unit	NO3	Norwegian spot price bidding area
COP	Coefficient of Performance	nZEB	Nearly Zero Energy Building
CO_{2eq}	CO_2 equivalent	OP	Off-peak
DHW	Domestic hot water	PV	Photovoltaic
EPBD	European Performance of Buildings Directive	RBC	Rule-based control
FH	Floor heating	SFP	Specific fan power
GSHP	Ground source heat pump	SH	Space heating
HDS	Heat distribution system	SP	Spot price
hGHE	Horizontal ground heat exchanger	SPF	Seasonal performance factor
HVAC	Heating, ventilation and air-conditioning	t_{aa}	Average annual temperature
HRU	Heat recovery unit	TMY	Typical meteorological year
KPI	Key performance indicator	T_{SP}	Temperature set-point
LL	Living Lab	ZEB	Zero Emission Building
MPC	Model-predictive control		

the heating system (EN15251) so that constant indoor temperatures as well as domestic hot water (DHW) temperatures are met. In this way, the heating system does not take into account external physical variables for building control such as price variations or limitations of electrical power that can be delivered by the grid. Furthermore, the approach does not consider any flexibility of occupants to variations of the indoor temperature and neither that a heating system can have storage capacity.

A suitable control strategy for the heat pump system can improve the building performance significantly. Among others, such a control strategy can apply rule-based or model-predictive control (MPC). Rule-based control (RBC) uses pre-defined set points for temperatures, electricity CO_2 levels or prices for running the energy system in an efficient way. MPC applies a simplified building model for predicting future system states and optimizes an objective function over a sliding planning horizon. The objective function optimizes the schedule for a chosen parameter, for example minimum energy costs for operation. Both, rule-based control as well as MPC can lead to considerable energy and operation cost savings [2] [3].

In this paper, nine rule-based control strategies are investigated using detailed dynamic simulations (IDA ICE). Each control is applied to a Norwegian residential ZEB located in Trondheim and their performances are compared with regards to eight different key performance indicators (KPI). The terminology is taken according to NS-EN15603:2008 [4].

2. Description of residential ZEBs

2.1. Characteristics of the Living Lab

The studied building, shown in Figure 1, is a Norwegian residential zero emission building [5] constructed in Trondheim, Norway. The so-called Living Lab (LL) is a single-family building and is used for several interdisciplinary research studies [6], ranging from investigations of the occupant behavior to testing of different ventilation strategies or control strategies for the heating system. The Norwegian Research Centre on Zero Emission Buildings (ZEBs) focuses on the balance of CO_2 emissions during the building life cycle. Different performance levels have been defined depending on how many stages of the building life cycle are included in the emission balance [7]. The LL is designed to be a ZEB-OM meaning that on-site generation compensates for embodied emissions as well as emissions from the operation phase. The building envelope specifications follow the Norwegian passive house standard NS3700 [8] and are presented in Table 1.

The LL, which is located at the Gløshaugen Campus of the Norwegian University of Science and Technology (NTNU), has a floor area of approximately 100 m^2 and a volume of around 500 m^3 [5]. The building has four rooms (machinery room not part of the protected volume): two bedrooms, one bathroom and one large room combining a kitchen, a living room and a working space. The building has lightweight construction with a wooden frame construction.

Table 1. Building envelope specifications of the Living Lab [9] and comparison of the U-value with NS3700.

Construction element	Construction element specification	Construction thickness [mm]	U-value $\left[\frac{W}{m^2K}\right]$	
			Living Lab	NS3700
External wall	Timber framed construction, mineral wool insulation, timber cladding	479	0.11	-
Internal wall	Timber cladding, mineral wool insulation	120	0.345	-
Floor	Raised timber framed construction, mineral wool insulation, parquet timber flooring	469	0.1	-
Roof	Timber framed construction, mineral wool insulation, integrated phase change material, in-roof photovoltaic panels	523	0.1	-
Window south side	Triple glazed unit with insulated aluminum frame, double skin	-	0.67	≤ 0.8
Window east/west side	Aluminum clad timber framed triple glazed units, integrated vacuum insulated panels	-	0.8	≤ 0.8
Window north side	Triple glazed unit with insulated aluminum frame, double skin	-	0.97	≤ 0.8
Air tightness $\left[\frac{1}{h}\right]$	0.5 ACH at 50 Pa	-	-	≤ 0.6
Thermal bridges $\left[\frac{W}{m^2K}\right]$	0.03	-	-	0.03

The maximum acceptable SH demand for a passive house is calculated following the standardized equation [8]

$$SH = 15 + 5.4 \cdot \frac{250 - A_{floor}}{100} + \left(2.1 + 0.59 \cdot \frac{250 - A_{floor}}{100}\right) \cdot (6.3 - t_{aa}) \quad (1)$$

leading to 26.9 kWh/(m²·a) for a floor area of 105 m² and an average annual temperature of 4.9 °C for Trondheim.

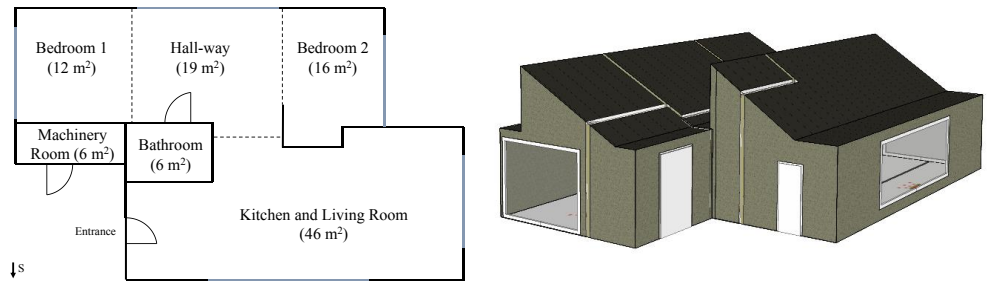

(a) (b)

Figure 1. (a) Floor plan (dashed lines show the delimitation of the modelled zones) and (b) sketch of the studied building

2.2. Energy system

A ground source heat pump (GSHP) connected to a horizontal ground heat exchanger (hGHE) and solar thermal collectors provides heating energy to a water storage tank (for both, space heating and DHW). All components are commercially available products. For such a highly-insulated building, the DHW demand is dominant over the space-heating needs [10]. The GSHP has 3.2 kW (0/35°C) nominal power and a COP of 3.7. If the water temperature has to be heated to 55°C, the nominal power and COP are 2.6 kW and 3.0 respectively. It is a one-stage heat pump cycle where the water is recirculated through the heat pump until it reaches 55°C. The water tank consists of a 240 litre DHW tank installed on the top of a 160 litre SH tank [11]. Depending on which part of the water tank is heated up, the temperature supplied by the heat pump changes. The total tank height is 1990 mm and the inner diameter is 580mm. Each of the tank parts has one auxiliary electric heating coil with a capacity of 3 kW [5]. The hGHE is a 150 m long surface collector field and is used as the heat source to the GSHP. The energy gained from the flat-plate solar thermal collector (STC) can either be used to recover the ground temperature of the hGHE or for heating the water in the tank. The STC is installed at the south façade and has an area of 4.2 m²

and an optical efficiency of 82%. The photovoltaic (PV) system consists of 48 polycrystalline panels and has a total installed power (DC) of about 12.5 kW. The panels have a rated efficiency of 16% [5]. There are two possible water-based heat distribution system (HDS) installed in the LL, a radiator with a design supply temperature of 55°C and a floor heating (FH) system with a design supply temperature of 33°C. On top of this, heating by ventilation air is also possible by increasing its temperature up to 40°C. There are eight different FH loops in the LL, which are usually used to heat up the building, and which can be run independently. The radiator, which is installed at the wall in the middle of the building, is only used, when FH is not used. The LL is equipped with a balanced mechanical ventilation system. The air handling unit (AHU) has a rotary heat wheel with nominal heat recovery efficiency of 85%. The AHU has a nominal flow rate of 120 m^3/h.

3. Rule-based control strategies

3.1. Working principle of rule-based controls

Rule-based control (RBC) strategies use pre-defined conditions (or decision rules) to change the current state of a system. Regarding HVAC systems, these pre-defined conditions can be set-points for indoor temperatures or indoor CO_2 levels. In case of a decreasing indoor temperature, the heating system is started as soon as a pre-defined set point for the lowest indoor temperature is reached and hence the zone is heated up. RBCs are commonly used for testing different scenarios in order to optimize the energy use of HVAC systems or to improve the energy flexibility towards the grid [2] [12]. The strategies can be easily implemented into dynamic building simulation tools, such as IDA ICE.

Regarding energy flexibility towards the power grid, RBC strategies can be coupled with electricity prices in order to investigate load-shifting scenarios where the electricity demand is moved to off-peak hours by activating thermal energy storages. The electricity prices follow the electricity production and can change significantly throughout the day. Practically, knowing these changes, RBC strategies can be used to preferentially run the heating system during low-price hours. Figure a shows the trend of the electricity spot price in Trondheim as well as the electricity production of the NO3 region throughout two exemplary days during 2015. Trondheim is situated in the NO3 region which is one of the five bidding areas of the power market in Norway [13]. Even though the electricity production of the grid is in the same range for the two exemplary days, the electricity price levels are significantly different (Figure a). The trend of the electricity production does not necessarily show a pre-dominant trend for the period of the year. In addition, RBC strategies considering these price variations can lead to economic savings for the electricity consumer. Low and high thresholds can be introduced in order to increase or decrease a temperature set-point depending on the spot price. The principle is illustrated in Figure b. Similar ideas have been proposed by Dar et al. [14] and Georges et al. [2] as a measure to describe flexibility of the heating system. In this study, it is examined how much energy flexibility can be provided by the GSHP in combination with a water storage tank depending on different control strategies. The corresponding cost savings for the building operation are also compared.

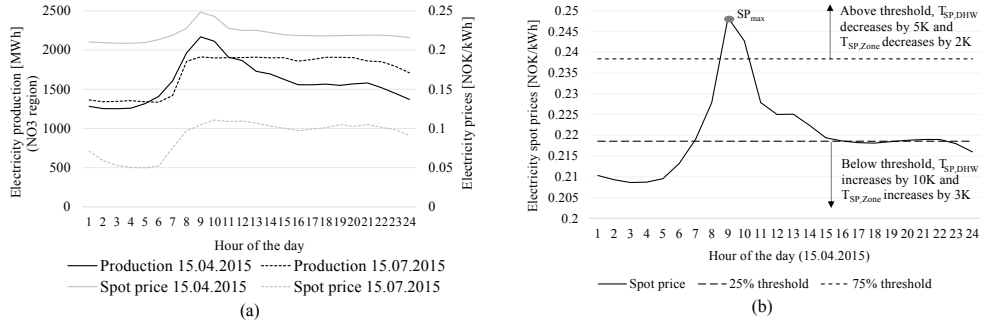

Figure 2. (a) Electricity spot prices throughout two exemplary days [13] and (b) principle of heating control based on electricity spot prices

3.2. Investigated strategies

Nine different rule-based control strategies for the heating system are investigated (here termed C1 to C9). C1 is a constant set-point heating and is used as the reference case since it is a common way to operate passive houses.

C2 investigates intermittent heating (time-scheduled set-points) even though it is usually not recommended for passive houses (due to the power needed to restart the building after a night setback). C3, C4 and C5 investigate peak-shaving strategies assuming that the peak in the power grid is between 7a.m. and 10a.m. C6, C7 and C8 are based on the electricity spot price with the aim of shifting the electricity consumption to low-price hours. C9 aims at increasing the PV self-consumption. The investigated control strategies are:

- C1, constant set-points (CS): The set-point of the indoor temperature is 21°C in the common rooms (hall-way and kitchen) and is kept constant at all times. The set-point temperature is 19°C for the bedroom and 24°C in the bathroom, considering the bathroom door is closed at all times. The set-point temperature for stored DHW is 55°C.
- C2, intermittent heating (IH): The indoor temperature set-point is 21°C during the day (6a.m.-10p.m.) and 18°C during the night for the common rooms. For the bathroom, it is 22°C during unoccupied times (0a.m.-5a.m. and 10a.m.-4p.m.), otherwise 26°C. The temperature set-point for the bedrooms is 16°C from 9p.m. to 6a.m. and 19°C during the day. The set-point temperature for the stored DHW is 55°C.
- C3 (OP/DHW): The DHW tank is pre-heated before typical peak hours. The set-point of the DHW tank is increased to 65°C during periods preceding peak power (5a.m.-6.30a.m.) and decreased to 50°C during peak periods in the grid (6.30a.m.-9.30a.m.). The temperature set-points for SH in the different zones are the same as in C1.
- C4 (OP/SH): The building thermal mass is activated before typical peak hours. The GSHP is supposed to run before the peak hours in the power grid (between 4a.m.-6.30a.m.) by increasing the SH set-point temperature in the common rooms by 3K. To decrease the consumption during peak power periods (7a.m.-10a.m.) the set-point temperature is decreased to 19°C. The DHW set-point remains at 55°C without any load shifting.
- C5 (OP/DHW&SH): This control combines C3 and C4 where both, the DHW storage tank and the thermal mass are activated.
- C6 (SP/DHW): The DHW tank is charged as a function of the electricity spot price. The control of the heat pump includes electricity day-ahead prices with constant thresholds for low prices and high prices for one full day. Each day at midnight the new thresholds are determined by taking into account the spot prices of the day ahead. The thresholds are set at 25% and 75% of the difference between the minimum and maximum spot price of the day above the minimum price of the day ahead, respectively (see Figure b). If the spot price of the current hour is below the daily low-price threshold, the upper temperature set-point of the DHW tank is increased from 55°C to 65°C. If the spot price of the hour is above the high-price threshold, the upper temperature set-point in the tank is decreased from 55°C to 50°C, so that the heat pump starts heating later and thus consumes less energy at high prices. If the spot price is between the two thresholds, the DHW set-point remains at 55°C. The temperature set-points for SH in the different zones are the same as in C1.
- C7 (SP/SH): The thermal mass is charged based on the electricity spot price. The same principle as for DHW heating in C6 is implemented for the zone heating. During high-price periods the set-point temperature is decreased by 2K and during low-price periods it is increased by 3K. This temperature control is done in the floor and kitchen. Even though the low prices typically occur during the night, a control for increasing the temperature set-point in the bedrooms is not desired for practical reasons. The DHW remains at 55°C.
- C8 (SP/DHW&SH): This control combines C6 and C7 allowing changes for both set-points. The principle is shown in Figure b.
- C9 (PV/SC): Increase of the water storage tank temperature based on on-site PV generation to increase electricity self-consumption. The temperature set-point of the water storage tank is increased by 10K as soon as the PV generation is above 860 W. This value is chosen to make sure that the heat pump runs continuously (without frequent on/off) which requires to run above 30% of the nominal compressor capacity. A power of 860 W considers electricity consumption for lighting, appliances and the compressor and was chosen because the software distributes on-site PV generation equally among all consumers.

4. Modelling approach

4.1. Simulation software tool

The building simulation is carried out in IDA ICE 4.7.1. IDA ICE is a dynamic multi-zone simulation software, which enables the user to investigate the energy consumption or the indoor thermal climate of a building. The software applies equation-based modelling [15].

4.2. Complexity of the model

The model of the building envelope can be validated by comparing the annual net SH needs [kWh/(m²·a)] to the NS3700 standard. The SH demand of the building model of IDA ICE is 27.0 kWh/(m²·a) and thus the envelope model is reasonably accurate compared to 26.9 kWh/(m²·a) calculated in equation (1).

The parameters of the heat pump model should be optimized to be consistent with manufacturer data at nominal conditions. The best fit is obtained when the error between the computed condenser and compressor power and the manufacturer data is minimal. With the help of parametric runs in IDA ICE it is possible to change the parameters (termed B, C, E and F) of the IDA ICE heat pump model. The optimization is then done using GenOpt. Other assumptions and simplifications are presented in Table 2. In general, idealized models for the components of the energy system are applied.

Table 2. Modelling assumptions and simplifications of the study.

Parameter	Model assumption/simplification
Indoor temperature set point	Chosen manually, depending on the control strategy
Internal gains	According to NS3700
Occupant behaviour	Synthetic occupancy schedules and Finnish DHW consumption profiles are used
Energy system model	Hot water tank: idealized tank combining DHW and SH with a volume of 400 litres
	GSHP: IDA ICE heat pump model with continuous power modulation from 0 to 100% and no maximum temperature limitation; nominal capacity is 4.54 kW with COP 4 (not the real heat pump installed in the LL)
	PV: constant panel efficiency (16%) throughout the year
	Solar thermal: constant collector efficiency throughout the year
	HDS: only floor heating is applied
	AHU: real ventilation flow rates which were measured in the building
Weather data	TMY data from Trondheim (Værnes) is used
Electricity prices	Hourly electricity spot prices for Trondheim in 2015 plus additional fees on top of the spot price

4.3. Occupant behavior

Occupants have different behavior in terms of occupancy patterns, SH set-point temperature, DHW needs, lighting and electrical appliances, resulting in different energy usage. The Norwegian passive house standard NS3700 defines time-constant SH set-point temperatures as well as space-uniform internal gains (from lighting, electrical appliances and occupants) to determine the net SH needs. For a same thermal comfort level, set-point temperatures can deviate from these fixed standard values as long as the indoor operative temperature corresponds to the same PMV level [16]. In order to be more realistic, different occupancy profiles are defined for this study (see Table 3). These synthetic profiles are meant to describe a realistic day rhythm of a four-person-family. The parents are both working and the children are going to school.

Table 3. Synthetic occupancy profiles defined for this study.

Room	Occupancy	
	Weekdays	Weekends
Kitchen	Occupied from 7-9am (0.5) and 17-19pm (0.5)	Occupied from 9-11am (0.5), 13-14pm (0.5) and 17-20 (0.5)
Floor	Occupied from 7-9am (0.5) and 18-20pm (0.5)	Occupied from 9-11am (0.5), 13-14pm (0.5) and 18-21pm (0.5)
Bedrooms	Occupied from 22pm-8am (1)	Occupied from 22pm-9am (1)
Bathroom	Occupied from 7-9am (0.5) and 19-22pm (0.1)	Occupied from 9-11am (0.5) and 19-21pm (0.1)

A realistic DHW consumption profile is included in the model. It is based on hourly consumption profiles for DHW in detached houses in Finland [17]. Because of the similar climate conditions it is assumed that the same profile can be applied for Norway. Comparing it to other DHW consumption data found in [17], the chosen profile seems to be a representative user profile. The corresponding DHW demand for a 4 persons household adds up to 29.8 kWh/(m²·a) which is comparable to the Norwegian Standard NS3700.

4.4. Presentation of the applied key performance indexes

Eight key performance indexes are used to evaluate the effect of the investigated control strategies:

- The net heating needs including SH and DHW presented in kWh/(m²·a).
- The annual energy use for heating is the energy input to the heating system [4], here the delivered electricity to the compressor of the heat pump and the electric resistances.
- The energy costs during operation are based on the delivered and exported energy to the building. It results from the energy use for lighting, electrical appliances, fans and pumps as well as for the heat pump and the electricity production from PV. Two different cost scenarios are presented: one scenario without any feed-in tariff for the exported electricity from PV and one scenario with a feed-in tariff being the hourly electricity spot price. The energy costs are calculated for each hour *i* (n=8760 hours i.e. 1 year) by

$$E_{Cost}\left[\frac{NOK}{year}\right] = \sum_{i=1}^{n} E_{del,i.}\,[kW] \cdot 1h \cdot Price_{el.,i}\left[\frac{NOK}{kWh}\right] \tag{2}$$

  A negative cost means that money is earned by feeding electricity into the grid (for the cost scenario with a feed-in tariff). The variable electricity prices consist of the spot prices and additional fees. The additional costs depend on the size of the installed fuse of the building and on the energy consumption of the building. A single-family building usually has a 63A fuse with 230V. For this fuse, the energy price that has to be paid on top of the spot price is 0.40 NOK/kWh (in 2015) [18]. Both prices are considered in the energy cost analysis. The different heating scenarios will lead to different annual electricity costs, since the additional fee depends on the energy consumption.
- The amount of energy in kWh/(m²·a) which is delivered to the building during the peak hours of the grid. Here, the peak hour period of the power grid is assumed to be between 7-10a.m.
- CO_{2eq} balance on the operation of the ZEB: the balance is based on the delivered and exported energy. For constant and symmetric (same for import and export) CO_{2eq} factors, the annual emissions can be calculated by

$$Em_{op}\left[\frac{kgCO_{2eq}}{m^2 \cdot a}\right] = f(i) \cdot (Q_{exp} - Q_{del}) \tag{3}$$

  where Q_{del} is the annual electricity delivered to the building, Q_{exp} is the annual exported electricity from the building to the grid and f(i) is the annual averaged CO_2 factor. The CO_2 factor is assumed to be 0.132 $kgCO_2$ eq./kWh which is commonly used by the Norwegian ZEB Centre [19]. If Em_{op} is positive, the building achieves a "plus energy" balance for operation.
- Two indexes are used to characterise the grid interaction of the building. The *load cover factor*, also known as "*self-generation*", is the percentage of the electrical demand, which is covered by on-site electricity generation [20]. It can be calculated by

$$\gamma_{load} = \frac{\int_{\tau_1}^{\tau_2} min[g(t) - S(t) - \zeta(t), l(t)]dt}{\int_{\tau_1}^{\tau_2} l(t)dt} \tag{4}$$

  where τ is the time resolution, g (t) is the on-site electricity generation, l (t) is the energy load and t is total time of observation. The time resolution is one hour and the total time period is one year. The *supply cover factor*, also known as "*self-consumption*", is the percentage of the on-site generation that is used by the building [20]. It is calculated by

$$\gamma_{supply} = \frac{\int_{\tau_1}^{\tau_2} min[g(t) - S(t) - \zeta(t), l(t)]dt}{\int_{\tau_1}^{\tau_2} g(t)dt} \tag{5}$$

  For the calculation of both indexes, energy storage balances, S(t), and energy losses, ζ(t), are neglected.
- The accumulated run time of the heat pump (duration curve) shows how many hours of the year the heat pump is running on a part load higher than 30% of the nominal compressor power. Since the heat pump is here modelled with an idealized power modulation from 0 to 100%, the absolute number of these hours does not have real physical meaning and thus rather gives an indication whether a control promotes on/off cycling or a more continuous heat pump operation.

5. Results

Compared to the reference case C1, each of the control strategies C2-C9 focuses on the improvement of at least one of the KPIs. The results are presented in Table 4. The results show that a trade-off between the performance indicators has to be made. It is not possible to achieve the lowest energy consumption and have the lowest energy costs, but at the same time improve the potential for energy flexibility. Activating the building flexibility requires storing heat at a higher temperature which most often leads to an increased energy consumption. The annual energy consumption for heating has been lowest for C2 (IH) being 17.9 kWh/(m^2·a), corresponding to an energy saving of 8%, but C2 also showed an increased energy consumption during peak hours. The highest energy use for heating occurred for C8 (SP/DHW&SH) with 24.4 kWh/(m^2·a). Lower operational costs were achieved with C2 (IH) and C9 (PV/SC) (14%).

Table 4. Comparison of the investigated control strategies (green for best case, red for worst case).

	Net heating needs $\left[\frac{kWh}{m^2 \cdot year}\right]$	Heating energy use $\left[\frac{kWh}{m^2 \cdot year}\right]$	Energy costs during operation $\left[\frac{NOK}{year}\right]$		Energy delivered to the building 7-10 $\left[\frac{kWh}{m^2 \cdot year}\right]$	Accumulated heat pump run time at P > 0.3 P_{nom} $\left[\frac{h}{year}\right]$	CO_2 eq. balance $\left[\frac{kg\ CO_2}{m^2 \cdot year}\right]$	Grid interaction indexes	
			w/o feed-in tariff	with feed-in t.				Self-gen.	Self-cons.
C1-CS	56.7	19.4	1645	-69	4.52	3150	8.93	0.52	0.23
C2-IH	54.7	17.9	1588	-133	5.34	2520	9.13	0.53	0.23
C3-OP/DHW	56.7	19.6	1731	-33	3.90	3120	8.91	0.48	0.21
C4-OP/SH	60.8	20.8	1717	12	5.01	3280	8.74	0.51	0.23
C5-OP/DHW&SH	60.6	20.9	1792	38	4.43	3430	8.72	0.48	0.21
C6-SP/DHW	56.9	22.2	2078	266	4.32	2740	8.56	0.41	0.19
C7-SP/SH	61.7	21.3	1733	66	4.99	3550	8.67	0.51	0.23
C8-SP/DHW&SH	61.7	24.4	2207	401	4.76	2890	8.26	0.40	0.19
C9-PV/SC	56.7	22.2	1414	-153	4.37	3220	8.55	0.61	0.28

Using pre-defined schedules for loading the thermal mass and the water storage tank before peak hours in the grid only had a limited effect on the load shifting. Loads were shifted only, if the peak hours were actually within the pre-defined peak hour period. C3 and C5 indeed led to slightly decreased energy consumptions during these peak hours. With the default tank implementation in IDA ICE, C4 (OP/SH) did not manage to activate the thermal mass before peak periods but rather transferred the energy from the storage tank to the floor heating system.

All price-based control strategies generated a higher energy consumption, unfortunately leading to increased total energy costs. This is due to the control principle. The controller strictly increased or decreased the set-point of the temperature in the common rooms based on the price, which means that, for example, the zone set-point temperature was kept at 24°C all night long until the price was above the low-price threshold. This led to a significant increase in energy consumption that is not compensated by the low electricity price. Although the electricity consumption increased for the price-based controls, it can be seen from Figure 3 that the price-based controls were able to actively shift the electricity consumption to low-price hours. C9 (PV/SC) had the lowest delivered energy consumption because self-consumption of the on-site generated electricity was prioritized and thus operational costs based in delivered energy were decreased.

Generally, the running time of the heat pump (Figure 4Figure 3) using on/off cycles could be reduced when using a control that increases the temperature set-point for DHW heating compared to a control, which used constant standard set-point temperatures throughout the day for a whole year (C1). Due to the idealized power modulation assumed in the heat pump model, results of when the heat pump is operated below 30% of the nominal capacity cannot be interpreted as this would lead to on/off cycles in reality. This limitation will be addressed in further studies. It can be seen from Figure 4 that the control strategies with varying DHW set-points promote a more continuous operation of the heat pump. The Living Lab achieves a positive CO_{2eq} balance reaching values between 8.3 and 9.1 (kgCO_{2eq})/(m^2·a) and hence the building generates more on-site electricity than it consumes. The magnitude of these values are in agreement with studies from other Norwegian ZEBs [21].

C2 has the best CO_{2eq} balance because it has the lowest energy consumption. The annual self-generation of the building is 0.52 meaning that 52% of the electricity demand of the building can be covered by on-site electricity generation. The annual self-consumption is 0.23 meaning that 23% of the on-site generated electricity are used by

the building. Only C9 (PV/SC) is able to significantly improve both grid interaction indexes leading to a self-generation of 0.61 and a self-consumption of 0.28. The range of these grid interaction indexes are in good agreement with comparable studies on other net zero energy buildings [22].

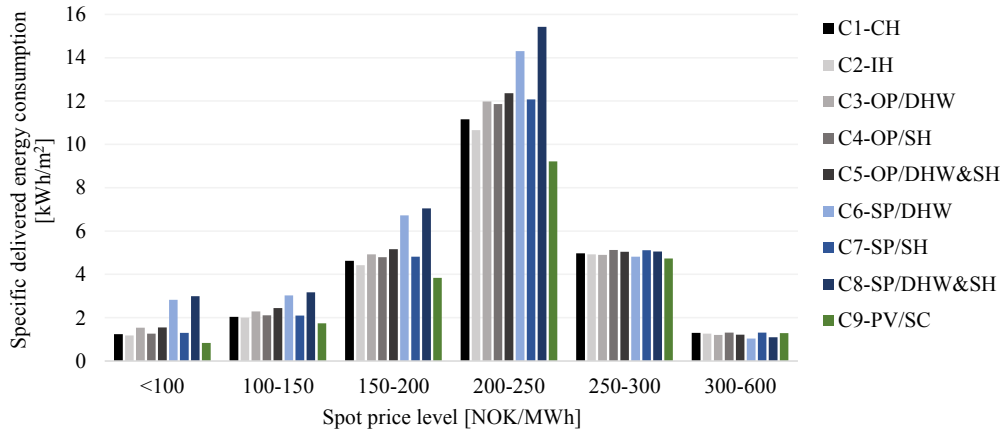

Figure 3. Specific delivered energy consumption per spot price level: average spot price during the space heating season was 210 NOK/MWh in 2015

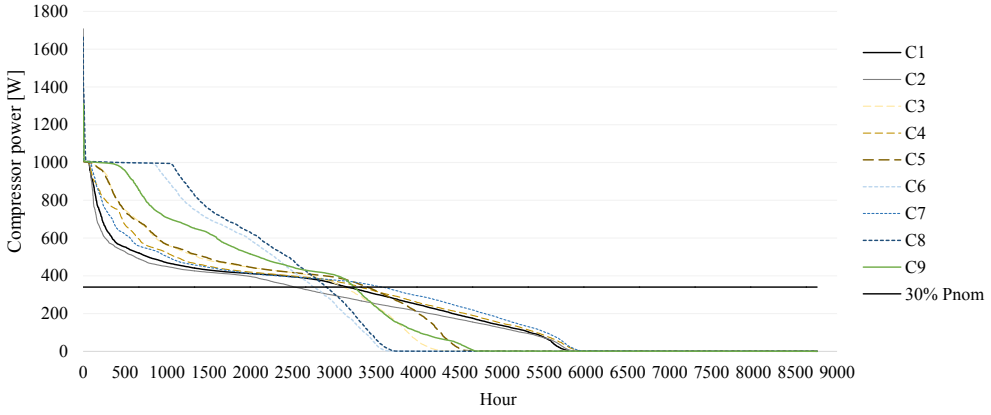

Figure 4. Duration curve of the heat pump (with idealized power modulation from 0 to 100%)

6. Discussion and conclusion

Nine rule-based control strategies for heating systems in a residential zero emission building have been investigated to assess their effect on different performance indicators. Three control strategies were based on pre-defined peak hours based on the power grid, whereas three other strategies were based on hourly electricity spot prices. One control promotes PV self-consumption in order to improve the grid interaction.

The controls for peak load shifting (C3-C5) managed to activate the water storage tank, but not the thermal mass of the buildings. Hence a better control for the activation of the thermal mass will be realized in the future. Furthermore, a control strategy based on the grid´s electricity generation will be implemented.

The price-based controls (C6-C8) successfully shifted the electricity consumption to low-price hours, but failed to achieve savings for annual operational costs. The control strategies with varying DHW set-points promoted a continuous heat pump operation and reduced the accumulated run time above 30% nominal capacity (C6 and C8).

Control strategy C9 proved to increase the self-generation as well as the self-consumption of the building and was thus able to improve the flexibility service to the grid.

Room temperature set-points of 19°C and 24°C were within the same PMV level (-1<PMV<1) (ASHRAE 55) and were thus assumed to be comfortable. Increased DHW set-points have a higher impact on load shifting than increased SH set-points due to the dominance of DHW needs in highly-insulated building envelope. The same control may not lead to similar conclusions for buildings with lower insulation levels. This study proves that a balance between a low energy consumption, energy costs, heat pump run time and a high load shifting potential has still to be found, for instance by advanced control strategies, such as MPC.

For further work, a more realistic heat pump control model will be implemented in this model. Up to now, the heat pump is used to heat up the DHW to 65°C, while in reality it would heat up the DHW to about 55°C and the last 10K temperature difference would be achieved by electrical resistance peak heating. Furthermore, a control based on the CO_2 intensity of the electricity generation in the power grid will be implemented in the model in order to address the aim of improving the CO_{2eq} emissions balance. Another control to be tested is the combination of C2 and the introduced price-based controls, as this will prevent high set-points during the night (usually low spot prices) and also to lower the number of start/stops of the heat pump. In addition, a sensitivity analysis against the lower and upper spot price thresholds (for the present price-based control) will be performed. Finally, the storage tank volume in combination with the heat pump capacity will be optimized for increased flexibility towards the grid.

Acknowledgements

This work has been performed in the framework of the IEA EBC Annex 67 Energy Flexible Buildings as well as IEA HPT Annex 49 Design and Integration of Heat Pumps for nZEB.

References

[1] European Council for an Energy Efficient Economy, "eceee.org," [Online]. Available: http://www.eceee.org/policy-areas/buildings/EPBD_Recast. [Accessed 31 10 2016].

[2] E. Georges, G. Masy, C. Verhelst, V. Lemort and P. André, "Smart Grid Energy Flexible Buildings Through The Use Of Heat Pumps In The Belgian Context," in *International High Performance Buildings Conference*, Purdue, 2014.

[3] Y. Ma, A. Kelman, A. Daly and F. Borrelli, "Predictive Control for Energy Efficient Buildings with Thermal Storage," *IEEE Control Systems Magazine,* pp. 44-64, February 2012.

[4] Standard Norge, "NS-EN 15603:2008 Energy performance of buildings - Overall energy use and definition of energy ratings," Standard Norge, 2008.

[5] F. Goia, L. Finocchiaro and A. Gustavsen, "The ZEB Living Laboratory at the Norwegian University of Science and Technology: a zero emission house for engineering and social science experiments," in *7. Passivehus Norden - Sustainable Cities and Buildings*, Copenhagen, 2015.

[6] M. Korsnes, T. Berker and R. Woods, "Compliance and deviation. How occupants interact with a high performance zero emission building," in *DEMAND Centre Conference 2016: "What energy is for: the making and dynamics of demand"*, 2016.

[7] S. M. Fufa, "A Norwegian ZEB Definition Guideline," SINTEF Academic Press and Norwegian University of Science and Technology, Trondheim, 2016.

[8] Standard Norge, "NS 3700:2013 Criteria for passive houses and low energy buildings - Residential buildings," 2013.

[9] S. Grynning, F. Goia, L. Finocchiaro and A. Gustavsen, "The ZEB Living Lab: a multi-purpose experimental facility," in *IEA Annex 58 meeting*, Ghent, 2014.

[10] M. J. Alonso, J. Stene, M. Bantle and L. Georges, "Simulations of Heat Pumps for Nearly Zero Enery Buildings - Country Report IEA HPP Annex 40, Task 2 - Norway," Trondheim, 2015.

[11] OSO Hotwater, "OSO Optima EPC series". Patent 328503, 02 2014.

[12] J. LeDréau and P. Heiselberg, "Energy flexibility of residential buildings using short term heat storage in the thermal mass," *Energy,* pp. 991-1002, 2016.

[13] Nordpool. [Online]. Available: http://www.nordpoolspot.com/. [Accessed 07 10 2016].

[14] U. Dar, I. Sartori, L. Georges and V. Novakovic, "Advanced control of heat pumps for improved flexibility of Net-ZEB towards the grid," *Energy and Buildings,* vol. 69, pp. 74-84, 2014.

[15] EQUA, EQUA, [Online]. Available: http://www.equa.se/en/ida-ice. [Accessed 28 May 2016].

[16] Standard Norge, "ISO 7730:2005 Ergonomics of the thermal environment," 2005.

[17] K. Ahmed, P. Pylsy and J. Kurnitski, "Hourly consumption profiles of domestic hot water for different occupant groups in dwellings," *Solar Energy,* no. 137, pp. 516-530, 2016.

[18] TrønderEnergi. [Online]. Available: https://tronderenerginett.no/nettleie/privat/priser-fra-1.jan-2016. [Accessed 31 10 2016].

[19] L. Georges, M. Haase, A. H. Wiberg, T. Kristjansdottir and B. Risholt, "Life Cycle emissions analysis of two nZEB concepts," *Building Research & Information,* vol. 43, no. 1, pp. 82-93, 2015.

[20] J. Salom, A. J. Marszal, J. Widén, J. Candanedo and K. B. Lindberg, "Analysis of load match and grid interaction indicators in net zero energy buildings with simulated and monitored data," *Applied Energy,* vol. 136, pp. 119-131, 2014.

[21] A. H. Wiberg, L. Georges, T. H. Dokka, M. Haase, B. Time, A. G. Lien, S. Mellegård and M. Maltha, "A net zero emission concept analysis of a single-family house," *Energy and Buildings,* vol. 74, pp. 101-110, 2014.

[22] R. Luthander, J. Widén, D. Nilsson and J. Palm, "Photovoltaic self-consumption in buildings: A review," *Applied Energy,* vol. 142, pp. 80-94, 2015.

ISBN 978-82-326-4046-1 (printed version)
ISBN 978-82-326-4047-8 (electronic version)
ISSN 1503-8181

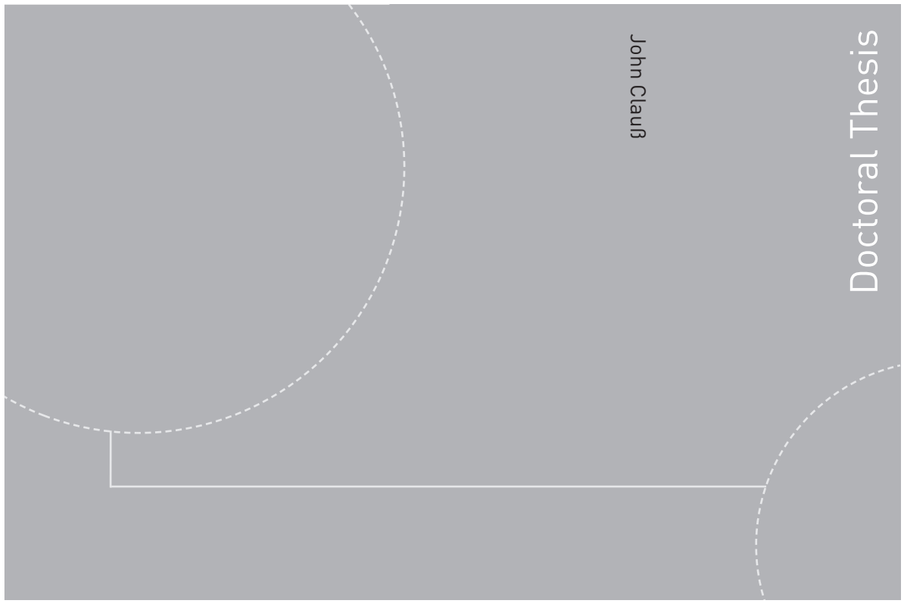

Doctoral theses at NTNU, 2019:225

John Clauß

Energy flexibility of Norwegian residential buildings using demand response of electricity-based heating systems

A study on residential demand side flexibility, heating system control, and time-varying $CO_{2eq.}$ intensities of the electricity mix

NTNU
Norwegian University of
Science and Technology
Faculty of Engineering
Department of Energy and Process Engineering

NTNU
Norwegian University of
Science and Technology

Doctoral theses at NTNU, 2019:225

NTNU

NTNU
Norwegian University of
Science and Technology